Studies of The PTEN Tumour Suppressor In Endometrial Cancer

Rachel Crosland

A thesis submitted in partial fulfilment of the requirements of
Sheffield Hallam University
for the Degree of Doctor of Philosophy

JANUARY 2004

ABSTRACT

Somatic mutations in the PTEN gene (Phosphatase and Tensin Homologue Deleted on Chromosome Ten) have been found in many types of cancer, but most frequently in cancer of the endometrium.

The PTEN gene encodes a D3' lipid phosphatase of the second messenger phosphatidylinositol 3,4,5-trisphosphate (PIP3), which activates protein kinase B/Akt. Constitutive activation of Akt has been found in cells that lack functional PTEN, thus by dephosphorylating PIP3, this enzyme modulates several cellular functions e.g. proliferation, differentiation and migration.

The PTEN protein comprises a 403 amino acid, 55KDa protein which is present in the cytoplasm but has also been detected in the nucleus of some cells. The function of nuclear versus cytoplasmic PTEN has not yet been determined. Little is known about modulation of PTEN expression by molecules such as hormones and cytokines. It has been reported, however, that NGF, BDNF and vitamin D3 analogues can up-regulate PTEN. The steroid hormones oestrogen and progesterone have been proposed as mediators of PTEN transcription, since their expression in endometrium reflects the menstrual cycle. The role of TGFβ1 in PTEN expression of PTEN in human cells has been also investigated, but the results are contradictory. Compounds which stimulate up-regulation of PTEN represent potential anti-tumour therapies and therefore merit investigation. To further investigate the role of PTEN in endometrial cancer the following approaches were taken.

The effect of TGF-β1 on two endometrial carcinoma cell lines, HEC-1B and Ishikawa were investigated. The cell lines were stimulated with TGF-β1 in the presence or absence of serum, and changes in mRNA and protein levels of PTEN and other genes analysed by RT-PCR and Western blotting. The morphology, cell number and cell viability were also assessed. Modest up-regulation of PTEN mRNA was detected in both cell lines, but little change in protein levels was observed. In accordance with published data, TGF-β1 suppressed the growth of, and changed the morphology of both cell lines.

To study PTEN sub-cellular localisation, full-length human PTEN cDNA was used in RT-PCR to generate a 1.2Kb fragment which was cloned into a green fluorescent protein expression vector pEGFP-N1 to create pRC-2. Sequencing of pRC-2 confirmed the in-frame cloning of wild-type PTEN. Lipid-based

transfection was used to transiently transfect HEC-1B, Ishikawa and Cos-7 cells. Strong perinuclear and cytoplasmic localisation was detected in these cell lines, and localisation to the endoplasmic reticulum was observed. Stimulation with TGF-β1 and 17-β-estradiol had no discernable effect on sub-cellular localisation of PTEN in either HEC-1B or Ishikawa cell lines.

A mutational study was performed using a large repository of archival endometrial carcinomas and normal cervical controls. PCR was used to amplify PTEN exons 5 and 8 from extracted DNA and the fragments separated by single-strand conformation polymorphism (SSCP) analysis. A number of samples exhibiting bandshifts were detected in both exons.

ACKNOWLEDGEMENTS

My gratitude and thanks goes to Dr Maria Blair and Prof Mike Wells for their supervision of this project and invaluable support throughout.

I would like to thank everyone in the BMRC for their friendship and guidance, with special thanks to Dr Andrew Fairclough for excellent technical advice, Dr. David Anderson for his constant support and to Dr Clare Fenech, Mr Greg Parker and Ms Carina Pinto.

CONTENTS

LIST OF FIGURES

3.3 Results of Mutation Analysis of PTEN in Endometrial Samples bySSCP

LIST OF TABLES

LIST OF GRAPHS

LIST OF ABBREVIATIONS

AA/aa	Amino Acid
Akt/PKB	Akt / Protein Kinase B
AR	Androgen Receptor
CBP	CREB Binding Protein
CDK	Cyclin Dependent Kinase
CK2	Casein Kinase 2
CM	Complete Medium
CMV-EGFP-N1	Plasmid containing green fluorescent protein tag
DSP	Dual-Specificity Phosphatase
EC	Endometrial carcinoma
ECM	Extracellular Matrix
EGF(R)	Epidermal Growth Factor (Receptor)
ER	Endoplasmic Reticulum
ERK	Extracellular signal-Regulated Kinase
FAK	Focal Adhesion Kinase
FH / FOX0	Forkhead (Transcription Factor)
HEC-1B	Human Endometrial Carcinoma cell line-1B
Ig	Immunoglobulin
IGF(R)	Insulin-like Growth Factor (Receptor)
IKK	IκB Kinase
IκB	Inhibitory unit of NF-κB
ISK	Ishikawa cell line
JNK	c-Jun N-terminal kinase
Kb	Kilobase
KDa	KiloDalton
LF2K	Lipofectamine 2000
MAPK	Mitogen Activated Protein Kinase
mTOR	Mammalian Target of Rapamycin
MDE	Mutation Detection Enhancement gel
NF-κB	Nuclear Factor Kappa-B
NLS	Nuclear Location Signal/Sequence
PAGE	Polyacrylamide gel electrophoresis
PEST	Proline-Glutamate-Serine-Threonine

PCR	Polymerase chain reaction
PDGF(R)	Platelet-Derived Growth Factor (Receptor)
PDZ	Protein Dimerization Zipper
PI(3,4,5)P3	Phosphatidylinositol 3,4,5-trisphosphate
PI(3,4)P2	Phosphatidylinositol 3,4-bisphosphate
PI3-K	Phosphatidylinositol 3-kinase
PLC	Phospholipase C
pRC-2	Clone containing full-length human PTEN cDNA
PTEN	Phosphatase and Tensin Homologue Deleted on Chromosome Ten
PTEN-2	Murine testis-specific PTEN homologue
P-PTEN	Phospho-PTEN
PtdIns	Phosphatidylinositol
PTP	Protein Tyrosine Phosphatase
RT	Reverse Transcription
rTK	Receptor Tyrosine Kinase
SAPK	Stress-Activated Protein Kinase
Ser	Serine
SDS	Sodium dodecyl sulphate
SH	Src Homology domain
SSCP	Single Strand Conformation Polymorphism
TAE	Tris-acetate EDTA
TBE	Tris-borate EDTA
TEMED	N,N,N',N'-tetarmethylethylenediamine
TGF-β1	Transforming Growth Factor-beta 1
Thr	Threonine
TNF-α	Tumour Necrosis Factor-alpha
TPIP	TPTE and PTEN homologous inositol lipid phosphatase
TPTE	Transmembrane phosphatase and tensin himology
Tyr	Tyrosine
VEGF	Vascular Endothelial Growth Factor

RESEARCH MEETINGS ATTENDED

British Cancer Research Meeting, 1-4th July 2001, Leeds, UK.

Abstract published in the British Journal of Cancer, July 2001, Volume 85, Supplement 1.

Pathology 2003, 1-4th July 2003, Bristol, UK.

Poster presented (number 119) and abstract published in the meeting Programme.

CHAPTER 1

INTRODUCTION

1.1 Intracellular Signalling and Phosphatidylinositol 3-kinase (PI-3K)

The regulation of cell growth and death is crucial to the survival of all multi-cellular organisms. Environmental stimuli, such as growth factors, control the delicate balance between cellular life and death by producing the desired response from the target cell. Binding of a stimulating molecule to a transmembrane receptor is a common event, which activates transmission of the specific signal via the generation of intracellular second messengers such as cyclic AMP and phosphoinositols (PIs). Once activated these transient molecules elicit activation, usually by phosphorylation, of a downstream target. The signalling cascade may involve many molecules and be highly redundant, but the net effect includes the modulation of gene expression to exert control over cell growth and metabolism.

1.1.1 Signalling Through Receptor Tyrosine Kinases

The generation of intracellular signals can be achieved by the binding of extracellular growth factors or cytokines to specific receptor tyrosine kinases, which are activated by tyrosine phosphorylation. Ligand binding to a receptor tyrosine kinase, which can exhibit autoinhibition in the absence of ligand (Schlessinger 2003), causes rapid phosphorylation of the cytosolic domain which may induce receptor dimerisation. This can then be followed by the activation of G-proteins (Nystrom & Quon, 1999).

G-proteins are 3-subunit transmembrane complexes which bind GTP or GDP, and of which there are four subclasses. The G-protein is directly linked

to the enzyme which catalyses second messenger generation, for example by various isoforms of phospholipase C (PLC). Phosphorylation of the G-protein results in the activation of the enzyme, and for the PLCs in the generation of inositol-3,4,5-trisphosphate (IP3) and diacylglycerol (DAG) from phosphatidylinositol-4,5-bisphosphate (PI4,5P2). IP3 stimulates calcium release from the endoplasmic reticulum (ER), and DAG activates protein kinase C (PKC) to stimulate proliferation. In addition, DAG is phosphorylated by DAG-kinases to phosphatidic acid and transported to the ER, where it is combined with inositol to perpetuate the generation of phosphoinositides (Payrastre, et al, 2001 & Vazquez-Prado, et al 2003).

Signalling through receptor tyrosine kinases (rTKs) can also occur in a G-protein independent manner. Activation by ligand binding causes rapid dimerisation of receptors (eg for EGF and PDGF) or conformational changes in dimeric receptors, for example for insulin and IGF-1 (Hubbard, et al, 1998). This permits activation of the cytoplasmic tyrosine kinase domain by autophosphorylation of tyrosine residues in this region. An activated rTK is then capable of engaging a wide range of downstream molecules containing src homology domains (SH2), including growth factor receptor bound protein 2 (GRB-2) and phosphatidylinositol 3-kinase (PI3K). SH2 domains are characterised by binding specifically to phosphorylated tyrosine motifs and can therefore regulate the catalytic functions or localisation of their substrates (Baca, 2003).

Binding of the SH2 domain of PI3K, a heterodimer which is composed of a regulatory p85 and catalytic p110 subunit, causes a conformational change in p85. This change permits activation of p110 and localises the activated PI3K

to the plasma membrane for the 3' phosphorylation of phosphatidylinositols (PtdIns). These products are not cleaved by PLC and represent a distinct signal transduction mechanism (Vanhaesebroeck, et al, 1999c).

Convergent signalling pathways can be activated by binding of ligand to non-receptor tyrosine kinases, such as src and JAK (Janus kinase) as observed in B- and T-cell antigen receptor signalling (Stephens, et al., 1993). PI3K recruitment and activation via p85 may occur due to these kinases binding to intermediates containing src homology-3 (SH3) domains. SH3 domains bind proline rich motifs on both upstream and downstream molecules simultaneously and mediate multiple protein-protein interactions (Jiang & Qui 2003). The overall effect, as with activation of rTKs, is the localisation of active PI3K enzyme to the plasma membrane.

Finally, as signalling is a redundant mechanism, PI3K may also be activated by the Ras family members which initiate the mitogen activated protein kinase (MAPK) pathways (Vanhaesebroeck, et al, 1997). Ras, like PI3K, is a common effector of pathways activated by many growth factor receptors and binds GTP with high affinity when activated. PI3K recruitment by GTP-Ras occurs via direct interaction with the p110 subunit, restoring catalytic function without binding to p85.

1.1.2 The PI-3K Pathway Intracellular Signal Transducers

The activation and recruitment of PI3K to the plasma membrane is the starting point of lipid-mediated signal transduction via a serine/threonine phosphorylation cascade. Three distinct classes of PI3Ks have been identified based upon p110 lipid substrate specificity and mechanism of regulation, with Class IA being most commonly associated with signalling through receptor tyrosine kinases and the only class to activate protein kinase B (PKB) (Vanhaesebroeck et al., 1999 & Fruman, et al., 1998). All mammalian Class I PI3Ks exhibit inhibition by low levels of the small cell-permeable compounds wortmannin and LY294002, which are unrelated structurally but which bind covalently to p110 (Wymann, et al, 1996) or competitively inhibit ATP binding (Vlahos, et al, 1994) . The PI3K class and associated inositol lipid products are shown in Table 1.

PI3K Class	Features	Substrates	Inositol products	Downstream Roles
I	Activated by rTKs & G-proteins	PI	PI3P	Proliferation Vesicular Trafficking Cytoskeletal Rearrangements Gene Expression
		PI4P	PI3,4,5P3	
		PI4,5P2	PI3,4,P2	
II	Possess C2 domain	PI	PI3P	
		PI4P	PI3,4P2	
III	Forms heterodimers	PI	PI3P	Vesicular Transport from Golgi Gene Expression

Table 1 PI3K Classes, their products and cellular roles

The catalytic p110 subunit exists as isoforms α, β and δ which associate with regulatory/adaptor p85 isoforms α, β and γ (Hu *et al.*, 1993) to achieve lipid kinase activity. The p110γ isoform, however, binds an adaptor protein p101 and is activated by the βγ subunits of G proteins, as is the p110β subunit

(Stoyanov et al., 1995 & Kurosu et al., 1997). These isoforms are expressed in a tissue specific manner and have distinct roles in transducing signals generated through distinct receptors. For example, p110α transduces PDGF-derived signals and p110β is the transducing factor for insulin (Hooshmand-Rad, *et al.*, 2000). p110δ is predominantly expressed in mature B and T cells and mediates antigen-receptor signalling (Zhang, Vanhaesebroeck & Rittenhouse, 2002), whereas p110γ is required for T-cell development and CD4/CD8 lineage commitment (Rodriguez-Borlando, et al, 2003).

It is thought that the isoform-specific protein kinase activity of p110 subunits towards themselves (by autophosphorylation) and their adaptor proteins contributes to the functional specificity of PI3Ks (Vanhaesebroeck et al., 1999b and c). The isoforms of p85 mentioned above contain a range of domains (Cohen *et al.,* 1995) including multiple SH2/3 and a region for binding p110 isoforms to regulate kinase activity (Klippel *et al.*, 1994). Recent work by Okkenhaugik & Vanhaesebroeck (2001) also indicates a regulatory role for p85 in actin cytoskeleton rearrangement.

Membrane localised PI3K specifically phosphorylates the D3 position of the inositol ring of phosphatidylinositides to generate phosphatidylinositol-3,4-bisphosphate (PI3,4P2) and phosphatidylinositol-3,4,5-trisphosphate (PI3,4,5P3, also written as PIP3). These PtdIns are almost absent unless the cell is stimulated by a growth factor, unlike other cellular PtdIns which are constitutively expressed (Carpenter et al., 1996). These include phosphatidylinositol-4,5-bisphosphate (PI4,5P2), which is involved in the PLC/DAG pathway as previously mentioned, and phosphatidylinositol-3-phosphate (PI3P) which has a role in membrane trafficking via the

recruitment of proteins containing FYVE domains and in receptor sorting (Leevers, et al., 1999 & Petiot, et al, 2003). PI3Ks generate molecules which activate many downstream effectors, (discussed in detail below), the disregulation of which is implicated in pathological disorders such as cancer, allergy and cardiovascular diseases.

PI3Ks are now the target of novel drugs to selectively inhibit specific isoforms of the kinase, in the hope of eliminating disease without abolishing entire signalling pathways (Arcaro, et al 2002 & Wymann, M. P., et al 2003). Recently, the p110δ/γ subunits of PI3K have been found to be essential non-redundant mediators of immune function, with implications for treating autoimmunity and transplant rejection (Okkenhaug & Vanhaesebroeck, 2003)

1.1.3 Downstream Targets of PI3K Activation

Membrane associated PI3,4P2 and PI3,4,5P3 generated by Class I PI3K are capable of activating PKB by binding to downstream target molecules via Pleckstrin homology (PH) domains, some of which target the inositol lipids and their head groups with high affinity (Vazquez & Sellers, 2000).

Proteins containing PH domains for PI3,4P2 and PI3,4,5P3 in this pathway include the Ser/Thr kinases PKB, also known as Akt, and PDK-1 (phosphoinositide-dependant kinase-1). Akt/PKB exists as α, β and γ isoforms which are widely expressed in tissues, consisting of an N-terminal PH domain, a kinase domain and a C-terminal regulatory tail (Wymann, et al, 1998). These latter two domains contain ser/thr sites (Ser473 and Thr308) which must be phosphorylated to fully activate the kinase (Alessi, et al, 1996a). The PH domain of Akt/PKBα preferentially binds to PI3,4,5P3,

causing its translocation from the cytoplasm to the membrane and a conformational change. This change exposes an activation loop containing Thr308 and Ser473, (or equivalent residues in the other isoforms), and initiates the phosphorylation of Thr-308 by PDK-1.

The mechanism of Ser473 phosphorylation is thought to occur through integrin-linked kinases functioning as adaptors to recruit a Ser473 kinase (Lynch et al., 1999), or by other rTKs (eg for IGF) by virtue of an interaction between PDK-1 and the C-terminal fragment of PRK-2 (protein kinase C-related kinase-2. This fragment, termed PDK1-interacting fragment (PIF) has been observed to convert PDK1 in a manner which permits it to phosphorylate Ser473 of Akt/PKB. Recent findings implicate Ser473, but not Thr308, as being the target residue for modulation of Akt/PKB activity (Wan & Helman, 2003, Dery, et al 2003, & Woods, et al, 2003). The interaction with PIF also causes a three-fold activation of PDK-1 by PI3,4,5P3 or PI3,4P2 but not PI4,5P2 (Balendran et al., 1999a). As PDK-1 complexes with other PKC family members, these interactions may form the basis by which modulation of PDK-1 towards Akt/PKB is achieved (Pullen et al., 1998, Le Good et al., 1998, & Balendran, et al, 1999b).

In addition to Akt/PKB, PDK-1 is also capable of activating p70-S6 kinase to initiate cell cycle progression via increased translation of immediate-early genes such as cyclin D (Takuwa, et al, 1999) and E2F transcription factor (Brennan, et al, 1999). Some components of the PI3K pathway demonstrate the ability to travel between the nucleus and cytoplasm, including PI3K, Akt/PKB and insulin signal mediators. Recently, PDK-1 has also been verified as existing in the nucleus, and this may represent a mechanism for

sequestering the protein to prevent it from participation in the cytosolic signalling cascade (Lim, M. A., et al 2003).

1.1.4 Downstream Targets of Akt

Once activated, Akt/PKB is capable of phosphorylating serine and threonine residues in small peptides *in vitro* containing the motif RXRXXS/T∗, where X is any amino acid and ∗ is phenylalanine or leucine (Alessi et al., 1996). Many of Akt/PKBs substrates are inactivated by this phosphorylation, at least *in vitro*, and therefore include pro-apoptotic factors such as BAD, Caspase 9, GS3Kβ and Forkhead transcription factors (Downward, 1998). Overexpression of Akt/PKB isoforms is anti-apoptotic and delays cell death, as observed in cancer cell lines representing pancreas (Cheng et al., 1996), breast (Nakatani et al., 1999) and ovary (Cheng, et al., 1992). An overview of the possible substrates of Akt/PKB are illustrated in Figure 1.

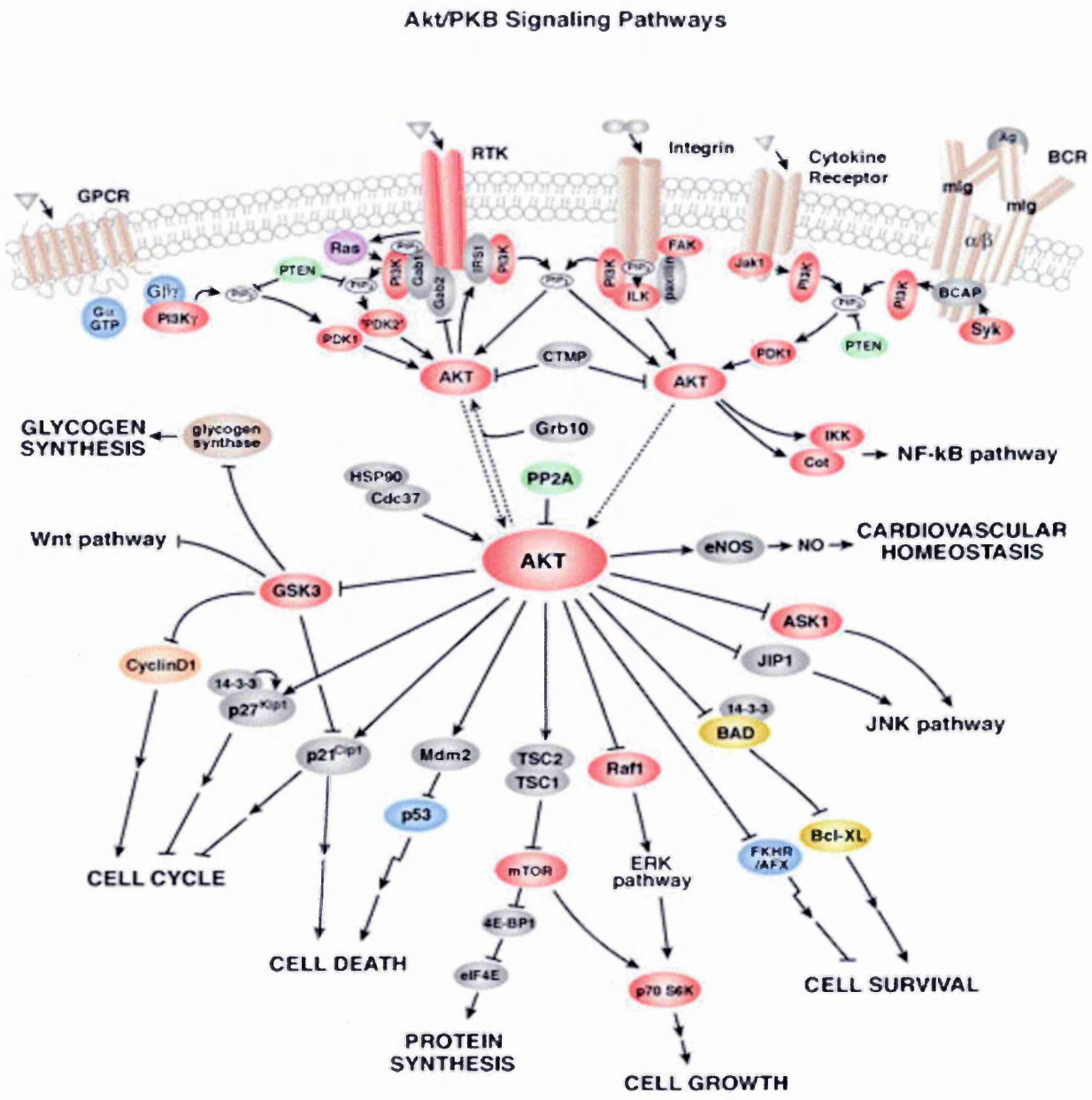

Figure 1 Akt/PKB Pathways Figure legends overleaf.

Taken from www.cellsignal.com

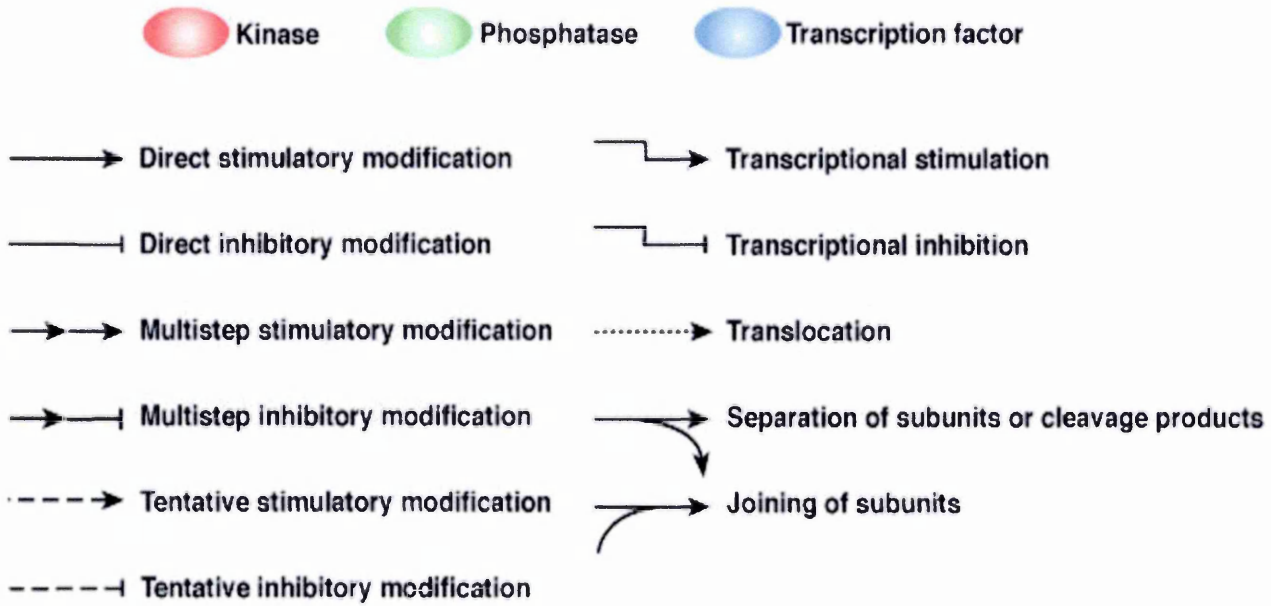

Figure 1 Akt/PKB Pathways, Legend The serine/threonine kinase Akt/PKB has a critical regulatory role in diverse cellular processes, including cancer progression. The Akt cascade is activated by receptor tyrosine kinases, integrins, B-cell receptor (BCR) and T-cell receptors, cytokine receptors, G-protein coupled receptors, and other stimuli that induce the accumulation of PI3,4,5P_3, by the phosphoinositide 3-kinase (PI3K). Akt is a major regulator of insulin signalling and glucose metabolism. Akt controls cell growth through its effects on the mTOR and p70 S6 kinase pathways, as well as the cell cycle and cell proliferation through its direct action on the CDK inhibitors, p21 and p27, and indirectly by affecting the levels of cyclin D1 and p53. Akt is also major mediator of cell survival by directly inhibiting different pro-apoptotic signals such as Bad and the Forkhead transcription factors, or indirectly by modulating two central regulators of cell death such as p53 and NF-κB. Akt signalling in endothelial cells play a critical role in the regulation of vascular homeostasis and angiogenesis, and have turned Akt/PKB into important therapeutic target for the treatment of cancer, diabetes and stroke. Modified from www.cell-signal.com

BAD

The BAD protein (Bcl-2/Bcl-X_L-antagonist, causing cell death) exists as a heterodimer with either Bcl-2 or Bcl-X_L, which are anti-apoptotic, and inhibits their function. When phosphorylated on Ser136 or Ser112, BAD is bound by 14-3-3 adaptor proteins and releases Bcl-2/Bcl-X_L which inhibit apoptosis. (Downward, 1999). Not all cell types express BAD, however, and other mechanisms of cell survival regulation exist independently of BAD phosphorylation and Akt/PKB activation (Hinton & Welham, 1999).

Caspase-9

Caspase-9 is an important protease in the initiation of the terminal apoptotic cascade and directly cleaves and activates the executioner molecule caspase-3 (Alnemri, 1999 and Wolf, et al, 1999). Akt/PKB has been shown to phosphorylate and inactivate human caspase-9 (Cardone, et al, 1998 and Takeuchi & Ito, 2003) but the phosphorylated residue is not conserved in rat, mouse or monkey homologues (Fujita, et al, 1999). There is also evidence that Akt/PKB may intervene at an earlier stage in the apoptotic cascade, prior to caspase-9 activation, by stabilising the mitochondrial membrane (Kennedy, et al, 1999).

ASK1

The apoptosis signal-regulating kinase-1 (ASK1) is a recently discovered substrate of Akt/PKB. ASK1 is a mitogen-activated protein kinase kinase kinase (MAPK kinase kinase) which acts upstream of p38 (Liao & Hung, 2003) and c-Jun N-terminal kinase (JNK) pathways, which are activated by

stress and pro-inflammatory cytokines to induce apoptosis. Work by Kim, et al (2001) demonstrated phosphorylation of ASK1 by Akt/PKB at Ser83 in a consensus region similar to other Akt/PKB substrates. The two proteins also co-immunoprecipitated in a manner observed in Akt/PKB-BAD interactions (Datta, et al, 1997) and could associate constitutively, but activation of Akt/PKB was necessary for ASK1 phosphorylation.

Modulation of ASK1 by Akt/PKB phosphorylation results in an inhibition of JNK and p38, which initiate and modify transcription through a range of transcription factors including ATF-2 and AP-1. These factors promote apoptosis via expression of Bcl homologues such as Bax and Bak, and may therefore indicate a transcription-based regulatory mechanism for Akt/PKB in apoptosis (Kyriakis, 1999 and Tibbles & Woodgett, 1999). Recently, Atk/PKB has been shown to bind to JNK interacting protein-1 (JIP1) in mouse primary neurones. This interaction inhibited JIP1-mediated activation of JNK pathway kinases and thus decreased apoptosis (Kim, et al 2002).

Additional targets in the stress-activated protein kinase (SAPK) pathways may include the Rac1 G-protein which activates the JNK pathway (Kwon, et al, 2000). The involvement of Akt/PKB is complex, and illustrates the cross-talk between lipid signalling and MAP kinase cascades. This is further complicated by observation that although a single stimulus may activate multiple pathways, not all of these pathways are required to elicit the appropriate cellular response (Kirit, et al, 2000).There is additional evidence that Akt/PKB may phosphorylate multiple targets simultaneously and act as a central regulator of multiple signalling pathways (Kim, et al, 2001).

Forkhead Transcription Factors

Akt/PKB is known to interfere with apoptosis at the transcription level via two mechanisms, the first of which involves members of the Forkhead (FH) transcription factor family. Three members of this superfamily, FKHR, FKHRL1 and AFX have been shown to be phosphorylated by Akt/PKB on three residues (Kops, et al, 1999, Rena et al, 1999 and Brunet et al, 1999). During cellular stimulation, FH transcription factors are translocated from their normal location in the nucleus to the cytoplasm (Brunet, et al, 1999). It is thought that phosphorylation by Akt/PKB prevents FH target gene transcription by promoting nuclear export of the FH proteins to the cytosol where they are sequestered by 14-3-3 adaptor proteins, thus preventing access to their pro-apoptotic target genes (Guo, et al, 1999 and Biggs, et al, 1999).

Recent findings have implicated Akt/PKB-regulated FH transcription factors, now termed FOXO (Burgering & Medema, 2003) in the control of expression of proteins directly involved in the cell cycle. A clone of HL60 human leukaemia cells with constitutive Akt/PKB (HL60AR) displayed higher levels of phosphorylated FH transcription factors Fox01 (FKHR) and Fox03 (FKHRL1) than parental cells. These factors were permanently restricted to the cytoplasm resulting in increased proliferation. The cyclin-dependent kinase (CDK) inhibitor $p27^{Kip1}$ protein was observed to be both decreased and hyperphosphorylated, levels of cyclin D1 were increased as were the activities of cdk2, 4 and 6, and the retinoblastoma (Rb) protein was also phosphorylated (Cappellini, et al, 2003). These findings indicate control of the cell cycle by Akt/PKB via nuclear exclusion of FOXO transcription factors,

and similar results have been observed in hepatocytes (Wolfrum, et al, 2003) and glioma cells (Ciechomska, et al, 2003). FOXO factors are capable of both inhibiting proliferation and initiating apoptosis via distinct mechanisms, and could be especially important in cells of the immune system (Birkenkamp & Coffer, 2003).

NFκB & IκB kinases (IKK)

The second anti-apoptotic transcription-based mechanism employed by Akt/PKB involves the transcription factor nuclear factor κ-B (NF-κB), which is at the endpoint of many signalling pathways. NF-κB exists in the cytoplasm bound to its inhibitor, IκB, until it is phosphorylated by IκB kinases (IKKs) and degraded, allowing NF-κB to translocate to the nucleus (Mercie, et al, 1998 and Dent et al, 2003). Here, transcription of anti-apoptotic genes occurs, including inhibitor-of-apoptosis (IAP) proteins c-IAP1 and 2 (Wang, 1998). Akt/PKB has previously been shown to associate with IKKs (Kane, et al, 1999) and to mediate IKKα phosphorylation at Thr23 (Ozes, et al, 1999). As with human caspase-9, the predicted phosphorylation site on IKKα does not lie within the optimal consensus sequence for Akt/PKB (Ozes et al, 1999), and may involve additional mediators such as protein kinase CK2 (Romieu-Mourez, et al, 2002) which is upregulated in some tumours.

GSK3β & Insulin Signalling

Akt/PKB appears to have a crucial role in mediating insulin signalling, as over-expression of activated Akt/PKB elicits the same effects as insulin in responsive cells (Barthel, et al, 1999), and PI3K inhibitors prevent insulin signalling (Shepherd et al, 1998). Although the exact mechanism is unknown, Akt/PKB has been shown to phosphorylate and inactivate glycogen synthase kinase-3β on Ser9 (Grimes & Jope, 2001). GSK3β phosphorylates cyclin D1 on Thr286 (Diehl, et al, 1998), causing its degradation by the proteasome and preventing G1-S transition of the cell cycle. Phosphorylation and inhibition of GSK3β would therefore allow the accumulation of cyclin D1 and progression of the cell cycle.

Other targets of Akt/PKB downstream of the insulin receptor include insulin receptor substrates -1&-2 (IRS-1&-2), mammalian target of rapamycin (mTOR) and phosphodiesterase-3B (PDE-3B). IRS-1 is tyrosine-phosphorylated and activated by the insulin receptor allowing association with p85α of PI3K. Akt/PKB appears to positively regulate IRS-1 by phosphorylation of one or more of four possible Ser residues in a feedback mechanism which protects active IRS-1 from dephosphorylation by protein tyrosine phosphatases (Paz et al, 1999). Recently Ser302 has been shown to be one of the residues phosphorylated (Giraud, et al, 2003 and Johnston, Pirola & Van Obberghen, 2003). IRS-2 is modulated through both mRNA transcription and protein regulation, but the exact mechanism is unknown (Hirashima, et al, 2003).

The mTOR protein is critical in the integration of signals which detect nutrient availability and allow cell cycle progression, and is inhibited by rapamycin

and its analogues. (Abraham, 2002). mTOR is a downstream target of Akt/PKB and PDK-1 (Section 1.1.3) which activate the protein and initiate an increase in the synthesis of proteins required for cell cycle progression such as cyclin D1. This pathway has been found to be elevated in several cancer cell lines including pancreas, lung and prostate, and inhibitors of mTOR are potential anti-tumour agents (Gera, et al, 2003 and Gao, et al, 2003).

In response to insulin binding, Akt/PKB also phosphorylates and activates PDE-3B on Ser273. PDE-3B is present in adipocytes and pancreatic β cells where it controls cellular levels of the second messengers cAMP and cGMP, and prevents lipolysis (Kitamura et al, 1999), and possibly promotes cell survival and cell cycle progression (Ahmad et al, 2000)

Endothelial Nitric Oxide Synthase (eNOS)

eNOS is produced by endothelial cells in response to VEGF and shear stress and activated by Akt/PKB, which can phosphorylate eNOS on Ser1177 (Dimmeler, et al, 1999). Recently, insulin has also been shown to regulate eNOS expression, but not activity, via increasing the binding of the transcription factors AP-1 and Sp1 (Fisslthaler, et al, 2003). Increased eNOS expression has been implicated in the onset of diabetes and hypertension (Pieper, 1998). Nitric oxide (NO) production by eNOS causes vasodilation and can modulate apoptosis, exerting both pro- and anti-apoptotic effects depending on concentration and cell type (Pervin, Singh, & Chaudhuri, 2003). NO produced in response to VEGF increases angiogenesis, and may be a mechanism by which tumours increase their blood supply.

BRCA1

The breast cancer susceptibility gene BRCA1 encodes a nuclear phosphoprotein that acts as a tumour suppressor and is inactivated in breast and ovarian cancers. BRCA1 is regulated through the cell cycle by CDK2 and also in response to DNA damage by Cds1, and its phosphorylation prevents its activity in attenuating the cell cycle (Lee, et al, 2000). The growth factor family of heregulins have been implicated in the survival of breast cancer cell lines, and are known to inactivate BRCA1 via Akt/PKB-mediated phosphorylation of Thr509 (Altiok, et al, 1999). Furthermore, inactivation of BRCA1 has been shown to be enhanced by the extracellular matrix (ECM), which often interacts abnormally with tumour cells to promote invasion of surrounding tissue (Miralem & Avraham, 2003).

In addition to the substrates discussed in detail above, new targets of Akt/PKB are continually adding to the repertoire of this kinase in regulating cell survival via multiple pathways. Recent discoveries include the negative regulation of Elk-1 mRNA translation, a transcription factor downstream of MAPK signalling (Figueroa & Vojtek, 2003) and the MAP kinase activator Raf in some cell lines (Zimmerman & Moelling, 1999). Direct phosphorylation and inhibition of the CDK inhibitor $p27^{kip1}$ at Thr198 and Thr157 by Akt/PKB has been reported, preventing constraint of G1 progression by relocalising $p27^{kip1}$ to cytoplasmic 14-3-3 proteins (Shin, et al, 2002 and Fujita, Sato & Tsururo, 2003). Akt/PKB also causes IGF-induced phosphorylation of WNK1 (with no K [lysine] protein kinase-1) on Thr60, a kinase that is mutated in an inherited hypertensive disorder (Vitari, et al, 2003).

1.2 PTEN Tumour Suppressor & PI3K Signalling

The importance of regulating intracellular signalling is dramatically illustrated by the many disorders resulting from mutation or otherwise inactivation of the genes which govern these pathways. The most prominent pathological process is cancer, described as a disease of the cell cycle, whose many forms provide insight into the complexities of cell life and death. Many genes have been characterised in the role of guardian of the cell cycle, termed proto-oncogenes and tumour suppressors. Of the latter p53 and Rb are perhaps the best understood, but recently a new tumour suppressor was isolated. Called PTEN, this gene rivals p53 for the most commonly mutated gene in human cancer.

1.2.1 PTEN - A Tumour Suppressor Discovered Twice

In 1997 a novel tumour suppressor gene was simultaneously discovered by two groups focussing on the high incidence of mutations and allelic loss on human chromosome 10. The gene, which localised to the long q arm at locus 23.3, was named PTEN (Phosphatase and Tensin Homologue Deleted on Chromosome Ten, (Li, et al, 1997) and MMAC-1 (Mutated in Multiple Advanced Cancers-1, Steck, et al, 1997) respectively. A third group submitted their findings shortly afterwards, named the gene TEP-1 (TGF-β Regulated and Epithelial Cell Enriched Phosphatase-1, (Li & Sun, 1997). As the names suggest, analysis of PTEN cDNA revealed a sequence coding for a 403 amino acid 55KDa protein of 9 distinct exons, with N-terminal homology to the cytoskeletal proteins auxilin and tensin. The sequence also contained a highly conserved catalytic motif IHCKAGXXRTG at residues

122-133 (Denu & Dixon, 1995 and Tonks & Neel, 1996), which is found in protein tyrosine and dual-specificity phosphatases (PTP and DSP). DSPs, such as yeast CDC14 (Li, et al, 1997) and PTPs, such as the yeast PTEN homologue CDC25 (Flint, et al, 1997 and Li & Sun, 1997), are components of signal transduction and the cell cycle regulatory machinery in *S.cerevisiae*. The presence of the phosphatase motif therefore indicated a possibly crucial role for PTEN as a protein tyrosine phosphatase in cell cycle modulation, and therefore in the development of cancer.

1.2.2 PTEN Structure and Function

1.2.2.1 PTEN Gene and mRNA Structure

Although the cDNA sequence for PTEN (illustrated in Appendix II) has been known for some years, it is only recently that the 5' promoter region upstream of the PTEN genomic sequence has been described. A lack of classical promoter motifs, such as TATA boxes, added to the question of how PTEN mRNA was transcribed. Sheng, et al (2002) investigated this problem by constructing various minimal promoter cassettes from a 2212bp genomic fragment previously cloned by Steck, et al, (1998) named BAC-46B12. This fragment contained a portion of the 5' untranslated region of exon1 and a 5' portion of the flanking PTEN sequence. The investigation revealed nine potential transcription start sites from -958 to -821 prior to the initiation codon ATG (+1) in a 599bp fragment termed the minimal promoter region. Of these, three sites at -972, -869 and -837 were identified as potential major transcription initiation sites, with the 137bp prior to +1 being the absolute

minimum required for transcription. The minimal promoter region is shown schematically in Figure 2.

Additional features uncovered by Sheng, et al (2002) included several consensus sites for binding transcription factors including Sp1 and Egr-1(between -958 and -821), which may have opposing effects on promoter activity. The cyclin inhibitor $p15^{INK4B}$ is upregulated by TGF-β1 via Sp1 (Feng & Derynck, 2000), suggesting that Sp1 may play a role in PTEN expression. The presence of a p53 binding site was investigated but the group found that p53 caused only a modest increase in PTEN expression. The relationship between p53 and PTEN is discussed in detail further in this section.

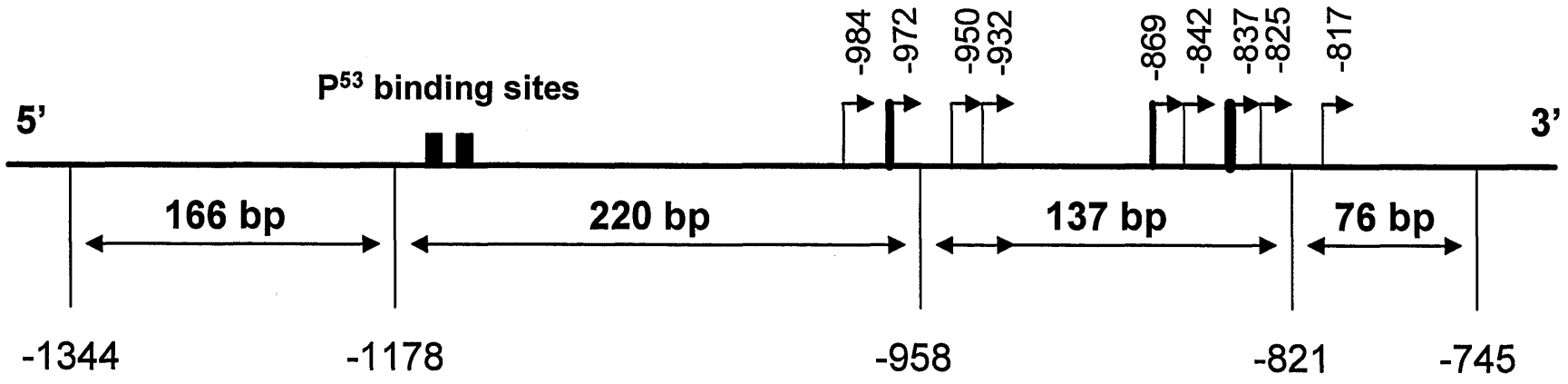

Figure 2 PTEN minimal promoter region

PTEN minimal promoter region showing nine transcription start sites. Arrowed bars represent transcription start sites relative to ATG(+1). Bold arrows show potential major transcription start sites, with -837 being the most common. The minimum promoter region from -958 to -821 contains six of the nine initiation sites and includes two Sp1 sites flanking an Egr-1 site. Adapted from Sheng, et al, 2002.

1.2.2.2 PTEN Protein: A Structure-Function Relationship

As previously mentioned, analysis of the PTEN sequence revealed an N-terminal phosphatase domain, and also C-terminal putative phosphorylation sites. Notably, the protein lacked a nuclear location sequence, and appeared to be cytoplasmically located. The determination of the crystal structure of PTEN by Lee, et al, (1999) gave greater insight into the functional aspects of this protein. The resolved structure is shown in Figure 3.

The structure revealed several interesting features of PTEN. Firstly, the PTP-like N-terminal domain forms part of an enlarged active site, and the C-terminus contains a C2 domain. Calcium independent C2 domains bind lipid vesicles in vitro, and the presence of a membrane-binding motif in addition to the active site is common in enzymes against inositol phospholipids substrates (Lee, et al 1999). A PDZ motif found in protein-protein interaction domains (Kocher, et al 2003) was located in the C-terminus, as were two PEST sequences which target proteins for degradation (Rogers, et al 1986). The domains are shown in cartoon form in Figure 3.

Initial studies to determine the physiological substrate(s) of PTEN indicated that phosphoproteins and peptides were not major targets, due to weak activity of the enzyme. Highly acidic peptides did undergo dephosphorylation by PTEN *in vitro* (Myers, et al, 1997 & Maehama & Dixon, 1998), but the major cellular substrate was found to be PI3,4,5P3 which is dephosphorylated to PI3,4P2. PTEN was therefore characterised as a lipid phosphatase, and its connection to the PI3K pathway was established (Myers, et al, 1998, Maehama & Dixon, 1999 & Stambolic, et al, 1998).

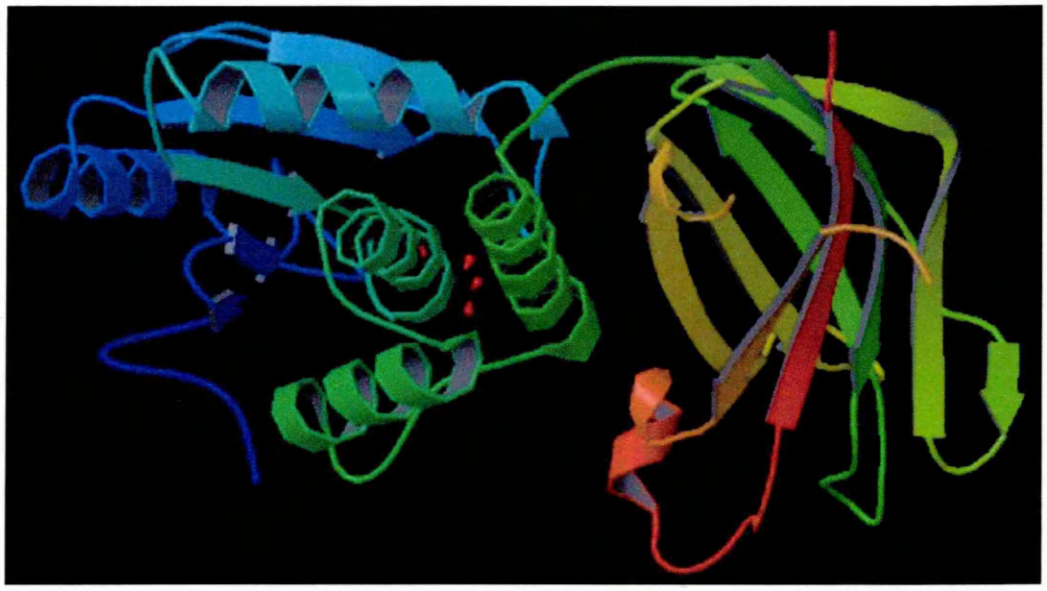

A

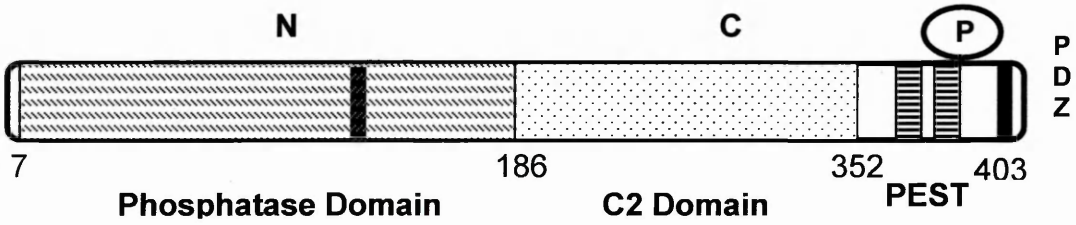

B

Figure 3 The Crystal Structure of PTEN

A .The structure of PTEN as determined by Lee, J. O., et al (1999), PDB 1DR5. The N-terminus is composed of β-sheets surrounded by α-helices and the C-terminus is composed of β-sheets. The catalytic site in the phosphatase domain is shown as red ball-and-stick area. **B**. Cartoon representation of PTEN. N-terminal phosphatase domain (aa 1-185 & catalytic motif 123-130), C-terminal domain (186-403) with C2 (186-351), PEST (350-375 & 379-396) and PDZ. Phosphorylation sites for CK2 (S380, T382 & T383) shown as a circled P.

In light of its substrate PI3,4,5P3, the features of the PTEN protein and their relevance to possible function are discussed below.

C-Terminal Domain

This domain contains C2, PDZ and PEST domains found in many other signal transducing molecules. The C2 domain, as previously mentioned, is associated with phospholipids and membrane binding. The C2 domain of PTEN does bind to phospholipid membranes *in vitro* (Rizo & Sudhof, 1998 & Hurley & Meyer, 2001) but lacks the acidic residues for Ca^{2+} binding seen in Ca^{2+}-dependant lipid phosphatases (Hurley, et al 2000). Functionally, mutations in this domain dramatically reduce lipid binding and cellular levels of PI3,4,5P3 are not reduced (Georgescu, et al, 2000 & Leslie, et al, 2001). Many mutation studies have shown that the minimal catalytic unit consists of the phosphatase and C2 units. Removal of a few bases in the C2 region is sufficient to disrupt all phosphatase activity, even against soluble PI3,4,5P3. Mutations in the C-terminal tail distal to the C2 domain however have little effect on catalysis (Georgescu, et al, 1999 & Tolkacheva & Chan, 2000.) It is thought that the C2 domain may not only allow PTEN to associate with membranes, but also to ensure the correct orientation of the active site relative to PI3,4,5P3 (Georgescu, et al, 2000).

The PDZ motif has been observed to affect the stability but not the activity of PTEN against lipid substrates (Georgescu, et al, 1999), but deletion of the PDZ disrupts cell spreading (Leslie, et al 2001). Work by Wu, et al, 2000a & Wu, et al, 2000b demonstrated a PDZ-specific interaction between PTEN and MAGI-2 and -3 (membrane-associated guanylate kinase inverted)

scaffold proteins. This interaction enhanced the ability of very low levels of PTEN to act on its substrate, suggesting such interactions may have a role in regulating PTEN activity and stability.

The two PEST sequences are also apparently required for stabilising the PTEN protein. Deletion of these motifs can cause a decrease in expression of the protein, but can also increase phosphatase activity of some C2 domain mutants (Georgescu, et al, 1999 & 2000). When phosphorylated the second PEST sequence can decrease PTEN activity (Vazquez, et al, 2000), suggesting that modifications to the PEST sequences can alleviate abnormal C2 mutations. Possible conformational changes may occur to correct the function of C2 mutants in a manner observed for p53 mutants (Foster, et al, 1999).

Finally, the C-terminus also contains several phosphorylation sites located in the last 50 amino acid "tail" of exons 8 and 9. These sites may be essential for PTEN stability and have a role in regulating cellular levels and activity of the protein. Phosphorylation of the C-terminal tail has been observed by protein kinase CK2 (Torres & Pulido, 2001) and is discussed further in this section.

N-Terminal Domain

The N-terminal domain contains the catalytic phosphatase core with the conserved motif residing in exon 5 at amino acids 123-130 (see Figure 3). Although similar to other protein phosphatases (PTPases and DSPs), the active site of PTEN is somewhat larger. For example, the active cleft of PTP1B is narrow and deep whereas that of the DSP VHR is shallower

(Tonks & Neel, 2001). The enlarged active site of PTEN is deep but also broad to accommodate the large inositol ring headgroup, and highly basic reflecting its preference for acid substrates (Lee, et al, 1999). Mutations are common in this region with ~30% of somatic and germline changes affecting exon 5. Mutations, and their associated diseases, are discussed in Section 1.5. Recently, the N-terminus has been shown to be involved in membrane targeting, and along with the C2 domain may ensure correct orientation of PTEN relative to its acidic substrate. Moreover, disruption of the N-terminal motif prevents catalysis of substrate *in vivo*, which can be restored by adding a myristoylation signal which enables targeting to the plasma membrane (Walker, et al, 2004).

Nuclear Localisation

As PTEN targets PI3,4,5,P3 it is ubiquitously expressed in the cytoplasm and has no nuclear location sequence (repeated positive aa flanked by proline residues), therefore little study was allocated to nuclear PTEN. Now, however, several immunohistochemical studies have reported PTEN in the nucleus of normal cells, with a shift to cytoplasmic localisation in corresponding tumour cells (Perren, et al 2000, Gimm, et al 2000, Tachibana, et al 2002 & Whiteman, et al 2002). Nuclear PTEN has been associated with G_0-G_1 in MCF-7 breast carcinoma cells, whereas the protein accumulates in the cytoplasm during S-phase, suggesting PTEN may directly regulate the cell cycle in the nucleus (Ginn-Pease & Eng, 2003). Differential localisation of PTEN in immature, mature and differentiating neural cells also indicates a role for nuclear PTEN in CNS development (Lachyankar, et al 2000).

Regulation of Protein Activity

Phosphorylation of the C2 Domain

As previously mentioned the 50 amino acid C-terminal 'tail' of PTEN protein contains several phosphorylation sites. Ser380, Thr382 and Thr383 are required to be phosphorylated to stabilise the protein, but this stabilisation may also reduce activity (Vazquez, et al 2000) and association with PDZ proteins (Adey, et al 2000). Constitutive P-PTEN has been observed in acute myeloid leukaemias and is associated with advancement of the disease and poor clinical outcome (Cheong, et al 2003). The protein kinase CK2 has been shown to phosphorylate Ser370, 380 and 385, and Thr383 and this appears to prevent degradation by the proteosome, thus influencing PTEN protein levels. (Torres & Pulido, 2001). This has very recently been investigated *in vivo* using cilostazol, a 3-phosphodiesterase inhibitor used as an anti-platelet drug which is neuroprotective. This drug decreased CK2-mediated PTEN phosphorylation in both ischemic rat brains (Lee, J. H., et al 2003) and SK-N-SH neuroblastoma cells (Kim, et 2003b), thus permitting degradation of PTEN and activation of Akt/PKB. However, mechanisms controlling the degree to which PTEN is phosphorylated are unknown.

Vazquez, et al (2001) have proposed a mechanism in which phosphorylation of the tail causes a conformational change from 'open' to 'closed' and prevents the recruitment of PTEN into protein complexes by masking the PDZ domain. The recruitment of PTEN into the protein complex may permit targeting to the membrane to bind PI3,4,5P3, therefore phosphorylation of the tail would effectively inhibit the lipid phosphatase function of PTEN. A second proposal by Das, et al (2003) suggests that phosphorylation of the tail

does not block the PDZ domain, but interferes with the electrostatic membrane binding capability of the protein. By blocking membrane docking, phospho-PTEN is not degraded, but it is still not clear how even the membrane-bound form is degraded or whether a phosphatase exists to dephosphorylate PTEN.

Another phosphorylation-dependant mechanism of PTEN regulation may be via Src family kinases. Lu, et al (2003) demonstrated that Src family kinases, but not purified Src or Lck, can tyrosine-phosphorylate PTEN, suggesting an intermediary protein is involved. The 5'-phospholipid phosphatase SHP-1 can regulate Src kinases and dephosphorylate many Src targets (Somani, et al, 1997 & Cuevas, et al, 1999), and can regulate PI3,4,5P3 via PI3K (Freeburn, et al, 2002 & Lu, et al 2003). It is possible therefore that SHP-1 may restore the function of PTEN by acting as a PTEN phosphatase (Lu, et al 2003).

Recently, fluorescent microscopy has indicated that nuclear PTEN in VCSM cells is phosphorylated and its activity reduced, whilst the 5'-phospholipid phosphatase SHIP-2 is active. The presence of nuclear PI4,5P2 and PI3,4,5P3 has been reported in may cell lines, but their role in the nucleus is unclear (Deleris, et al 2003).

C2 phosphorylation also appears to protect PTEN from cleavage by TNFα-activated caspase-3, which also targets MAGI-2 scaffold proteins to which PTEN has been shown to associate with. Torres, et al, (2003) have identified several aspartate residues in the C2 domain of PTEN which are targeted by caspase-3, and these sites overlap with the CK2 phosphorylation sites in this region. The group demonstrated that phosphorylation by CK2 blocks caspase-3 cleavage, and may therefore protect PTEN from cleavage. During

apoptosis, cleavage of the C2 domain could change the interaction of PTEN with structural and regulatory proteins, such as MAGIs, and vault proteins which are involved in nuclear-cytoplasmic transport (Yu, et al 2002).

Inhibition of the Catalytic site

A study analysing the effect of oxidative stress on PTEN levels has revealed that reactive oxygen species (ROS), which are produced as a by-product of metabolism, by macrophages, and through growth factor signalling (Meng, et al 2002), could decrease PTEN activity (Leslie, et al 2003). ROS have previously been shown to inactivate and regulate PTPs by oxidising a critical cysteine in the active site (Tonks & Neel, 2001).These enzymes, including PTEN, therefore require reducing conditions for catalysis (Maehama & Dixon, 1998).

The findings of Leslie, et al (2003) indicated that as tumours, and some specialised immune cells such as phagocytes, produce high levels of ROS, this may represent a mechanism by which these cells down-regulate PTEN activity and thus evade apoptosis. Moreover, the ROS can be produced by the NADPH oxidase complex in the plasma membrane by binding PI3,4,5P3 (Welch, et al 2002). As PTEN's substrate PI3,4,5P3 is in close proximity to the ROS-producing complex, increases in PI3,4,5P3 via receptor signalling could be a mechanism of actually inhibiting PTEN.

1.2.3 PTEN & Attenuation of PI3K/Akt Signalling

Activation of the serine/threonine protein kinase Akt/PKB by PI3,4,5P3 is an important mechanism in cell survival, but one which must therefore be regulated. The observation that expression of PTEN caused an increase in levels of inactivated non-phosphorylated Akt indicated that PTEN prevents phosphorylation of Akt/PKB, thus antagonising PI3K activity. Conversely, deletion of PTEN results in constitutively activated, phosphorylated Akt (Cantley & Neel, 1999). By restraining Akt activation, PTEN could therefore prevent the activation of Akt substrates such as mTOR, PDE-3B and IKK, and promote activation of pro-apoptotic substrates such as BAD and FOXOs. The main physiological substrate of PTEN is the phosphatidylinositol lipid PI3,4,5P3, which is specifically dephosphorylated by PTEN at the 3' position on the inositol ring. The role of PTEN in the restriction of PI3K signalling and Akt/PKB activation is illustrated in Figure 4. Recently, an activation mechanism has been described for PI3,4,5P3 binding. In this model, PI4,5P2 binds to a distinct N-terminal site on PTEN and causes an allosteric conformational change in the active site which favours PI3,4,5P3 binding. A feedback loop therefore exists as PTEN regenerates its activator PI4,5P2 from PI3,4,5P3 (Campbell, et al 2003).

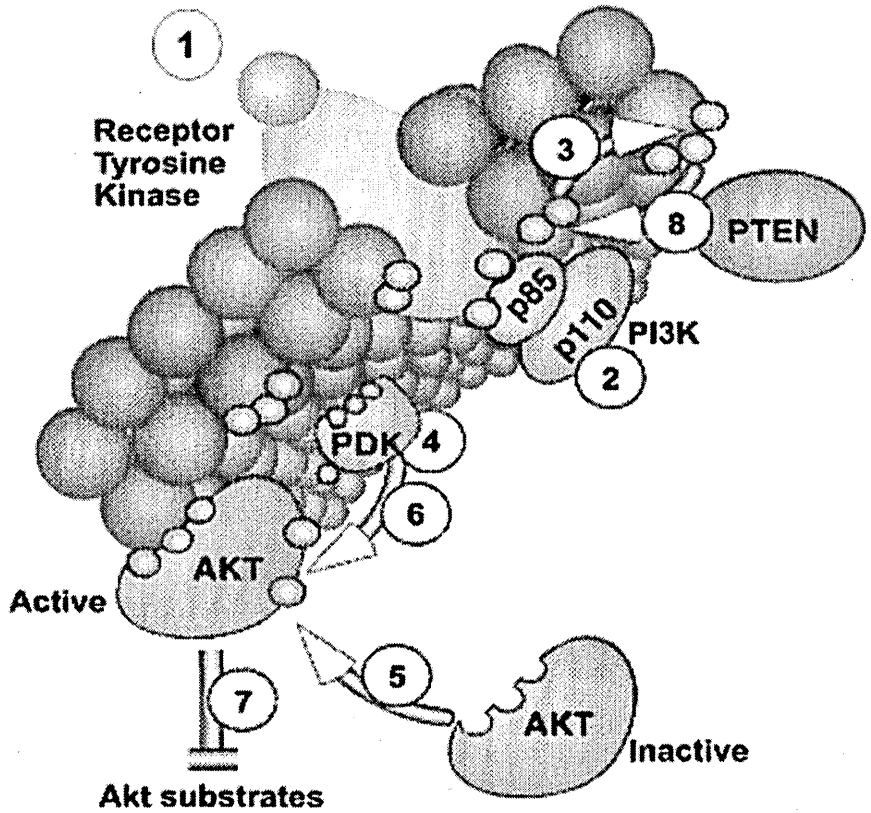

Figure 4 PTEN & the Akt/PKB Pathway

1. Growth factor binds to receptor and induces autophosphorylation, **2.** PI3K is recruited to the receptor via p85 subunit, **3.** Active PI3K phosphorylates PI4,5P2 (2 balls) to PI3,4,5P3 (3 balls),**4.** PI3,4,5P3 binds PDK ser/thr kinases, **5.** PI3,4,5P3 binds Akt ser/thr kinases, **6.** PDK phosphorylates and activates Akt, **7.** Activated Akt phosphorylates downstream targets, **8 .**PTEN antagonises the pathway by dephosphorylating PI3,4,5P3 to PI4,5P2. Adapted from Vazquez & Sellers, 2000.

Several components of the Akt/PKB pathway, including PTEN, are highly conserved in *C. elegans* (DAF-18) and *D. melanogaster (*dPTEN*)*, underlining an evolutionarily important mechanism in development and homeostasis (Huang, et al 1999, & Gao, et al 2000). Work by Myers, et al (1998) and Furnari, et al (1999) revealed human mutations of PTEN in both germline and sporadic tumours which disrupted the lipid phosphatase activity. Additionally, PTEN-null cell lines (Myers, et al (1998) and murine PTEN-/- fibroblasts (Stambolic, et al, 1998) showed increased levels of PI3,4,5P3. The PI3K inhibitor LY294002 can also mimic the effects of PTEN by effectively blocking Akt/PKB phosphorylation (Li & Sun, 1998).

Although PTEN reduces activation of Akt and therefore prevents cell cycle progression, the ultimate fate of the cell depends upon the cell type. PTEN can either cause G1 arrest or apoptosis via inhibition of the PI3K pathway, and evidence for these outcomes will be discussed.

1.2.3.1 PTEN & Induction of Cell Cycle Arrest

The mechanism by which PTEN can induce cell cycle arrest has been studied in a variety of cell types, but the consensus implicates inhibitors of cyclin-dependent kinases $p27^{Kip1}$ as a target for PTEN. The induction of G1 cell cycle arrest in PTEN-null cell lines by addition of wild-type PTEN has been noted in the glioblastoma cell lines U87-MG and U178 (Li & Sun, 1998, Furnari, et al 1998 & Cheney, et al., 1998), 768-O renal carcinoma cells (Ramaswamy, et al 1999) MCF-7 (Weng, et al 1999) and ZR-75 (Hlobilkova, et al., 2000) breast cancer cell lines, several thyroid carcinomas (Weng, at al, 2001a), two bladder cancer cell lines (Tanaka, et al 2000) and several cell

lines of endometrial origin (Matsushima-Nishiu, et al 2001). This effect was only observed under low-serum conditions, suggesting that serum components such as mitogens can modulate the function of PTEN. Furthermore, addition of mutant forms of PTEN into the glioblastoma cell lines indicated that only the lipid phosphatase activity was essential for growth suppression by G1 arrest (Furnari, et al, 1998).

P27^{Kip1}

It has been shown by several groups that G1 growth arrest by PTEN is effected by up-regulation of p27^{Kip1} and down-regulation of cyclin D1 (Cheney, et al 1999, Medema, et al 2000, Weng, et al 2001b & Gottschalk, et al 2001), cyclin D3 (Zhu, et al 2001) or cyclins A, and B (Seminario, et al, 2003), and inhibition of Rb phosphorylation (Lu, et al, 1999, Paramio, et al 1999 & Radu, et al 2003). Notably, the expression of p27^{Kip1} is reduced in various tumour cell lines (Graff, et al 2000, Gesbert, et al 2000 & Yang, et al 2000).

By mutating key residues in the active site of PTEN, Weng, et al (2001b) determined that PTEN down-regulates cyclin D1 through its ambiguous protein phosphatase activity but up-regulates p27^{Kip1}, p57 and p21 (Wu & Li, 2000) via downstream events orchestrated through the lipid phosphatase activity. The p27^{Kip1}, p57 and p21 CDK inhibitors are therefore up-regulated via the inhibition of Akt/PKB by PTEN, possibly via activation and nuclear translocation of Forkhead transcription factors (FOXOs).

Nakamura, et al (2000) demonstrated that a constitutively expressed form of FKHR (Fox01) which could not be phosphorylated by Akt/PKB could cause

G1 arrest or apoptosis in PTEN-null cells. PTEN also appears to be capable of affecting not only transcription of $p27^{Kip1}$ but also the stability of the protein. Inhibition of Akt/PKB by PTEN causes a decrease in the levels of the ubiquitin E3 ligase SCF^{SKP2} which degrades $p27^{KIP1}$, thus contributing to $p27^{KIP1}$ protein accumulation (Mamillapalli, et al 2001 & Nakayama, et al 2001). Interestingly, treatment of nasopharangeal carcinoma cells with ceramide induced G1 arrest and up-regulation of $p27^{Kip1}$ in a PTEN/PI3K independent manner, possibly via dephosphorylation of Akt by CAPP, a ceramide-activated protein phosphatase (Zhu, et al 2003).

GSK3β and β-catenin

Other possible elements involved in the induction of G1 arrest by PTEN as a protein phosphatase are GSK3β, involved in insulin-mediated signalling and the signalling/cell adhesion protein β-catenin (Polakis, 1998). β-catenin is involved in many pathways, with complex regulation, and when activated enters the nucleus to effect gene transcription (Stambolic, 2002). Two possible mechanisms of control by PTEN over the level of cyclin D1 have recently been proposed by Radu, et al, 2003.

The first is via phosphorylation of nuclear cyclin D1 by GSK3β-mediated phosphorylation and inactivation of β-catenin, and the subsequent export of cyclin D1 to the cytoplasm for degradation. GSK3β is activated when Akt/PKB is inhibited, thus PTEN may inhibit transcription and promote degradation of cyclin D1 by preventing nuclear accumulation of the protein. In support of this mechanism, levels of activated nuclear β-catenin have been shown to be reduced by exogenous PTEN expression (Persad, et al 2001).

Additionally, some tumours show activating mutations in the degradation targeting box of β-catenin, which is normally phosphorylated to cause nuclear exclusion and breakdown of the protein (Koch, et al 1999, Fukuchi, et al 1998 & Palacios & Gamello, 1998).

The second mechanism proposes that PTEN decreases cytoplasmic 'free' cyclin D1 by a GSK3β-independent pathway, which has been reported previously (Germain, et al (2000), although the exact mechanism of degradation is unknown. The novel tumour suppressor MDA-7 has recently been shown to down-regulate PI3K, redistribute β-catenin to the cytoplasm and up-regulate GSK3β and PTEN levels in breast and tumour cells, adding another regulatory mechanism to these pathways (Mhashilkar, et al 2003).

1.2.3.2 PTEN & Induction of Apoptosis

Reconstitution of wild-type PTEN into some PTEN-deficient cell lines may induce apoptosis rather than cell cycle arrest. Restoration of wild-type PTEN to several breast cancer cell lines induced G1 arrest followed by apoptosis (Li, et al., 1998) and similar results have been observed in endometrial cell lines (Sakurada, et al., 1999). Apoptosis was also induced by PTEN restoration into glioma cell lines (Davies, et al, 1998, Wick, et al 1999 & Tian, et al.,1999). Under serum-starved conditions apoptosis is induced rapidly in breast cancer cells (Lu, et al, 1999) and more slowly in prostate carcinoma cells (Davies, et al, 1999). One explanation is that under conditions where apoptotic stimuli are absent (eg Fas ligand, TNF) PTEN causes early G1 arrest. PTEN could then inhibit survival by growth factors and induce

apoptosis, depending upon the strength of the proliferative extracellular signal (Di Christofano & Pandolfi, 2000).

cIAP (Inhibitor of Apoptosis) Proteins

It has been shown that PTEN reconstitution into PTEN-null endometrial cell lines Ishikawa and RL-95-2 causes a decrease in expression of the survival factor cIAP-1 (Gagnon, et al, 2003). Human inhibitors of apoptosis, (IAP), proteins belong to a family consisting of six members which can inhibit the proteolytic activity of caspase-3, -6 and -7. Downstream activation of pro-casapase 9 is therefore prevented, and the cell escapes apoptosis induced by pro-apoptotic stimuli such as Fas, chemotherapeutic agents and serum starvation (Wang, et al 2003).

NFκB

PTEN may also initiate apoptosis via the inhibition of NFκB induced by TNF-α. This has been shown to occur via two possible mechanisms. Firstly, by inhibition of Akt/PBK which can activate IKKα and NFκB, in a manner that appears to be cell-type specific (Gustin, et al 2001). Secondly, PTEN has been shown to inhibit NFκB independently of IκB degradation (Koul, et al 2001), possibly by preventing TNF-mediated activation of the p65 transactivation domain of NFκB, which is essential for activating the NFκB complex (Mayo, et al 2002). The exact mechanisms are yet to be determined, and may involve complex feedback regulation of PTEN itself by the NFκB pathway (Kim, et al, 2003).

1.2.4 Expanding the Cellular Role of PTEN

PTEN has become established as a key player in the regulation of phospholipid signalling through Akt/PKB, but a definitive *in vivo* substrate for its *in vitro* protein phosphatase activity remains elusive. Additionally, other downstream effects of PTEN are becoming apparent, suggesting that the tumour suppressor could be involved in multiple signalling pathways involving both protein and lipid phosphatase functions.

1.2.4.1 PTEN & Cell Migration

As PTEN is a protein phosphatase *in vitro* against acidic phospho-Tyr/Ser/Thr peptides, it has been postulated that the integrin-mediated signalling proteins FAK (focal adhesion kinase) and Shc may be targets. These proteins are involved in cell motility and spreading, and modulation by PTEN could contribute to growth suppression. Loss of PTEN is correlated with anchorage-independence, and in PTEN-null tumour cells expressing exogenous PTEN, forced detatchment from the ECM causes up-regulation of PTEN (Wu, et al 2002). PTEN does exhibit dephosphorylation of FAK and Shc *in vitro*, and work by Gu, et al (1998) & Tamura, et al (1998 & 1999) proposed this to be the case *in vivo* using U87-MG cells.

However, lipid phosphatase mutants of PTEN with intact protein phosphatase activity have been shown to have no effects on FAK phosphorylation or motility (Maier, et al, 1999 & Liliental, et al, 2000), and other groups have been unable to repeat the original work in U87-MG. Additionally, evidence may link PTEN directly to FAK and Shc through its normal lipid phosphatase role in the Akt/PBK pathway (Lopez-Ilascala, et al, 1997 & Casamassima &

Rozengurt, 1998), thus implicating PTEN in MAPK pathway responses. Work in human PC3 cells implicates the integrin-linked kinase (ILK) in attachment. Here, ILK is bound and activated by the ILK-activating proteins CH-ILKBP and localised to focal adhesions, where Akt/PKB is stimulated and GSK3β is inhibited. The generation of PI3,4,5P3 further activates ILK, causing re-organisation of F-actin and paxillin to direct attachment and migration. PTEN appears to disrupt the ILK:CH-ILKBP complex by an unknown mechanism (Attwell, et al 2003).

It now appears that mechanisms exist to compartmentalise PTEN during chemotaxis and prevent it from disrupting complexes forming at the leading edge of the motile cell. Recent studies in mammalian leukocytes and the amoebae *D. discoideum* have shown that when sensing cAMP as a chemoattractant, PI3K localises to the leading edge of the cell where a PI3,4,5P3 gradient forms. This enhances signalling through Akt/PKB and directional movement, whilst PTEN is localised to the posterior away from the concentrated PI3,4,5P3.

Cells lacking PTEN show multiple, random pseudopodia and a lack of directional movement (Comer & Parent, 2002 & Iijima & Devreotes, 2002). The localisation mechanisms of PI3K and PTEN are currently under investigation. In *D. discoideum,* recent work suggests that activation of chemoattractant receptors provides G-protein-coupled binding sites on the cytosolic face of the plasma membrane which bind PI3Ks at the leading edge (Huang, et al 2003).

A study of chemotaxis in neutrophils concurred with the findings in *D. discoideum,* and described a mechanism for localising PTEN via the

cytoskeletal proteins PIXα (PAK-associated guanidine nucleotide exchange factor) and Cdc42. In this system, the two proteins direct F-actin formation at the leading edge, but PIXα actively repels PTEN (Zhong, et al 2003).

1.2.4.2 PTEN and Regulation of Pathways Other Than PI-3 kinase

MAPK Signalling

The MAP and ERK kinase pathways are activated in response to binding of cell surface receptors such as EGF, or the interaction of integrins with the extracellular matrix to control adhesion, growth and differentiation. The pathways are redundant and partake in complex cross-talk; a diagrammatic overview of MAPK/ERK is shown in Figure 5. The Shc adaptor couples receptor tyrosine kinases and associated receptors to these pathways, and is believed to be regulated by recruitment from the cytosol to the plasma membrane. Here, it binds Grb-2/Sos complexes and causes transfer of the guanine nucleotide exchange factor Sos to Ras, resulting in Ras activation (Plyte, et al 2000). Downstream of Ras are members of the Raf family which activate MAPKs/ERKs and/or JNK/SAPK to effect gene transcription.

PTEN has been shown to be involved in the MAP/ERK kinase pathway in several ways. Firstly, PTEN can act in a Shc-dependant manner, dephosphorylating this protein and inhibiting the formation of Grb-2/Sos complexes and thus activation of Ras (Gu, et al 1998). Secondly, PTEN can inhibit MAPK and ERK via Shc-independent mechanisms involving Gab1 and IRS. Gab1 contains a PH domain that interacts with PI3,4,5P3-rich membranes (Ong, et al 2001) via PI3K and the tyrosine phosphatase SHP2.

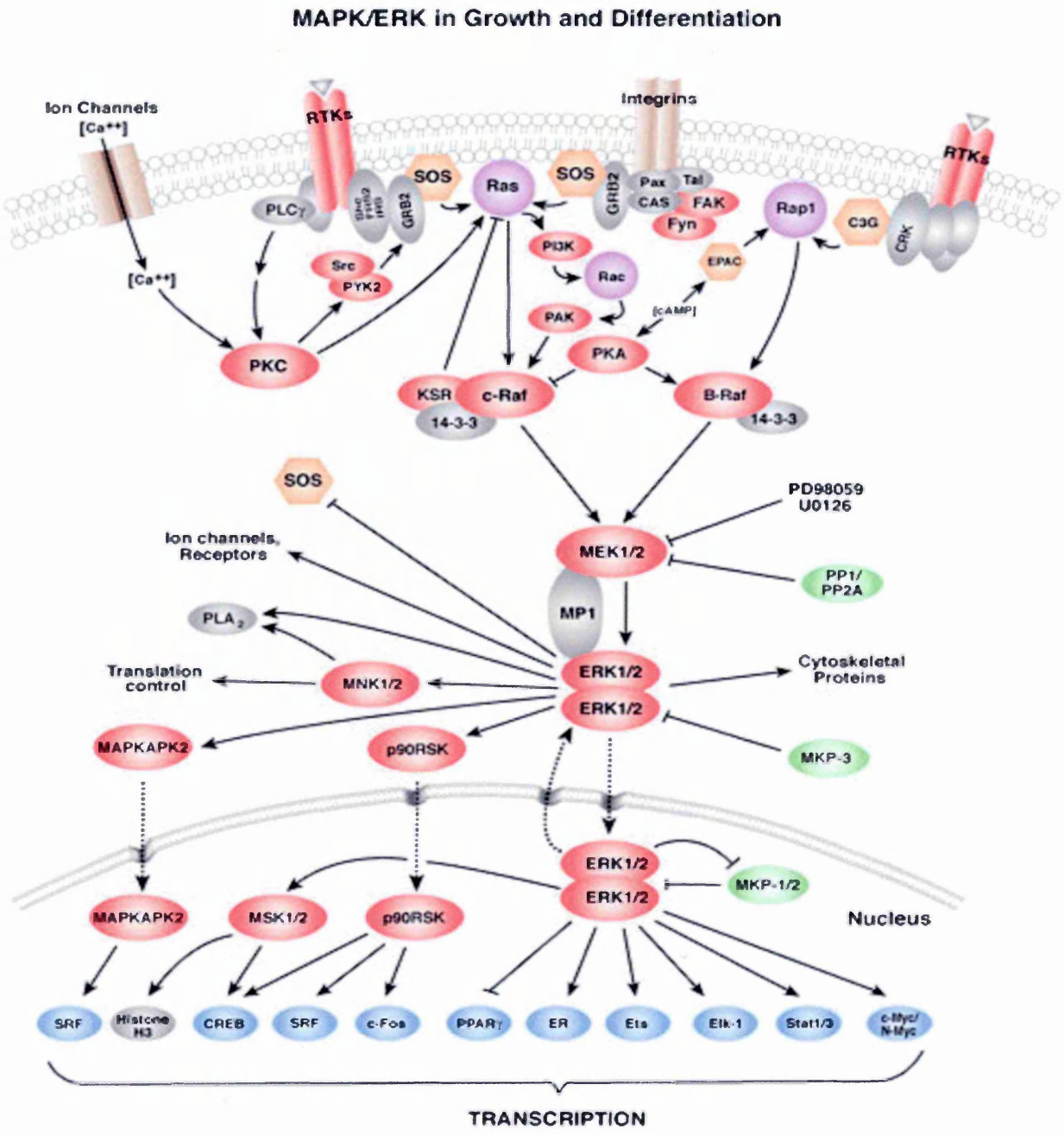

Figure 5 MAPK/ERK Pathways Taken from www.cellsignal .com

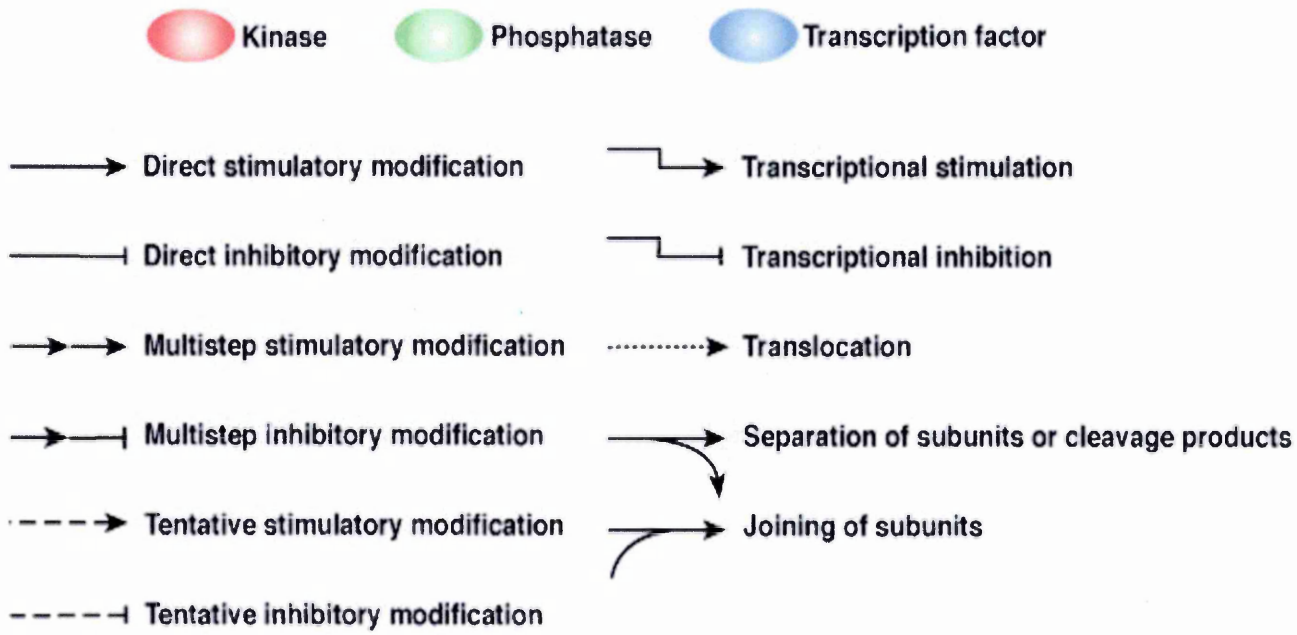

Figure 5 MAPK/ERK Pathways, Legend The MAPK/Erk signalling cascade is activated by a wide variety of receptors involved in growth and differentiation including receptor tyrosine kinases (RTKs), integrins, and ion channels. The specific components of the cascade vary greatly among different stimuli, but the architecture of the pathway usually includes a set of adaptors (Shc, Grb2, etc.) linking the receptor to a guanine nucleotide exchange factor (Sos, C3G, etc.) transducing the signal to small GTP binding proteins (Ras, Rap1), which in turn activate the core unit of the cascade composed of a MAPKKK (Raf), a MAPKK (MEK1/2) and MAPK (Erk). An activated Erk dimer can regulate targets in the cytosol and also translocate to the nucleus where it phosphorylates a variety of transcription factors regulating gene expression. Taken and modified from www.cellsignal .com

Dephosphorylation of PI3,4,5P3 could prevent Gab1 from interacting with SHP2, thus inhibiting MAPK activation (Yart, et al 2001). Recently, Gab1 decoys have been shown to inhibit EGF-induced ERK and Atk/PKB activation in tumour cell lines lacking functional PTEN (Ren & Wu, et al 2003).

Several groups have now reported that PTEN negatively regulates ERK-mediated signalling of estradiol in endometrial carcinoma (Zhang, et al 2003) and hepatoma cell lines (Marino, et al 2003), and that ERK may regulate PTEN levels. Binding of PDGF to its receptor activates both PI3-K and ERK/MAPK pathways. Work by Mahimainathan & Ghosh (2004) has demonstrated that PTEN binds directly to the cytosolic domain of the PDGF receptor through its C2 and C-terminal domains, causing dephosphorylation of the autophosphorylated tyrosine residues in the receptor. The group propose that PTEN may inactivate other receptors, such as for EGF, in this manner to regulate signalling in the absence of ligand binding.

A role for PTEN in negatively regulating BCR (B-cell antigen receptor)-mediated proliferation has recently been described (Brown, et al 2004). The low-affinity IgG receptor FcγRIIb, involved in immune regulation, is thought to recruit PTEN and the immune cell-restricted 5' inositol phosphatase SHIP (Kalesnikoff, et al 2003). PTEN converts PI3,4,5P3 to PI,4,5P2, whilst SHIP uncouples BCR from the GTPase Ras and converts PI3,4,5P3 to PI3,4P2, the overall effect being to prevent ERK/MAPK activation.

The involvement of PTEN in insulin signalling is well known, and it is believed that it may achieve attenuation of the pathway via direct dephosphorylation of IRS-1. This would prevent the formation of an IRS-1/Grb2/Sos complex and thus MAPK activation (Weng, et al 2001c & Yeon, et al 2003). Up-regulation

by PTEN of IRS-2, which is a component of insulin signalling, has also been observed (Simpson, et al, 2001). Work by Weng, et al (2003) has demonstrated that in MCF-7 breast cancer cells, PTEN can inhibit insulin-mediated signalling, but not EGF-mediated signalling, by blocking phosphorylation of the transcription factor ETS-2. This was shown to occur independently of PI3K via ERK/MAP kinases, and involved the protein phosphatase activity of PTEN. The apparent specificity of PTEN as a protein phosphatase for different receptor tyrosine kinases implies that the role of PTEN may be cell-type specific, and that therapeutic targeting of PI3K/Akt in some cancers may not be effective.

Hypoxia & Angiogenesis

Under 'normoxic' conditions, PTEN has been shown to downregulate hypoxia-inducible factor 1α (HIF-1α), normally expressed under low oxygen conditions or by EGF stimulation (Zhong, et al 2000 & Zundel, et al 2000). HIF-1α is a transcriptional activator of genes for glucose transporters, glycolytic enzymes and VEGF, the latter of which is commonly up-regulated in tumours and increases vascularisation. Recently, restoration of PTEN into glioma cells has shown that PTEN down-regulates HIF-1α and VEGF expression, with an increase in $p27^{Kip1}$ orchestrated via PI3K and not p38/MAPK (Gomez-Manzano, et al 2003 & Abe, et al 2003). Similar findings have been made in gastric carcinomas, where a lack of PTEN causes increased MMP-7 expression, (Zheng, et al 2003) which could synergise with VEGF to contribute to increased angiogenesis and invasiveness. Conversely, over-expression of wild-type PTEN in primary microvascular

endothelial cells stimulated with VEGF caused inhibition of angiogenesis (Cai, et al 2003). Interestingly, in cells lines with abnormally expressed pro-apoptotic Myc, which cannot activate p53 death genes (Bringold & Serrano, 2000), PTEN and HIF transcription were unaffected and hypoxia-induced death occurred by other mechanisms (Brunelle, et al 2003). It is now known that a close relationship exists between PTEN and p53, which will be discussed in Section 1.3.

Androgen Insensitivity

Androgen insensitivity is a feature of some prostate cancers, and it has been demonstrated that androgens can protect prostate cancer cells from PTEN-induced apoptosis via Akt/PKB (Li et al 2001). This is probably due to aberrant ligand binding and activation of the androgen receptor (AR), or activation via MAPK pathways (Ueda, et al 2002) which could explain why the AR is required for survival. Unsurprisingly, loss of functional PTEN could enhance AR signalling and progression to the androgen independent state (Nan, et al 2003). The exact mechanisms involved are controversial, but evidence exits for two Akt consensus sites, Ser213 and 791, in AR which Akt can phosphorylate to activate the receptor (Lin, et al 2001).

Antagonism of PI3K by PTEN therefore leads to negative regulation of AR signalling in an Akt-dependant manner (Sharma, et al 2002), and down-regulation of the AR co-activator β-catenin has also been observed in this model (Trucia, et al 2001). Another group have recently detected binding of FKHR/FOX01 to the NT region of AR which prevents transcription of pro-

apoptotic genes. As Akt/PKB can also inhibit FOXOs, this may represent multiple mechanisms by which prostate cancers survive (Li, et al 2003).

Inositol Phosphates and PTEN Substrate Specificity

It is accepted that inositol lipids and inositol phosphates have their own dedicated phosphatases and kinases, with little cross-over in substrate specificity. Until recently, PTEN was thought to exhibit negligible activity towards inositol phosphates and has been shown to be a poor 3' phosphatase towards inositol 1,3,4,5-tetrakisphosphate (Ins(1,3,4,5)P4) (Maehama & Dixon, 1999). Evidence was presented for the hydrolysis of inositol 1,3,4,5,6-pentakisphosphate (InsP5) by PTEN *in vitro* via its 3'-phosphatase activity to Ins(1,4,5,6)P4 (Caffrey, et al 2001). Ins(1,4,5,6)P4 is an antagonist of PI3,4,5P3 (Eckmann, et al 1997) and these substrates could theoretically compete for PTEN binding. Ins(1,4,5,6)P4 is also associated with transcriptional regulation (Odom, et al 2000), and Rho-GTPase activation (Zhou, D et al, 2001).

Work by Orchiston, et al (2003) suggest that wild-type PTEN, which is active against 3' phosphatidylinositol phospholipids, does not regulate inositol phospholipids *in vivo*. This group used a C2 domain mutant form of PTEN (M-CBR3) initially described by Lee, et al (1999). The mutant had little effect on 3'-phosphoinositide lipids, but selectively dephosphorylated InsP5. Decreased levels of InsP5 corresponded with a decrease in cell growth and anchorage-independence, suggesting that InsP5 acts as a proliferative agent of unknown physiological role.

1.3 Regulation of PTEN Expression

Despite the large amount of data regarding the role of PTEN in the control of various important pathways, detail regarding the regulation of mRNA and protein levels has only recently begun to emerge. Several mechanisms have been proposed for the regulation of PTEN expression, including transcriptional control via interaction with p53, PPARγ and Egr-1, promoter methylation (see Section 1.5) and modulation of protein expression by cytokines.

1.3.1 Transcriptional Control of PTEN mRNA

Interaction of the PTEN Promoter with p53

The tumour suppressor p53 is well-characterised and one of the most commonly mutated genes in cancer. The p53 protein acts as a transcription factor to induce growth arrest or apoptosis by up-regulating pro-apoptotic genes such as p21, and Bax. Activity of the p53 protein is regulated by a feedback loop with MDM2, which p53 up-regulates. MDM2 protein binds to p53, inhibits its transcriptional activity and causes nuclear exclusion and proteasome degradation (Freedman & Levine 1998). p53 can be inactivated by growth factors and hormones such as oestrogen, and expression of such stimulatory factors is often uncontrolled in tumours, as is the case in breast carcinomas (Molinari, et al 2000).

The discovery of a putative p53 binding site in the promoter of PTEN between -1190 and -1157 (Stambolic, et al 2001) indicated a possible transcriptional mechanism for PTEN regulation (see Figure 2). This group reported transactivation of PTEN by p53 via transfection into the PTEN-null

U87-MG glioblastoma cell line, and defined the region between -1001 and -427 as a positive regulatory element which drives constitutive PTEN expression. Both mRNA and protein levels of PTEN were significantly increased. Analysis of p53-mediated apoptosis revealed that the p53 binding sites in the PTEN promoter were essential for efficient p53-mediated cell death, and a lack of functional PTEN inhibited this process (Mayo & Donner, 2002).

Recent evidence of decreased PTEN expression in p53-/- mice supports the idea that p53 up-regulates PTEN (Hesselager, et al 2003) and that p53 and PTEN proteins can physically bind *in vivo* and *in vitro* to regulate PI3K signalling and also to protect p53 from MDM2-mediated degradation (Zhou, et al 2003). Moreover, the PI3K inhibitor LY294002 was shown to synergise with introduction of exogenous PTEN into U87-MG cells to transactivate p53 expression and its target genes $p21^{Waf-1}$ and IGFBP3 (Su, et al 2003).

The requirement of both PTEN and p53 for effective suppression of tumours has been reinforced by work using irradiated mice. Here, PTEN heterozygotes were just as sensitive to irradiation and lymphoma development as p53 heterozygotes, suggesting that the two genes are complementary (Mao, et al 2003).

The hepatitis B virus X protein (HBx), which is involved in hepatocellular carcinoma, has been shown to interfere with p53 binding to its binding site on the PTEN promoter and thus down-regulates PTEN transcription (Chung, et al 2003). Hepatitis B infection may therefore promote tumourigenesis via inhibition of PTEN through decreased p53 transactivation, and the resulting downstream activation of Akt/PKB.

PPARγ

The nuclear receptor peroxisome proliferator-activated receptor gamma (PPARγ) is a transcription co-factor that has been shown to regulate differentiation and/or cell growth in a number of cell types (Chen, et al 2003a). It acts as an anti-inflammatory mediator and may also act as a tumour suppressor, and is a therapeutic target for type-II diabetes. Patel, et al (2001) demonstrated that the PPARγ ligand rosiglitazone (an insulin-sensitising drug) upregulates PTEN expression in human macrophages, MCF7 breast cancer cells and Caco2 colorectal cancer cells, and decreases Akt/PKB phosphorylation. Two PPARγ binding elements were identified in the PTEN promoter at positions –15376 and –13339bp upstream of the PTEN transcription start site (assigned at -1035 relative to the translational start site).

Other groups have shown PPARγ-mediated up-regulation of PTEN in pancreatic tumour cell lines (Farrow & Evers, 2003), and vascular endothelial cells (Goetze, et al 2002). These results suggest that PTEN up-regulation may be one mechanism by which PPARγ agonists ameliorate inflammation and tumourigenic processes. One problem with this is that PPARγ agonists, such as rosiglitazone, are used successfully to treat type II diabetes (Poulsen, et al 2003), which logically could cause potentially harmful elevation of PTEN. However, as PTEN also up-regulates IRS-2 which leads to an insulin-mediated increase in Akt/PKB activity (Simpson, et al 2001), PPARγ agonists would be beneficial in this disease.

Egr-1

The immediate-early *Egr-1* is a transcription factor that is known to respond to the breast cancer mitogen insulin-like growth factor II (IGF-II) via IRS-1 (Tsuruzoe, at al 2001), and up-regulates the IGF-II promoter in response to hypoxia (Bae, et al 1999). Work by Virolle, et al (2001) identified a functional *Egr-1*-binding site (GCGGCGGCG) in the PTEN 5' untranslated region between positions –947 and –939, which up-regulated PTEN transcription in response to irradiation in mice. Moorehead, et al (2003) demonstrated induction of PTEN transcription via *Egr-1* in developing mammary cells stimulated with IGF-II, but not in mammary cells undergoing involution (Moorehead, et al (2001). The differences in response seen between developing and involuting mammary cells may reflect the divergent hormonal exposure of the cells. Moorehead, et al (2003) also proposes that the induction of PTEN could involve a regulatory loop where IGF-II signals through *Egr-1* to induce PTEN, and then *Egr-1* also induces IGF-II.

TGF-β1

Transforming growth factor-β1 is a pleiotropic cytokine which is capable of exerting a huge range of cellular effects, including proliferation, differentiation and apoptosis. Several papers have reported modulation of expression of PTEN by TGF-β1, but the data is conflicting. Li & Sun, (1997) first described rapid down-regulation of PTEN (TEP1) mRNA by TGF-β1 in a responsive asynchronously growing HaCaT keratinocyte cell line. A second group have also demonstrated PTEN mRNA down-regulation in pancreatic adenocarcinomas over-expressing TGF-β1 and synchronous (serum-starved)

cell lines treated with TGF-β1 (Ebert, et al 2002). These two reports concluded that a reduction in PTEN may impart a growth advantage under TGF-β1 stimulation, and may contribute to aggressiveness in the pancreatic study.

A third report, however, described the up-regulation of PTEN mRNA in a synchronous U937 monoblastic leukaemia cell line in response to TGF-β1 (Lee, et al 1999b). The study also found up-regulation of anti-apoptotic Bcl-XL and resistance to Fas-mediated apoptosis. These apparently contradictory findings could be due to various factors, including cell type, dose of cytokine, and incubation times and conditions of growth. In light of current understanding, the results presented by (Lee, at al 1999) may be explained by the inhibition of PTEN protein by one or more of the various mechanisms previously described.

The TGF-β superfamily contains over 30 members with three isoforms, β1, 2 and 3, but only TGF-β1 will be discussed here. TGFβ isoforms signal through ser/thr kinase receptors type I and II (TβRI and II). Binding of TGF to the constitutively active TβRII initiates recruitment of the receptor/ligand to TβRI and transphosphorylation of TβRI at its GS-box (juxtamembrane gly/ser-rich region). This creates a binding site for Smads, the signal transducing elements of TGFβ which are activated by phosphorylation of their C-termini, and the internalisation of the receptor into endosomes for recycling.

Eight vertebrate Smads have been identified. These include receptor-activated Smads (R-Smads) Smad2 and 3 for the TGF-beta/activin pathway, or Smad1/5/8 for the bone morphogenetic pathway, (BMP). C-terminal phosphorylation of Smads by activated receptors results in their binding to

the common signalling transducer (Co-Smad) Smad4 and translocation to the nucleus. The R-Smads also compete for binding to TβRI with inhibitory Smads (I-Smads) Smad 6 and 7 (Attisano & Lee-Hoeflich, 2001).

The Smads have a conserved, modular structure composed of MH1, linker and MH2 domains. The MH1 domain contains a DNA-binding motif, an NLS and regions for binding transcription factors such as ATF-2, c-Jun/Fos, Forkheads and Sp1 (Shi, et al 2003). The linker contains consensus sites for MAPK phosphorylation, which causes sequestration of R-Smads to the cytoplasm and prevents nuclear translocation, for example the R-Smad1 is phosphorylated by ERK (Kretzschmar, et al 1999). In both R- and I-Smads this region also contains sites recognised by E3 ubiquitin ligases Smurf1 and 2 for degradation, and in the Co-Smad4 the linker has an additional nuclear export signal (NES).

The MH2 domain mediates many protein-protein interactions including Smad-receptor association and the formation of Smad homo- and heteromeric complexes consisting of up to six units. For example, Smads 2,3, and 4 are required as a complex to effect transcription of the CDK $p15^{INK4B}$ via SP1 transcription factor (Li, et al 1995 & Feng, et al (2000). These complexes are thought to permit differential signalling thresholds to act on target gene expression.

Phosphorylated Smads are released from microtubules (Dong, et al 2000), and inhibitory I-Smads, and bind to endosomes containing transport proteins (Di Guglielmo, et al 2003), all of which increase Smad activation (Lutz and Knaus, 2002). Association with Smad4 and other R-Smads follows, and the complexes translocate to the nucleus via their NLS. Here, many genes are

activated as previously mentioned, but others are repressed to inhibit cell cycle progression, such as c-myc (Chen, et al (2002). An overview of TGF-β1 signalling through Smads in shown in Figure 6.

TGF-β Signaling Pathway

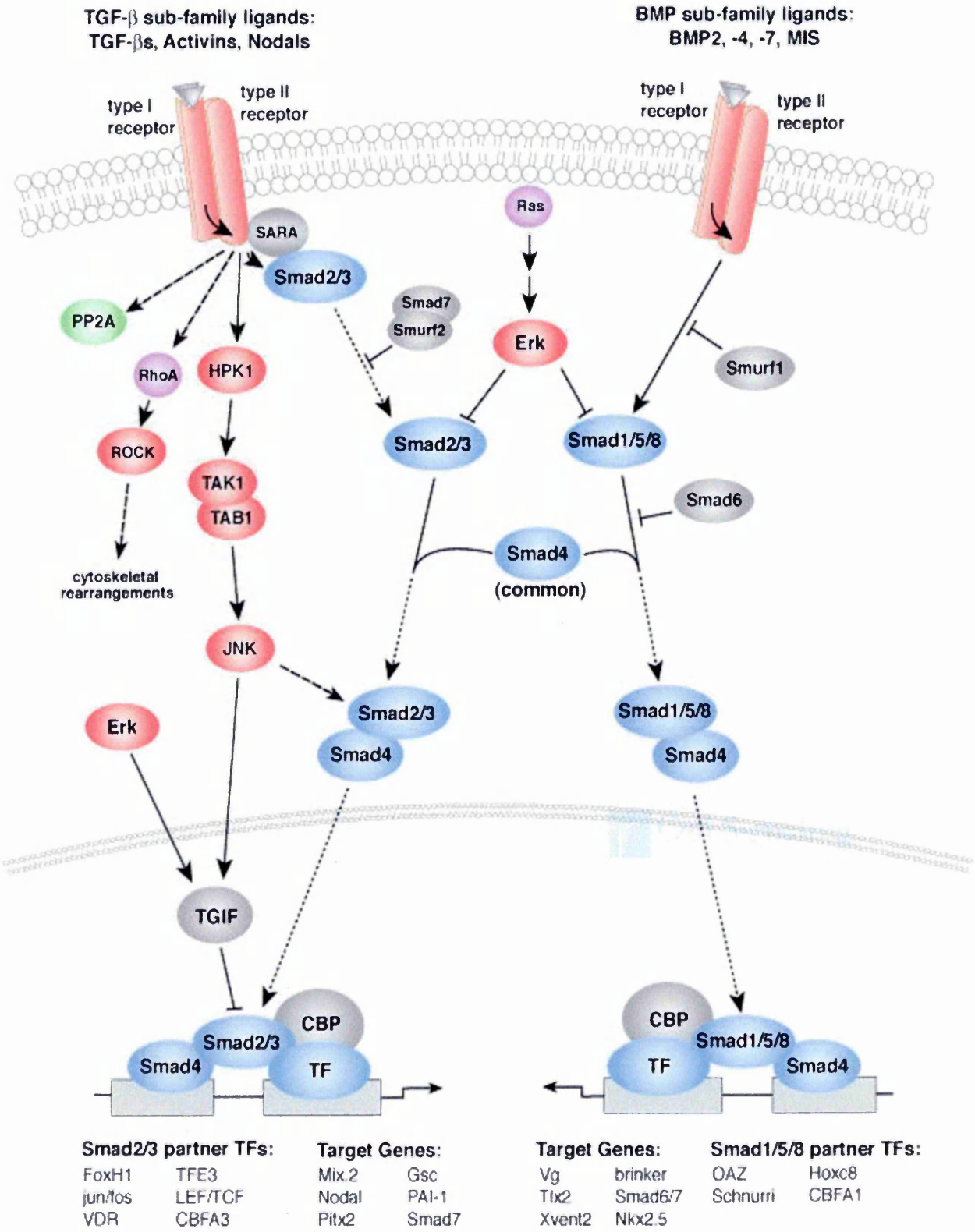

Figure 6 TGFβ1 Signalling to the Nucleus

Figure legends are overleaf. Taken from www.cellsignal.com

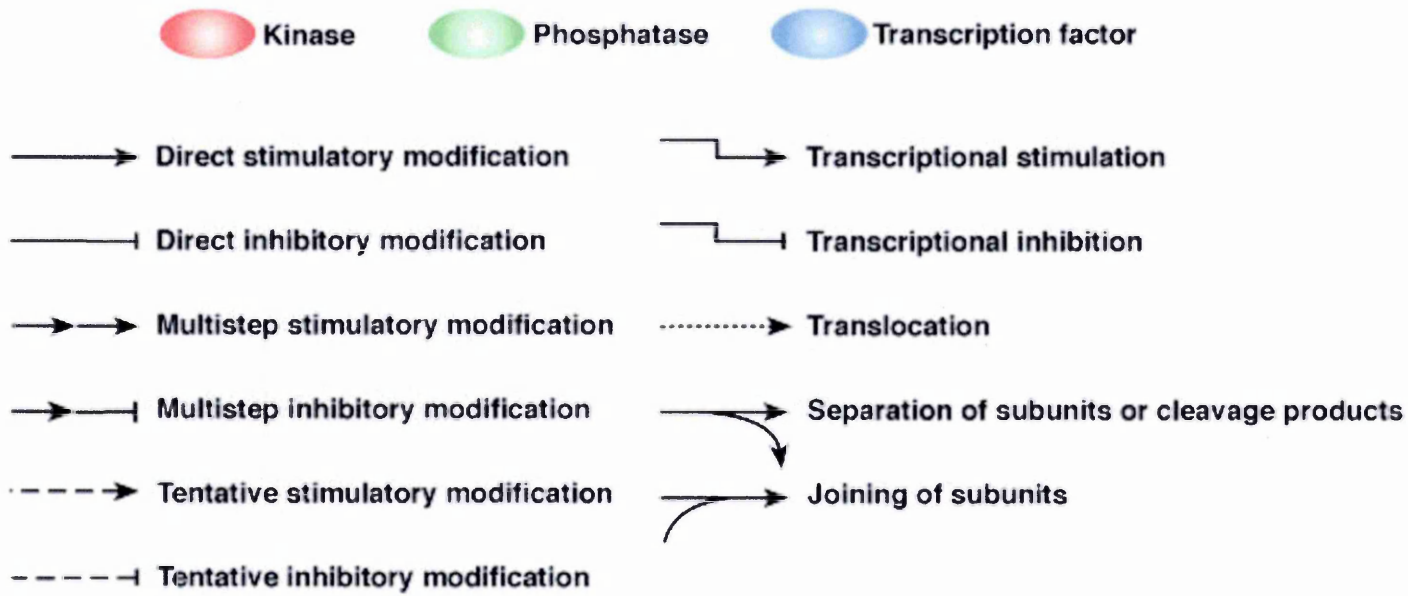

Figure 6 TGFβ1 Signalling to the Nucleus, Legend TGF-β signalling is initiated with ligand-induced oligomerization of ser/thr receptor kinases and phosphorylation of the cytoplasmic signalling molecules Smad2 and 3 for the TGF-beta/activin pathway, or Smad1/5/8 for the bone morphogenetic pathway, (BMP). C-terminal phosphorylation of Smads by activated receptors results in their binding to the common signalling transducer Smad4 and translocation to the nucleus. Activated Smads regulate diverse biological effects by partnering with transcription factors resulting in cell-state specific modulation of transcription. The activin and BMP pathways are attenuated by MAPK signalling at a number of levels, while the expression of inhibitory, or I-Smads 6 and 7 is induced by both activin/TGF-β and BMP signalling as part of a negative feed-back route. Modified from www.cellsignaling.com

In addition to the traditional Smad-dependant signalling, TGF-β1 also activates p38 MAPK/ERK/JNK pathways which are able to regulate Smads themselves. However, the activation-response kinetics are too rapid to be Smad-dependent, suggesting an alternative mechanism (Massague, 2000). Activation of Ras by TGF-β1 by has been observed in induction of ERK/MAPK (Yue, & Mulder, 2001), and the TGFβ-activated kinase-1 (TAK1) is a MAPKKK that can activate both p38MAPK and JNK (Dowdy, et al 2003). TAK1 can also activate anti-apoptotic NF-κB by phosphorylating IκB, thus TGF-β1 may also be involved in NF-κB-mediate responses (Bhat, et al 2003). Work by Vasudevan, et al (2004) has demonstrated that NF-κB is capable of inhibiting PTEN transcription through its p65 subunit by sequestering the transcriptional co-activators CBP/p300. Thus, during pro-apoptotic TNF stimulus, NF-κB can prevent apoptosis by down-regulating mRNA and protein levels of PTEN.

Other pathways may be activated in a cell-type specific manner. These include Cdc42 and Rac, also involved in MAPK and cytoskeletal arrangement, and Rho-like small GTPases which may effect gene expression responses (Derynck & Zhang, 2003). Additionally, TGF-β1 can down-regulate Rb and a variety of associated CDKs and cyclins to cause G1 arrest (Hu, et al 2001 & Bhowmick, et al 2003).

TGF-β1 has also been widely implicated in cancer, but its involvement is complex. During the early stages of tumourigenesis, the cytokine acts to suppress tumour formation via its cell-cycle restrictive functions detailed above. However, during neoplastic change, many tumours show progressive lack of responsiveness to growth inhibition by TGF-β1 and actually produce

large amounts of the protein (Boyd & Kaufman, 1990 & Lei, et al 2002). This seems to provide autocrine stimulus to the cells which increases angiogenesis and motility, via up-regulation of plasminogen activator inhibitor-1 (PAI-1) (Kutz, et al (2001) and has an immunosuppressive effect (Reiss, 1999).

Tumours may display mutant TGF receptors which signal in an aberrant manner, most commonly in TβRII, (Oft, et al 1998, Heldin, et al 1999 & Waite & Eng, 2003) and/or Smads, have reduced levels of the CDK inhibitors such as $p27^{Kip1}$, increased MDM2 which inactivates p53 (Gold, 1999) and increased cyclin D1 (Kornmann, et al 1999). Steroid hormones such as oestrogen are also implicated in abnormal TGF-β1 signalling, and have been shown to down-regulate TβRII and allow ovarian cancer cells to evade TGF-β1-mediated growth suppression (Evangelou, et al, 2000 & Frasor, et al 2003).

Of particular relevance to this thesis, TGF-β1 has been shown to activate PI3K through Smad2 (Bakin, et al 2000), ERK/MAPK (Lhuillier & Dryer, 2003) and may invoke EGF receptor activation, (Vinals & Pouyssegur 2001).

1.3.2 Post-Translational Modulation of PTEN Protein Expression

Progesterone & oestrogen

The high incidence of PTEN loss or mutation in some cancers, and in particular endometrial carcinomas (see Section 1.5), has indicated that steroid hormones could play a role in PTEN regulation. Studies on PTEN expression in the endometrium, which undergoes complex morphological changes in response to cyclic levels of oestrogen and progesterone, have

shown that these hormones do indeed regulate PTEN mRNA and protein expression levels.

Mutter, et al (2000) demonstrated that levels of PTEN mRNA in endometrial cells were higher during the post-ovulatory secretory phase compared to the proliferative phase of the menstrual cycle. The secretory phase has a high progesterone level whilst the proliferative phase is dominated by oestrogens, suggesting that progesterone is responsible for changes in PTEN levels. The protein levels and localisation were more complex and cell-type specific. Oestrogen-driven dividing epithelial and stromal cells were seen to have nuclear and cytoplasmic protein, with increased nuclear localisation during decidualisation and menstrual apoptosis. During the secretory phase, progesterone levels rise which caused epithelial cells to lose PTEN protein whereas stromal cell levels increased, particularly in the cytoplasm.

An investigation into PTEN expression in the endometrium was made in the light of the current evidence for PTEN protein regulatory mechanisms. Guzeloglu-Kayisli, et al (2003) have described PTEN expression in the menstrual cycle and early pregnancy consistent with the work of Mutter, et al (2000). This group showed that estradiol increased phospho-PTEN after 5-15 minutes of treatment in stromal cells, which could account for the observation that during the proliferative phase these cells are resistant to apoptosis. Additionally, the oestrogen receptor-α is activated by CK2 which inactivates PTEN, providing an additional feedback mechanism for increased oestrogen signalling and PTEN down-regulation. Progesterone increased PTEN protein levels after 24 hours in stromal and glandular cells, and in decidual and glandular cells during pregnancy.

This suggests that this hormone may dephosphorylate PTEN and increase protein activity levels in a long-term manner, to cause the increase in apoptosis observed in these cells. In conclusion, Guzeloglu-Kayisli, et al 2003 proposed that the two steroid hormones may target PTEN to affect the concentration and spatial localisation of the protein in different endometrial compartments.

Other Positive Modulators of PTEN Protein Expression

Several additional factors have also demonstrated the ability to up-regulate PTEN expression, these being a vitamin D3 analogue, nerve growth factor (NGF), brain-derived neurotrophic factor (BDNF) and bone morphogenetic protein (BMP).

Vitamin D3 Analogues

Vitamin D3 is a secosteroidal hormone involved in bone metabolism, which is also capable of inhibiting proliferation and inducing differentiation in tumours of diverse origin (Banerjee & Chatterjee, 2003). The growth inhibition effects of this molecule are thought to be via G_0/G_1 arrest and up-regulation of CDK inhibitors such as $p27^{KIP1}$, $p21^{Waf1}$ and induction of p53 and apoptosis (Yang & Burnstein, 2003, Audo, et al 2003 & Flanagan, et al 2003). Despite its efficacy against tumours, it is of little clinical use as at the doses required for effectiveness a side effect of treatment is calceamia (Kensler, et al 2000). Novel D3 analogues have been designed to be anti-proliferative without the dangerous side effects (Chen, et al 2003b).

The novel D3 analogue Gemini-19-nor was shown to be more potent in mediating growth, G_0/G_1 arrest and $p27^{KIP1}$ expression, apoptosis and differentiation than vitamin D3 in leukaemic, breast and prostate cancer cell lines. Interestingly HL-60 myeloid leukaemic cells, which are wild-type for PTEN, also demonstrated up-regulation of PTEN protein during Gemini-19-nor -induced differentiation (Hisatake, et al 2001). This group also showed up-regulation of PTEN in HL-60 cells treated with the phorbol diester TPA and all-*trans*-retinoic acid (ATRA), which induced macrophage-like or granulocyte-like differentiation respectively in this cell line.

These results suggest that PTEN is involved in myeloid differentiation, and may indicate that vitamin D3 analogues are a potential therapy for myeloid leukaemias. Another D3 analogue, Seocalcitol (EB1089), has been shown to inhibit the growth of aggressive pituitary tumours without increasing PTEN expression (Liu, et al 2002), highlighting the cell-type specificity of PTEN involvement.

NGF & BDNF

It has been reported that NGF, which stimulates neurite extension, upregulates PTEN mRNA levels in rat neuronal pheochromocytoma PC12 cells (Li & Sun, 1997). An increase in PTEN protein has also been observed in the same cell line stimulated with NGF (Lachyankar, et al 2000). This group also demonstrated increased PTEN protein in immature and mature mouse CNS stem cells during BDNF-induced differentiation. PTEN protein could only be detected weakly in immature astrocytic cells and was absent in mature astrocytes. This indicates that PTEN plays a role in neural

development and the extension of neurites, and that perhaps the absence of PTEN in glial precursors (astrocytes) is important for glioma development.

Bone morphogenetic protein (BMP).

BMP signals through the TGFβ-family receptor BMPR1A, and mutations in this receptor have been noted in patients with Cowden disease, a proliferative disorder associated with PTEN mutation (see Section 1.4). Recently, Waite & Eng, (2003b) demonstrated up-regulation of PTEN protein in MCF-7 breast cancer cells stimulated with BMP2. The increase in PTEN protein was due to inhibition of degradation, through inhibition of association of PTEN with ubiquitin-conjugating enzymes UbCH7 and UbC9.

1.4 PTEN and Disease

It is now apparent that mutation or loss of PTEN is a feature of many malignant and non-malignant human proliferative disorders, ranging from aggressive carcinomas to benign hamartomas. Aberrations in genomic PTEN contribute to tumourigenic phenotypes in a cell-type specific manner and may be germ-line or somatic. The incidence of PTEN mutation or loss is strikingly high for some cancers, notably endometrial, but almost absent from haematological malignancies. The current understanding of the contribution of PTEN mutation or loss in human proliferative diseases is discussed below.

1.4.1 Germline Mutations

PTEN Hamartoma-Tumour Syndrome (PHTS)

PHTS broadly identifies several related autosomal dominant disorders

resulting from germline PTEN mutations, which display overlapping phenotypes. Diagnosis can be problematic as the disorders can share both phenotypic features and identical PTEN mutations. It is likely that individual genotypes, with loss or mutation of other disease-related genes, contribute to this lack of distinction, as a small number of patients do not have PTEN mutations (Merks, et al 2003 & Waite & Eng, 2002). The four main disorders, Cowden disease (CD), Bannayan-Ruvalcaba-Rily syndrome (BRRS), Lhermitte-Duclos disease (LDD), and Proteus syndrome (PS) are described below.

Cowden Disease (CD)

CD is associated with a susceptibility to breast and thyroid cancers, increasing the risk of breast cancer in affected females to 25-50% and lowering the age of tumour development by approximately 10 years from the population average. Affected individuals commonly display hamartomas, or mucocutaneous lesions (papillomas and trichilemmomas), carcinomas of breast, thyroid follicular carcinoma and macrocephaly.

Approximately 10-50% of CD cases are familial, but the true figures are unknown due to underdiagnosis. Up to 80% of CD cases contain a germline mutation of PTEN, and mutation of PTEN correlates with tumour aggressiveness (Zhou, et al 2003b & Marsh, et al 1998). Many such mutations in the PTEN gene have been described, and ~65% of these appear to affect the first 5 exons coding for the phosphatase domain and the promoter region (Eng, 2003).

In a murine model developed by Podyspanina, et al (1999), mice containing a deletion in exon 5 developed neoplasms in multiple organs reminiscent of CD and BRRS . Cases of CS without intragenic PTEN mutation could be due to mutations in BMPR1A (Waite & Eng 2003b), or promoter mutation which has been detected in ~10% of samples (Zhou, et al 2003b).

Bannayan-Ruvalcaba-Rily syndrome (BRRS)

This familial disorder is characterised by lipomatosis, speckled penis, hemanigiomatosis and macrocephaly, and ~60% of patients harbour a germline PTEN mutation (Hendriks, et al 2003) Such mutations occur in the four exons at the 3' region of the gene which mainly encode the C2 domain (Eng, 2003). Deletion and translocation of PTEN have also been described in some cases (Marsh, et al 1999 & Ahmed, et al 1999). Once again, BRRS patients with PTEN mutations are more likely to develop breast cancers, and BRRS and CS are now regarded as phenotypic variations of the same syndrome. The causes of the remaining ~40% of BRRS cases without PTEN mutation are unknown (Dahia, 2000), but PTEN deletion has been detected in ~11% of these cases (Zhou, et al 2003b).

Lhermitte-Duclos Disease (LDD)

LDD is regarded as a neurological manifestation of CD, and is characterised by hamartomatous overgrowth of cerebellar ganglion cells, which replace granular and Purkinje cells (Vantomme, et al 2001). Patients suffer ataxia and seizures due to increased intracranial pressure, and PTEN haploinsufficiency is sufficient to mimic these symptoms in mice (Li, et al

(2003b). LDD is usually sporadic rather than familial, but it is unclear as to how PTEN mutations contribute to this disease, which has only recently been recognised as part of PHTS.

Zhou, et al (2003b), presented data suggesting a high incidence (83%) of adult-onset LDD cases had germline mutations in PTEN, resulting in little or no protein expression in 75% of the samples which also had elevated P-Akt. They also propose that LDD in children and adults have distinct underlying causes, as very few children diagnosed with the disease carry PTEN mutations. The majority of somatic PTEN mutations in LDD are truncating (Koch, et al 1999), but there have been reports of germline mutations in exon 5 more usually seen in CD patients, which reduce phosphatase activity (Sutphen, et al 1999 & Robinson & Cohen, 2000).

Proteus Syndrome (PS)

PS, like LDD, has only recently been included under the PHTS grouping and is a rare sporadic, hamartomatous disorder of vascular, skeletal, and soft tissues with mosaic distribution. Patients can present with asymmetry of the skull, body, limbs and partial gigantism of the hands or feet, hypertrophy of long bones, haemangiomas, lipomas, macrocephaly, and focal growths of the skin and vascular tissues (Bilkay, et al 2003). PS-like (PSL) cases show less pronounced symptoms, and are more stable with less sporadic outbreaks of abnormal growth (Zhou, et al 2000b). Up to 20% of PS cases and 50% of PSL cases harbour germline PTEN mutations (Eng, 2003). Mutations unique to PS, which are not seen in CD, BRRS or LDD are W211R and C211X, and in PSL the mutation M35T (Zhou, et al 2001c).

As previously mentioned, the various phenotypes of PHTS diseases can arise from the same PTEN mutations. Common mutations in CD, BRRS and PS are Q110X, R130X, R233X, R335X, (CpG dinucleotides in the phosphatase domain) and P246L (C2 domain), emphasising the importance of these regions for PTEN function. Mutations in the CpG islands could possibly increase promoter silencing by methylation, and in the C2 domain mutations can have profound effects on the stability of PTEN protein, as previously described.

1.4.2 Somatic Mutations

Over 300 somatic mutations of PTEN have now been described in various types of tumour, including endometrium, breast, prostate and melanomas. ~ 70% of mutations in PTEN are frameshift, missense or splice mutations which truncate the protein. Approximately half of the ~100 missense mutations, or ~23% of all mutations, are found in the exon 5 phosphatase domain and may affect activity. Additionally, the structural abnormality known as loss of heterozygosity (LOH), where mutations in one allele lead to the deletion of the other, has been detected in ~90% of tumours. LOH is difficult to accurately detect, therefore this figure may not be truly representative (Bonneau & Longy, 2000).

Glioblastoma (GB)

PTEN mutations have been described in several neurological tumours as a late event which correlates with tumour progression and aggressiveness (Davies, et al 1999b) rather that predisposition (Sanson, et al 1999).

Glioblastoma (GB) is the most common and most malignant form of astrocytic tumour in adults, with a survival rate of <1 year (Reis, et al 2000). Loss of PTEN is seen in ~20-30% of primary tumours (Kato, et al 2000, Zhou, et al 1999 & Backlund, et al 2003) and is often accompanied by amplification of EGFR and aberrations in the Rb1 pathway and p53 (Reis, et al, 2000). LOH and promoter methylation have also been observed in GB (Baeza, et al 2003).

The molecular mechanisms underlying this disease remain elusive, but it has been proposed that mutations in EGFR and p53 are very early events, and that disruption of the Rb1 pathway (e.g., pRb, CDK4), in conjunction with "second hit" loss of PTEN may be progression factors. This could provide a diagnostic tool for the early detection and treatment of this disease (Backlund, et al 2003, Krex, et al, 2003). Studies in PTEN knockout mice suggest that inhibitors of mTOR, a downstream target of Akt/PKB, correct abnormal growth and could be useful in the treatment of LDD and glioblastoma (Kwon, et al 2003).

Together with the phenotypes observed in LDD and various murine models, the crucial role of PTEN in the development of the CNS has been highlighted (Di Christofano, et al 1998). Expression of PTEN protein in human foetuses has been observed to be the highest in the central and peripheral nervous systems, and with less intensity in adult brains (Gimm, et al 2000b). PTEN appears to be important for orchestrating brain architecture, cell size and migration, and has a much more important role in the development and maintenance of this organ than previously thought (Li, et al 2003).

Prostate Cancer

As in GB, PTEN mutation is a late event in prostate cancer which correlates to increasing grade of the tumour. Abnormal PTEN has been observed in ~15% of primary tumours and ~60% of advanced prostate cancers, with a high LOH frequency of ~40% being related to metastatic potential (Fernandez & Eng, 2002 & Deocampo, et al 2003). Low expression of the CDKI p27 is also indicative of aggressiveness and poor outcome (Halvorsen, et al 2003). It is believed that promoter hypermethylation is more important in this cancer, and there have been many reports of PTEN silencing in prostate tumours (Whang, et al, 1998 & Rennie & Nelson, 1999). Additionally, as prostate cancers frequently display androgen independence (See Section 1.2.4.2), loss of PTEN function may facilitate the activation of AR signalling and progression to this state in prostate cancer (Snabboon, et al 2003).

A recently developed murine model of the precancerous prostatic intraepithelial neoplasia (PIN) may be useful in the further elucidation of the molecular mechanisms in prostate carcinoma (Abate-Shen, et al 2003). The mouse model carries a heterozygous mutation in the *NKX3.1* prostate-specific homeobox gene which is deleted in ~80% of early lesions. Heterozygous loss of PTEN in this model leads to androgen independence, invasiveness and metastasis also observed in advanced prostate adenocarcinoma.

Malignant Melanoma

Frequent PTEN mutations have also been described in ~30% of late-stage malignant melanomas (Guldberg, et al 1997)and up to ~60% in advanced metastatic disease (Birck, et al 2000) , but PTEN loss again appears to be

absent in early tumours (Poetsch, et al 2001). LOH of the PTEN locus is also very common in advanced melanomas, affecting of 30-50% of tumours and is associated with poor prognosis (Robertson, et al 1998 & Healy, et al 1998).

Breast Cancer

Primary sporadic carcinomas of the breast also harbour PTEN mutation, but at a much lower level of <5% compared to the cancers listed above (Rhei, et al 1997), and is therefore not implicated in the early stages of this disease (Ueda, et al 1998). LOH is observed in ~40% of invasive carcinomas in conjunction with loss of oestrogen receptors and increasing tumour grade (Bose, et al 1998). PTEN does not appear to be involved in inheritable breast cancer unless Cowden disease is also present, where it causes a predisposition to early-onset breast cancer (Mincey, 2003 & Carroll, et al, 1999).

More recently, loss of protein expression has been studied by several groups. Decreased or lack of PTEN was observed in ~38-50% of metastatic tumours, and also correlated with loss of oestrogen receptors and invasiveness (Depowski, et al 2001 & Bose, et al 2002).

In primary advanced breast adenocarcinoma, ~33% of tumours had decreased or no PTEN protein with LOH (Perren, et al (1999). The evidence indicates that PTEN loss is a late event in breast carcinogenesis which correlates with increased progression (Bose, et al 2002), and mutation in other genes such as p53 and BRCA1/2 (Kurose, et al 2002 & Buchholz, et al 2002). Constitutive activation of erbB2 autocrine signalling and increased P-Akt/PKB has been observed in breast cancer cell lines negative for PTEN,

and may be one mechanism promoting progression in these cells (Nicholson, et al 2003).

Endometrial Carcinoma (EC)

Endometrial cancers are the most common gynaecological malignancy affecting ~188,000 females worldwide per year (WHO, 2003), and are now recognised as having the highest rate of somatic PTEN mutation (Tashiro, et al 1997). Endometrial carcinomas (EC) display ~30-50%, adenocarcinomas (EAC) 50-85% and ~20% of the precursor lesion endometrial hyperplasia (EH) exhibit PTEN mutations. The figures for EAC represent the highest PTEN mutation rate in primary tumours, with all the mutations being in tumours of the endometrioid (Type I) variety which accounts for 80-90% of all ECs (Mutter, et al 2000). The predisposition to EC via PTEN mutation has been demonstrated in knockout mice, which develop atypical hyperplasia, the endometrioid precursor to EC (Podyspanina, et al 1999).

Mutation of PTEN appears to be an early event in EC, as aberration in the gene can be detected in early hyperplasias, (Levine, et al 1998), and such mutations may provide a diagnostic marker for the disease (Mutter, at al 2000, Gao, et al 2003b & Ricci, et al 2003). PTEN loss and Akt phosphorylation are indicative of poor prognosis, and survival rates are lower in patients who are immunohistochemically PTEN-negative (Terakawa, et al 2003). LOH at the PTEN locus has also been reported to be present in ~20-50% of advanced endometrial carcinomas, and may indicate progression of the disease (Tsuda, et al 2002 & Toda, et al 2001). The current mutational spectra for PTEN in EC is shown in Table 2.

Some correlation has also recently been reported between the amplification of the oncogene cMYC and PTEN mutation in early and advanced EC. In $PTEN^{+}/cMYC^{-}$ tumours, PTEN mutations were most frequent in exons 1-5, and less frequent in exons 7-8 (66.7% and 33.3%, respectively). In contrast, in $PTEN^{+}/cMYC^{+}$ carcinomas the PTEN mutations were found mainly in exons 7-8 (85.7%). The group implicate subtle genetic variations and interaction with different PTEN mutations for the different subsets of EC (Konopka, et al 2003).

Table 2 Mutation Spectrum of PTEN in Endometrial Cancers					
Exon/Intron	Nucleotide Exchange	Mutation	Protein/mRNA Change	2nd Mutation	Histology
E1	c.36insA	Frameshift	Stop at 43	No LOH	EC
E1	c.37delA	Frameshift	Stop at 23	?	EC
E1	c.37A-->G	Missense	K37Q	?	ECIII
E1	c.45ins T	Frameshift	Stop at 43	?	EC
E1	c.49C-->T	Nonsense	Q17X	LOH	EC
E1	c.54delGGAT	Frameshift	Stop at 23	Dble Mut	EC
E1	c.59G-->A	Missense	G20E	LOH	EC
E1	c.70G-->A	Missense	D24N	LOH	EC
E1	c.70insC	Frameshift	Stop at 43	LOH	EC
E1	c.76A-->C	Missense	T76P	?	ECIII
E2	c.80delAT	Frameshift	Stop at 42	?	EC
E2	c.89delC	Frameshift	Stop at 53	?	EC
E2	c.94delATT	In-Frame Del	I32del	Dble Mut	EC
E2	c.95delT	Frameshift	Stop at 53	MIN	EC
E2	c.96delT	Frameshift	Stop at 53	?	EC
E2	c.97del3	In-Frame Del	I33del	LOH	EC
E2	c.97delA	Frameshift	Stop at 53	No LOH	EC
E2	c.97delATTG	Frameshift	Stop at 53	?	EC
E2	c.98T-->G	Missense	I33S	No LOH	EC
E2	c.118G-->T	Nonsense	E40X	?	EC
I2	IVS2-1G-->T	Splicing		LOH	EC
E3	c.165-6del17	Splicing		?	ECI
E3	c.170insT	Frameshift	Stop at 62	?	ECI
E3	c.171ins38	Frameshift	Stop at 98	Dble Mut	EC
E3	c.176C-->A	Nonsense	S59X	LOH	EC
E3	c.184delA	Frameshift	Stop at 98	Dble Mut	EC

E3	c.190delCA	Frameshift	Stop at 72	?	ECI
E3	c.202delTA	Frameshift	Stop at 72	LOH	EC
E3	c.202insTAT	Frameshift	Stop at 74	?	EC
E3	c.202T-->C	Missense	Y68H	?	AEH
E4	c.218delAA	Frameshift	Stop at 76	MIN	EC
E4	c.223insA	Frameshift	Stop at 77	MIN	EC
E4	c.227delAT	Nonsense	Y76X	LOH	EC
E4	c.242T-->G	Frameshift	F to C	?	EC
I4	IVS4+1G-->A	Splicing		MIN	EC
E5	c.276delT	Frameshift	Stop at 86	Dble Mut	EC
E5	c.269T-->C	Missense	F90S	Dble Mut	EC
E5	c.275A-->G	Missense	D96G	LOH	EC
E5	c.277C-->G	Missense	H93D	MIN	EC
E5	c.277C-->T	Missense	H93Y	MIN	EC
E5	c.284C-->T	Missense	P95L	MIN	AEH
E5	c.284C-->T	Missense	P95L	MIN	EC
E5	c.296insTA	Frameshift	Stop at 112	?	EC
E5	c.309insT	Frameshift	Stop at 106	?	EC
E5	c.309del11	Frameshift	Stop 105	?	EH
E5	c.319G-->T	Missense	D107Y	?	EC
E5	c.356T-->A	Missense	V119D	Dble Mut	EC
E5	c.360del75	In-Frame Del		MIN	EC
E5	c.367C-->T	Missense	H123Y	MIN	EC
E5	c.370T-->A	Missense	C124S	?	EC
E5	c.382del14	Frameshift	Stop at 159	?	AEH
E5	c.386G-->A	Missense	G129E	?	EC
E5	c.387delA	Frameshift	Stop at 133	?	EC
E5	c.388C-->G	Missense	R130G	?	EC
E5	c.388C-->G	Missense	R130G	Dble Mut	EC
E5	c.388C-->G	Missense	R130G	MIN	EC

E5	c.388C-->T	Nonsense	R130X	?	EC
E5	c.388C-->T	Nonsense	R130X	MIN	EC
E5	c.388C-->T	Nonsense	R130X	Dble Mut	EH
E5	c.389del7	Frameshift	Stop at 131	?	AEH
E5	c.389del9	In-Frame Del		?	EC
E5	c.389G-->A	Missense	R130Q	LOH	EC
E5	c.389G-->T	Missense	R130Q	?	AEH
E5	c.389G-->T	Missense	R130L	?	AEH
E5	c.389G-->T	Missense	R130L	?	EC
E5	c.392del20	Frameshift	Stop at 172	?	AEH
E5	c.397G-->A	Missense	V133I	LOH	EC
E5	c.405insA	Frameshift	Stop at 179	Dble Mut	EC
E5	c.405del19	Frameshift	Stop at 140		ECIII
E5	c.415delTT	Frameshift	Stop at 178	?	EH
E5	c.416T-->G	Nonsense	L139X	?	EH
E5	c.445C-->A	Nonsense	Gln to Stop	?	AEH
E5	c.459T-->C	No Change	No Change	?	EC
I5	c.486insA	Frameshift	Stop at 166	Dble Mut	EC
I5	c.486ins8	Frameshift	Stop at 169	?	AEH
E6	IVS5+2delT	Splicing		LOH	EC
E6	c.491delA	Frameshift	Stop at 166	?	ECI
E6	c.509G-->A	Missense	S170N	?	EC
E6	c.517C-->T	Missense	R173C	?	AEH
E6	c.517C-->T	Missense	R173C	?	EC
E6	c.517C-->T	Missense	R173C	LOH	EC
E6	c.527T-->G	Nonsense	Y176X	Dble Mut	EC
E6	c.530delATTAT	Frameshift	Stop at 178	Dble Mut	EC
E6	c.537del4	Frameshift	Stop at 181	?	AEH
E6	c.545insA	Frameshift	Stop at 189	MIN	EC
E6	c.559delG	Frameshift	Stop at 198	?	EC

E6	c.572T-->C	Missense	V191A	?	EH
I6	c.IVS6+1G-->T	Splicing		LOH	EC
I6	c.IVS6+1G-->T	Splicing		MIN	EC
E7	c.632insG	Frameshift	Stop at 242	?	ECI
E7	c.640C-->T	Nonsense	Q214X	?	EC
E7	c.640C-->T	Nonsense	Q214X	LOH	EC
E7	c.640C-->T	Nonsense	Q214X	MIN	EC
E7	c.646G-->A	Missense	V216M	LOH	EC
E7	c.654C-->A	Nonsense	C218X	Dble Mut	EC
E7	c.667delA	Frameshift	Stop at 225	?	EC
E7	c.697C-->T	Nonsense	R233X	Dble Mut	EC
E7	c.697C-->T	Nonsense	R233X	?	AEH
E7	c.703G-->T	Missense	E235X	LOH	EC
E7	c.710insAA	Frameshift	Stop at 242	LOH	EC
E7	c.721delT	Frameshift	Stop at 255	LOH	EC
E7	c.727del13	Frameshift	Stop at 251	?	EC
E7	c.733C-->T	Nonsense	Q245X	Dble Mut	EC
E7	c.733del8insA	Frameshift	Stop at 253	No LOH	EC
E7	c.737insGT	Frameshift	Stop at 256	?	AEH
E7	c.738delG	Frameshift	Stop at 255	MIN	EC
E7	c.750T-->A	Nonsense	C250X	Dble Mut	EC
E7	c.750delTG	Frameshift	Stop at 251	?	ECI
E7	c.762del14	Frameshift	Stop at 298	?	EC
E7	c.792del13	Frameshift	Stop at 271	No LOH	EC
E7	c.795delA	Frameshift	Stop at 275	?	EC
E7	c.795delA	Frameshift	Stop at 275	Dble Mut	EC
E7	c.795delA	Frameshift	Stop at 275	LOH	EC
E7	c.795delA	Frameshift	Stop at 275	MIN	EC
E7	c.799delAA	Frameshift	Stop at 296	Dble Mut	EC
E7	c.800insA	Frameshift	Stop at 297	?	ECI

E7	c.800delA	Frameshift	Stop at 275	?	EC
E7	c.801insA	Frameshift	Stop at 297	?	EC
E7	c.802ins171	Frameshift		?	EC
I7	INS7+1G-->T	Splicing		LOH	EC
E8	c.820delT	Frameshift	Stop at 275	?	ECI
E8	c.850G-->A	Missense	Q to K	?	EC
E8	c.863delA	Frameshift	Stop at 290	Dble Mut	EC
E8	c.864del5	Frameshift	Stop at 295	?	EC
E8	c.867delA	Frameshift	Stop at 290	?	ECII
E8	c.877G-->T	Nonsense	G293X	MIN	EC
E8	c.892C-->T	Nonsense	Q298X	LOH	EC
E8	c.885insA	Frameshift	Stop at 297	?	ECII
E8	c.895G-->T	Nonsense	Q299X	?	ECII
E8	c.901del10	Frameshift	Stop at 303	No LOH	EC
E8	c.923delGT	Frameshift	Stop at 310	?	AEH
E8	c.937delA	Frameshift	Stop at 315	?	EC
E8	c.940insG	Frameshift	Stop at 324	?	ECI
E8	c.950del4	Frameshift	Stop at 319	Dble Mut	EC
E8	c.950del5	Frameshift	Stop at 320	MIN	EC
E8	c.952delCTTA	Frameshift	Stop 319	?	AEH
E8	c.952delCTTA	Frameshift	Stop 320	Dble Mut	EC
E8	c.952delCTTA	Frameshift	Stop at 319	Dble Mut	EC
E8	c.953delTTAC	Frameshift	Stop at 319	?	AEH
E8	c.955delACTT	Nonsense	T319X	LOH	EC
E8	c.955delACTT	Nonsense	T319X	MIN	EC
E8	c.956delCTTT	Frameshift	Stop at 342	?	EC
E8	c.956insA	Frameshift	Stop at 324	Dble Mut	EC
E8	c.962insA	Frameshift	Stop at 324	?	EC
E8	c.962insA	Frameshift	Stop at 324	Dble Mut	EC
E8	c.962insA	Frameshift	Stop at 324	MIN	EC

E8	c.962insA	Frameshift	Stop at 324	No LOH	EC
E8	c.963delA	Frameshift	Stop at 343	?	EC
E8	c.963delA	Frameshift	Stop at 343	Dble Mut	EC
E8	c.963delA	Frameshift	Stop at 343	MIN	EC
E8	c.963delA	Frameshift	Stop at 343	No LOH	EC
E8	c.963delAA	Frameshift	Stop at 324	?	EC
E8	c.968delA	Frameshift	Stop at 343	?	EH
E8	c.968delA	Frameshift	Stop at 343	?	EC
E8	c.968insA	Frameshift	Stop at 324	?	ECI
E8	c.969insA	Frameshift	Stop at 324	?	EC
E8	c.976del55	In-Frame Del + Spl		Dble Mut	EC
E8	c.984del4	Frameshift	Stop at 343	?	EC
E8	c.987del4	Frameshift	Stop at 343	?	EC
E8	c.988delAA	Frameshift	Stop at 341	?	EC
E8	c.992A-->G	Missense	D331G	No LOH	EC
E8	c.999ins7	Frameshift	Stop at 344	?	ECI
E8	c.1003C-->T	Nonsense	R335X	?	EC
E8	c.1004del11	Frameshift	Stop at 338	?	ECI
E8	c.1008C-->A	Nonsense	Y336X	LOH	EC
E8	c.1009delT	Frameshift	Stop at 343	?	EC
E8	c.1012T-->A	Missense	S to T		
E8	c.1021T-->G	Missense	F to V	?	ECII
E9	c.1043C-->T	Missense	T348I	?	AEH
E9	c.1043insA	Frameshift	Stop at 360	Dble Mut	EC

Table 2. Mutation Spectrum of PTEN in Endometrial Cancers, Legend

Mutations are numbered according to the PTEN DNA code and starting from A in the start codon of the protein.

E: Exon, **I:** Intron, **del:** deletion, **ins:** insertion, **In-Frame Del:** In-Frame deletion.

AEH: atypical endometrial hyperplasia, AH, **EH:** endometrial hyperplasia, **EC (I/II/III):** endometrial carcinoma (Grades I/II/III) **LOH:** Loss of heterozygosity, **MIN:** microsatellite instability, **Dble mut:** Two point mutations in same tumour, **IVS:** intronic variant sequence, **?:** No information.

Table adapted from Bonneau & Longy (2000), Sun, et al (2001), & Minaguchi, et al (2001)

The location of mutations in PTEN also appears to have significance in EC. There have been several reports of PTEN mutations giving a better prognosis in endometrioid tumours (Risinger, et al 1998 & Maxwell, et al 2000), although the specific mutations were not analysed. Minaguchi, et al (2001) described better survival rates in patients with mutations outside of exons 5, 6 and 7, although the tumours were histopathologically indistinguishable from those with PTEN mutations inside these exons. They associated exon 8 mutation with a better prognosis as these mutations affect only the C2 domain and may still retain phosphatase activity (refer to Section 1.2.2). Exon 7 mutation was however correlated with poor outcome as most mutations here are frameshifts or nonsense, which lead to truncation of the CBR3 region of the phosphatase domain and the C2 domain. This mutation would be comparable to an exon 5 catalytic site mutation and most likely would disrupt PI3,4,5P3 binding.

In addition to mutation, PTEN promoter methylation has been detected in ~20% of EC lesions and correlated with increasing tumour grade and metastasis (Salvessen, et al 2001 & Risinger, et al 2003).

Microsatellite instability (MSI) due to replication errors occurs frequently in hereditary tumors and appears to be an early event in EC. MSI is caused by mutations in DNA mismatch repair genes hMLH1 and hMSH2, but errors are seen in hMLH1 more often in EC (Piero, et al 2002). Reports have detected loss of hMLH1 and PTEN expression in 55% of EC samples (Orbo, et al 2003), and also in endometriosis, which has the potential to become malignant (Martini, et al 2002). MSI has been associated with a favourable prognosis in endometrioid EC (Maxwell, et al 2001, Wong, et al 1999 &

Tibilietti, et al, 1999), and colorectal cancers (Gryfe, et al 2000). One possible reason for the more favourable prognosis is that lymphocytic invasion is higher in EC lesions with MSI, suggesting augmentation of host immune recognition of these tumours (Kihana, et al 1998).

PTEN mutations in EC could provide useful prognostic and therapeutic information, and aid in the decision to perform surgical removal of metastatic tumours or to offer treatments such as chemotherapy or radiotherapy. Additional studies on PTEN genetic alterations, regulation and cellular localisation in EC cells may help to clarify the tumor suppressor function of PTEN in this disease.

Other Malignancies

Aberrations of PTEN have now been reported in a wide range of other cancers, but the implications of PTEN mutation are less well understood in these diseases with regard to initiation and progression. Decreased PTEN expression has been detected in higher grade gastric cancer (Zheng, et al 2003b), colorectal cancer (Zhou, et al 2002), bladder (Aveyard, et al 1999) and pancreatic cancer (Perren, et al 2000).

PTEN mutation has also been analysed in haematological malignancies. Abberant PTEN has been detected in ~20% of acute myeloid leukaemias [AML] (Liu, et al 2000 & Aggerholm, et al 2000). The high incidence of loss of protein expression in the presence of high levels of PTEN mRNA in primary leukaemia and Non-Hodgkins' lymphoma indicate that gene silencing, probably by promoter methylation, is important in haematological cancers (Dahia, et al 1999). Recently, high levels of P-PTEN, P-Akt/PKB

and phosphorylated Forkhead factors have been detected in this disease indicating poor prognosis (Cheong, et al 2003a & b). Conversely, PTEN mutations are rarely seen in lymphoma (Melendez, et al 2003), although lower expression levels have been observed (Abbott, et al 2003).

Loss of PTEN may also play a role in autoimmune diseases, as it has been shown that in during clonal selection T-cells with PTEN deficiency become resistant to CD95-induced death and gain long-term activity (Strauss, et al 2003). Loss of PTEN also disrupts B-cell immunoglobulin class switching and differentiation in the spleen (Anzelon, et al 2003) and can increase autoantibody titres (Suzuki, et al (2003).

1.4.3 PTEN Promoter Methylation

Promoter methylation is an alternative method of silencing tumour suppressor genes (Herman, 1999) and has been observed in a variety of tumour types for many cancer-related genes including p16 (Yu, et al 2002), BRCA1 (Baldwin, et al 2000) and Rb (Simpson, et al 2000). Methylation occurs at 'CpG islands', dinucleotides which are usually present within or near the promoter. Hypermethylation by DNA methyltransferases prevents transcription of the downstream gene, and elevated expression of DNA methyltransferase I is frequently observed in cancers (Warnecke & Bestor, 2000).

Several papers have reported methylation of the PTEN promoter in a number of tumour cell types, including gastric carcinomas (Kang, et al 2002), endometrial carcinomas (Salvesen, et al 2001), thyroid cancers (Frisk, et al 2002) and prostate carcinomas (Whang, et al, 1998). Soria, et al (2002) also

report methylation of the PTEN promoter in non-small cell lung carcinoma (NSCLC) which often presents constitutive Akt/PKB. This group were able to demethylate PTEN in a NSCLC cell line with 5-axa-2'-deoxycytidine which restored mRNA transcription. They report that as demethylating agents are undergoing clinical trials, their finding is of particular therapeutic significance. It is noted by Zysman, et al (2002) that many of the methods used to determine the methylation status of the PTEN promoter cannot differentiate between PTEN and the pseudogene ψPTEN which are discussed below.

1.5 The PTEN Pseudogene & Tissue-Specific PTEN Homologues

ψPTEN, the Pseudogene

Shortly after the discovery of PTEN, a highly conserved processed pseudogene (Mighell, et al 2000), named ψPTEN was located on human chromosome 9p21 (Dahia, et al 1998). ψPTEN differed from PTEN by 19 nucleotides and 12 amino acids (see Appendix III), had no initiation methionine and was intronless. Despite these features, several groups have described varying levels of transcription of ψPTEN mRNA in a range of tissues but were unable to detect any protein expression (Fujii, et al, 1999, Yokoyama, et al 2000).

PTEN Homologues TPTE, PTEN-2 and TPIP

Several PTEN homologues have now been reported in both human and mouse genomes. In 1999 a testis-specific conserved PTEN homologue called TPTE (transmembrane phosphatase and tensin homology) was cloned from human chromosome 21. Multiple copies also mapped to chromosomes

13, 15, 22 and Y, but this group did not characterise the protein (Chen, et al 1999). Work by Guipponi, et al (2000) has described the DNA structure of the copy on the short arm of chromosome 21 as having 24 exons spanning 87Kb. The same group also cloned murine TPTE, of which 3 major transcripts a, b, and c were described, each coding for proteins containing a protein tyrosine phosphatase motif and four potential transmembrane domains which localised to the golgi (Guipponi, et al 2001).

A highly conserved murine PTEN homologue, named PTEN 2, has recently been identified (Wu, et al (2001). This form appears to be expressed only in the testis and is localised to the golgi, possibly via an extended N-terminus containing four potential transmembrane domains. This association with the golgi may indicate a specialist role in membrane trafficking and regulation of terminal spermatocyte development. PTEN 2 also demonstrates enzymatic activity against PI3,4,5P3, and has a greater specificity for 3' and 5' phospholipids than PTEN although the reason for this is unclear.

Walker, et al, (2001) have also described another human PTEN homologue termed TPIP (TPTE and PTEN homologous inositol lipid phosphatase). This homologue has two splice variants, TPIPα and β, the former which has phosphatase activity and binds membranes, and the latter which is inactive and cytosolic. TPIPα contains up to three possible transmembrane domains that are absent in TPIPβ, and localises to the endoplasmic reticulum (ER), where it may regulate phosphoinositide signalling. This group also demonstrated that TPTE was catalytically inactive against phospholipids, but protein phosphatase activity was not assessed. Additionally, none of the three homologues could regulate Akt/PKB.

1.6 Project Aims

Overview

Endometrial carcinoma is the most common gynaecological malignancy and has the highest rate of PTEN mutation over any other cancer. Over 100 mutations have been described, but none of the studies have been performed using archival endometrial material. A repository of ~50 patients was made available for use in this project, consisting of a histologically normal cervical sample and up to three tumour samples of varying histological grade. These samples permitted the analysis of the PTEN sequence in both normal and tumour cells. The role of TGF-β1 in the regulation of PTEN levels is contradictory and may be cell-type specific, and has not yet been assessed in endometrial cells. Compounds which upregulate PTEN may have therapeutic value and therefore merit investigation. The subcellular localisation of PTEN has been reported to be both cytoplasmic and nuclear, and this may depend on both cell-type and stimulating compound. As PTEN levels respond to cyclic hormones in the endometrium, the cloning of PTEN into a plasmid encoding a green fluorescent protein tag (EGFP) would enable rapid study of PTEN protein behaviour in endometrial cell lines under hormone and cytokine stimulation. Specific project aims are detailed overleaf.

Specific Aims

The major aims of this project were threefold:

1. To analyse PTEN mRNA and protein expression in endometrial cell lines stimulated with TGF-β1.

The transcriptional and post-translational effects of this cytokine were evaluated in two cell lines of endometrial origin, HEC-1B and Ishikawa, to compare the response of cells with wild-type PTEN (HEC-1B) or mutant PTEN (Ishikawa). Expression of PTEN, phospho-PTEN and several other genes were studied using RT-PCR and Western blot to determine the nature of any changes in expression produced by exposure to TGF-β1. Expression levels of PTEN mRNA and protein were correlated to time and dose of cytokine stimulation. As serum in the growth medium can contain varying levels of TGF-β1, stimulation of endometrial cell lines with cytokine was also performed in low-serum conditions and the results compared to normal serum conditions. The effect of TGF-β1 on cell morphology and viability was also investigated.

2. To determine the sub-cellular localisation of PTEN protein in endometrial cell lines.

Localisation of PTEN protein has not previously been described in cell lines of endometrial origin. To assess localisation of PTEN in endometrial cell lines, the cloning of full-length human PTEN tagged with green fluorescent protein (GFP) was undertaken. Cell lines were transfected with PTEN-GFP and the localisation of the protein to cellular compartments observed. The effect of treatment with compounds reported to change PTEN expression

(TGF-β1 and oestrogen) were also evaluated to determine whether the localisation of PTEN could be altered by such compounds.

3. To detect novel mutations of PTEN exons 5 and 8 in DNA derived from archival endometrial material.

Mutation of PTEN is especially prevalent in endometrial cancer, and by describing such mutations the specific role of PTEN in this disease can be analysed. Using PCR fragments amplified from tumour DNA for PTEN exons 5 and 8, the presence of sequence variations in the samples were detected by Single-Strand Conformation Polymorphism (SSCP) analysis. Samples with sequences differing from a PTEN control sample were detected as bands with aberrant mobility. Samples displaying such bandshifts may contain polymorphisms or mutations, which can be determined by automated sequencing of the PCR products.

CHAPTER 2

MATERIALS & METHODS

2.1 MATERIALS & SUPPLIERS

2.1.1 Reagents & Kits

McCoy's 5A Modified Medium, (M8403), Sigma

Minimal Essential Medium Eagle's, (M2289), Sigma

Human recombinant TGFβ-1, (240-B), R&D Systems, UK

Protease Inhibitor Cocktail for Mammalian Cells, (P8340), Sigma

Bradford Reagent, (B6916), Sigma

Colour SDS Molecular Weight Markers, High Range, (C3312), Sigma

Biotinylated SDS Molecular Weight Markers, (MW-SDS-100B), Sigma

ECL Blocking Powder, Amersham

Western Blotting Detection System, (RPN 2209), Amersham

CellTiter One Solution Cell Proliferation Assay Solution, (G3580), Promega

Normal Goat Serum, (G9023), Sigma

GenElute Plasmid Miniprep Kit, (PLN-10), Sigma

GeneRuler 1Kb molecular weight marker 0.25mg/ml, (SM0313), MBI Fermentas

Poly-D-Lysine, (P7405), Sigma

DAPI, (D8417), Sigma

Fluoromount G, (0100-01), Southern Biotechnology

Lipofectamine, (18324), Liopfectamine 2000, (11668), Invitrogen

ß-17 Estradiol (E8875) Sigma

CMV-PEGFP-N1 Courtesy of Dr E Blair, Dept Molecular Biology, University of Leeds, UK

CMV-pECFP-N1 Courtesy of Dr C Fenech, Sheffield Hallam University, UK

2x MDE gel solution, (50620),Bio Whittaker Molecular Applications

PlusOne DNA Silver Staining Kit, (17-6000-30), Amersham Pharmacia Biotech

100bp Molecular Weight Marker, (N3231S), NEB

Sequencing performed to order by:

Lark Technologies Inc

Radwinter Road

Saffron Waldon

Essex CB11 3HY

2.1.2 Antibodies

Mouse monoclonal IgG1anti-PTEN, Clone A2B1, 0.5 mg/m,l (68731A), BD Transduction Laboratories

Mouse monoclonal IgG anti-PTEN, Clone 6H2.1, 0.5 mg/ml Alexis Biochemicals

Mouse monoclonal anti-β-Actin, Clone AC15, (A5441), Sigma

Mouse monoclonal IgG1anti-PAI-1, 0.25 mg/ml, (612024), BD Transduction Laboratories

Mouse monoclonal IgG1anti-p27KIP1, Clone G-173-524, 0.5 mg/ml, (554069), BD Transduction Laboratories

Mouse monoclonal IgG2a anti-Phospho-AKT Ser 473, Clone 4E2, (#9276), NEB

Rabbit Polyclonal anti-Phospho-PTEN Ser 380, (#9551) NEB

Vector Elite anti-mouse IgG detection kit & anti-Universal detection kit, Vector Laboratories

AlexaFluor 594 goat anti-mouse IgG (H+L) Highly cross-adsorbed, 2 mg/ml, (A-11005), Molecular Probes

Anti-Hsp47, (Colligin), mouse monoclonal 0.85mg/ml, (SPA-470), Stressgen

Anti-Mannosidase II, Courtesy of Prof D Parkinson, Sheffield Hallam University

2.1.3 Oligonucleotides

The oligonucleotides used for PCR were synthesized by Sigma-Genosys with HPLC purification. Lyophilised oligonucleotides were re-suspended in 0.5-1ml of sterile water, aliquoted and stored at –20°C. The location of each PTEN primer is illustrated in Appendix II.2.

PTEN 1# Forward Exonic
5' CGGCATATGACAGCCATCATCAAAGAGATC3'

PTEN 2a# Reverse Exonic
5' CCC GTC GAC TCA GAC TTT TGT AAT TTG TG 3'

PTEN 3# Forward Exonic
5' CGG CAT ATG TGT GAT CAA GAA ATC GAT AGC 3'

PTEN 4# Reverse Exonic
5' CCCGTCGACTCACCCATAGAATCTAGGG3'

PTEN 5A* Forward intronic
5' TATTCTGAGGTTATCTTTTA 3'

PTEN 5B* Reverse exonic
5' CTTTCCAGCTTTACAGTGAA 3'

PTEN 5C* Forward exonic
5' GCTAAGTGAAGATGACAATCA 3'

PTEN 5D* Reverse intronic
5' AGAAAAAACATCAAAAAATAA 3'

PTEN 8A* Forward intronic
5' ACACATCACATACATACAAGTC 3'

PTEN 8B* Reverse Exonic

5' GTGCAGATAATGACAAGGAATA 3'

PTEN 8C* Forward Intronic

5' TTAAATATGTCATTTCATTTCTTTTTC3'

PTEN 8D* Reverse Exonic

5' CTTTGTCTTTATTTGCTTTGT 3'

PTEN 10[#] Forward Exonic

5' CCC **GTC GAC** GGA CTT TTG TAA TTT GTG TAT 3'

PTEN 11[#] Reverse Exonic

GGC **GAA TTC** AGC ATG ACA GCC ATC ATC AAA GAG 3'

PTEN 10b[#] Forward Exonic

5' CAC CAC CT**G TCG AC**T GGA CTT TTG TAA TTT GTG TAT 3'

PTEN11a[#] Reverse Exonic

5' CGG ACT **GAA TTC** AGC ATG ACA GCC ATC ATC AAA GAG 3'

(*Sal* I sites are highlighted in red and the *Eco*RI sites in blue).

GAPDH 472F[∫] Forward Exonic

5' TGA TGA CAT CAA GAA GGT GGT GAA G 3'

GAPDH 472R[∫] Reverse Exonic

5' TCC TTG GAG GCC ATG TGA GGC CAT G 3'

PAI-1F[‡] Forward Exonic

5' GCT GAA TTC CTG GAG CTC AG 3'

PAI-1R[‡] Reverse Exonic

5' CTG CGC CAC CTG CTG AAA CA 3'

TPIPF[†] Forward Exonic

5' TAT TCT GAT AAG AAT TTT TCA TCT GC 3'

TPIPR[†] Reverse Exonic

5' CCT CGG CAG TTA AAA ATA TTT CG 3'

Bcl-2A[∂] Forward Exonic

5' GTT CGG TGG GGT CAT GTG TGT GGA GAG CG 3'

Bcl-2B[∂] Reverse Exonic

5' TAG CTG ATT CGA CGT TTT GCC TGA 3'

Denotes primer sequence taken from *Risinger *et al* (1997), [†]Walker, *et al*, (2001). All other primers designed from Entrez sequences [#]AF067844, [‡]M16006, [§]BC040499, [‡]X05744, [∂]M14745, [ƒ]NM002046.

2.1.4 Enzymes

Red Hot Taq Polymerase, 5U/µl, (AB 0406/B), ABGene

Superscript II RNAse H- Reverse Transcriptase, 200U/µl, (18064-014), Invitrogen

Placental RNAse Inhibitor, 50,000U/ml, (R2520), Sigma

Platinum *Pfx* DNA Polymerase, Invitrogen

Sal I, 20,000 U/ml, (R0138S), NEB

Eco RI, 20,000 U/ml, (R0101S), NEB

Mse I, 10,000 U/m,l (R0525S), NEB

Hha I, 20,000 U/ml, (R01395), NEB

T4 DNA Ligase, 400,000 U/ml, (M0202S), NEB

RNase A, (R6513), Sigma

2.1.5 Bacterial Strains and Cell Lines

E. coli JM109 courtesy of Dr A. Fairclough, Sheffield Hallam University

E. coli DH5α Subcloning Efficiency Chemically Competent Cells, (18265-017), Invitrogen

HEC-1B cell line courtesy of Dr Sue Laird, Sheffield Hallam University, UK

Ishikawa cell line purchased from ECACC (99040201)

2.2 ANALYSYS OF EXPRESSION OF PTEN AND SELECTED GENES IN HEC-1B & ISHIKAWA CELL LINES STIMULATED WITH TGF-ß1

To assess the effect of TGF-ß1 on mRNA expression in HEC-1B and Ishikawa cells, RT-PCR was used to amplify mRNA species for PTEN, GAPDH and PAI-1.

2.2.1 Cell culture

Human endometrial cell lines HEC-1B and Ishikawa were routinely maintained in McCoy's 5A and Minimal Essential Eagles medium respectively (see Appendix I.1), at 37°C in 5% CO2 atmosphere. Cells were passaged at a ratio of 1:10 every three to four days when 80% confluence was reached. The growth medium was discarded, 5 ml of Trypsin-EDTA solution added and cells were incubated at 37°C until they detached from the flask surface. Trypsinised cells (0.5ml) were then diluted in 9.5 ml of fresh complete medium in a new flask and returned to the incubator.

2.2.2 TGF-ß1 stimulation

To analyse the effect of TGF-ß1 on gene expression in HEC-1B and Ishikawa cell lines, cell populations were expanded in 250 ml flasks, prior to passaging 5ml of cells into 75 ml flasks. The cells were grown to 100% confluence in complete medium then washed once with fresh complete medium. For serum-starved samples the cells were washed with reduced-serum medium (Appendix I.1) and incubated in reduced-serum media for 24 hours.

Solutions of TGF-ß1 at concentrations of 2ng/ml and 5ng/ml of TGF-ß1 were freshly prepared from a sterile 2μg/ml stock of the human recombinant cytokine by diluting with complete or reduced-serum medium. Concentrations were chosen based on previous work by Lee, et al (1999). Medium was discarded from the cells and replaced with medium containing TGF-ß1 at the appropriate concentration, then cells were returned to the incubator for four, eight or twenty-four hours prior to RNA extraction. Duplicate flasks were prepared for each concentration and time, and controls included cells without TGF-ß1 at each time point and a pre-starvation '10% serum' sample for the serum-starved experiments.

2.2.3 Analysis of RNA Expression

2.2.3.1 RNA Extraction

Medium was discarded from each flask and the cells washed with sterile 1x PBS. The PBS was discarded and 2.5ml cold TRI Reagent (Sigma) added per flask in accordance with the manufacturers' recommendations. The cells were resuspended by repeated pipetting and immediately transferred to sterile Eppendorf tubes, using two tubes per sample. The cells were incubated on ice for 5 minutes to lyse before the addition of 150μl of ice-cold chloroform and a further incubation on ice for 10 minutes. The samples were centrifuged at 12,000 rpm for 15 minutes at 4°C in a Heraeus microcentrifuge and the upper layer transferred to fresh sterile tubes. An equal volume of ice-cold isopropanol was added to each sample and the tubes incubated for 20 minutes at –70°C.

The RNA was pelleted by centrifugation at 12,000 rpm for 15 minutes at 4°C and the supernatant discarded. The pellets were washed with 375μl of ice-cold 80% ethanol, centrifuged at 10,000 rpm for 5 minutes at 4°C and the supernatant carefully aspirated. The RNA samples were air dried at room temperature for 10 minutes and dissolved in 20μl of ice-cold sterile water and immediately stored at –70°C.

2.2.3.2 RNA Quantitation and RT-PCR

For each RNA sample 2.5μl aliquots of RNA were added to 497.5μl of ice-cold sterile water to give a dilution of 1:200 and stored on ice. The absorbance at 260nm and 280nm was determined for each sample on a Cecil Aquarius spectrophotometer, using water to zero the machine at each wavelength. Readings were obtained from the spectrophotometer for each sample for the concentration at 260nm, and the purity ratio of 260 / 280 as calculated by the machine. Measurements were performed in duplicate. Each sample was adjusted to a concentration of 1μg/μl with ice-cold sterile water.

2.2.3.3 cDNA Synthesis

For cDNA synthesis, Superscript II RNAase H- RT enzyme (Invitrogen) was used according to the manufacturers' instructions. This enzyme lacks the ability for RNA hydrolysis, thus increasing product yield (www.invitrogen.com). Briefly, a master mixture containing 3μl 5mM dNTPs, 3μl 0.1M DTT, 6μl 5x RT buffer, 0.5μl Oligo $(d)_{16}T$ and 14.5μl sterile water per reaction was prepared on ice and mixed by brief vortexing. Aliquots of 27μl were added to each reaction tube. For each RNA sample two reactions

were prepared, consisting of a positive 'cDNA' containing 1μl of RNA (1μg), and a '-RT' also containing 1μl of RNA. An additional reaction tube without RNA (-RNA) was included in which sterile water (1μl) replaced RNA. The samples were mixed and heated at 65°C for 5 minutes on a thermal cycler, then immediately transferred to ice for 3 minutes. To each tube 1μl of placental RNase Inhibitor and Reverse Transcriptase were added; 1μl of sterile water was pipetted into the tubes labeled '-RT' in the place of RT. The samples were then incubated at 42°C for 1 hour on a thermal cycler and the cDNAs and controls stored at –20°C.

2.2.3.4 PCR

PCR was performed using cDNA diluted 1:4 with sterile water and a master mixture containing 2.5μl 10x Taq Buffer, 2.5μl 2mM dNTPs, 1μl 50mM $MgCl_2$, 100pM forward primer, 100pM reverse primer, 15μl sterile water and 1μl BioTaq Red DNA Polymerase per reaction. The master mixture was mixed by flicking gently and 24μl was aliquoted into each reaction tube, to which 1μl of diluted cDNA was added. The PCR reactions were mixed gently, briefly microfuged and placed in the thermal cycler on the appropriate programme (Appendix V). Samples were stored at 4°C when the PCR cycle had ended. PCR products were analysed by electrophoresis of 10μl aliquots using a 2% agarose gels as described below. Samples were loaded as a time-course for each concentration of TGF-ß1 and control.

2.2.3.5 Analytical Scale Agarose Gel Electrophoresis of DNA

Analytical agarose gels were prepared by adding 300mg or 600mg of molecular grade agarose to 30ml of 1x TAE buffer (Appendix I.8) to give 1% or 2% gels respectively (Maniatis, Sambrook & Fritsch, 1989). The gel slurry was heated for 1 minute in a microwave oven on full power until the agarose had fully dissolved, and then allowed to cool briefly before the addition of 1.5μl of 10mg/ml ethidium bromide solution. The molten agarose was poured into a gel former with a comb inserted and allowed to set for 30 minutes at room temperature.

The comb was removed from the prepared gel which was then placed in a mini-submarine electrophoresis tank and submerged in 1xTAE buffer to the manufacturer's indicated mark. 10μl of PCR product was added to 2μl of loading dye (Appendix I.8) and the entire sample loaded through the buffer into a pre-formed well of the gel. 1μl of 100bp molecular weight marker was also included in one well. Electrophoresis was carried out at a constant 110V for approximately 45 minutes and the gel visualized on a UV transilluminator and photographed using a KODAK DC120 digital camera.

2.2.3.6 Densitometric Analysis of RT-PCR products

Gels were analysed using Kodak 1D Image Analysis Software (Version 2.0.1) using a 100bp molecular weight marker as a standard for mass calculations, and the band intensities expressed in nanograms.

2.2.4 Analysis of Protein Levels in HEC-1B and Ishikawa Cell Lines stimulated with TGF-ß1

2.2.4.1 Protein Extraction and Quantification

For preparation of whole-cell extracts, TGF-ß1 stimulation was carried out in 75 ml cell culture flasks as described in section 2.2. Following stimulation, the flasks were removed from the incubator, the medium discarded and the cells washed twice with ice-cold sterile PBS. The PBS was discarded and 750μl of ice-cold phosphoprotein lysis buffer (Appendix I.2) added to each flask, with brief homogenization by pipetting. The cell lysates were transferred to sterile 1.5 ml Eppendorf tubes and incubated on ice for 30 minutes to allow complete lysis of the cells. The lysates were cleared of insoluble material by microfuging for 10 mins at 13,000 rpm at 4°C and the supernatant transferred to clean tubes on ice.

2.2.4.2 Determination of Protein Concentration by the Bradford Assay

Protein concentration in each sample was determined using the Bradford Assay. This simple, rapid method quantitates the amount of protein in a sample by the proportional binding of coomassie blue dye to the protein, which can be measured at an absorbance of 595nm (Friedenauer & Berlet, 1989). For each sample, 5 μl was diluted in 995μl of sterile water to give a 1:200 dilution; 500μl of these dilutions were then transferred to clean 1.5ml Eppendorf tubes and 500μl of Bradford Reagent (Sigma) added to each tube. The reactions were vortexed and incubated at room temperature for five

minutes, prior to recording the absorbance of each sample at 595 nm using disposable plastic cuvettes. All samples were prepared in duplicate.

Average absorbance values were used to calculate the concentration of protein in the undiluted samples by reading from the BSA standard curve (Appendix IV) and adjusting for the dilution factor. The volume of each sample required to give 10 μg of protein was calculated and aliquots prepared for storage at -20°C.

2.2.4.3 Separation of Proteins by SDS-PAGE

SDS-polyacrylamide gels were prepared based on the Laemmli two-phase system of protein separation (Laemmli, 1970) using the Bio-Rad minigel (8x10cm) format system. Proteins separated by this method are denatured to single strands by the presence of SDS, which exposes the charged amino acid residues. Exposure of these residues permits electrotransfer of the proteins to a membrane, and subsequent detection by western blotting using antibodies.

The glass plates were cleaned with ethanol prior to assembly and an 8% resolving gel mix (Appendix I.3) pipetted between the plates. The gel was overlayed with ethanol and allowed to polymerize at room temperature for one hour. The ethanol overlay was then discarded and the surface of the gel washed six times with distilled water and freshly prepared 4% stacking gel mix (see Appendix 1.3) pipetted on top of the resolving gel. A 10-well Teflon comb was carefully inserted into each stacking gel, avoiding air bubbles, and pressed down into the solution to give approximately 5 mm of stacking gel between the bottom of the wells and the resolving gel interface.

The stacking gel was left to polymerize for 30 minutes, then the combs carefully removed and the wells washed thoroughly with 1x Running buffer (Appendix I.3). The prepared gels were clamped into the electrophoresis module and both anode and cathode chambers filled with 1x Running buffer according to the manufacturer's recommendations.

Protein samples were prepared by mixing 10 μg of each sample with 1μl of loading buffer (Appendix I.9) and boiling at 100°C for 1 minute on a thermal cycler, with the lid heater set at 110°C. A coloured molecular weight marker was also boiled at 100°C for 1 minute, according to the manufacturer's instructions.

The entire volume of each sample was loaded into the wells of the SDS-PAGE gel using gel loading pipette tips, ensuring that the samples sank to the bottom of each well. To one well of each gel was added 4 μl of boiled colour marker and 0.5 μl of a biotinylated molecular weight marker (Appendix II). Gels were connected to a power supply and electrophoresed at 120 V for 90 minutes.

2.2.4.4 Electrotransfer of Proteins to PVDF Membrane

Following separation of proteins by SDS-PAGE, the gels were carefully removed from the tank and released from the glass plates into a volume of ice-cold Towbin Buffer (Appendix II.3) sufficient to cover the gel, in separate containers. An 8x10 cm piece of PVDF membrane was cut for each gel, pre-wet for a few seconds in methanol and submerged in Towbin buffer. The gels and PVDF were allowed to equilibrate on the bench for 15 minutes; the fiber

pads and blotting paper sheets were also wetted with buffer for the same period of time.

The transfer was set up as shown below in Figure 7.

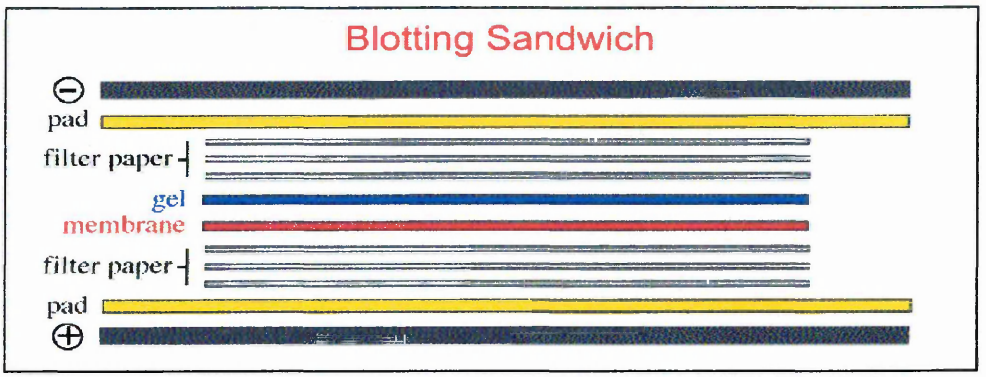

Figure 7 Western blotting transfer assembly

The assembled sandwiches were inserted into the blotting module and placed into the tank along with a small magnetic stirrer bar and an ice pack. The tank was filled with Towbin buffer to the manufacturer's recommended level, the lid and electrodes attached and electrotransfer performed at 150V for 1 hour with stirring (transfer protocol modified from www.bdbiosciences.com/pharmingen/protocols) After the transfer was completed, the PVDF membranes were removed from the sandwiches and air dried on paper towels. To assess the efficiency of the transfer, a gel was carefully retrieved and equilibrated in destain solution for 15 minutes prior to staining with coomassie blue overnight (Appendix I.3). The stained gel was then destained to show the presence of any residual protein in the gel.

2.2.4.5 Detection of Proteins by Western Blot and Enhanced Chemiluminesence

PVDF membranes which had been electroblotted were pre-wet with methanol for a few seconds, then washed 3 times with T/P-BST, (Appendix II), for 5 minutes per wash. A sufficient volume of buffer was used to completely cover the membrane, and gentle shaking was applied during all stages of the Western process. The colour marker, placed to the left at all times, was used to orientate the membrane so that the proteins faced upwards. The Western protocol was modified from existing protocols (www.bdbiosciences.com/pharmingen/protocols and Maniatis, Sambrook & Fritsch, 1989). Membranes were incubated in the blocking buffer (Appendix I.3) for 1 hour at room temperature, then washed 3 times as previously described. The primary monoclonal antibodies were diluted in 1% BSA/PBST at 1:300 (α-PTEN), 1:20,000 (α-ß-Actin), and 1:2000 (α-PAI-1). The blots were incubated with primary antibodies at room temperature for 90 minutes, washed three times, and incubated with anti-mouse secondary antibody diluted to 1:800 in 1% BSA/PBST at room temperature for 40 minutes. Anti-phospho-PTEN antibodies were used according to the manufacturer's instructions. The membranes for all primary antibodies were washed three times prior to incubation with Vector ABC reagent (avidin-biotin-horesradish peroxidase complex), prepared according to the manufacturer's instructions, for 30 minutes and again washed three times.

The ECL reagent was prepared according to the instructions supplied and applied to the membrane for 1 minute. Excess reagent was removed by touching the corners of the membranes with absorbent tissue, and the

membranes quickly sandwiched between two sheets of cling film with the colour marker to the left. Membranes were taken to the darkroom and exposed to film for 1 minute before developing according to the instructions supplied with the film and manual processing chemicals.

2.2.4.5.1 Densitometric Analysis of Protein levels

Photographic films which had been produced by the method described in 2.2.3 were scanned by Mr R Stewart, Academic Unit of Pathology, University of Sheffield and scanning densitometric analysis performed. The software used in the analysis was QuantityOne version 2.4 from the PDI Discovery package (Pharmacia).

2.2.5 HEC-1B Cell Proliferation Assay

To assess the effect of TGF-ß1 on HEC-1B cell proliferation, a Cell Titer 96 Aqueous One Solution Cell Proliferation Assay was used, according to the protocol. This MTT-based assay measures the cellular reduction of the assay reagent to a blue formazan product, which can only be performed by metabolically active cells (Mosmann, 1989). Briefly, cells were seeded on three 96 well plates corresponding to 4, 8 and 24 hours stimulation and grown to confluence in complete medium (Appendix I.1). Cells were serum-deprived in reduced-serum medium (Appendix I.1) for 24 hours and then stimulated with 0, 1, 2, 4, 5, 7 and 10 ng/ml TGF-ß1 in reduced serum medium. Controls either consisted of unstimulated cells prior to serum-starvation or they did not contain cells (growth medium and assay solution alone). Four replica wells were performed for each condition. Results were

obtained by reading the absorbance of the wells at 490nm in an automated plate reader, 1 hour after the addition of the assay solution.

2.2.6 Assessment of the effect of cell density on PTEN expression in HEC-1B cells.

To determine the effect of increasing cell density on PTEN expression levels in the HEC-1B cell line, cells were seeded at $4.5x10^5$ and $9x10^5$ cells per small (T25) culture flask. Cells were grown in complete medium for 1, 2, 3 and 4 days, plus 4 days with a growth medium change on day 3 (modified from Boyd & Kaufman, (1990). RNA extraction, cDNA synthesis and PCR were performed as described in Section 2.2.3. PCR products were analysed by running 10µl of each sample on a 2% agarose gels.

2.2.7 Morphological changes in HEC-1B and Ishikawa cell lines in response to TGF-ß1

The effect of TGF-ß1 on the morphology of HEC-1B and Ishikawa cells was investigated using a modified protocol previously described by Boyd & Kaufman, (1990). The cells were plated in triplicate onto two 24 well culture plates at an initial density of $1x10^4$ cells/well in 1ml of complete medium. Cells were allowed to attach for 24 hours, then they were rinsed twice with reduced-serum medium (Appendix I.1) and maintained in this medium for 48 hours to induce synchronization. The medium was replaced with fresh reduced-serum medium containing 10ng/ml TGF-ß1 or an equivalent volume of vehicle, (4mM sterile HCL with 1% BSA). The medium containing TGF-ß1 or vehicle was replaced daily.

The morphology was observed after 48 and 72 hours by taking phase contrast light micrographs at x 200 magnification with a Leica DM/L inverted microscope using a Polaroid MicroSLR unit and 661 film. After photographing the cells, a cell count was performed by washing each well twice with PBS, trypsinising for 15 minutes and resuspending the cells in 1ml of complete medium. Cells were counted on a haemocytometer and the triplicate results shown graphically.

2.3 CLONING OF FULL LENGTH HUMAN PTEN INTO CMV-pEGFP-N1 & ANALYSIS OF SUBCELLULAR LOCALISATION.

2.3.1 Cloning Strategy

PCR primers were designed to amplify full length PTEN from cDNA. These primers, the sequences of which are shown in Section 3.1, were designed to add restriction endonuclease sites to the PCR product for directional cloning into the CMV-pEGFP-N1 vector (Figure 8).

The forward primer, (PTEN 10), contained a 5' *Eco*RI site (blue), and the reverse primer, (PTEN 11), contained a 5' *Sal*I site (red). This should promote the ligation of double digested insert into pEGFP vector in one orientation only, and thus ensure that the correct strand of the cloned PTEN cDNA is transcribed. The overall cloning strategy is illustrated in Figure 9.

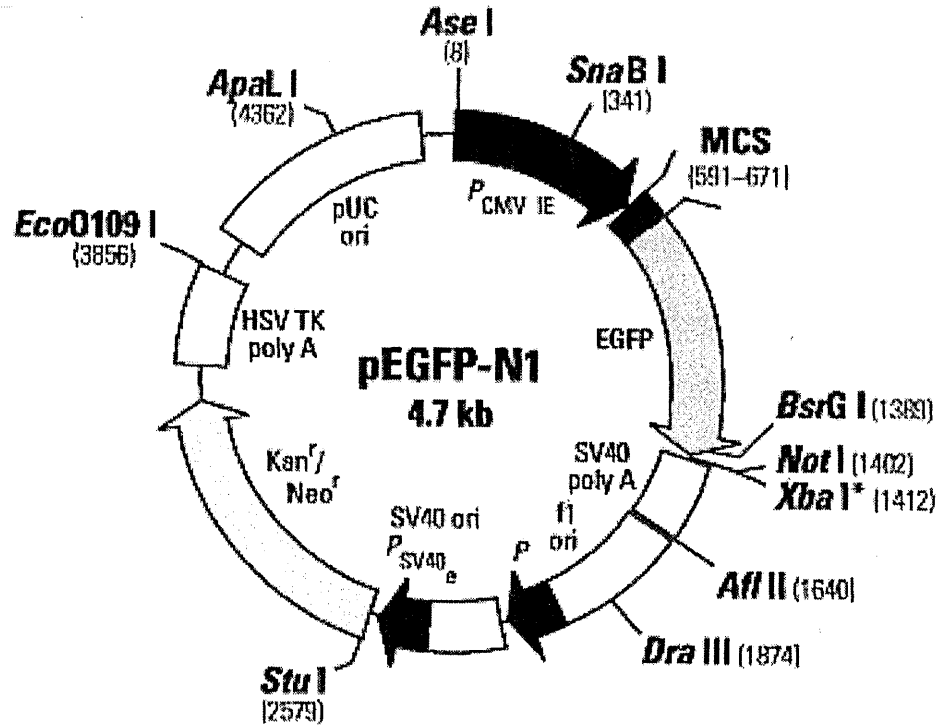

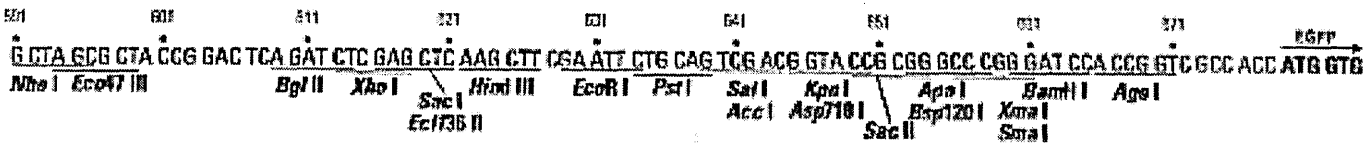

Figure 8 CMV-pEGFP-N1 and MCS Taken from www.invitrogen.com

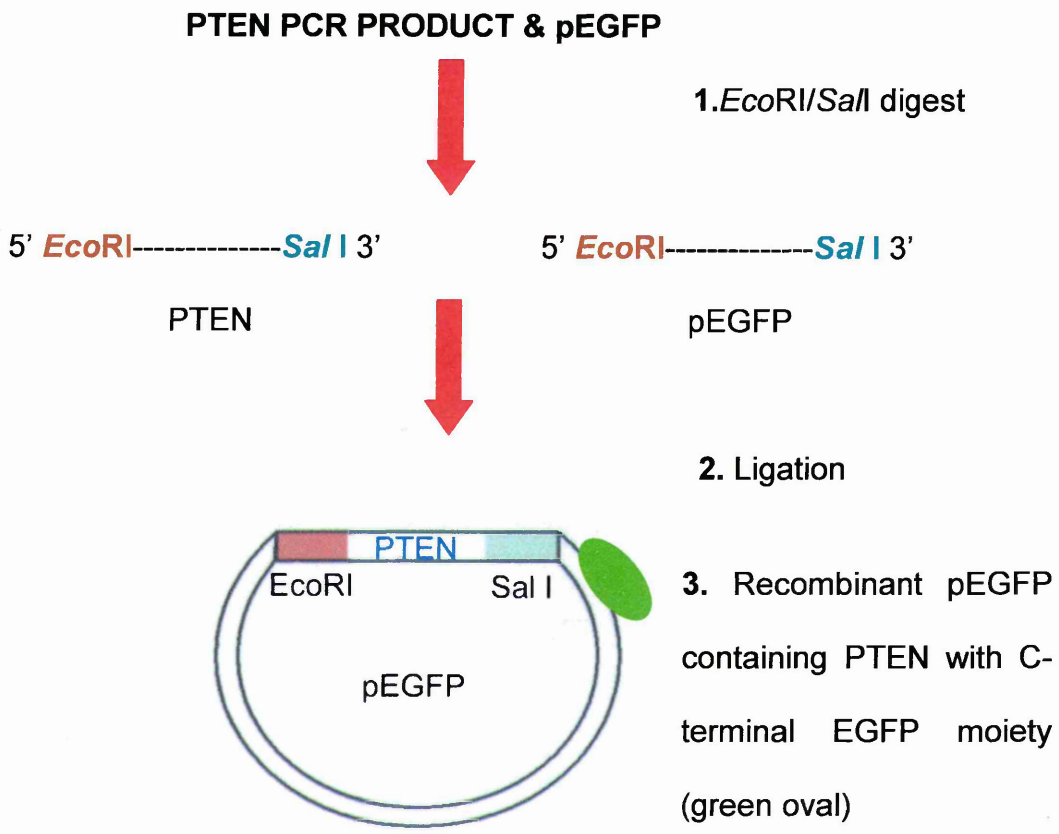

Figure 9

Cloning strategy showing **1.** Digestion of PTEN & pEGFP, **2.** Ligation of cut fragments to produce **3.** Recombinant directional clone

2.3.2 Extraction of RNA from whole human blood

Fresh human venous blood was collected from four staff members into vacutubes containing EDTA and the tubes marked anonymously. Mononuclear cells were harvested using Histopaque (Sigma), according to the manufacturers' guidelines. Briefly, 5 ml of Histopaque was added to four sterile 15 ml Falcon tubes and carefully overlayed with 5 ml of each blood sample, ensuring that the blood did not mix with the Histopaque. The blood samples were centrifuged at 19,000 rpm for 30 minutes at room temperature using a Sorvall RT7 Plus centrifuge, and the mononuclear cells carefully collected from the interface using a sterile Pasteur pipette into clean 15 ml Falcon tubes.

The mononuclear cells were washed by adding 10 ml of sterile 1x PBS (Appendix I.3) followed by centrifugation at 2000 rpm for 5 minutes at room temperature using a Sorvall rotor. This step was repeated and the pelleted cells resuspended in 1 ml of cold TRI reagent for RNA isolation. Quantitation of the resulting RNA was performed as described in Section 2.2.3.

2.3.3 RT-PCR of Full Length Human PTEN for Cloning

2.3.3.1 Analytical Scale Digestion of cDNA With Restriction Endonucleases *Mse* I and *Hha* I

cDNA synthesis was performed using 5μg of total RNA isolated from each of the four members of staff, as described in 2.2.3.3 To verify that the cDNA produced was free of genomic DNA contamination, each cDNA sample was amplified by PCR with exonic primers PTEN 1 and 4, using the PTEN I PCR programme and conditions previously described in Chapter 2. These primers

amplified the N-terminal region of PTEN, yielding a fragment of 450bp in length which could be cleaved by *Mse* I and *Hha* I restriction endonucleases to distinguish between PTEN from mRNA or contaminating genomic ΨPTEN pseudogene (Liu & Kagan, 1999).

PTEN derived from cDNA contains a unique *Mse* I site, and the pseudogene contains a unique *Hha* I site within the PCR fragment (Appendix III). Each of the PCR products were therefore subjected to a restriction digest with each enzyme in separate reactions. 5 μl of PCR product was mixed in a sterile 0.2 ml Eppendorf tube with 1μl of the appropriate 10x restriction buffer, (supplied with each enzyme), and 3μl of sterile water. 1μl of the appropriate enzyme was added (10U of *Mse*I or 20U of *Hha*I) and mixed by gentle flicking prior to incubating at 37°C for 2 hours on a thermal cycler.

The digestion was terminated by the addition of 2μl of loading buffer (Appendix I.8) and the products analysed by agarose gel electrophoresis on a 2% gel as previously described in Section 2.2.3.5.

2.3.4 PCR amplification of PTEN with High Fidelity Pfx Polymerase

2.3.4.1 Optimisation of PCR using Platinum Pfx Polymerase

Full length PTEN was amplified from each of the four staff cDNA samples using 0.5μl of the high fidelity proofreading DNA polymerase Platinum Pfx (Invitrogen), exonic primers PTEN 10b and 11a, and 3mM magnesium on the Pfx3lx PCR programme (Appendix V), to yield a fragment of 1.2 Kb. 10μl of each PCR product was analysed by agarose gel electrophoresis on a 1% gel

with 1μl of 1Kb molecular weight marker, as previously described. The PCR programme was modified to increase the yield of product (Appendix V).

2.3.4.2 Scaled-up PCR of PTEN

Four PCR reactions were performed simultaneously using the Pfx3lx2 PCR programme and conditions previously described in Section 2.3.4.1. They were pooled and a 10μl aliquot was analysed on a 1% agarose gel.

2.3.5 Preparation of the PTEN fragment for ligation

2.3.5.1 Gel purification of the PTEN fragment

Full length PTEN PCR product was separated by 1% agarose gel electrophoresis and the product band carefully excised from the gel with a sterile scalpel. DNA was purified from the agarose slices using two columns from a Qiagen Gel Extraction Kit, according to the manufacturers' instructions. Sterile water (30μl) was used to elute the DNA from each column, and the eluates were pooled.

2.3.5.2 Small-Scale Digestion of the PTEN PCR Product with Restriction Endonucleases *Eco* RI and *Sal* I

Restriction digestion was performed by mixing 28μl of gel purified PCR product with 4μl of 10x *Eco*RI buffer, 4μl of 1μg/ml BSA and 2μl each of *Eco*RI and *Sal*I in a total volume of 40μl. The digest was incubated at 37°C for 2 hours.

2.3.5.3 Purification of the *Eco* RI-*Sal* I digested PTEN Fragment and assessment of yield

The digested PTEN fragment was purified directly from solution using a Qiagen Gel Extraction Kit, according to the manufacturers' instructions for the clean-up of enzymatic reactions. 30µl of sterile water was used to elute the purified DNA from the spin column, and the elutate stored at –20°C. Yield was assessed as described in 2.3.7.3.

2.3.6 Transformation of *E.*coli with CMV-pEGFP-N1

2.3.6.1 Preparation of chemically competent JA221 cells by calcium chloride method

Aseptic technique was used for all bacterial manipulations, using a protocol modified from Maniatis, Sambrook & Fritsch, (1989). A 1ml aliquot of JA221 cells stored as a 50% glycerol stock at -80°C was thawed on ice. The 1ml of cells was inoculated into 100ml of LB in a 1L sterile flask and incubated at 37°C for 16 hours with shaking at 250 rpm. The following morning 10ml of the saturated culture was diluted into 90ml of LB and grown at 37°C and 250 rpm for approximately 2 hours, until and an absorbance (A^{650}) of 0.5-0.6 was reached.

The culture was then transferred into sterile pre-chilled 50ml Falcon tubes and incubated on ice for 10 minutes to inhibit further growth. The cells were centrifuged at 3,500 rpm at 4°C for 5 minutes in a pre-chilled Sorvall Super T21 centrifuge and the medium carefully removed. The cell pellets were

resuspended in 10ml of ice-cold 0.1M $MgCl_2$, incubated on ice for 5 minutes, and then centrifuged at 3,500 rpm at 4°C for 5 minutes.

Following careful aspiration of the supernatant, the cell pellets were gently resuspended in 1.5ml of ice-cold 0.1M $CaCl_2$ and held on ice in preparation for transformation. The cells were treated very carefully at this stage, as the cell membranes are highly permeable and easily ruptured if too much shear force is applied to the tube.

2.3.6.2 Transformation of Competent JA221 with CMV-pEGFP-N1

Using the competent JA221 described above, a 200µl aliquot of cells was added to a sterile thin-walled polypropylene culture tube for transformation using pre-chilled pipette tips, based on a protocol modified from Maniatis, Sambrook & Fritsch, (1989). 1µl of CMV-pEGFP-N1 was added to the cells and mixed by swirling gently with the pipette tip; the cells were then incubated on ice for 30 minutes to allow the plasmid DNA to bind to the bacterial cell wall.

To induce bacterial uptake of the DNA, the cells were heat-shocked by placing the tube in a water bath at exactly 42°C for 90 seconds, then transferred immediately to ice for 2 minutes. 800µl of room-temperature SOC medium (Appendix I.4) was added to the cells, which were incubated at 37°C for 1 hour at 220 rpm to allow expression of the kanamycin resistance gene encoded by the plasmid.

2.3.6.3 Plating out of the transformants

From the transformed cells prepared in Section 2.3.6.1, a 100µl aliquot was spread onto an L-Agar plate containing 50µg/ml kanamycin (Appendix I.4) using a sterile spreader and the plate inverted and placed in an incubator at 37^{0}C overnight. The plate was inspected for colony formation the following morning and stored inverted in a refrigerator until required.

2.3.7 Preparation of CMV-pEGFP-N1 Plasmid for Cloning

2.3.7.1 Small Scale Isolation of CMV-pEGFP-N1 DNA by Alkaline Lysis

From the plate prepared as described in Section 2.3.6.3, a single colony was picked using a sterile inoculating loop into 5ml of LB with kanamycin, (Appendix I.4), and incubated at 37°C for 16 hours at 250 rpm (Maniatis, Sambrook & Fritsch, (1989). Culture (3ml in total) was microcentrifuged in a 1.5ml Eppendorf tube at 13,000 rpm for 5 minutes, and the pellet resuspended by vortexing in 100µl of ice-cold Solution I (Appendix I.5).

Solution II (200µl, Appendix I.5) was added to the cell suspension and the tube gently inverted 5 times to lyse the cells. After incubation on ice for 3 minutes the lysate was observed to become clear, indicating complete lysis, and 150µl of ice-cold Solution III (Appendix I.5) was then added.

The tube was inverted twice and incubated on ice for 5 mins, prior to microcentrifugation at 13,000 rpm for 5 minutes at 4°C. 400µl of supernatant was transferred to a fresh sterile tube, an equal volume of phenol:chloroform:isoamyl alcohol added and the solution vortexed for 10 seconds. The phases were separated by centrifugation at 13,000 rpm for 2 minutes and 350µl of the supernatant transferred to a fresh sterile tube. To

precipitate the plasmid DNA 700µl of100% ice-cold ethanol was added to the tube, mixed by inversion and incubated at -20°C for 20 minutes.

The DNA was pelleted by centrifugation at 13,000 rpm for 5 minutes at 4°C and washed with 1 ml of ice-cold 70% ethanol. A final centrifugation at 13,000rpm for 10 minutes at 4°C was used to bring the pellet back to the bottom of the tube and the ethanol carefully aspirated.

The pellet was air-dried on the bench for approximately 2 hours until the DNA appeared transparent and dry, then resuspended in 40µl of 5mg/ml RNase A solution. Presence of the plasmid was confirmed by 1% agarose gel electrophoresis using 1µl of stock plasmid and a 1Kb molecular weight marker for a size comparison and to give an estimation of yield. Plasmid DNA was stored at -20°C until required.

2.3.7.2 Small-Scale Digestion of CMV-pEGFP-N1 with restriction endonucleases *Eco*RI and *Sal* I

Double digest of the plasmid was performed essentially as described in Section 2.3.5.2, using 5µl of plasmid DNA (extracted as described in Section 2.3.7.1) in a 20µl digest with 2µl of *Eco*RI (40U) and *Sal*I (40U).

2.3.7.3 Gel Extraction of the *Eco*RI-*Sal* I Linearised Plasmid

To remove the unwanted small fragment generated during the restriction digest, the digest was fractionated on a 1% agarose gel and the 4.7Kb band corresponding to linearised vector carefully excised using a sterile scalpel. The DNA was extracted using a Qiagen Gel Extraction Kit according to the manufacturers' instructions into 30µl of sterile water. Yield was assessed by

analysing 5µl of the purified digested vector and 5µl of purified digested PTEN on a 1% agarose gel. The purified plasmid was stored at -20°C until required.

2.3.8 Ligation

After assessing the yield of the double-digested PTEN fragment and plasmid, three ligation reactions were carried out at DNA molar ratios of approximately 1:1, 1:3 and 1:5 of vector : insert. This ensured that one of the reactions would contain the optimal amounts of each digested DNA fragment for efficient ligation. Ligations were performed by adding to the appropriate volumes of DNA 2.5µl of ligase buffer and 1µl of T4 DNA Ligase (NEB), in a total volume of 25µl. The reactions were incubated at 10°C for 16 hours on the block of a thermal cycler according to the instructions provided with the ligase.. A control ligation was also performed using 1µl of 100bp molecular weight marker under the same conditions, or at room temperature. To determine whether ligation had occurred, 10 µl of the three ligations and control reaction were subjected to 1% agarose gel analysis.

2.3.9 Introduction of Recombinant Plasmid DNA into E.coli cells

2.3.9.1 Transformation of Chemically Competent DH5α

Chemically competent DH5α (Invitrogen) were transformed with 5µl of each ligation reaction (Section 2.3.8), according to the manufacturers' recommendations, essentially as described in 2.3.6.2.

2.3.9.2 Plating Out and Analysis of the Transformants

LB-Agar plates containing 50μg/ml Kanamycin were prepared as described in Appendix I.4. Volumes of 20 or 50μl of each of the three transformation reactions were pipetted onto an agar plate and spread over the surface using a sterile spreader. A control plate was included which contained no antibiotic, onto which 20μl of DH5α was spread from the remainder of the stock competent cells. The plates (8 in total) were incubated at 37°C for 16 hours to allow colony formation. The number of colonies on each plate was noted by counting.

2.3.9.3 Confirmation of the presence of full length PTEN in the recombinant plasmids

Two medium-sized colonies were selected from each plate and inoculated into 5 ml of LB with 50 μg/ml kanamycin using sterile toothpicks, and grown for 16 hours at 37°C with shaking at 250 rpm. Each culture, (3ml), was used to isolate plasmid DNA by the alkaline lysis method as described in Section 2.3.7.1; to the remaining 2ml of culture an equal volume of sterile glycerol was added, shaken, and frozen at -70°C.

The extracted plasmid DNA was analysed by running 1μl of each plasmid preparation against 0.5μl of uncut pEGFP on a 1% agarose gel. A 1μl aliquot of each plasmid was then double-digested with 1μl each of *Eco*RI, *Sal*I and BSA in a total volume of 20μl as described previously. 10μl of each digest were analyzed by 1% agarose gel electrophoresis against 0.5μl of undigested pEGFP and 1μl of double-digested pEGFP.

2.3.10 Preparation of pRC-2 (clone 6A) plasmid DNA for Sequencing

Upon careful analysis of the results of gel electrophoresis of the double-digested plasmid samples, the clone 6A was selected and named pRC-2. To propagate the clone, the pRC-2 glycerol stock was thawed and 20µl spread onto an L-Agar/Kan selective plate, as described in Section 2.3.9.2. After 16 hours of incubation at 37°C a single colony was picked for overnight growth in selective LB as described in 1.7.3. From this preparation a stab culture was taken by dipping a sterile inoculating loop into the culture and 'stabbing' it into a selective L-agar tube (Appendix I.4). The tube was incubated at 37°C overnight then packaged on ice and sent for sequencing to Lark Technologies.

2.3.11 Subcellular Localisation and Distribution of PTEN

2.3.11.1 Preparation of Ultrapure Supercoiled Plasmid

To improve the transfection rate of pRC-2 into all the cell lines, the plasmid was prepared by an alternative technique to the one described in Section 2.3.7.1. Fresh LB selective plate was streaked with pRC-2 glycerol stock. An overnight culture was grown from a single colony picked from the plate and the plasmid isolated using a GenElute Plasmid Miniprep Kit, according to the manufacturer's instructions. Plasmid DNA was analysed by agarose gel electrophoresis, the concentration measured spectrophotometrically at 260nm and a stock solution of 1µg/µl prepared.

2.3.11.2 Transfection of cell lines with pRC-2 by Lipid-Mediated Transfer

Initial transfections were performed on the COS-7 and HEC-1B cell lines using the pRC-2 plasmid at a stock concentration of 1µg/µl. Cells lines were seeded on 13mm round coverslips placed in the wells of 24 well culture plates and grown to 50% confluence 24 hours prior to transfection with 0.6, 0.7, 0.8, 0.9 or 1.0µg of plasmid, as recommended by the manufacturers of the Lipofectamine reagents (Invitrogen).

Two commercial transfection reagents were tested; Lipofectamine and Lipofectamine 2000 (LF2K), using 2µl of each reagent combined with each concentration of plasmid. These cationic lipid reagents bind to DNA and permit transfer across the cell membrane, and are commonly used in place of electroporation or calcium phosphate methods (Maniatis, Sambrook & Fritsch, 1989). The lipid reagents were used to transfect the cells according to the manufacturer's instructions and these cells were then maintained in culture for 24 hours post-transfection to allow expression of the fusion protein.

The cells were washed twice with PBS, fixed in 200µl of ice-cold methanol for 10 minutes (Beppu, et al, 1994), and the nuclei stained with DAPI (1µg/ml) for 5 minutes. The stain was washed off twice with PBS and the coverslips mounted on microscope slides using a small drop of Fluoromount G aqueous mountant.

Slides were analysed by manual fluorescence microscopy using a U-V filter for DAPI and FITC filter for EGFP The microscope used was an Olympus BX60 microscope with a JVC 3-CCD digital camera and Image Grabber PC

V1.2 (Neotech Ltd,1995) software. Transfection efficiency using Lipofectamine and LF2K was recorded for each cell line.

2.3.12 Optimisation of Transfection

Adherence of the cells during fixing was improved by seeding onto coverslips that had been treated with polylysine. Prior to adding the cells, the coverslips were submerged in 200µl of a 5µg/ml solution of polylysine (Sigma) in sterile PBS for 20 minutes, according to the manufacturers' recommendations. The polylysine was aspirated, allowed to air dry for a few minutes and the cells pipetted into the wells of the culture plate. The experiment described above in 2.3.1.2 was repeated using polylysine-treated coverslips and HEC-1B and Ishikawa cell lines. Conditions resulting in the highest transfection rate and expression of EGFP were noted for each cell line.

2.3.13 Stimulation of Transfected Cell lines

The effect of TGF-ß1 and estrogen on the localization of pRC-2 was investigated in the HEC-1B and Ishikawa cell lines. The cell lines were transfected with 0.8-1.0µg of pRC-2 using 2µl Lipofectamine prior to treatment with the relevant compound.

2.3.13.1 Oestrogen

Transfected cells were stimulated with 10 or 100nM ß-Oestradiol (Appendix I.6) for various periods of time, based on work by Campbell, et al (2001). The

complete growth medium was replaced with reduced-serum medium (Appendix I.1) and the appropriate volume of hormone from the stock solution. HEC-1B cells were stimulated for 30 minutes and 1, 2, 6, or 24 hours. Ishikawa cells were stimulated for 24 or 48 hours using reduced-serum medium with and without phenol red, to ascertain whether this molecule (which has structural similarity to oestrogen) was affecting the results. After each time point the coverslips were washed, fixed, DAPI stained and mounted for microscopic analysis as described in Section 2.3.11.2.

2.3.13.2 TGF-ß1

Transfected cells were stimulated with 2 or 5ng/ml of TGF-ß1 (Appendix I.6) for 30 minutes, 1, 2 and 6 hours. After transfection the complete growth medium was replaced with reduced-serum medium (Appendix I.1) and the appropriate volume of cytokine from the stock solution. When stimulation was complete the coverslips were prepared for microscopic analysis as previously described.

2.3.14 Localisation of pRC-2 to Subcellular Compartments

To determine the sequestration of pRC-2 to subcellular compartments, transfected HEC-1B and Ishikawa and were used in double-labelling experiments. Monoclonal antibodies to the ER protein Colligin (Stressgen), PTEN (BD) and ß-Actin (Sigma), were used according to the manufacturers' guidelines. A polyclonal antibody against the golgi protein Mannosidase II

The supernatant was carefully removed and the pellet reuspended in 20 ml of Buffer A, prior to centrifugation at 3000 rpm for 15 minutes at room temperature. The supernatant was again discarded and the pellet reuspended in 1 ml of Buffer B (Appendix I.7), and transferred to a sterile 1.5 ml Eppendorf tube.

5M Sodium perchlorate (300µl) was added to the samples, which were mixed end-over-end for 10 minutes at room temperature followed by microcentrifugation at 14,000 rpm for 10 minutes at 4°C in a Heraus Microcentaur. To fresh Eppendorf tubes 600 µl of supernatant was transferred and 700 µl of ice-cold chloroform added. The samples were mixed end-over-end for 3 minutes at 4°C and then centrifuged at 14,000 rpm for 10 minutes at 4°C.

The top layer of each sample was carefully transferred to a clean tube and two volumes of ice-cold ethanol added, with gentle mixing. A final centrifugation at 14,000 rpm for 15 minutes at 4°C was performed, and the supernatant aspirated from resulting DNA pellets, which were air dried for 10 minutes. The dried pellets were reuspended in 200-500 ml of sterile distilled water and stored at –70°C.

2.4.1.2 Extraction of Patient DNA from archival material

DNA from archival material was extracted and made available for my use by kind permission of Dr Ken Feeley, University of Sheffield Medical School. The extractions were performed by a member of Dr Feeleys technical staff.

was kindly donated by Prof David Parkinson, and used according to his recommendations. Cell lines transfected as described previously were fixed in methanol, blocked for 1 hour with normal goat serum (NGS, Appendix II.6) and incubated with α-Colligin (1:200), α-Mannosidase II (1:70), α-PTEN (1:200) and α-ß-Actin (1:20,000) in NGS for 1 hour. The cells were washed twice with PBS and incubated with secondary α- mouse / rabbit Alexafluor 594 (1:200) in NGS for 45 minutes according to the enclosed instructions; the cells were then washed, DAPI stained and mounted.

2.4 MUTATIONAL ANALYSIS OF PTEN EXONS 3 & 5 IN ENDOMETRIAL DNA SAMPLES BY SINGLE STRAND CONFORMATION POLYMORPHISM ANALYSIS (SSCP)

2.4.1 Preparation of DNA Samples for SSCP Analysis

2.4.1.1 Extraction of DNA from whole human blood

Fresh human venous blood was collected from staff members into vacutubes containing EDTA and the tubes marked anonymously for processing using a method modified from Maniatis, Sambrook & Fritsch, (1989). Each blood sample (10-20ml) was transferred to sterile universal tubes and Buffer A (Appendix I.7) added to make a total volume of 50 ml. The samples were mixed end-over-end for 4 minutes at room temperature, followed by centrifugation at 3000 rpm for 15 minutes at room temperature in a Sorvall RT7 Plus centrifuge.

2.4.2 PCR of Patient & Control DNA for SSCP Analysis

PCR was carried out on patient DNA samples extracted from paraffin embedded archival tissue, and on control DNA prepared as described in Section 2.4.1.1. Oligonucleotide primers designed to amplify PTEN Exons 5 and 8, (Risinger et al, 1997), in two overlapping fragments of approximately 200bp in length for each exon were used. Primers 5A/5B and 5C/5D (Section 2.1.3) produced PCR products of 137bp and 186bp respectively, and 8A/8B and 8C/8D produced PCR products of 122bp and 245bp respectively.

PCR was performed using 1-5μl of patient DNA, 3mM magnesium chloride, 0.2 mM dNTPs, 0.5μl of RedHot Taq polymerase and 50pM of forward and reverse primer in 1 x reaction buffer, in a total volume of 25μl. Reactions were carried out using the PTEN I programme for all primer pairs 5C/D and 8A/B or the RIS2-2 programme for primers 5A/B (Appendix V). The PCR products (10μl) were analysed by agarose gel electrophoresis.

2.4.3 Preparation of Control PCR products for sequencing

To verify that the PCR products amplified from the control DNA were wild-type, and therefore suitable for use as SSCP controls, PCR fragments for each primer pair were sequenced following the extraction from 2% agarose gels using a Qiagen Gel Extraction Kit. The purified fragments were vacuum desiccated and sent to Lark Technologies where they were automatically sequenced using the respective PCR primers.

2.4.4 SSCP analysis

2.4.4.1 Large gel format, Hoefer 18 x 24cm

SSCP was performed essentially as described by Rhei, et al (1997) and Aveyard, et al (1999). A large format gel was used to enable the samples to be electrophoresed slowly overnight, (to minimize heat generation), and to give maximum separation of bands. The SSCP plates were cleaned thoroughly with ethanol and assembled using 1mm spacers. Gels were prepared at concentrations of either 0.5 x MDE, for exon sections 5CD and 8AB, or 0.6 x MDE for exon sections 5AB and 8CD all with 5% or 10% glycerol (Appendix I.9) and cast between the assembled glass plates.

Teflon combs (15 wells) were inserted into the gels, which were allowed to polymerize at room temperature for 3 hours. The polymerized gels were then chilled to 4°C for 2 hours, the combs were removed and the wells rinsed thoroughly with chilled 0.6 x TBE running buffer (Appendix I.9). The gels were then clamped into the gel tank and submerged in running buffer.

PCR products were prepared for SSCP analysis by mixing 2-4μl of sample with an equal volume of formamide buffer (Appendix I.9) and sterile water to a total volume of 10μl. Samples were then heated at 95°C for 10 minutes on a thermal cycler before being transferred to ice for 2 minutes. 10μl of each sample were loaded into the wells of the gel using gel loading tips; 0.5μl of molecular weight marker was also included in one well of each gel. The samples were subjected to electrophoresis at 18W constant power for 16 hours with an ambient temperature of 4°C.

2.4.4.2 Silver staining

Upon completion of electrophoresis the plates were removed from the tank and the gels developed initially using a silver staining protocol based on that of Merril, (1990). Briefly, the gels were fixed for 10 minutes, incubated with a silver solution for 15 minutes and washed with distilled water, prior to developing for 15 minutes. The gels were washed again and then a final fixer solution applied for 10 minutes (Appendix I.9).

To improve the sensitivity of detection a PlusOne DNA Silver Staining kit was later used for all gels, according to the manufacturer's instructions. Stained bands were visualized on a visible light box and photographed using a Kodak DC120 digital camera before being sealed in BioDesign gel wrap and allowed to dehydrate at room temperature for 24 hours. Bands observed for each patient sample were compared to those corresponding to the control DNA samples on each gel, and samples exhibiting bandshifts or extra bands were subjected to a repeated gel run.

For samples with confirmed bandshifts, the remaining PCR product was packaged on ice with aliquots of the relevant primer pairs and sent to Lark Technologies for sequencing.

CHAPTER 3

RESULTS

3.1 ANALYSIS OF EXPRESSION OF PTEN AND SELECTED GENES IN HEC-1B AND ISHIKAWA CELL LINES STIMULATED WITH TGF-ß1

The aim of this section was to evaluate the response of PTEN to stimulation by TGF-β1 in endometrial cell lines. Several studies of this nature have previously been published describing the response of PTEN to TGF-β1 in other cell lines, including keratinocytic and myeloid, but the data from these papers is conflicting and appears to be cell-line specific. Compounds which up-regulate PTEN expression may represent a useful therapeutic strategy in the non-surgical treatment of tumours.

To assess any biologically significant changes in PTEN expression, both mRNA and protein levels were studied in two epithelial cell lines of endometrial adenocarcinoma origin. The HEC-1B cell line, representing a moderately differentiated grade II carcinoma (Crescenzi & Palumbo, 2001), possesses wild-type PTEN (Yaginuma, et al 2000) and expresses the protein (Figure 10.1). Conversely, the Ishikawa cell line represents a well differentiated carcinoma, but has a frameshift deletion in exon 8 of PTEN (codon 289 deletion of A) which codes for a rapidly degraded protein truncated at codon 290 (Yaginuma, et al 2000).

For experimental control purposes RNA and protein expression of the housekeeping genes GAPDH and β-Actin were studied. Housekeeping genes, including those indicated, are constitutively expressed and necessary for cell survival, with highly stable expression levels that are unlikely to change under experimental conditions. The TGF-β1 responsive gene PAI-1

was also analysed, as levels of this gene have been widely reported to increase during TGF-β1 stimulation in many cell lines (Keeton, et al 1991, Fujimoto, et al 1996 & Jiang, et al 2003). mRNA expression of the pro-apoptotic protein Bcl-2 in HEC-1B was also analysed by RT-PCR, as this protein has been reported to be down-regulated in this cell line (Crescenzi, et al 2000). Levels of phospho-PTEN protein were also analysed using an antibody specific for phosphorylated Ser380, as phosphorylation of the PTEN tail influences stability, degradation and activity of the protein.

Stimulation with cytokine was performed in the presence of either 10% or 1% foetal calf serum, which contains varying amounts of TGF-β1. The 10-fold reduction in serum concentration was therefore used to discount any effects of cytokine in the growth medium. Cellular morphology, density, and proliferation were also studied to further elucidate any correlation between TGF-β1 stimulation and PTEN expression.

3.1.1 Analysis of mRNA expression

Cells were grown under serum-starved and non-starved conditions in order to assess any differences in response to TGF-β1 under different growth conditions. The cells were then treated with either 2ng/ml or 5ng/ml TGF-β1, RNA was extracted and quantitation of the yield and purity of RNA from each sample was performed. These procedures are detailed in Chapter 2, Sections 2.2.1 to 2.2.3. The results shown in Appendix VII indicated a good yield of RNA, the quality of which would be shown by electrophoresis. All samples were diluted to 1μg/μl prior to use in PCR.

Semi-quantitative analysis of mRNA for PTEN, PAI-1 and GAPDH

RT-PCR was performed as described in Chapter 2 Section 2.2.3 and the products separated by agarose gel electrophoresis (Chapter 2, Section 2.2.3.5). Results are displayed in Figures 10 to 14 as a time course (4 to 24 hours) with TGF-ß1 concentrations of 2ng/ml in red, 5ng/ml in blue and the control (no TGF-ß1) in white. A Yellow line indicates PCR control minus cDNA template and duplicate sets of data are labelled A and B. A 100bp ladder was included on each gel. Densitometric analysis of PCR products was performed as described in Chapter 2 and shown in Tables 3 to 7. Results below the detection limit of the software are indicated by the notation "nd" (no data). Using Microsoft Excel, the overall results of PTEN mRNA expression for each experiment were expressed graphically by plotting the mean mass of DNA for each set of data points (Graphs 1 to 3). Error bars were added after calculating the standard error of the mean values.

Results for HEC-1B serum non-starved electrophoresis are shown in Figures 10.1 to 10.4, and densitometric analysis is shown in Table 3 and Graph 1. This experiment was performed once, in duplicate. Results for HEC-1B serum starved electrophoresis experiments 1 and 2 are shown in Figures 11.1 to 11.4 and Figures 12.1 to 12.4, respectively, and densitometric analysis is shown in Table 4 and Table 5 respectively. Overall results for both independent experiments (performed in duplicate) are illustrated in Graph 2.

Results for Ishikawa serum non-starved electrophoresis are shown in Figures 13.1 to 14.4, and densitometric analysis is shown in Tables 6 and 7. This experiment was performed once in duplicate, and cDNA synthesis performed twice, in duplicate. Results for both experiments are illustrated in Graph 3.

Serum non-starved HEC-1B

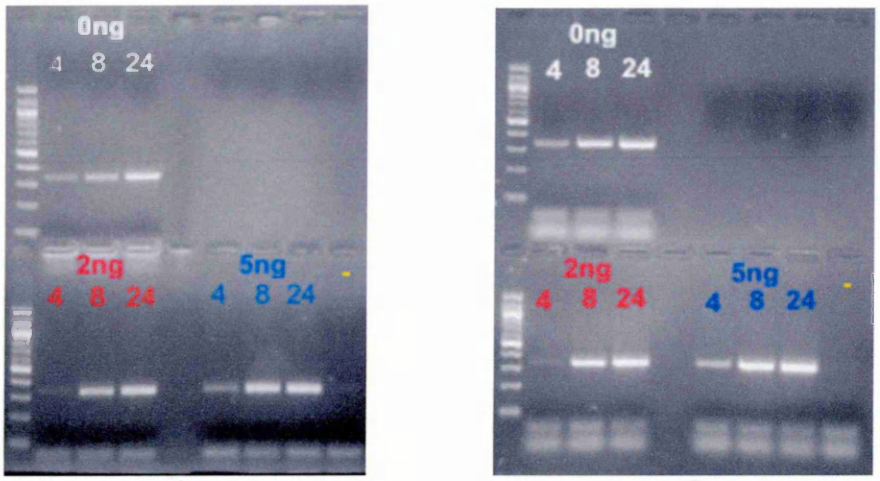

A B

Fig 10.1 PTEN expression in non-starved HEC-1B with duplicates A and B. No TGF-β1 control shown in white, 2ng/ml TGF-β1 in red, 5ng/ml TGF-β1 in blue over 4, 8 & 24 hours. PCR control (no DNA) is a yellow dash.

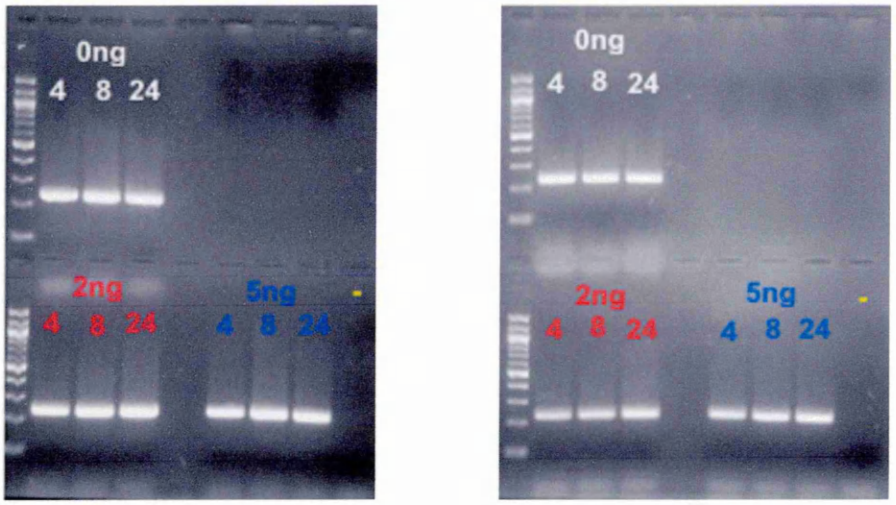

A B

Fig 10.2 GAPDH expression in non-starved HEC-1B with duplicates A and B. No TGF-β1 control shown in white, 2ng/ml TGF-β1 in red, 5ng/ml TGF-β1 in blue over 4, 8 & 24 hours. PCR control (no DNA) is a yellow dash.

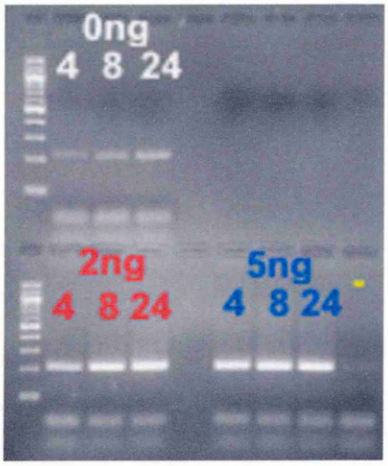

A

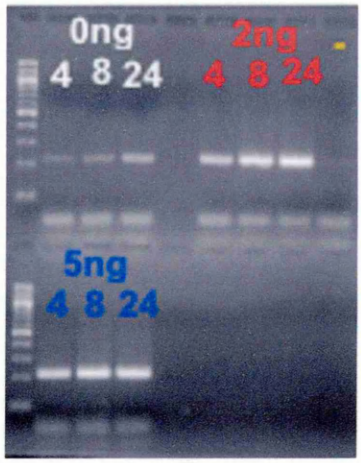

B

Fig 10.3 PAI-1 expression in non-starved HEC-1B with duplicates A and B. No TGF-β1 control shown in white, 2ng/ml TGF-β1 in red, 5ng/ml TGF-β1 in blue over 4, 8 & 24 hours. PCR control (no DNA) is a yellow dash.

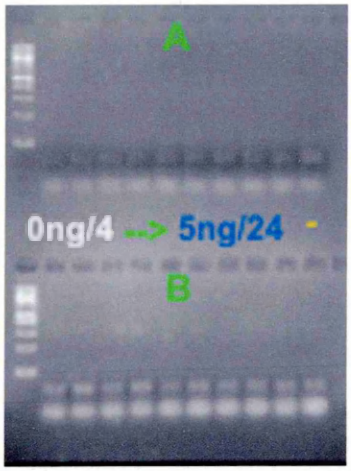

Fig 10.4 –RT controls for PTEN expression in non-starved HEC-1B, all samples and duplicates A/B. PCR control shown as yellow dash.

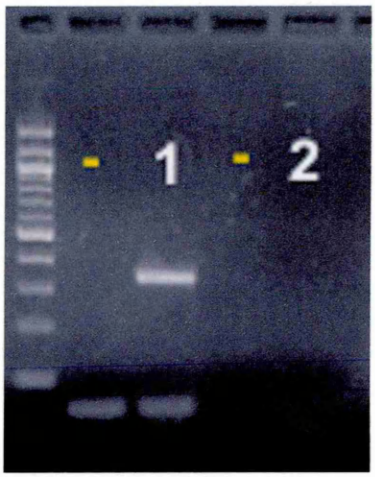

Fig 10.5 Expression of 1: PTEN and 2: TPIP with PCR control (yellow dash) in HEC-1B.

Serum non-starved HEC-1B stimulated with TGF-β1

This experiment was performed once, with duplicate flasks A and B from which cDNA was prepared for RT-PCR using primers for PTEN, PAI-1 and GAPDH. The analysis of RT-PCR products shown in Figure 11.1 show a subtle time and dose-dependant increase in PTEN mRNA expression in samples stimulated with TGF-β1 when compared to the controls. The response of PAI-1 in Figure 10.3 indicated a strong time and dose-dependant increase in expression (approximately four-fold) compared to the unstimulated controls, in a manner concurrent with published data (Lee, et al 1999).

2ng/ml TGF- β1

From Figure 10.1 it was seen that under stimulation with 2ng/ml of cytokine, no increase in PTEN expression was detected at 4 hours. An average increase in expression of ~1.5-times was observed at 8 hours but little change at 24 hours was observed compared to the controls.

Figure 10.3 shows PAI-1 mRNA expression in response to cytokine stimulation. At 4 hours, an increase of ~4-times compared to the controls was observed. At 8 and 24 hours an increase in PAI-1 expression of ~3.5-times and 3-times respectively was detected in comparison to the controls.

5ng/ml TGF- β1

Samples stimulated with 5ng/ml of TGF-β1 exhibited an increase in PTEN expression at 4 hours of ~1.4 times. At 8 hours the average increase in

expression was ~2-times that of the controls and at 24 hours a small increase of ~1.2-times was observed.

Figure 10.3 shows PAI-1 mRNA expression in response to cytokine stimulation. At 4 hours, an increase of ~5-times compared to the controls was observed. At 8 and 24 hours an increase in PAI-1 expression of ~4-times and 3-times respectively was detected in comparison to the controls.

Expression levels of GAPDH shown in Figure 10.2 remained constant in all samples, indicating that TGF-β1 had no discernable effect on this housekeeping gene.

Figure 10.4 shows RT-PCR of reverse transcription controls using the PTEN primers 2a and 3. All samples are free of PCR product and therefore the cDNA samples prepared were free of DNA contamination. The results observed in Figures 10.1 to 10.3 were also shown by densitometric analysis of band intensities in Table 3.

The additional PCR shown in Figure 10.5 was performed using 4 hour control cDNA and primers for PTEN (2a & 3) and TPIP (TPTE and PTEN homologous inositol lipid phosphatase). Sequences of the primers are listed in Chapter 2, Section 2.1.3. This PCR was included to demonstrate that amplification of TPIP, a PTEN homologue, had not occurred and therefore all such PCR reactions were specific for PTEN only.

Expression of Bcl-2 mRNA was undetectable in the 1:4 dilutions of cDNA used to perform RT-PCR. Feint bands were visible in all samples when undiluted cDNA was used, indicating that this cell line expressed very little Bcl-2 mRNA, and stimulation with TGF-β1 did not noticeably alter expression levels. The results are not shown due to the feint bands being very difficult to

photograph. Very low expression of Bcl-2 protein has previously been reported in the HEC-1B cell line, and is indicative of malignant change from hyperplasia to carcinoma (Crescenzi & Palumbo, 2001).

Summary of Results

A modest up-regulation of PTEN mRNA was observed in cells stimulated with TGF-β1 compared to the controls. The increase in transcripts was more strongly observed in cells stimulated with 5ng/ml of cytokine, which was seen to be approximately double after 8 hours compared to the unstimulated controls.

Table 3 HEC-1B Serum non-starved PCR Densitometry					
PTEN PCR A			**PTEN PCR B**		
TGF-β1(ng) /Time (hrs)	Mass ng	Peak OD	TGF-β1(ng) /Time (hrs)	Mass ng	Peak OD
0ng/4	41.15	161	0ng/4	59.49	161
8	114	187	8	123.6	194
24	199.7	194	24	224.4	220
2ng/4	28.31	91	2ng/4	45.43	91
8	169.6	194	8	224.4	224
24	209.6	210	24	253.3	224
5ng/4	63.45	142	5ng/4	74.3	139
8	194.8	207	8	254.6	227
24	237.5	210	24	280.2	251
GAPDH PCR A			**GAPDH PCR B**		
TGF-β1(ng) /Time (hrs)	Mass ng	Peak OD	TGF-β1(ng) /Time (hrs)	Mass ng	Peak OD
0ng/4	332.11	252	0ng/4	321.9	251
8	330.31	252	8	320.64	253
24	332.13	252	24	321.71	253
2ng/4	330.4	251	2ng/4	313.2	250
8	332	253	8	319.81	253
24	334.2	254	24	320.21	254
5ng/4	331.16	253	5ng/4	320.3	252
8	332.11	254	8	320.6	254
24	333.5	254	24	321	252
PAI-1 PCR A			**PAI-1 PCR B**		
TGF-β1(ng) /Time (hrs)	Mass ng	Peak OD	TGF-β1(ng) /Time (hrs)	Mass ng	Peak OD
0ng/4	40.93	89	0ng/4	41.45	91
8	70.12	117	8	70.55	117
24	110.67	117	24	114.4	118
2ng/4	176.3	218	2ng/4	179.4	218
8	261.5	245	8	261.3	245
24	295.1	254	24	293.2	252
5ng/4	200	220	5ng/4	196.6	220
8	285.64	254	8	287.3	238
24	294.4	254	24	296.8	238

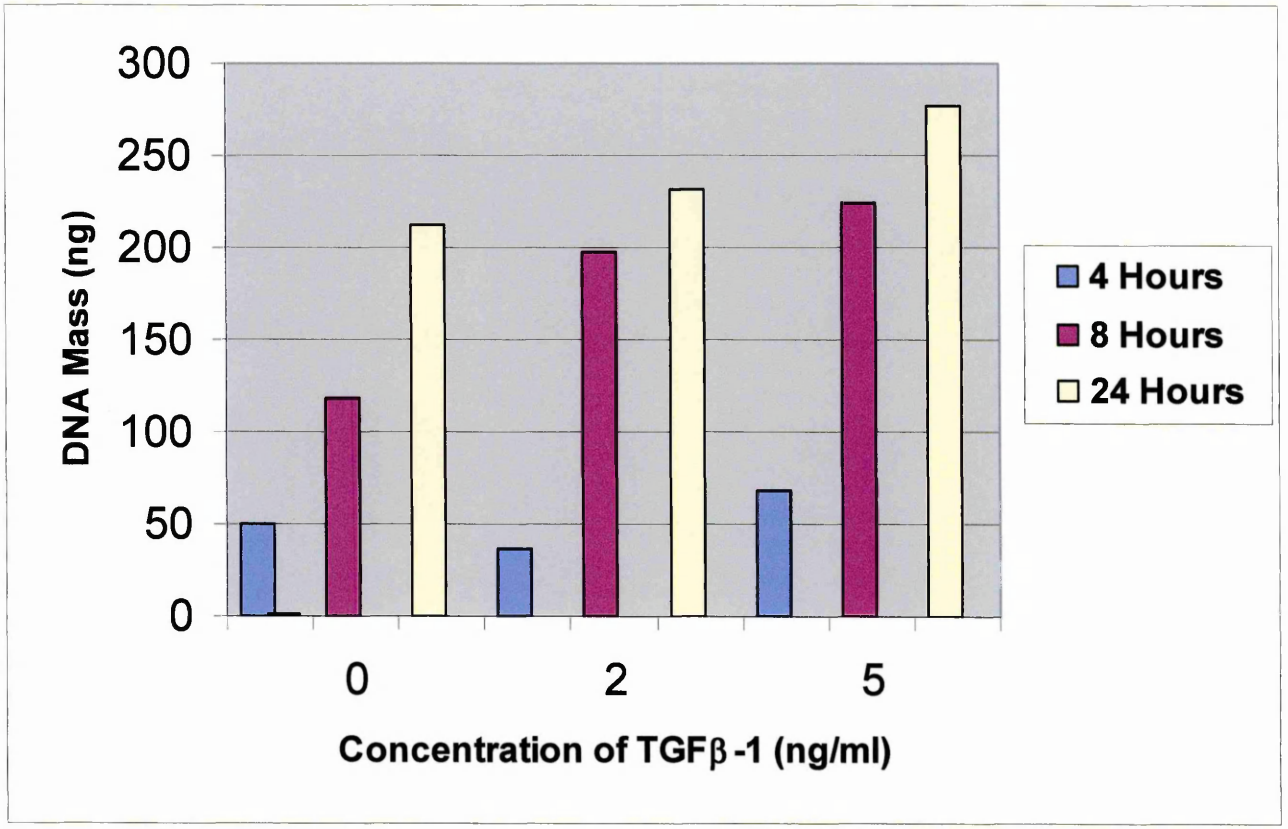

Graph 1 Expression of PTEN mRNA in serum non-starved HEC-1B stimulated with TGF-β1. Stimulation with cytokine was performed over 4 (blue bars), 8 (purple bars) & 24 hours (yellow bars) with 0ng/ml (control), 2ng/ml & 5ng/ml TGF-β1 in the presence of 10% foetal calf serum (complete medium). RT-PCR was performed using PTEN primers 2a and 3 and bands separated by gel electrophoresis prior to densitometric analysis. Data indicates a modest dose and time-dependant increase in PTEN mRNA expression compared to the controls. The stimulation experiment was performed once, in duplicate, (overall n=2) and data is presented as mean ± SEM of densitometry readings.

Serum starved HEC-1B, Experiment 1

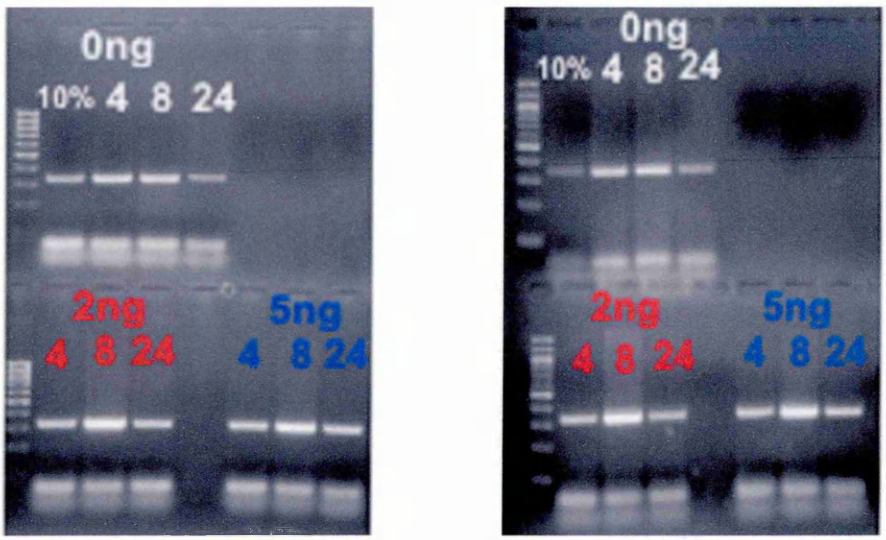

A B

Fig 11.1 PTEN expression in serum-starved HEC-1B with duplicates A and B. No TGF-β1 control shown in white, 2ng/ml TGF-β1 in red, 5ng/ml TGF-β1 in blue over 4, 8 & 24 hours. PCR control (no DNA) is a yellow dash.

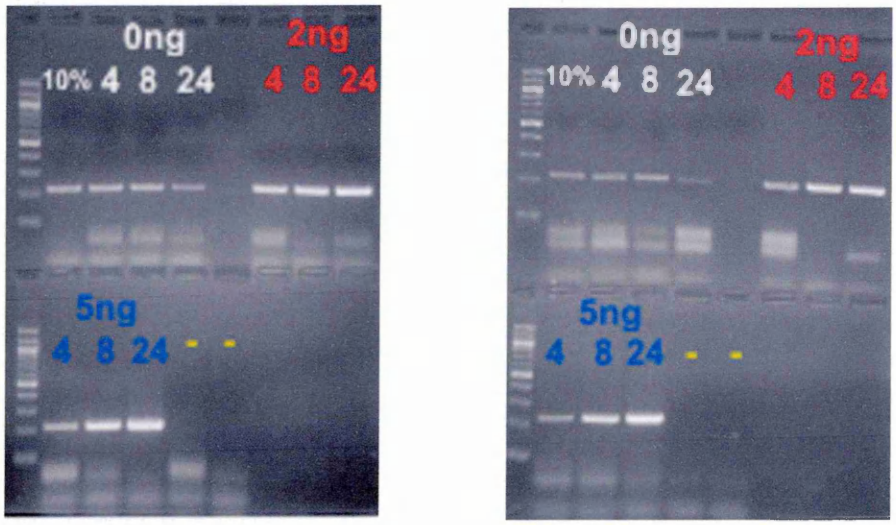

A B

Figure 11.2 PAI-1 expression in serum-starved HEC-1B with duplicates A and B. No TGF-β1 control shown in white, 2ng/ml TGF-β1 in red, 5ng/ml TGF-β1 in blue over 4, 8 & 24 hours. PCR control (no DNA) is a yellow dash.

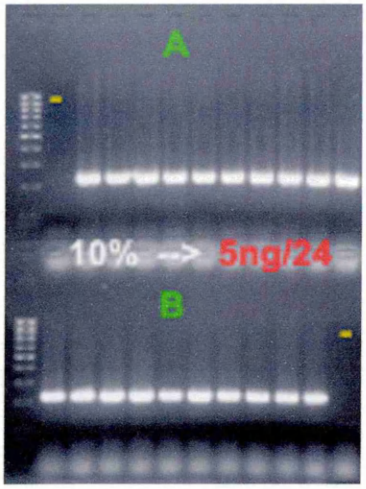

Fig 11.3 GAPDH expression in serum-starved HEC-1B with duplicates A and B. All samples from TGF-β1 (white) to 5ng/ml TGF-β1 (red) and duplicates A/B. PCR control shown as yellow dash

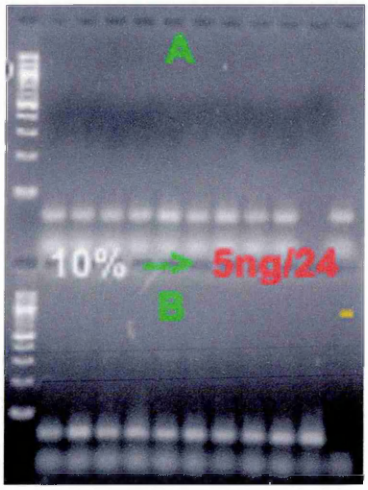

Fig 11.4 –RT controls for PTEN expression in serum starved HEC-1B. All samples from TGF-β1 (white) to 5ng/ml TGF-β1 (red) and duplicates A/B. PCR control shown as yellow dash.

Serum-starved HEC-1B stimulated with TGF-β1

This experiment was performed twice, with duplicate flasks A and B from which cDNA was prepared for RT-PCR using primers for PTEN, PAI-1 and GAPDH. The two experiments were performed independently and were donated experiments 1 and 2 respectively.

Experiment 1

The analysis of RT-PCR products shown in Figure 11.1 show a subtle time and dose-dependant increase in PTEN mRNA expression in samples stimulated with TGF-β1 when compared to the controls, with a slightly different response pattern to that observed in the non-starved experiments. Reduction of serum initiated a 2-fold increase in expression, as observed between the 10% serum controls and 4 hour serum-starved controls. Modulation of PTEN expression during serum starvation has been reported previously in neuronal cells (Kyrylenko, et al 1999). The response of PAI-1 in Figure 11.3 indicated a strong time and dose-dependant increase in expression (approximately three-fold) compared to the unstimulated controls.

2ng/ml TGF- β1

From Figure 11.1 it was seen that under stimulation with 2ng/ml of cytokine, no increase in PTEN expression was detected at 4 hours. An average increase in expression of ~2-times was observed at 8 hours and maintained over 24 hours compared to the controls.

Figure 11.2 shows PAI-1 mRNA expression in response to cytokine stimulation. At 4 hours, negligible increase of expression compared to the

controls was observed. At 8 and 24 hours an increase in PAI-1 expression of ~2-times and 3-times respectively was detected in comparison to the controls.

5ng/ml TGF- β1

Samples stimulated with 5ng/ml of TGF-β1 exhibited an increase in PTEN expression at 4 hours of ~2-times. At 8 hours the average increase in expression was ~2-times, which was again maintained over the 24 hour period when compared to the controls.

Figure 11.2 shows PAI-1 mRNA expression. At 4 hours, very little increase of expression compared to the controls was observed. At 8 and 24 hours an increase in PAI-1 expression of ~2-times and 3-times respectively was detected in comparison to the controls.

Expression levels of GAPDH shown in Figure 11.3 remained constant in all samples, indicating that TGF-β1 had no detectable effect on this housekeeping gene.

Again, Bcl-2 levels were undetectable in diluted cDNA samples but feint bands were detected using undiluted cDNA as observed for serum non-starved HEC-1B. TGF-β1 did not appear to alter expression of Bcl-2 mRNA from the slight bands seen in the controls (data not shown).

Figure 11.4 shows RT-PCR of reverse transcription controls using the PTEN primers 2a and 3. All samples are free of PCR product and therefore the cDNA samples prepared were free of DNA contamination. The results observed in Figures 11.1 to 11.3 were also shown by densitometric analysis of band intensities in Table 4.

Table 4 HEC-1B Serum-Starved Experiment 1 PCR Densitometry					
PTEN PCR A			**PTEN PCR B**		
TGF-β1(ng) /Time (hrs)	Mass ng	Peak OD	TGF-β1(ng) /Time (hrs)	Mass ng	Peak OD
10%	82.76	175	10%	63.6	128
0ng/4	124.4	205	0ng/4	122.63	206
8	115.6	208	8	116	214
24	69.99	156	24	68.91	158
2ng/4	141.5	192	2ng/4	143.2	205
8	264.7	250	8	264	250
24	130.7	196	24	126.4	193
5ng/4	149	215	5ng/4	149	214
8	254.7	247	8	255.1	246
24	132	212	24	130.2	202
GAPDH PCR A			**GAPDH PCR B**		
TGF-β1(ng) /Time (hrs)	Mass ng	Peak OD	TGF-β1(ng) /Time (hrs)	Mass ng	Peak OD
10%	332.4	255	10%	330.2	247
4	333.1	254	4	331.11	252
8	333	255	8	331	252
24	331.64	254	24	333.7	252
2ng/4	331.11	254	2ng/4	329.6	252
8	330.16	254	8	334.3	251
24	330.9	255	24	332	251
5ng/4	330	253	5ng/4	321.9	250
8	332	253	8	332	253
24	334.2	255	24	331.8	254
PAI-1 PCR A			**PAI-1 PCR B**		
TGF-β1(ng) /Time (hrs)	Mass ng	Peak OD	TGF-β1(ng) /Time (hrs)	Mass ng	Peak OD
10%	47.3	92	10%	60	146
0ng/4	54	102	0ng/4	61.4	143
8	56.4	122	8	61.1	147
24	40.2	87	24	47.5	96
2ng/4	60.8	147	2ng/4	76	151
8	89.6	174	8	113.3	196
24	110.3	193	24	176	219
5ng/4	61	149	5ng/4	64	155
8	92.5	188	8	120.7	204
24	121	201	24	200.6	241

Serum starved HEC-1B, Experiment 2

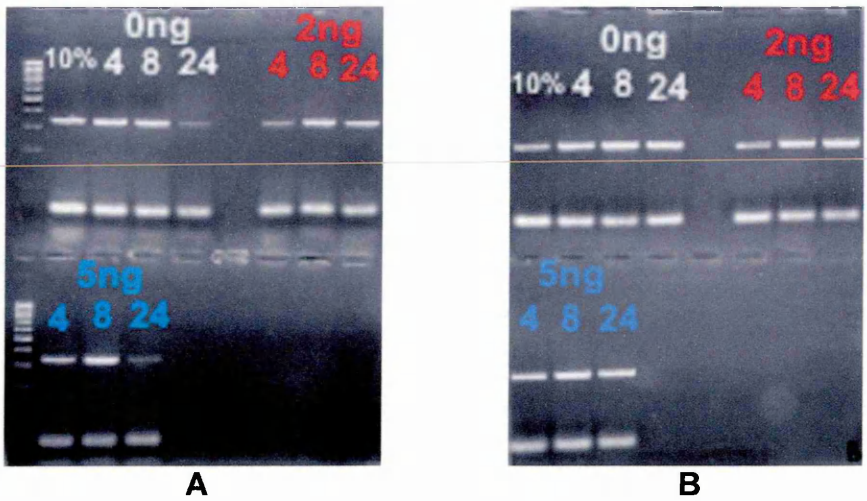

A B

Fig 12.1 Expression of PTEN in serum-starved HEC-1B with duplicates A and B. No TGF-β1 control shown in white, 2ng/ml TGF-β1 in red, 5ng/ml TGF-β1 in blue over 4, 8 & 24 hours. PCR control (no DNA) is a yellow dash.

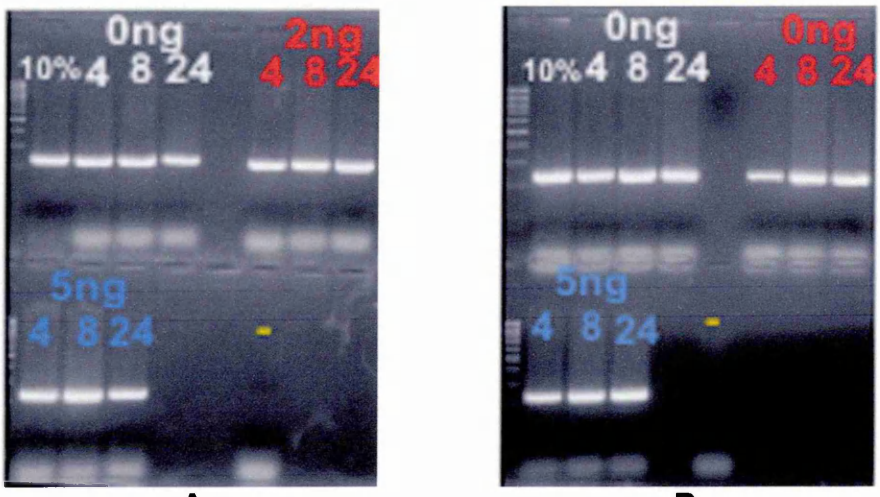

A B

Figure 12.2 Expression of GAPDH in serum-starved HEC-1B with duplicates A and B. No TGF-β1 control shown in white, 2ng/ml TGF-β1 in red, 5ng/ml TGF-β1 in blue over 4, 8 & 24 hours. PCR control (no DNA) is a yellow dash.

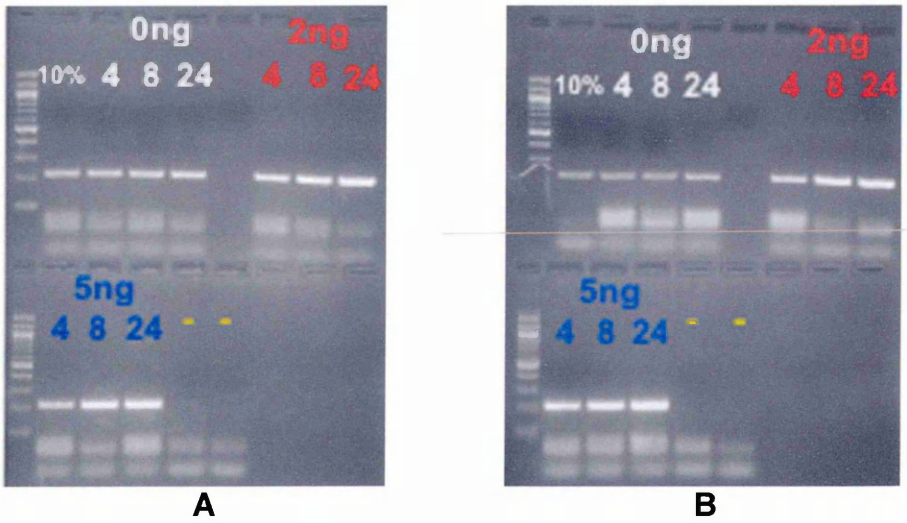

Fig 12.3 Expression of PAI-1 in serum-starved HEC-1B with duplicates A and B. No TGF-β1 control shown in white, 2ng/ml TGF-β1 in red, 5ng/ml TGF-β1 in blue over 4, 8 & 24 hours. PCR control (no DNA) is a yellow dash

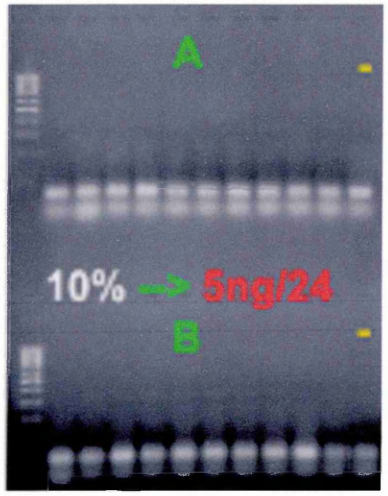

Fig 12.4 –RT controls for PTEN expression in serum-starved HEC-1B with duplicates A and B in green No TGF-β1 control (white), to 5ng/ml TGF-β1(red) over 4, 8 & 24 hours. PCR control (no DNA) is a yellow dash

Experiment 2

The analysis of RT-PCR products shown in Figure 12.1 again show a subtle overall increase in PTEN mRNA expression in samples stimulated with TGF-β1, with a two-fold peak at 8 hours as observed in serum-starved Experiment 1. This increase was again maintained over 24 hours as seen in Experiment 1 (Figure 11.1), with the exception of the 5ng/ml sample at 24 hours from flask A. This sample did not show the 2-fold increase in PTEN expression and was most likely due to experimental error.

Expression levels of GAPDH shown in figure 12.2 were constant, and PAI-1 in Figure 12.3 showed the same 3-fold increase in expression as seen in Experiment 1. Results for Bcl-2 were as described for serum-starved experiment 1, with only feint bands detected in RT-PCR with undiluted cDNA and no change in expression under TGF-β1 stimulation (data not shown). All RT-PCR controls were free of contamination as shown in Figure 12.4 and the results observed in Figures 12.1 to 12.3 were additionally shown by densitometric analysis of band intensities (Table 5).

Summary of Results for Experiments 1 & 2

A modest up-regulation of PTEN mRNA was observed in cells stimulated with TGF-β1 compared to the controls. The increase in transcripts was more strongly observed in cells stimulated with 5ng/ml of cytokine, which was seen to be approximately double after 4 hours compared to the unstimulated controls, and was maintained over the 24 hour period.

In both serum non-starved and serum-starved HEC-1B cells treated with TGF-β1, a modest time and dose-dependant increase in PTEN mRNA

expression was observed. This change in expression was quite similar regardless of serum levels, although serum-starvation did appear to yield a stronger induction of PTEN mRNA at 8 hours of stimulation with both concentrations of cytokine.

Notable, the response appeared to differ slightly between the controls for these experiments which were not treated with cytokine, indicating the presence of serum may alter PTEN mRNA levels. For example, PTEN expression in serum non-starved HEC-1B controls increases slightly in a linear manner over the 24 period of incubation. Cells which were serum-starved, however, demonstrated a gradual reduction in PTEN transcript levels in a linear manner over the 24 hour period. The significance of this is not clear from these results, but as a decrease in PTEN mRNA levels was observed in the controls in reduced serum medium this could be due to lower level of cytokines in the medium, including TGF-β1, reducing overall PTEN levels.

Table 5 HEC-1B serum-starved experiment 2 PCR densitometry					
PTEN PCR A			**PTEN PCR B**		
TGF-β1(ng) /Time (hrs)	Mass ng	Peak OD	TGF-β1(ng) /Time (hrs)	Mass ng	Peak OD
10%	149.7	200	10%	139	191
0ng/4	163.8	204	0ng/4	164.1	201
8	133.2	204	8	167.5	203
24	59.28	157	24	167.3	210
2ng/4	70.1	173	2ng/4	143.7	209
8	187.4	252	8	176.4	225
24	149.3	165	24	170	224
5ng/4	147.3	220	5ng/4	151.8	207
8	187.6	257	8	188.4	236
24	57.9	150	24	165.2	205
GAPDH PCR A			**GAPDH PCR A**		
TGF-β1(ng) /Time (hrs)	Mass ng	Peak OD	TGF-β1(ng) /Time (hrs)	Mass ng	Peak OD
10%	329.3	249	10%	334.7	245
0ng/4	329	241	0ng/4	332.6	244
8	329.11	241	8	334.4	245
24	323.21	241	24	333.28	243
2ng/4	330	247	2ng/4	329.8	244
8	330.4	246	8	333.71	246
24	333	246	24	334.67	247
5ng/4	332	244	5ng/4	330.5	241
8	334.2	245	8	333.5	243
24	332.5	245	24	333.2	245
PAI-1 PCR A			**PAI-1 PCR B**		
TGF-β1 (ng) /Time (hrs)	Mass ng	Peak OD	TGF-β1 (ng) /Time (hrs)	Mass ng	Peak OD
10%	63	147	10%	50	103
0ng/4	64	149	0ng/4	51.1	110
8	66.4	149	8	51	114
24	65	134	24	53.3	125
2ng/4	74	153	2ng/4	74.9	158
8	115.1	189	8	112.4	195
24	174.6	217	24	147	210
5ng/4	66	152	5ng/4	80	156
8	117.2	200	8	123.6	202
24	197	237	24	205	240

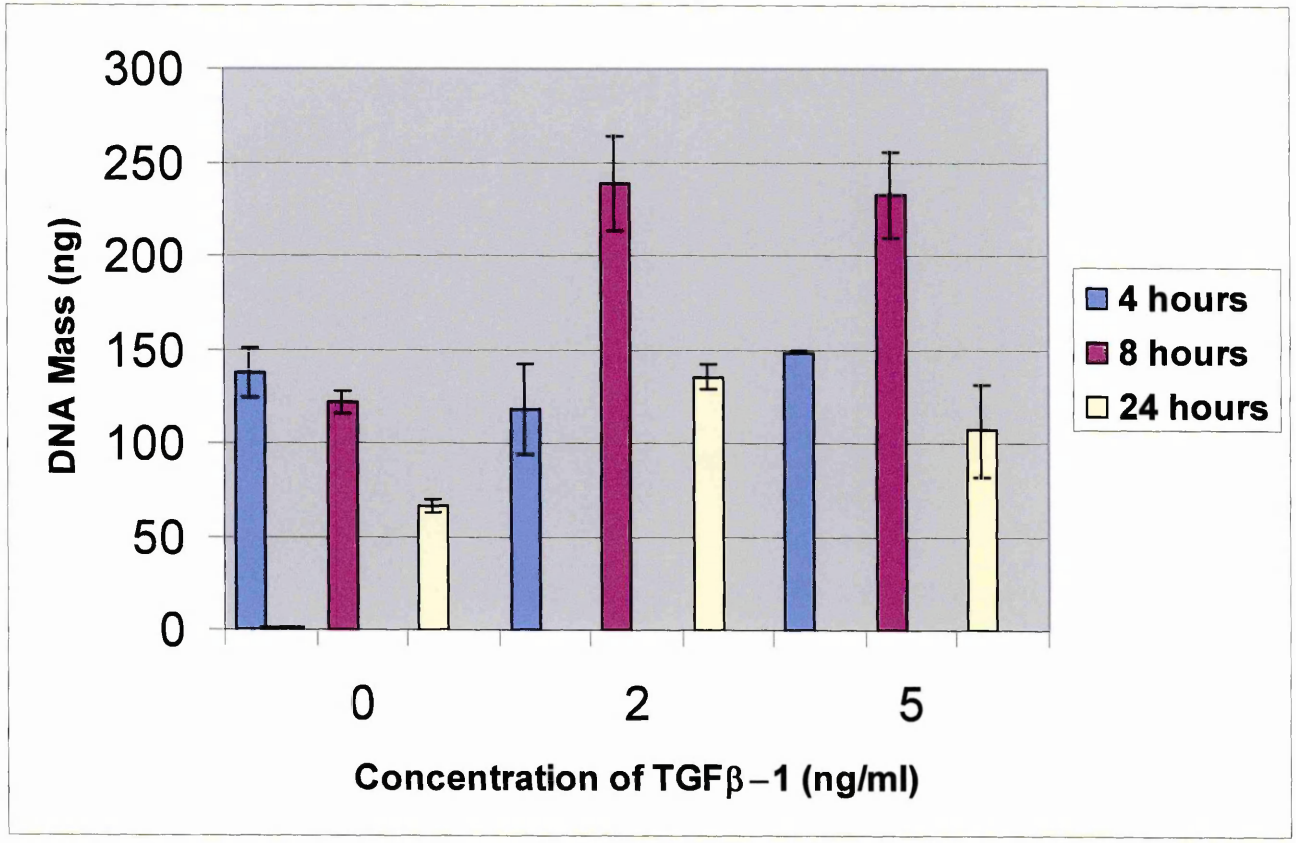

Graph 2 Expression of PTEN mRNA in serum-starved HEC-1B stimulated with TGF-β1. Stimulation with cytokine was performed over 4 (blue bars), 8 (purple bars) & 24 hours (yellow bars) with 0ng/ml (control), 2ng/ml & 5ng/ml TGF-β1 in the presence of 1% foetal calf serum (reduced serum medium). RT-PCR was performed using PTEN primers 2a and 3 and bands separated by gel electrophoresis prior to densitometric analysis. Data indicates a modest dose and time-dependant increase in PTEN mRNA expression after 8 hours compared to the controls. The stimulation experiment was performed twice, in duplicate, (overall n=4) and data is presented as mean ± SEM of densitometry readings.

Serum non-starved Ishikawa cells, Experiment 1

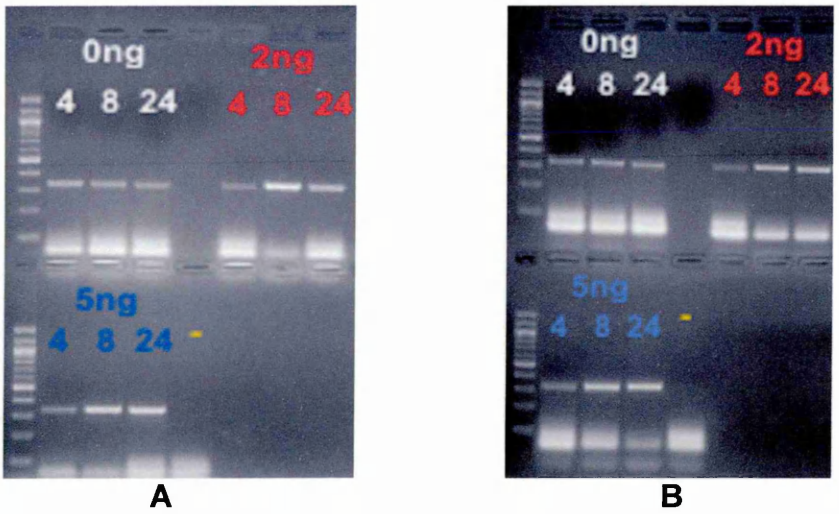

Fig 13.1 Expression of PTEN in non-starved Ishikawa with duplicates A and B. No TGF-β1 control shown in white, 2ng/ml TGF-β1 in red, 5ng/ml TGF-β1 in blue over 4, 8 & 24 hours. PCR control (no DNA) is a yellow dash

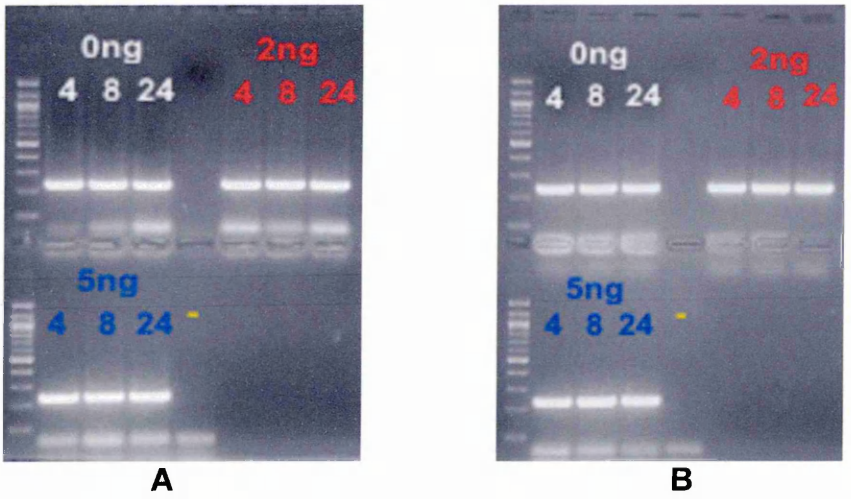

Fig 13.2 Expression of GAPDH in non-starved Ishikawa with duplicates A and B. No TGF-β1 control shown in white, 2ng/ml TGF-β1 in red, 5ng/ml TGF-β1 in blue over 4, 8 & 24 hours. PCR control (no DNA) is a yellow dash.

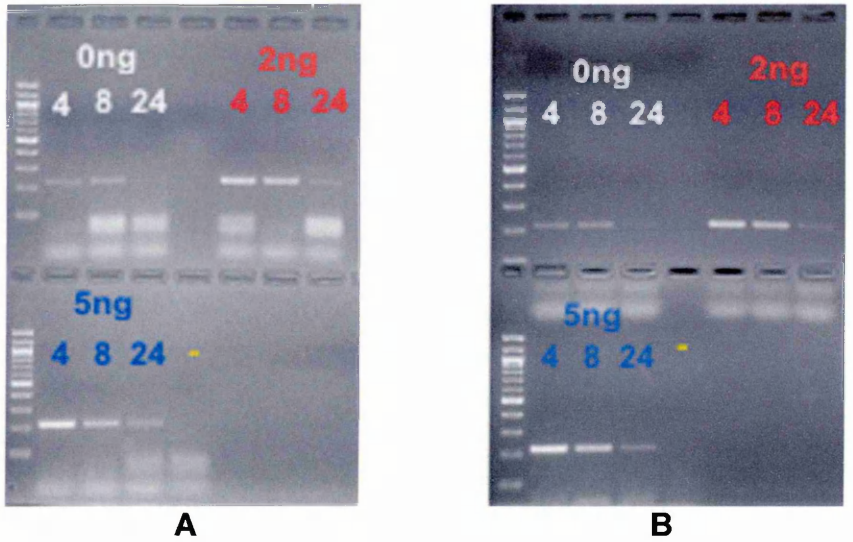

A B

Fig 13.3 Expression of PAI-1 in non-starved Ishikawa with duplicates A and B. No TGF-β1 control shown in white, 2ng/ml TGF-β1 in red, 5ng/ml TGF-β1 in blue over 4, 8 & 24 hours. PCR control (no DNA) is a yellow dash

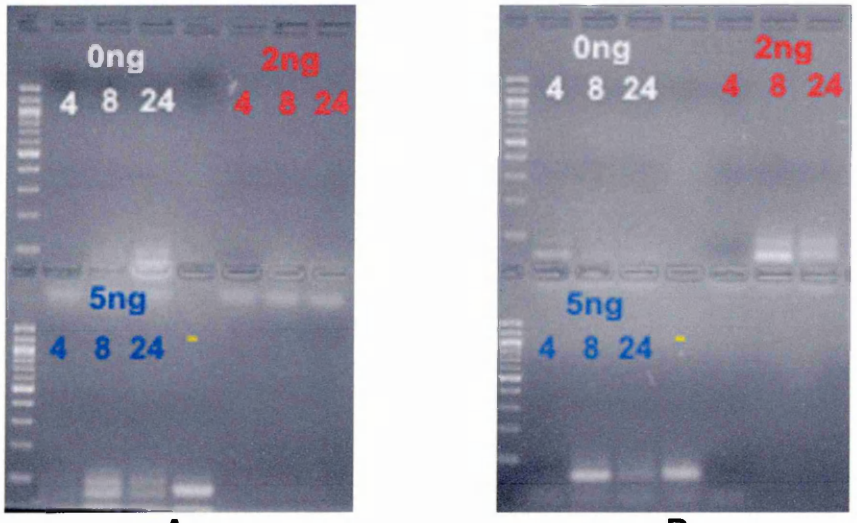

A B

Fig 13.4–RT controls for PTEN expression in non-starved Ishikawa with duplicates A and B. No TGF-β1 control shown in white, 2ng/ml TGF-β1 in red, 5ng/ml TGF-β1 in blue over 4, 8 & 24 hours. PCR control (no DNA) is a yellow dash

Serum non-starved Ishikawa cells stimulated with TGF-β1

This experiment was performed once, with duplicate flasks A and B. From these duplicate flask, cDNA was prepared twice on separate occasions for RT-PCR using primers for PTEN, PAI-1 and GAPDH. The two individual batches of cDNA were designated as experiments 1 and 2 respectively.

Experiment 1

The analysis of RT-PCR products shown in figure 13.1 show a modest time and dose-dependant two-fold increase in PTEN mRNA expression in samples stimulated with TGF-β1 at 8 hours, similar to that observed in serum non-starved HEC-1B. This cell line, which has a mutant copy of PTEN, also responded to cytokine stimulation by up-regulating expression of the TGF-β1-responsive gene PAI-1,but the expression pattern was different from that observed for HEC-1B. In ISK cells, induction of mRNA for PAI-1 was rapid and maximal at 4 hours, declining thereafter. This pattern of expression has also been described in A594 (Keska-Oja, et al 1988) and rat mesangial cells (Jiang, et al 2003).

2ng/ml TGF-β1

From Figure 13.1 it was seen that under stimulation with 2ng/ml of cytokine, no increase in PTEN expression was detected at 4 hours. An average increase in expression of ~2-times was observed at 8 hours and maintained over 24 hours compared to the controls.

Figure 13.3 shows PAI-1 mRNA expression in response to cytokine stimulation is essentially the reverse of that observed in HEC-1B. At 4 hours,

a ~2-fold increase in expression compared to the controls was observed. At 8 and 24 hours the levels of PAI-1 expression slowly diminished but was still detectable after 24 hours, whereas no bands were observed in the unstimulated controls.

5ng/ml TGF-β1

Figure 13.1 shows that under stimulation with 5ng/ml of cytokine, no increase in PTEN expression was detected at 4 hours. An average increase in expression of ~2-times was observed at 8 hours and maintained over 24 hours compared to the controls.

Figure 13.3 shows PAI-1 mRNA expression in response to cytokine stimulation. At 4 hours, a ~3-fold increase in expression compared to the controls was observed. At 8 and 24 hours the levels of PAI-1 expression diminished but was still detectable after 24 hours, with ~2-times the level of expression remaining at 24 hours compared to samples stimulated with 2mg/ml of cytokine.

Expression levels of GAPDH shown in Figure 13.2 are constant throughout, and all RT-PCR controls were free of contamination as shown in Figure 13.4. The results observed in Figures 13.1 to 13.3 were again shown by densitometric analysis of band intensities (Table 6).

Table 6 Ishikawa Serum Non-starved, Experiment 1 PCR Densitometry					
PTEN PCR A			**PTEN PCR B**		
TGF-β1(ng) /Time (hrs)	Mass ng	Peak OD	TGF-β1(ng) /Time (hrs)	Mass ng	Peak OD
0ng/4	59.86	141	0ng/4	57.3	121
8	52.73	113	8	62	148
24	49.9	92	24	61.52	154
2ng/4	42.85	89	2ng/4	43.7	81
8	120.04	198	8	114.9	193
24	63.7	150	24	93.8	172
5ng/4	51.4	113	5ng/4	66	115
8	118	195	8	120.1	197
24	114.1	186	24	121	196
GAPDH PCR A			**GAPDH PCR B**		
TGF-β1(ng) /Time (hrs)	Mass ng	Peak OD	TGF-β1(ng) /Time (hrs)	Mass ng	Peak OD
4	326.3	255	4	333.4	254
8	330	255	8	334	254
24	331.5	254	24	334	255
2ng/4	330.04	255	2ng/4	335.1	256
8	330	256	8	334.21	255
24	333.1	254	24	335	255
5ng/4	329	254	5ng/4	335.3	253
8	334.3	255	8	334	254
24	332	255	24	334.6	255
PAI-1 PCR A			**PAI-1 PCR B**		
TGF-β1(ng) /Time (hrs)	Mass ng	Peak OD	TGF-β1(ng) /Time (hrs)	Mass ng	Peak OD
0ng/4	40.56	89	0ng/4	43.12	96
8	43.15	95	8	45.5	99
24	nd	nd	24	nd	nd
2ng/4	71.8	159	2ng/4	94.33	176
8	62.71	147	8	70.4	155
24	25.4	58	24	24.91	57
5ng/4	124	192	5ng/4	121.3	192
8	64.1	142	8	69.7	157
24	41.51	94	24	41.6	93

Serum non-starved Ishikawa cells, Experiment 2

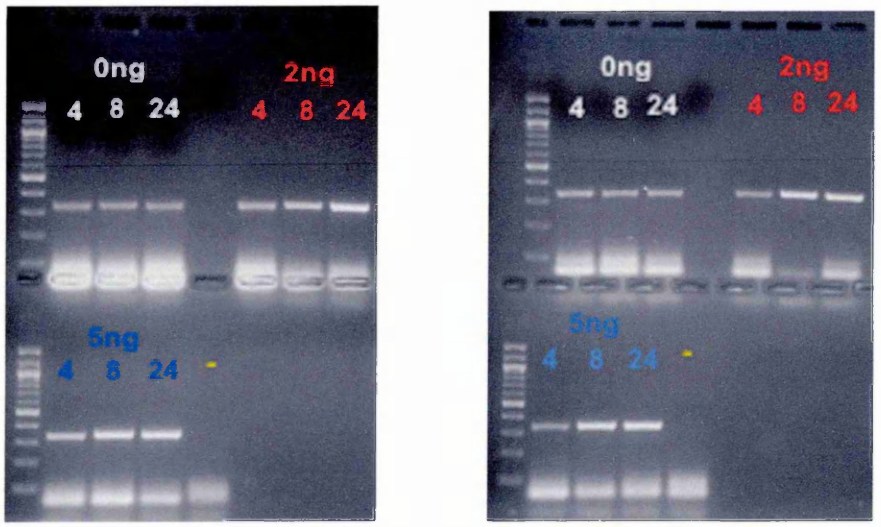

A B

Fig 14.1 Expression of PTEN in non-starved Ishikawa with duplicates A and B. No TGF-β1 control shown in white, 2ng/ml TGF-β1 in red, 5ng/ml TGF-β1 in blue over 4, 8 & 24 hours. PCR control (no DNA) is a yellow dash.

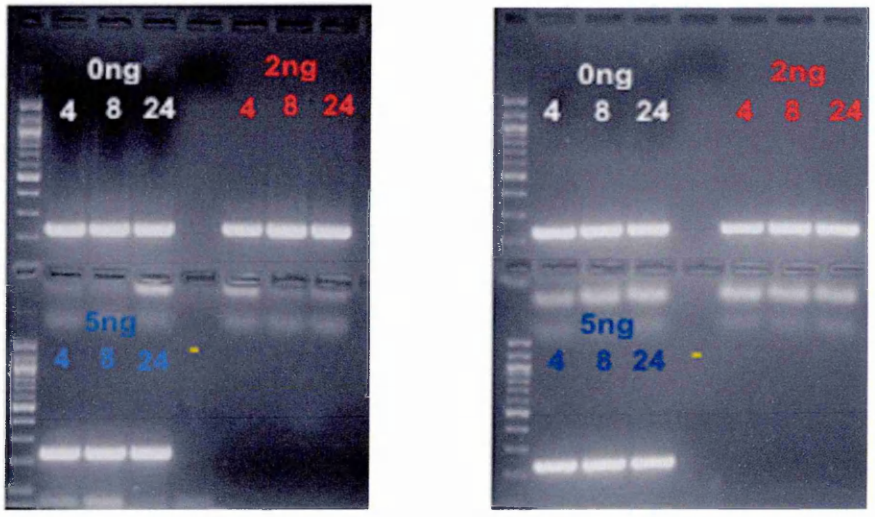

A B

Fig 14.2 Expression of GAPDH in non-starved Ishikawa with duplicates A and B. No TGF-β1 control shown in white, 2ng/ml TGF-β1 in red, 5ng/ml TGF-β1 in blue over 4, 8 & 24 hours. PCR control (no DNA) is a yellow dash.

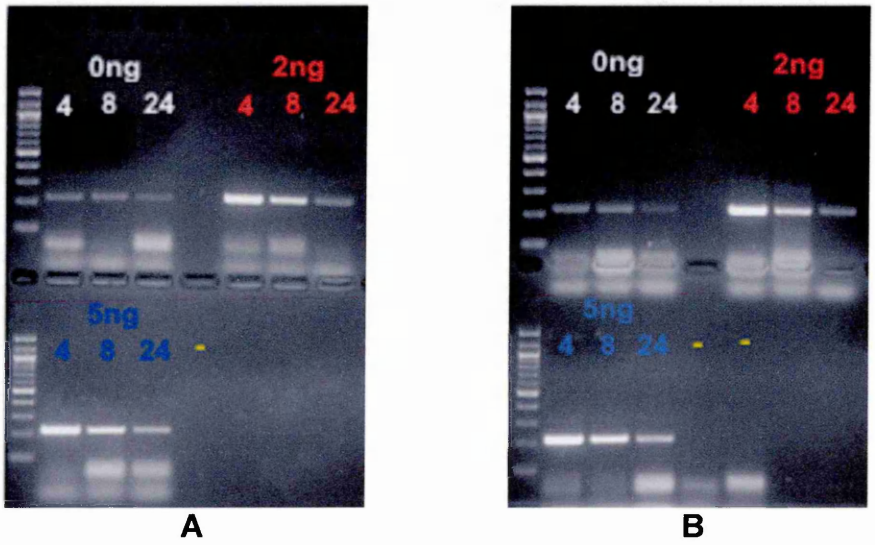

Fig 14.3 Expression of PAI-1 in non-starved Ishikawa with duplicates A and B. No TGF-β1 control shown in white, 2ng/ml TGF-β1 in red, 5ng/ml TGF-β1 in blue over 4, 8 & 24 hours. PCR control (no DNA) is a yellow dash

Serum non-starved Ishikawa cells stimulated with TGF-β1

This experiment was performed once, with duplicate flasks A and B. From these duplicate flask, cDNA was prepared twice on separate occasions for RT-PCR using primers for PTEN, PAI-1 and GAPDH. The two individual batches of cDNA were designated as experiments 1 and 2 respectively.

Experiment 2

Analysis of RT-PCR products shown in Figure 14.1 show the same time and dose-dependant two-fold increase in PTEN mRNA expression in samples stimulated with TGF-β1 after 8 hours to Ishikawa non-starved Experiment 1(Figure 13.1). This confirmed that the original RT-PCR results in Experiment 1 were correct, as the fresh cDNA used in Experiment 2 gave very similar results. Expression levels of GAPDH shown in Figure 14.2 and PAI-1in Figure 14.3 are also similar to Ishikawa Experiment 1, with the results for PAI-1 showing a three-fold increase with both concentrations of TGF-β1.

As PAI-1 expression in Ishikawa Experiment 1 was only induced 2-fold by 2ng/ml cytokine, this difference may be due to the use of a new batch of RT enzyme used in the cDNA synthesis for Ishikawa Experiment 2, causing slight variations in the cDNA. Band intensities from Figures 14.1 to 14.3 were again also shown by densitometric analysis (Table 7).

Summary of Results for Experiments 1 & 2

A modest up-regulation of PTEN mRNA was observed in cells stimulated with TGF-β1 compared to the controls. The increase in transcripts was observed to be comparable in cells stimulated with 2ng/ml or 5ng/ml of

cytokine, which was seen to be approximately double after 8 hours compared to the unstimulated controls, and was maintained over the 24 hour period.

The results obtained for serum non-starved Ishikawa and serum non-starved HEC-1B were very similar, with a time and dose-dependant increase in PTEN mRNA observed in response to cytokine stimulation. With regard to the control samples, the Ishikawa cell line did not appear to exhibit the slight up-regulation of PTEN over 24 hours in the absence of TGF-β1 that was seen in HEC-1B cells. This may indicate variation in the sensitivity of these two cell lines to serum components, or may be due to experimental difference, such as the source of serum used, which contains variable amounts of cytokines and other factors.

Table 7 Ishikawa Serum Non-Starved, Experiment 2 PCR Densitometry					
PTEN PCR A			**PTEN PCR B**		
TGF-β1(ng) /Time (hrs)	Mass ng	Peak OD	TGF-β1(ng) /Time (hrs)	Mass ng	Peak OD
0ng/4	61	146	0ng/4	62.4	150
8	59.32	142	8	61.73	150
24	59.4	145	24	61.8	152
2ng/4	64.03	153	2ng/4	60.11	155
8	120.6	201	8	125.7	207
24	127.61	205	24	122.96	206
5ng/4	65	151	5ng/4	61.3	150
8	129.01	209	8	126.2	210
24	126.95	205	24	125.58	207
GAPDH PCR A			**GAPDH PCR B**		
TGF-β1(ng) /Time (hrs)	Mass ng	Peak OD	TGF-β1(ng) /Time (hrs)	Mass ng	Peak OD
4	331.2	254	4	327	253
8	330	254	8	331.5	254
24	330.4	253	24	332	254
2ng/4	333.02	256	2ng/4	330	255
8	329.7	255	8	330.81	256
24	330.1	253	24	328.97	255
5ng/4	327	254	5ng/4	330	254
8	331.3	255	8	330.6	253
24	329	254	24	331.72	254
PAI-1 PCR A			**PAI-1 PCR B**		
TGF-β1(ng) /Time (hrs)	Mass ng	Peak OD	TGF-β1(ng) /Time (hrs)	Mass ng	Peak OD
0ng/4	54.8	99	0ng/4	55	96
8	57.2	98	8	50.3	97
24	43.01	51	24	45.42	53
2ng/4	196	239	2ng/4	199.12	242
8	112.1	190	8	114	187
24	40.37	88	24	43.6	92
5ng/4	197.5	238	5ng/4	201.81	240
8	113.9	189	8	118	197
24	64.04	152	24	69.11	154

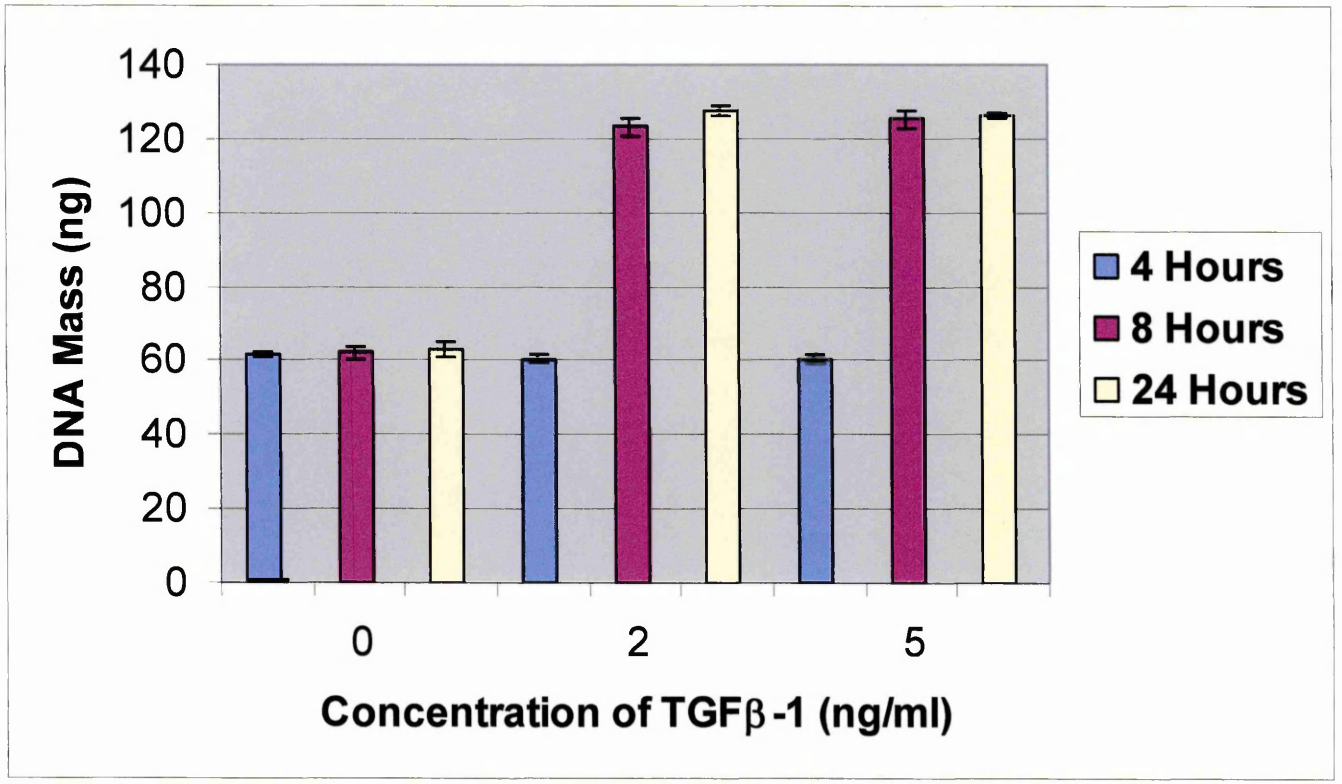

Graph 3 Expression of PTEN mRNA in serum non-starved Ishikawa stimulated with TGF-β1. Stimulation with cytokine was performed over 4 (blue bars), 8 (purple bars) & 24 hours (yellow bars) with 0ng/ml (control), 2ng/ml & 5ng/ml TGF-β1 in the presence of 10% foetal calf serum (complete medium). RT-PCR was performed using PTEN primers 2a and 3 and bands separated by gel electrophoresis prior to densitometric analysis. Data indicates a 2-fold time-dependant increase in PTEN mRNA expression after 8 hours compared to the controls. The stimulation experiment was performed once, in duplicate. cDNA from this experiment was prepared twice from the RNA stock, in duplicate (overall n=4). Data is presented as mean ± SEM of densitometry readings.

3.1.2 Analysis of PTEN, Phospho-PTEN, β-Actin and PAI-1 protein levels in HEC-1B and Ishikawa cell lines stimulated with TGF-ß1

To determine whether changes in mRNA expression elicited any modification of protein expression in response to TGF-β1 stimulation, total protein was extracted from HEC-1B and Ishikawa cells which had been treated with no cytokine or 2 and 5ng/ml TGF-β1, again under either serum-starved or non-starved conditions (Chapter 2, Section 2.2.4.1), and levels of specific proteins (PTEN, PAI-1, phospho-PTEN [P-PTEN] and β-Actin) determined by Western blotting. Determination of levels of PTEN and P-PTEN were required to ascertain any biological significance of PTEN mRNA up-regulation by TGF-β1.

3.1.2.1 Determination of protein concentration by the Bradford assay

To determine the concentration of protein in each sample obtained from stimulation with TGF-β1, a BSA standard curve was first prepared according to the instructions supplied with the Bradford reagent. Quantitation of the protein was necessary to enable the equal loading of 10μg onto the SDS-PAGE gel from each sample, so that expression levels could be compared. Briefly, serial dilutions of BSA were made in triplicate and the absorbance recorded at 595nm using disposable cuvettes after incubation with the reagent. The readings for each dilution were averaged and the results plotted as shown in Appendix IV.

Samples obtained from the stimulation experiments were measured in duplicate as described in Chapter 2, Section 2.2.4.2 and the average values shown in Table 8 with the volumes required for 10μg of protein.

Table 8 Protein Concentrations from HEC-1B & Ishikawa Stimulated with TGF-β1								
Flask	HEC-1B Non-Starved		HEC-1B Serum Starved 1		HEC-1B Serum-Starved 2		Ishikawa Non-Starved	
	μg/μl	For 10μg (μl)	μg/μl	For 10μg (μl)	μg/μl	For 10μg (μl)	μg/μl	For 10μg (μl)
10% A	x	x	0.75	13	0.36	6	x	x
B	x	x	1.64	6	0.29	7	x	x
0/4 A	1.02	9.8	1	10	0.45	22	1.72	5.81
B	1.04	9.6	1.3	8.1	1.17	8.5	1.1	9.1
0/8 A	0.94	10.6	1.5	6.7	0.24	42	1.14	8.77
B	0.82	12.2	1.78	5.1	0.85	11.76	1.34	7.46
0/24 A	1.16	8.6	1.68	5.95	0.6	17	1.34	7.46
B	1.16	8.6	1.66	6	0.5	20	1.82	5.49
2/4 A	1.02	9.8	1.28	7.8	0.74	14	1.2	8.33
B	1.02	9.8	1.54	6.5	0.7	14	1.44	6.94
2/8 A	0.84	11.9	1.66	6	0.84	12	1.2	8.33
B	1.1	9.1	1.41	7.2	0.76	13	1.44	6.94
2/24 A	0.94	10.6	1.67	6	0.6	17	1.46	6.85
B	0.78	12.8	1.27	8.3	0.72	13.8	1.44	6.94
5/4 A	1.02	9.8	1.24	8.1	0.74	14	1.5	6.67
B	1.04	9.6	1.69	5.9	0.76	13	1.4	7.14
5/8 A	1.1	9.1	1.72	5.8	0.7	14	1.26	7.93
B	1.1	9.1	1.52	6.5	0.78	12.8	1.4	7.14
5/24 A	1.1	9.1	1.36	7.4	0.6	17	1.63	6.13
B	0.7	0.7	0.98	10	0.38	26	1.88	5.32

3.1.2.3 Detection of proteins by Western blot with enhanced chemiluminesence (ECL) and densitometry.

Western blotting and detection by ECL were performed as described in Chapter 2, Section 2.2.4 for HEC-1B and Ishikawa cell lines, after fractionation of 10μg of each protein sample by 8% SDS-PAGE against a broad-range biotinylated molecular weight marker (Appendix I.4). Antibodies were used to detect PTEN, phospho-PTEN Ser380 (P-PTEN), β-Actin and PAI-1 as described in Chapter 2.

Both PTEN and phospho-PTEN (Ser380) levels were analysed using two separate antibodies (anti-PTEN from BD Biosciences and anti-P-PTEN Ser380 from NEB). This was performed only on the HEC-1B cell line which expresses wild-type PTEN, as the Ishikawa cell line does not express PTEN protein (Figure 18.1) due to a mutation of PTEN in this cell line (Yaginuma, et al, 2000). This was to determine if TGF-β1 was capable of modifying overall PTEN protein levels, which could indicate a potential use as an anti-tumour therapy, and also if the amount of phospho-PTEN was also changed. As phosphorylation of PTEN prevents degradation, but also inhibits catalytic activity (Vazquez, et al 2000), assessing the phosphorylation status under cytokine stimulus may aid in the elucidation of mechanisms of PTEN protein regulation by TGF-β1.

Scanned images of the developed films are shown in Figures 15 to 18 The intensity of each specific band, indicated by an arrow, was analysed (Chapter 2, Section 2.2.4.5.1) and displayed in Tables 9 to 12.

Results for HEC-1B serum non-starved are shown in Figures 15.1 to 15.4 and Table 9.

Results for HEC-1B serum-starved Experiments 1 and 2 are shown in Figures 16.1 to 16.2, Table 10 and Figures 17.1 to 17.4 and Table 11, respectively. The results for non-serum starved Ishikawa cells are presented in Figures 18.1 to 18.3 and Table 12.

HEC-1B Serum non-starved

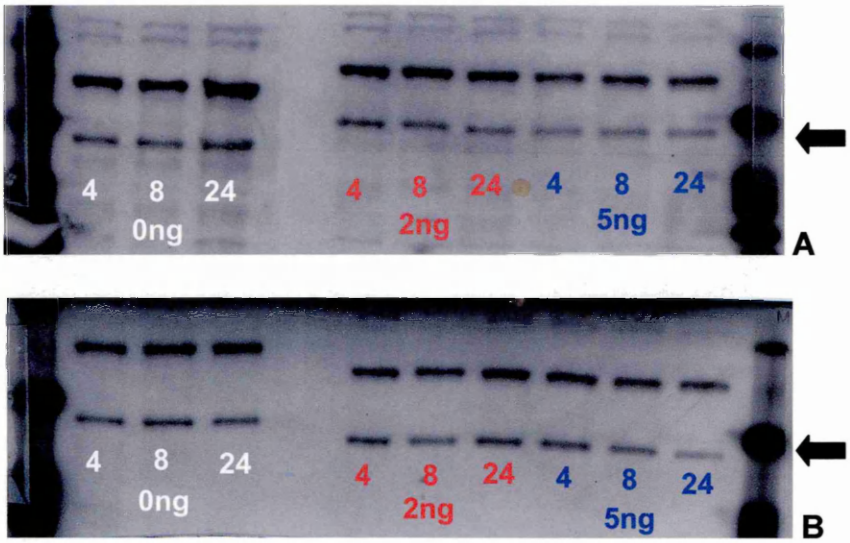

Figure 15.1 Anti-PTEN western blot for non-starved HEC-1B with duplicates A and B. No TGF-β1 control shown in white, 2ng/ml TGF-β1 in red,5ng/ml TGF-β1 in blue over 4, 8 & 24 hours Arrow indicates specific band at ~55KDa

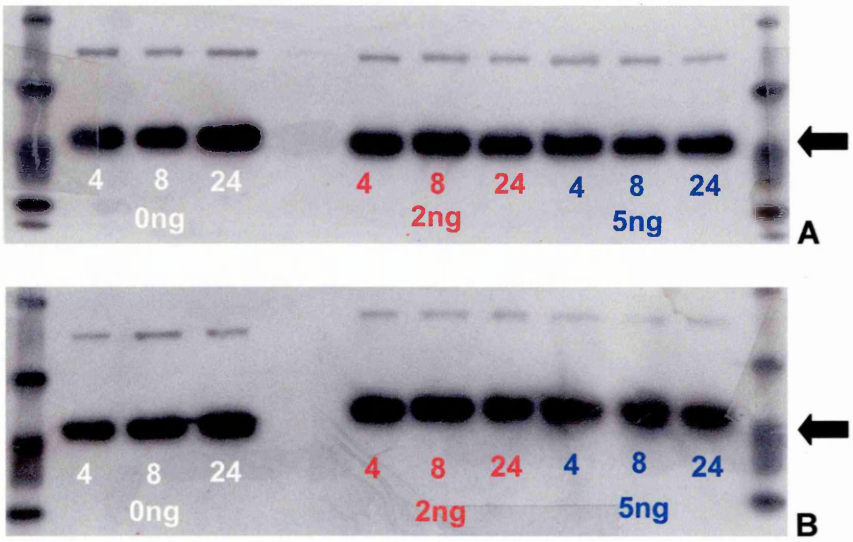

Figure 15.2 Anti-β Actin western blot for non-starved HEC-1B with duplicates A and B. No TGF-β1 control shown in white, 2ng/ml TGF-β1 in red,5ng/ml TGF-β1 in blue over 4, 8 & 24 hours. Arrow indicates specific band at ~43KDa.

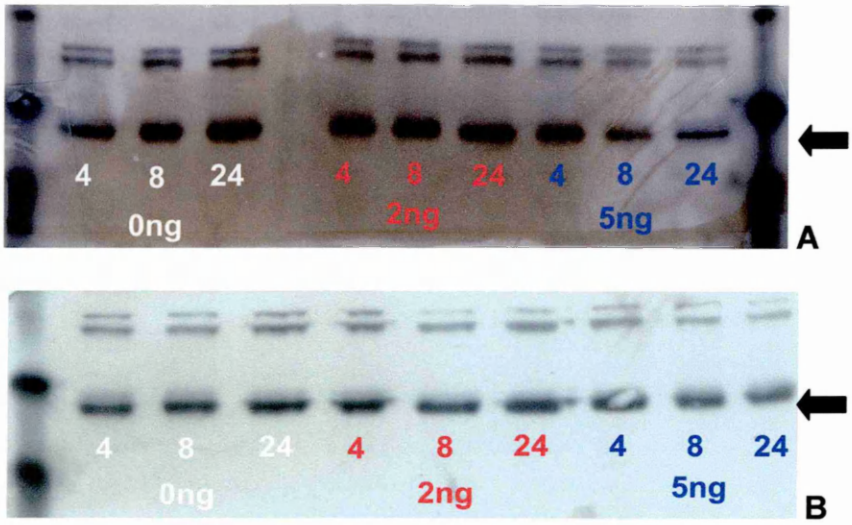

Fig 15.3 Anti-phospho-PTEN (Ser380) western blot for Non-starved HEC-1B with duplicates A and B. No TGF-β1 control shown in white, 2ng/ml TGF-β1 in red,5ng/ml TGF-β1 in blue over 4, 8 & 24 hours. Arrow indicates specific band at ~55KDa.

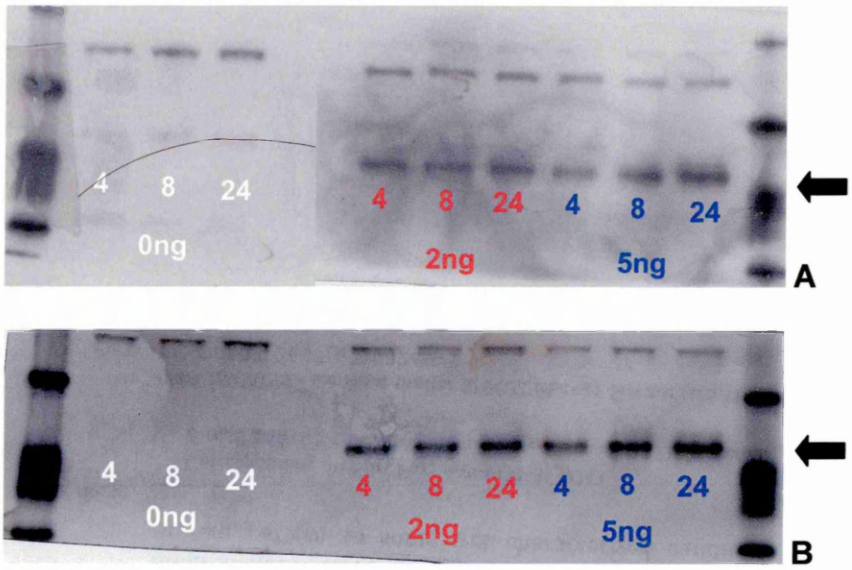

Fig 15.4 Anti-PAI-1 western blot for non-starved HEC-1B with duplicates A and B. No TGF-β1 control shown in white, 2ng/ml TGF-β1 in red,5ng/ml TGF-β1 in blue over 4, 8 & 24 hours. Arrow indicates specific band at ~47KDa.

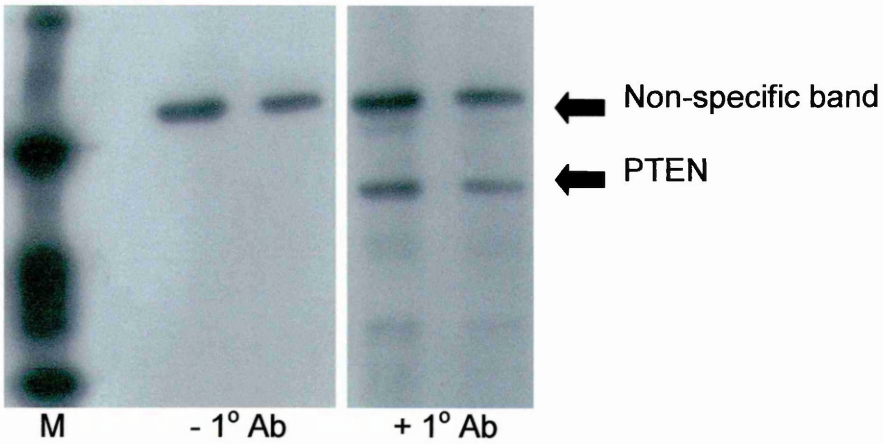

Fig 15.5 Anti-PTEN blot to show the source of the high molecular weight non-specific band with (+ 1°Ab) or without (-1° Ab) primary anti-PTEN antibody.

M= protein marker.

Serum non-starved HEC-1B stimulated with TGF-β1

This experiment was performed once, with duplicate flasks A and B from which total protein was prepared for Western blotting using antibodies against for PTEN, phospho-PTEN(Ser380), PAI-1 and β-actin.

As can be seen in Figure 15.1, expression of PTEN protein in HEC-1B (band in A and B samples at ~55KDa with respect to the marker) changes little between the samples, with only a very minor decrease after 24 hours with 5ng/ml of cytokine, and does not exhibit the increase observed in mRNA (Figure 10.1). Expression of PTEN protein was not assessed in the publications describing modulation of PTEN mRNA by TGF-β1(Lee, et al 1999 and Li and Sun, 1997), but PTEN protein was decreased in pancreatic cells after 24 hours of treatment with 10ng/ml of cytokine (Ebert, et al 2002). Levels of β-Actin in Figure 15.2 and phospho-PTEN in Figure 15.3 are also fairly constant.

It should be noted that the phospho-PTEN antibody used here is specific to Ser380. A new phospho-PTEN antibody is now available which recognises phosphorylated Ser380 and Thr382/383, and therefore could be used to detect changes at all three residues unlike the Ser380-specific antibody. The expression of PAI-1 protein (Fig 15.4) shows a similar pattern as for PAI-1 mRNA (Figure 10.3), with a time and dose-dependant increase of ~4-fold at 4 hours rising to ~5-fold at 24 hours for both concentrations of TGF-β1. Band intensities were also shown by densitometric analysis (Table 9).

The high molecular weight band of >90KDa observed in variable amounts in all the blots was due to non-specific binding by the ABC/secondary antibody complex. This band was present even in the absence of primary anti-PTEN

antibody (Figure 15.5), and therefore was not an artefact of non-specific binding by the primary antibody.

Summary of Results

Expression of PTEN and P-PTEN did not appear to undergo any detectable change in levels in cells stimulated with TGF-β1 compared to the controls. This would indicate that although the cytokine was capable of up-regulating PTEN mRNA, no change in protein levels were observed suggesting that TGF-β1 does not represent a novel anti-tumour therapy in the HEC-1B cell line.

Anti-PTEN A			Anti-PTEN B		
TGF-β1(ng) /Time (hrs)	Ave OD	Peak OD	TGF-β1(ng) /Time (hrs)	Ave OD	Peak OD
0ng/4	0.42	0.52	0ng/4	0.36	0.48
8	0.39	0.5	8	0.38	0.52
24	0.45	0.58	24	0.35	0.46
2ng/4	0.45	0.55	2ng/4	0.37	0.5
8	0.43	0.53	8	0.34	0.43
24	0.39	0.49	24	0.38	0.51
5ng/4	0.37	0.42	5ng/4	0.35	0.5
8	0.35	0.43	8	0.32	0.44
24	0.34	0.42	24	0.25	0.32
Anti-β Actin A			**Anti-β Actin B**		
TGF-β1(ng) /Time (hrs)	Ave OD	Peak OD	TGF-β1(ng) /Time (hrs)	Ave OD	Peak OD
0ng/4	0.48	0.73	0ng/4	0.46	0.74
8	0.5	0.75	8	0.5	0.82
24	0.55	0.85	24	0.53	0.85
2ng/4	0.52	0.77	2ng/4	0.54	0.85
8	0.51	0.78	8	0.57	0.87
24	0.44	0.7	24	0.53	0.74
5ng/4	0.45	0.7	5ng/4	0.45	0.7
8	0.44	0.68	8	0.4	0.64
24	0.43	0.67	24	0.42	0.65

Anti-P-PTEN A			Anti-P-PTEN B		
TGF-β1(ng) /Time (hrs)	Ave OD	Peak OD	TGF-β1(ng) /Time (hrs)	Ave OD	Peak OD
0ng/4	0.54	0.73	0ng/4	0.52	0.69
8	0.55	0.73	8	0.56	0.68
24	0.62	0.87	24	0.65	0.73
2ng/4	0.64	0.8	2ng/4	0.67	0.75
8	0.6	0.82	8	0.65	0.71
24	0.62	0.82	24	0.66	0.7
5ng/4	0.58	0.76	5ng/4	0.53	0.67
8	0.45	0.6	8	0.55	0.64
24	0.5	0.65	24	0.49	0.6
Anti-PAI-1 A			**Anti-PAI-1 B**		
TGF-β1(ng) /Time (hrs)	Mass ng	Peak OD	TGF-β1(ng) /Time (hrs)	Mass ng	Peak OD
0ng/4	0.13	0.14	0ng/4	nd	nd
8	0.14	0.15	8	0.12	0.12
24	0.13	0.14	24	0.11	0.12
2ng/4	0.37	0.45	2ng/4	0.41	0.53
8	0.38	0.44	8	0.43	0.55
24	0.35	0.42	24	0.54	0.68
5ng/4	0.25	0.3	5ng/4	0.42	0.54
8	0.28	0.37	8	0.48	0.56
24	0.33	0.46	24	0.57	0.66

Table 9 HEC-1B Serum non-starved Western blot Densitometry

HEC-1B Serum-starved, Experiment 1

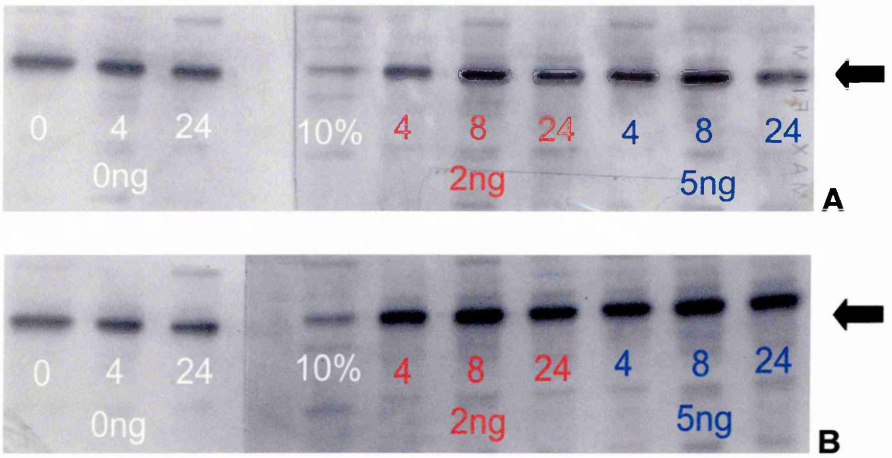

Fig 16.1 Anti-PTEN western blot for serum starved HEC-1B with duplicates A and B. No TGF-β1 control shown in white, 2ng/ml TGF-β1 in red,5ng/ml TGF-β1 in blue over 4, 8 & 24 hours. Arrow indicates specific band at ~55KDa.

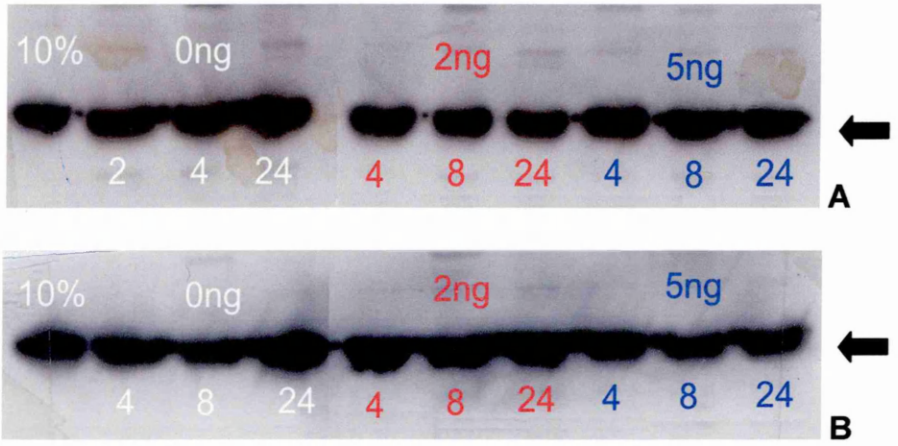

Fig 16.2 Anti-β actin western blot for serum starved HEC-1B with duplicates A and B. No TGF-β1 control shown in white, 2ng/ml TGF-β1 in red,5ng/ml TGF-β1 in blue over 4, 8 & 24 hours. Arrow indicates specific band at ~43KDa.

Table 10 HEC-1B Serum Starved Experiment 1 Western blot Densitometry					
Anti-PTEN A			**Anti-PTEN B**		
TGF-β1(ng) /Time (hrs)	Ave OD	Peak OD	TGF-1(ng) /Time (hrs)	Ave OD	Peak OD
10%	0.18	0.23	10%	0.26	0.34
0ng/4	0.22	0.33	0ng/4	0.24	0.35
8	0.24	0.35	8	0.24	0.35
24	0.23	0.35	24	0.24	0.35
2ng/4	0.28	0.37	2ng/4	0.4	0.52
8	0.35	0.47	8	0.44	0.59
24	0.32	0.44	24	0.4	0.55
5ng/4	0.31	0.45	5ng/4	0.4	0.56
8	0.33	0.48	8	0.43	0.6
24	0.25	0.36	24	0.39	0.54
Anti-β Actin A			**Anti-β Actin B**		
TGF-β1(ng) /Time (hrs)	Ave OD	Peak OD	TGF-β1(ng) /Time (hrs)	Ave OD	Peak OD
10%	0.45	0.68	10%	0.5	0.77
0ng/4	0.53	0.75	0ng/4	0.51	0.74
8	0.55	0.79	8	0.46	0.7
24	0.63	0.86	24	0.58	0.89
2ng/4	0.52	0.77	2ng/4	0.6	0.86
8	0.49	0.76	8	0.65	0.91
24	0.5	0.74	24	0.65	0.91
5ng/4	0.54	0.82	5ng/4	0.62	0.9
8	0.54	0.83	8	0.48	0.71
24	0.53	0.78	24	0.45	0.68

HEC-1B Serum-starved experiment 2

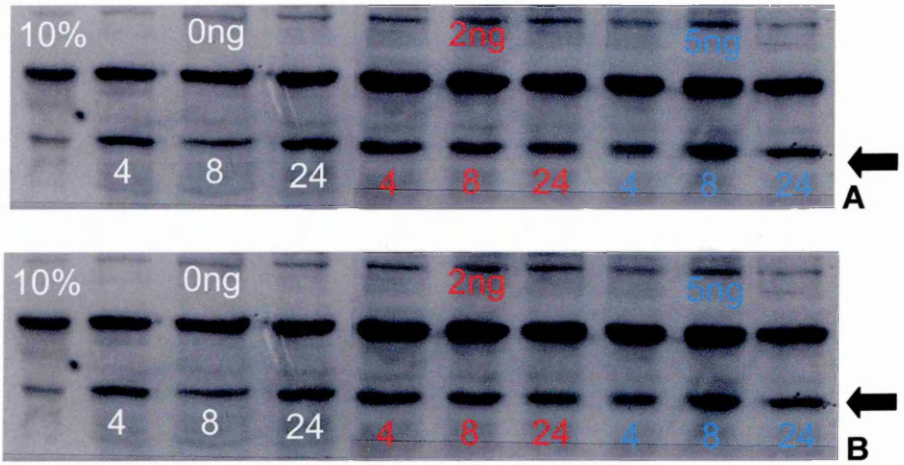

Fig 17.1 Anti-PTEN western blot for serum starved HEC-1B with duplicates A and B. No TGF-β1 control shown in white, 2ng/ml TGF-β1 in red,5ng/ml TGF-β1 in blue over 4, 8 & 24 hours. Arrow indicates specific band at ~55KDa.

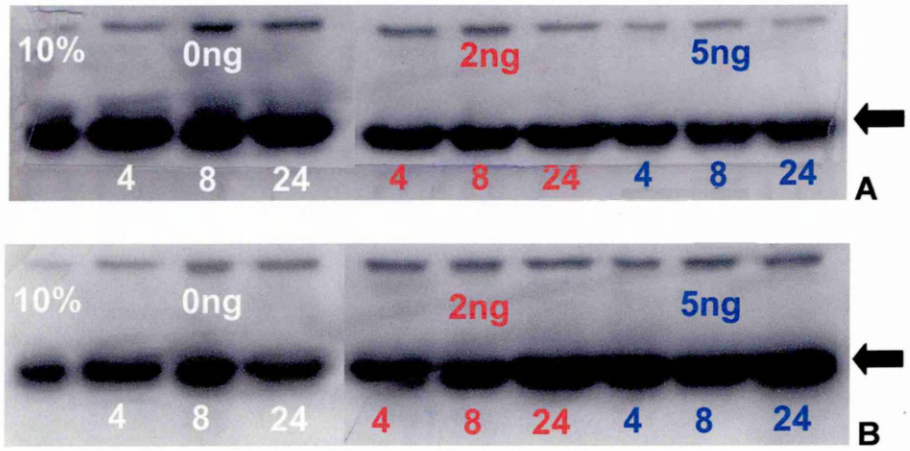

Fig 17.2 Anti-β actin western blot for serum starved HEC-1B with duplicates A and B. No TGF-β1 control shown in white, 2ng/ml TGF-β1 in red,5ng/ml TGF-β1 in blue over 4, 8 & 24 hours. Arrow indicates specific band at ~43KDa.

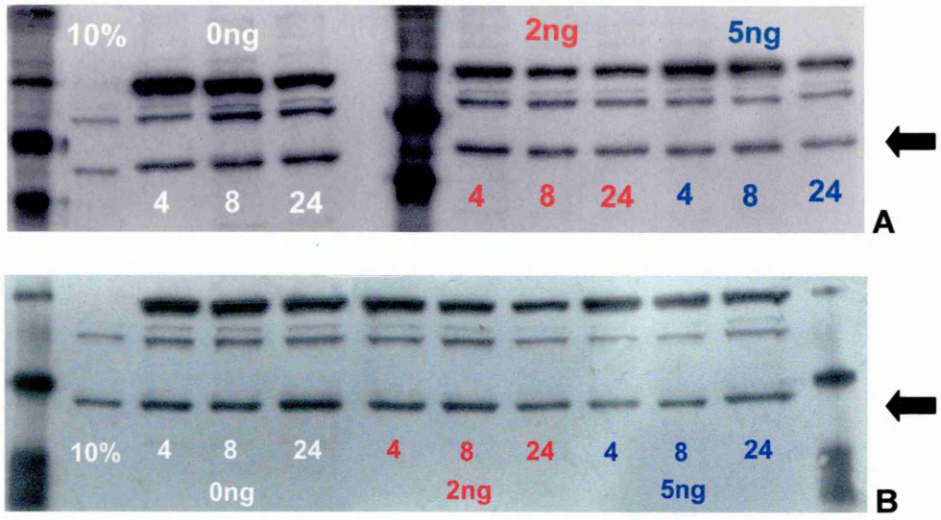

Fig 17.3 Anti-phospho-PTEN (Ser 380) western blot for serum starved HEC-1B with duplicates A and B. No TGF-β1 control shown in white, 2ng/ml TGF-β1 in red,5ng/ml TGF-β1 in blue over 4, 8 & 24 hours. Arrow indicates specific band at ~55KDa.

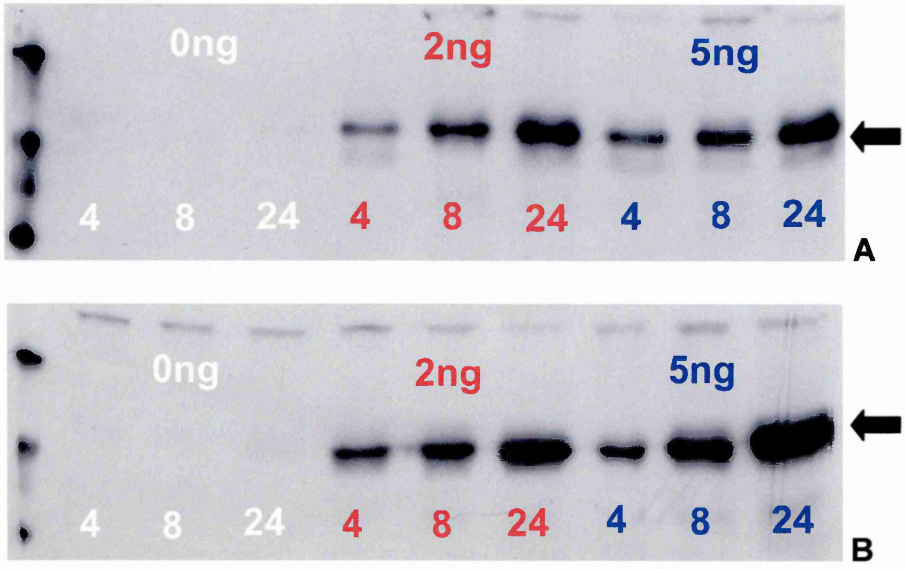

Fig 17.4 Anti-PAI-1 western blot serum starved HEC-1B with duplicates A and B. No TGF-β1 control shown in white, 2ng/ml TGF-β1 in red,5ng/ml TGF-β1 in blue over 4, 8 & 24 hours. Arrow indicates specific band at ~47KDa

Serum starved HEC-1B stimulated with TGF-β1

This experiment was performed twice in duplicate flasks A and B from which total protein was prepared for Western blotting using antibodies against for PTEN, phospho-PTEN(Ser380), PAI-1 and β-actin. Proteins extracted in experiment 1 were scraped into cold Tris, and therefore P-PTEN could not be detected in these samples. Proteins extracted in experiment 2 were isolated using a phosphoprotein lysis buffer (Appendix I.3) and could therefore by probed for P-PTEN.

Experiments 1 & 2

The results of both serum-starved HEC-1B experiments (Figures 16.1 and 17.1) show little change in PTEN expression levels, and again β-Actin remained constant (Figures 16.2 and 17.2). A slight decrease in phospho-PTEN levels was observed in a time and dose-dependant manner (Figure 17.3), but this decrease was very small and not completely consistent between duplicate samples. A strong response was observed for PAI-1 (Figure 17.4) which was undetectable in the controls. A continuous increase from 4 to 24 hours of stimulation was seen, giving approximately double the band intensity after 24 hours, with the strongest response from the 5ng/ml samples. These observations were reflected in the densitometry results shown in Tables 10 and 11.

Experiment 1 only included blots for PTEN and β-Actin due to the protein extraction method used (scraping into ice-cold Tris). The cell lysates initially prepared in this manner were very viscous, which gave difficulty loading onto the gels, and upon probing for phospho-PTEN were seen to have degraded

substantially. Phosphoprotein lysis buffer (protocol courtesy of Mr Mike Sharrard, University of York), was later employed to overcome this problem.

Summary of Results for experiments 1 & 2

Expression of PTEN and P-PTEN did not appear to undergo any detectable change in cells stimulated with TGF-β1 compared to the controls. This would indicate that although the cytokine was capable of up-regulating PTEN mRNA, no change in protein levels was observed. Reduction of foetal calf serum from 10% to 1% in these experiments also appear to have very little effect on PTEN and P-PTEN expression, even though reduction of serum was observed to mildly induce expression of PTEN mRNA (Figures 11 and 12, Section 3.1.1).

Again, as PTEN and P-PTEN levels remained unchanged with cytokine stimulation, TGF-β1 does not appear to represent an anti-tumour agent in this cell line.

Table 11 HEC-1B Serum starved Experiment 2
Western blot Densitometry

Anti-PTEN A			Anti-PTEN B		
TGF-β1(ng) /Time (hrs)	Ave OD	Peak OD	TGF-β1(ng) /Time (hrs)	Ave OD	Peak OD
10%	0.29	0.37	10%	0.17	0.21
0ng/4	0.44	0.63	0ng/4	0.35	0.49
8	0.42	0.59	8	0.37	0.52
24	0.54	0.75	24	0.45	0.65
2ng/4	0.58	0.8	2ng/4	0.43	0.61
8	0.49	0.69	8	0.41	0.61
24	0.48	0.62	24	0.4	0.55
5ng/4	0.45	0.56	5ng/4	0.38	0.52
8	0.56	0.74	8	0.37	0.53
24	0.48	0.71	24	0.42	0.49
Anti-β Actin A			**Anti-β Actin B**		
TGF-β1(ng) /Time (hrs)	Ave OD	Peak OD	TGF-β1(ng) /Time (hrs)	Ave OD	Peak OD
10%	0.7	0.94	10%	0.52	0.75
0ng/4	0.74	0.96	0ng/4	0.53	0.69
8	0.75	1.01	8	0.61	0.81
24	0.78	1.04	24	0.60	0.65
2ng/4	0.61	0.85	2ng/4	0.63	0.67
8	0.64	0.84	8	0.69	0.79
24	0.65	0.82	24	0.63	0.83
5ng/4	0.6	0.76	5ng/4	0.65	0.80
8	0.56	0.71	8	0.6	0.75
24	0.48	0.68	24	0.62	0.72

Anti-P-PTEN A			Anti-P-PTEN B		
TGF-β1(ng) /Time (hrs)	Ave OD	Peak OD	TGF-β1(ng) /Time (hrs)	Ave OD	Peak OD
10%	0.23	0.31	10%	0.22	0.27
0ng/4	0.35	0.51	0ng/4	0.28	0.38
8	0.36	0.53	8	0.27	0.37
24	0.37	0.58	24	0.34	0.44
2ng/4	0.36	0.55	2ng/4	0.33	0.43
8	0.29	0.46	8	0.3	0.38
24	0.25	0.41	24	0.24	0.31
5ng/4	0.25	0.39	5ng/4	0.24	0.31
8	0.25	0.39	8	0.27	0.35
24	0.21	0.33	24	0.29	0.37
Anti-PAI-1 A			**Anti-PAI-1 B**		
TGF-β1(ng) /Time (hrs)	Ave OD	Peak OD	TGF-β1(ng) /Time (hrs)	Ave OD	Peak OD
0ng/4	nd	nd	0ng/4	nd	nd
8	nd	nd	8	nd	nd
24	nd	nd	24	nd	nd
2ng/4	0.29	0.39	2ng/4	0.38	0.46
8	0.49	0.65	8	0.5	0.6
24	0.65	0.93	24	0.69	0.91
5ng/4	0.37	0.47	5ng/4	0.42	0.48
8	0.58	0.71	8	0.65	0.78
24	0.72	0.99	24	0.83	1.0

Table 11 (Continued)

HEC-1B Serum starved Experiment 2 Western blot Densitometry

Ishikawa Serum Non-Starved

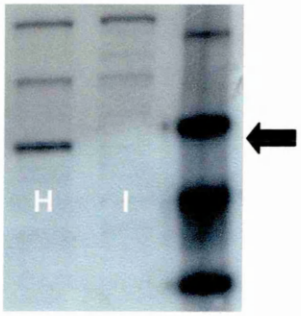

Fig 18.1 Anti-PTEN Western blot for non-starved Ishikawa & HEC-1B

H=HEC-1B, I=Ishikawa, arrow indicates specific band at ~54KDa

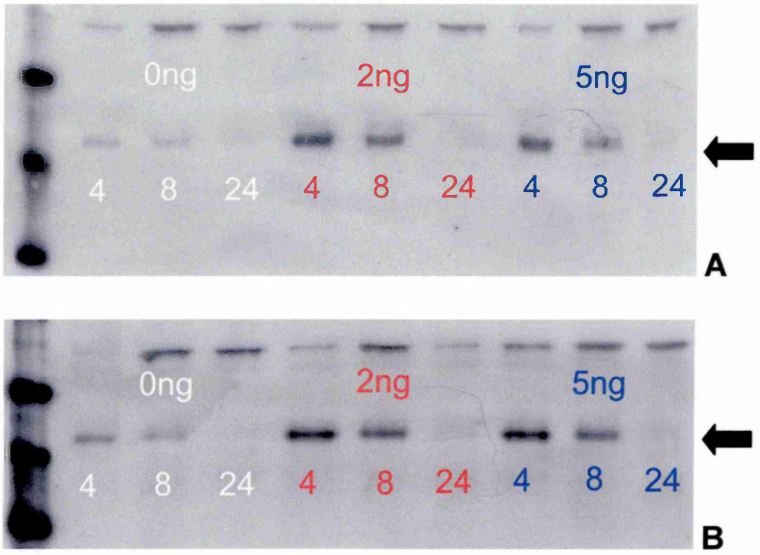

Fig 18.2 Anti-PAI-1 western blot for non-starved Ishikawa

with duplicates A and B. No TGF-β1 control shown in white, 2ng/ml TGF-β1

in red,5ng/ml TGF-β1 in blue over 4, 8 & 24 hours. Arrow indicates specific

band at ~47KDa

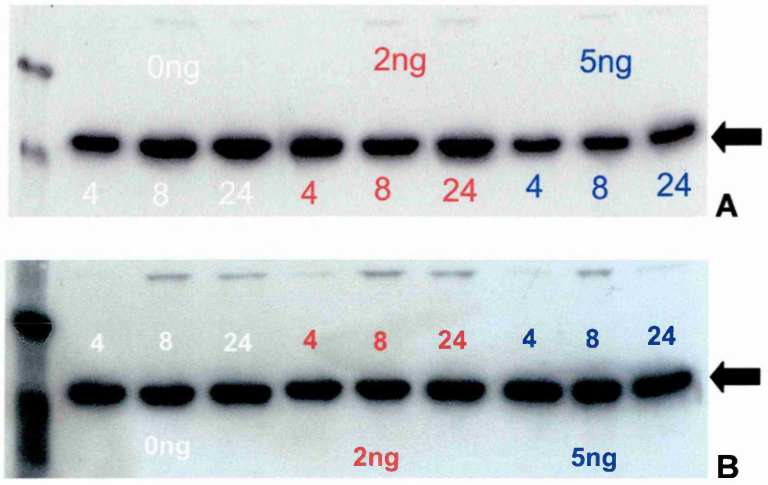

Fig 18.3 Anti-β actin western blot for non-starved Ishikawa with duplicates A and B. No TGF-β1 control shown in white, 2ng/ml TGF-β1 in red,5ng/ml TGF-β1 in blue over 4, 8 & 24 hours. Arrow indicates specific band at ~43KDa

Serum non-starved Ishikawa stimulated with TGF-β1

This experiment was performed once in duplicate flasks A and B from which total protein was prepared for Western blotting using antibodies against for PTEN, phospho-PTEN(Ser380), PAI-1 and β-actin.

The absence of PTEN protein in the Ishikawa cell line was confirmed by anti-PTEN Western blot using 10μg of protein from HEC-1B as a positive control and an equivalent amount of protein from Ishikawa cells. The blot shown in Figure 18.1 demonstrates the lack of detectable PTEN protein in the Ishikawa cell lysate, whilst the 54KDa band (black arrow) is visible in the HEC-1B cell lysate, and confirms previous reports (Guzeloglu-Kayishli, et al 2003).

The results of the Ishikawa serum non-starved experiment showed a more moderate response for PAI-1 (Figure 18.2), but with an inverse pattern compared to HEC-1B serum non-starved (Figure 15.4). For the Ishikawa cell line, PAI-1 induction by TGF-β1 occurred rapidly after 4 hours, then showed a steady decline up to 24 hours, where the signal is no longer detectable. This pattern of expression was also observed for mRNA expression levels shown in Figures 13 and 14, Section 3.1.1. Levels of β-actin protein remained constant throughout (Figure 18.3). These observations were verified by the densitometric analysis shown in Table 12.

Summary of Results

Expression of PTEN protein was absent in this cell line, in agreement with published material. A strong response to TGF-β1 was observed as a robust up-regulation of PAI-1 protein, reflecting the mRNA response previously

observed in Section 3.1.1, indicating a functional signalling pathway through the TGF-β1 receptor. The results for PAI-1 mRNA and protein up-regulation in both HEC-1B and Ishikawa cell lines indicates that the cytokine is capable of affecting PTEN mRNA expression regardless of whether PTEN is wild-type (HEC-1B) or mutated (Ishikawa).

Table 12 Ishikawa Non-serum starved Western blot Densitometry					
Anti-PAI-1 A			**Anti-PAI-1 B**		
TGF-b1(ng)/Time (hrs)	Ave OD	Peak OD	TGF-b1(ng)/Time (hrs)	Ave OD	Peak OD
0ng/4	0.19	0.23	0ng/4	0.23	0.26
8	0.16	0.2	8	0.18	0.22
24	nd	nd	24	nd	nd
2ng/4	0.31	0.47	2ng/4	0.39	0.58
8	0.24	0.36	8	0.30	0.49
24	nd	nd	24	nd	nd
5ng/4	0.3	0.41	5ng/4	0.4	0.55
8	0.24	0.38	8	0.33	0.4
24	nd	nd	24	nd	nd
Anti-β-Actin A			**Anti-β-Actin B**		
TGF-b1(ng)/Time (hrs)	Ave OD	Peak OD	TGF-b1(ng)/Time (hrs)	Ave OD	Peak OD
0ng/4	0.59	0.74	0ng/4	0.72	1.01
8	0.63	0.88	8	0.7	0.98
24	0.61	0.83	24	0.67	0.91
2ng/4	0.63	0.79	2ng/4	0.71	0.99
8	0.65	0.8	8	0.7	0.95
24	0.68	0.84	24	0.69	0.9
5ng/4	0.58	0.79	5ng/4	0.73	0.97
8	0.6	0.81	8	0.68	0.94
24	0.59	0.7	24	0.71	0.96

3.1.3 HEC-1B cell proliferation assay

From the results obtained in Section 3.1.1, further investigations were carried out to ascertain the relationship between changes in PTEN mRNA levels observed in the HEC-1B cell line and the growth of the cells under TGF-β1 stimulation. To determine the effect of TGF-β1 on the ability of HEC-1B cells to proliferate a simple, non-radioactive commercial cell proliferation assay was performed. This assay measures cellular reduction of the CellTitre reagent by the mitochondria of living cells to a coloured compound which can be measured using a standard plate reader. This method is an alternative to established techniques for measuring DNA synthesis such as ^{3}H-thymidine and 5-bromo-2-deoxyuracil (Brdu) incorporation.

HEC-1B cells were cultured on the wells of 24-well tissue culture plates in complete medium prior to serum starvation for 24 hours in reduced serum medium. The cells were stimulated with 1 to 10ng/ml of TGF-β1 for 4, 8 and 24 hours prior to addition of the assay reagent as described in Chapter 2, Section 2.2.5. Controls included no TGF-β1 and no cells (media only) and all readings were taken in quadruple from this experiment, which was performed once. Mean values for the quadruple readings were subtracted from the 'no cells' control and shown in bold, (Table 13); the results were also shown graphically (Graph 4).

The cell proliferation assay for HEC-1B cells stimulated with 1-10ng/ml TGF-β1 indicate no significant change in proliferation levels compared to the controls. Using this assay, TGF-β1 appeared to have no positive or negative effects on proliferation levels of HEC-1B over the time course and concentration of cytokine used.

Table 13 HEC-1B Cell Proliferation Assay Results								
Time (hours)	Ave no cells (n=4)	TGF-β1 concentration (ng/ml)						
		0	1	2	4	5	7	10
4	0.134	1.15	1.07	1.16	1.00	0.92	1.05	0.94
		1.11	1.12	0.99	0.97	0.94	1.07	0.99
		1.10	1.15	0.92	0.92	1.10	1.09	0.99
		0.96	1.17	1.01	1.01	0.92	0.96	0.94
Average A490 nm (n=4)		1.08	1.1	0.83	0.98	0.97	1.04	0.97
Average - no cells A490 nm		**0.95**	**0.97**	**0.70**	**0.84**	**0.84**	**0.91**	**0.83**
8	0.1437	1.18	1.04	1.03	1.26	1.07	1.06	1.42
		1.25	1.11	1.12	1.05	1.14	1.33	1.04
		1.28	1.28	1.16	1.02	1.19	1.05	1.10
		1.27	1.27	1.23	1.06	1.25	1.28	1.0
Average A490 nm (n=4)		1.26	1.17	1.13	1.1	1.16	1.18	1.16
Average - no cells A490 nm		**1.12**	**1.03**	**0.99**	**0.95**	**1.02**	**1.04**	**1.02**
24	0.1387	1.57	1.38	1.39	1.28	1.41	1.40	1.53
		1.75	1.62	1.18	1.52	1.65	1.37	1.68
		1.49	1.81	1.68	1.49	1.32	1.25	1.31
		1.67	1.53	1.46	1.47	1.61	1.65	1.48
Average A490 nm (n=4)		1.62	1.58	1.43	1.44	1.50	1.42	1.50
Average - no cells A490 nm		**1.48**	**1.44**	**1.29**	**1.30**	**1.36**	**1.28**	**1.36**

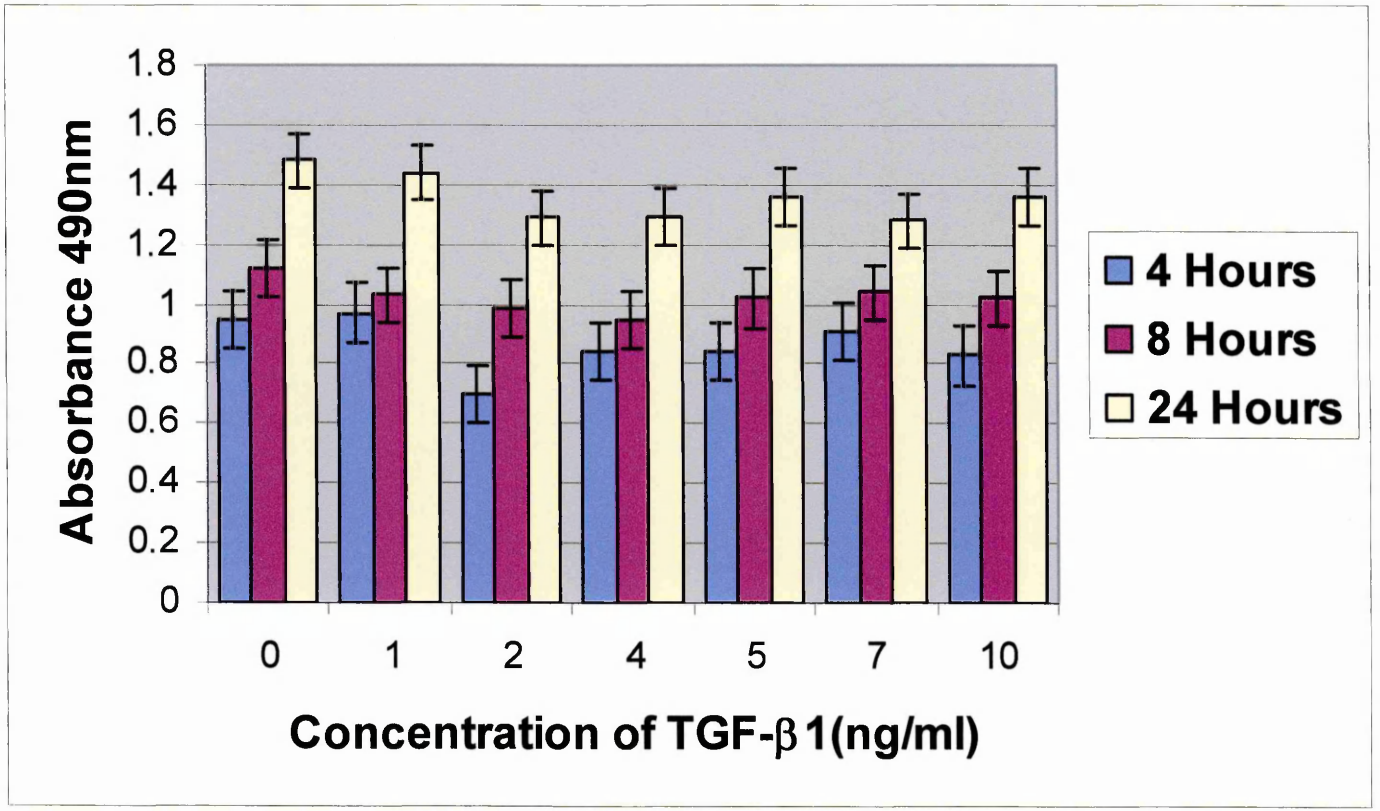

Graph 4 Results of HEC-1B cell proliferation assay with TGF-β1 stimulation. Stimulations were performed over 4 (blue bars), 8 (purple bars) & 24 hours (yellow bars) with 0ng/ml (control) or various concentrations of cytokine from 1-10ng/ml, in the presence of 1% foetal calf serum (reduced serum medium). CellTitre assay solution was added to the cells after the indicated time and the absorbance measured at 490nm. Data indicates no significant change in proliferation levels compared to the controls after 24 hours. The stimulation experiment was performed once, in triplicate (overall n=3). Data is presented as mean ± SEM.

3.1.4 Assessment of the effect of cell density on PTEN expression in HEC-1B cells.

To determine whether the minor increase in PTEN mRNA expression observed in the HEC-1B cell line in the absence of cytokine stimulation (Figures 10, 11 and 12) could be due to increasing cell density and contact inhibition, rather than TGF-β1, cells were cultured at low or high initial densities for several days. The effect of increasing cell density on PTEN expression was performed as described in Chapter 2, Section 2.2.6. Briefly, HEC-1B cells seeded at $4x10^5$ or $9x10^5$ cells per flask were cultured for 4 days in CM, or for 4 days with a media change on day 3. The media change was included to show the effects of replenishment of fresh CM, containing unknown quantites of cytokines, on PTEN expression. RNA was extracted for RT-PCR as previously detailed in Chapter 2, Section 2.2.3. Results are shown in Appendix VIII and Figures 19 to 21.

The expression of PTEN mRNA shown by RT-PCR in Figure 19 demonstrates a steady increase of PCR product over days 1 to 4, with the highest expression levels observed for the samples which received a media change on day 3 (MC). The increase in PTEN expression in day 3 MC samples may be due to renewal of stimulating factors, such as TGF-β1 in the fresh medium. No difference was discernable between cells seeded at $4x10^5$ or $9x10^5$ cells per flask, therefore initial density had no effect on PTEN expression levels, which increased in a linear manner for both densities, with comparable band intensities. Figure 20 shows that no changes in expression of the internal control GAPDH occurred over the course of the experiment, and Figure 21 indicates that no DNA was present as a contaminant in the cDNA.

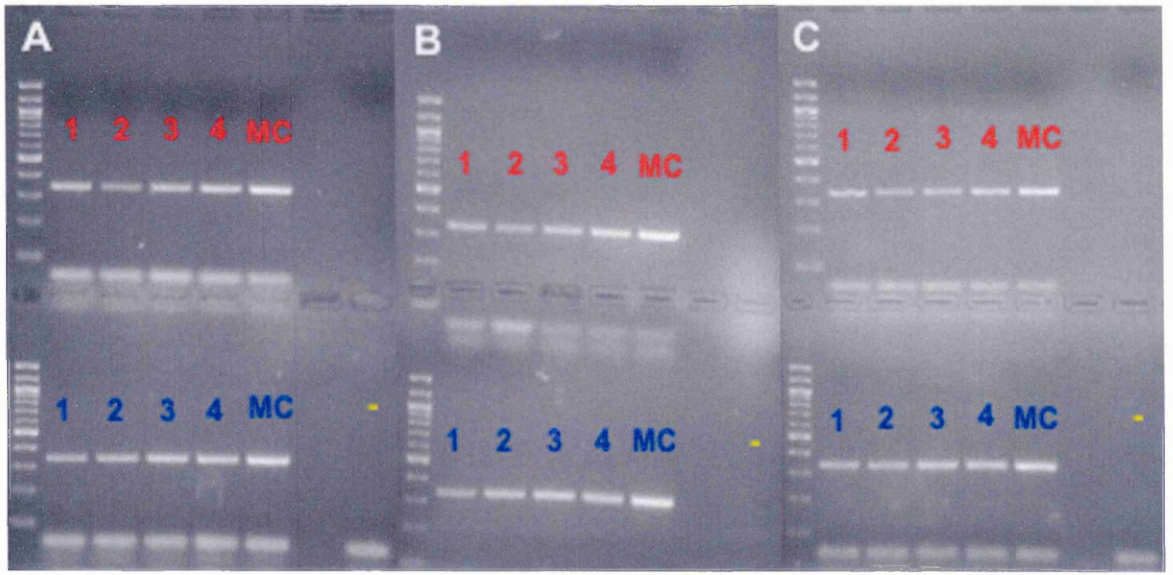

Figure 19

Agarose gel elecrophoresis of PTEN expression in HEC-1B cells over 4 days, with a media change on day 3 (MC). Red (upper panels) & blue (lower panel) indicate an initial seeding density of $4x10^5$ and $9x10^5$ respectively, yellow band is PCR control (no DNA). Triplicates A, B & C are shown. 100bp marker in lane 1.

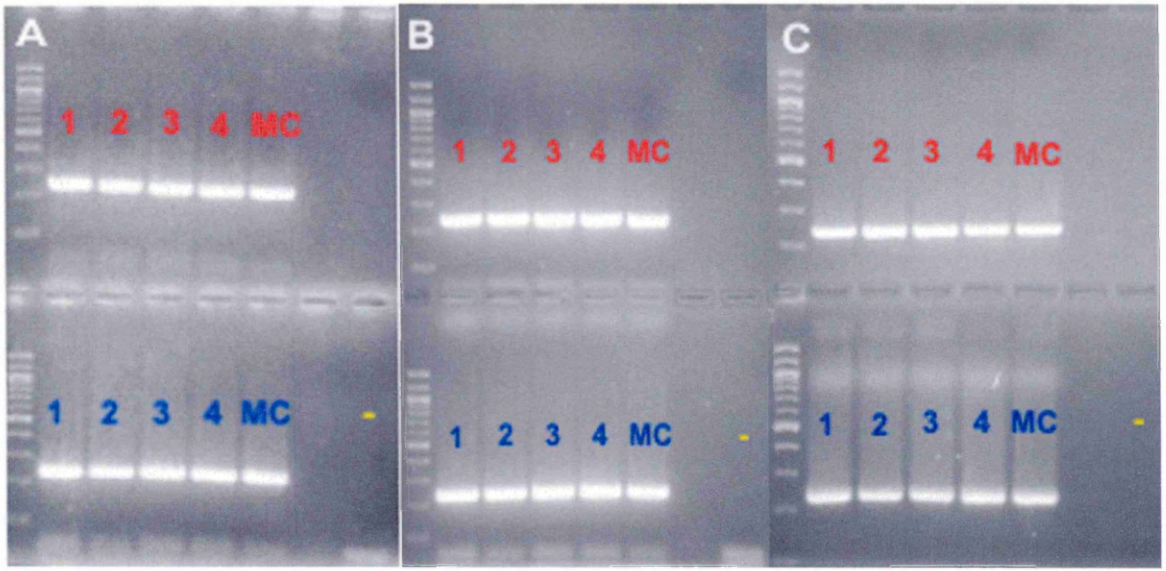

Figure 20

Agarose gel elecrophoresis of GAPDH expression in HEC-1B cells over 4 days, with a media change on day 3 (MC). Red (upper panels) & blue (lower panel) indicate an initial seeding density of $4x10^5$ and $9x10^5$ respectively, yellow band is PCR control (no DNA). Triplicates A, B & C are shown. 100bp marker in lane 1.

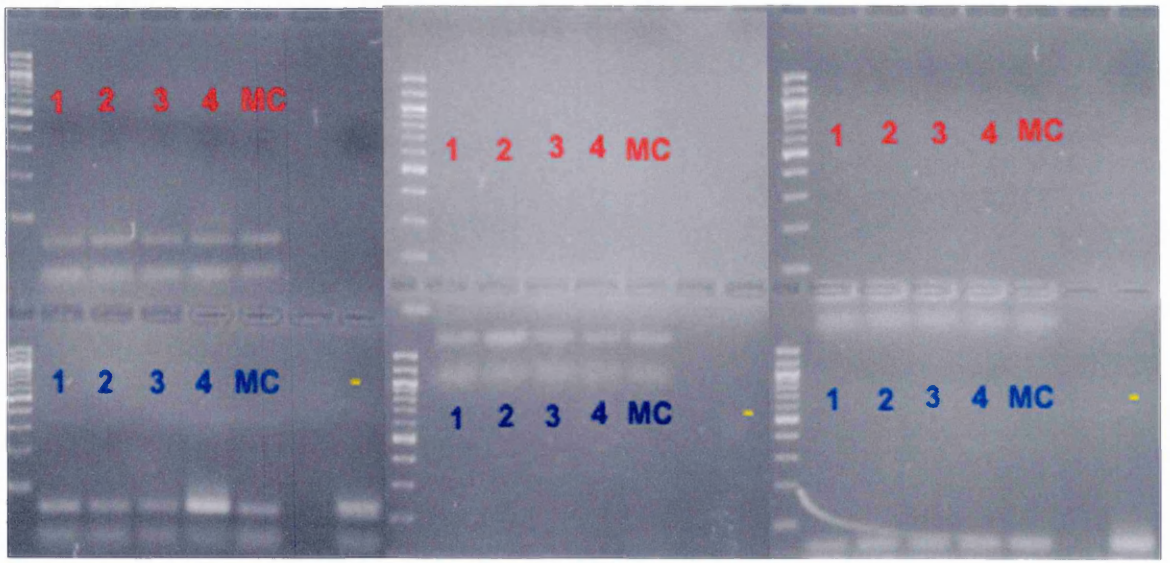

Figure 21

Agarose gel electrophoresis of –RT controls for PTEN expression in HEC-1B cells over 4 days, with a media change on day 3 (MC). Red (upper panels) & blue (lower panel) indicate an initial seeding density of $4x10^5$ and $9x10^5$ respectively, yellow band is PCR control (no DNA). Triplicates A, B & C are shown. 100bp marker in lane 1.

3.1.5 Morphological changes in HEC-1B and Ishikawa cell lines in response to TGF-ß1

As cell density alone did not appear to affect PTEN expression levels (Section 3.1.4), the effects of TGF-β1 on the morphology of both Ishikawa and HEC-1B cell lines was evaluated. Although the cytokine did not modify PTEN protein levels in the experiments described previously, decreased proliferation and increased cell volume has been described in HEC-1B stimulated with TGF-β1(Boyd & Kaufman, 1990). This may involve changes in phospho-PTEN levels which could possibly be detected with the new commercial anti-phospho-PTEN (Ser380/Thr383/384) antibody. A decrease in P-PTEN levels may indicate increased PTEN protein activity and degradation and a decrease in Akt-mediated proliferation.

HEC-1B and Ishikawa cell lines were cultured in medium containing 10% foetal calf serum, then cultured for a further 48 hours in medium containing 1% serum to reduce any effects of TGF-β1 in the medium. Cells were then cultured in reduced-serum medium in the absence or presence of TGF-β1 at a concentration of 10ng/ml for 48 and 72 hours as described in Chapter 2, Section 2.2.7. This experiment was performed once, with triplicate wells. The live cells were photographed under phase contrast using Polaroid film (Figures 22 to 25). The cells were trypsinised and counted using a haemocytometer and the average figures from the triplicate wells are shown in Graphs 5 and 6.

HEC-1B Morphological Changes

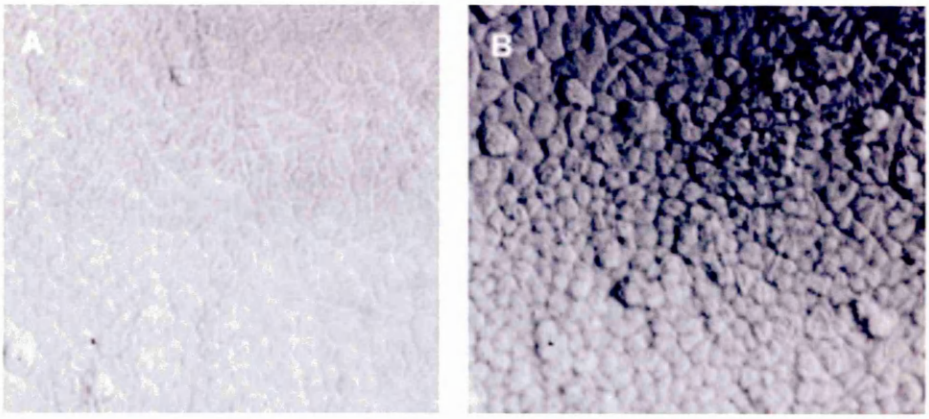

Fig 22 Morphological changes in HEC-1B under reduced-serum conditions with no TGF-β1 at A: 48 hours and B: 72 hours Live cells visualised after 48 & 72 hours using phase contrast microscopy. Magnification x20

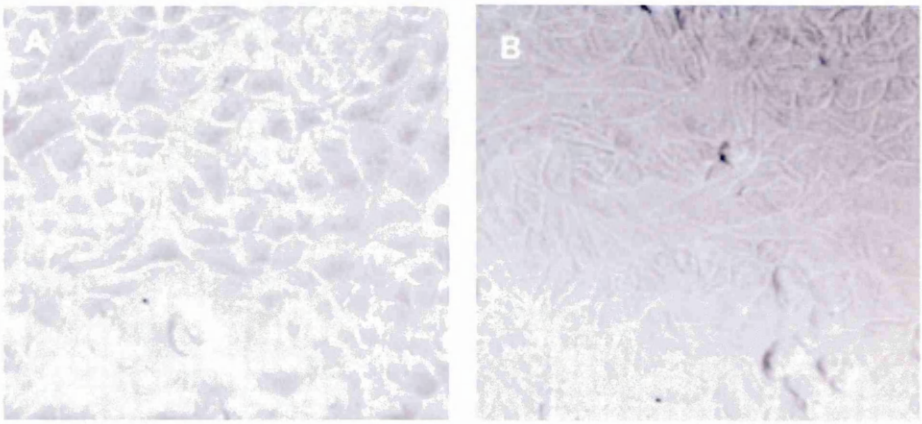

Fig 23 Morphological changes in HEC-1B with 10ng/ml TGF-β1 at A: 48 hours and B: 72 hours Live cells visualised after 48 & 72 hours using phase contrast microscopy. Magnification x200

Table 14 HEC-1B cell count x 10^4		
	48 hours	72 hours
No TGF-β1	13.5	28.5
	12	36.5
	11.5	26
Average	**12.3**	**30**
10ng/ml TGF-β1	8	17
	8.5	15
	7	14.5
Average	**7.8**	**15.5**

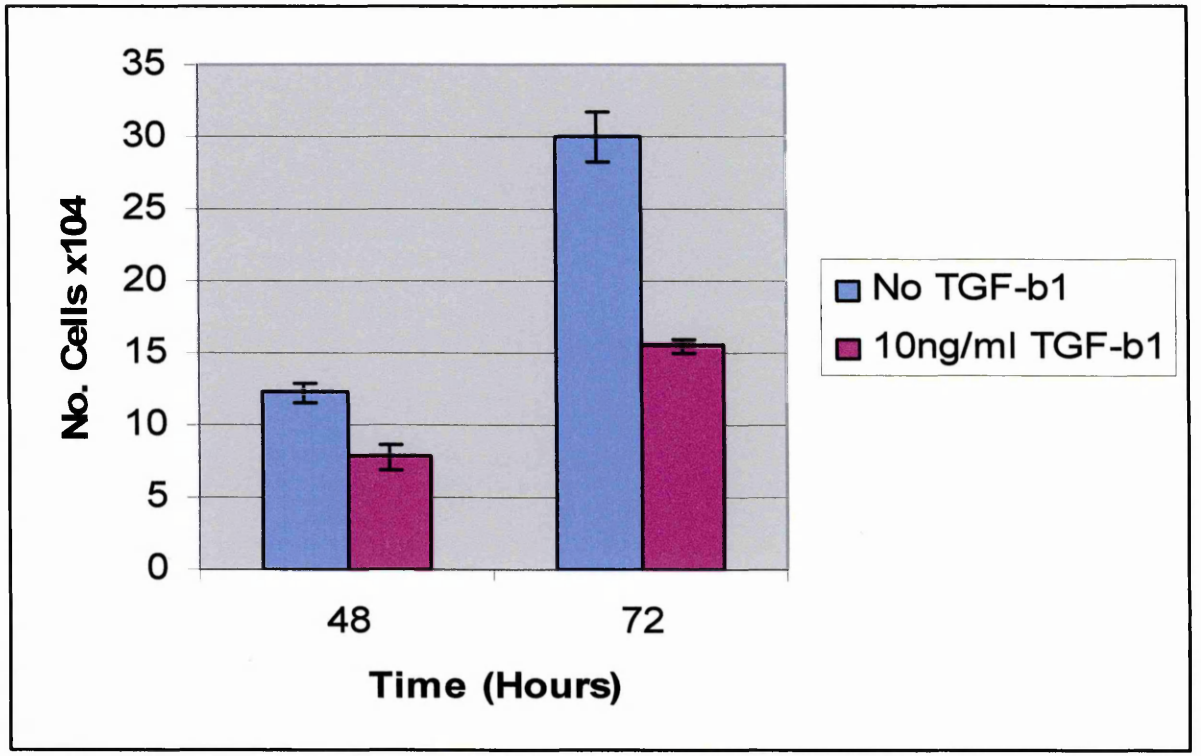

Graph 5 HEC-1B cell counts from morphology study following treatment with 10ng/ml TGF-β1. Cells were cultured in reduced-serum (1%) medium and either untreated (blue) or treated with 10ng/ml TGF-β1(purpie) for 48 and 72 hours prior to counting of trypsinised cells using a haemocytometer. Data indicates a reduction in cell numbers with TGF-β1 treatment compared to unstimulated controls. The stimulation experiment was performed once, in triplicate (overall n=3). Data is presented as mean ± SEM.

By comparing Figure 22 and 23, it can be seen that treatment of HEC-1B cells with TGF-β1 had the effect of increasing cell volume. Untreated cells were small and rounded, with a characteristic "cobblestone" appearance. After 48 hours of stimulation the cells were significantly larger, and after 72 hours had assumed a flattened profile. After performing cell counts of the stimulated and unstimulated HEC-1B cells (Table 14), the results were expressed in Graph 5.

After both 48 and 72 hours there was almost twice the number of untreated cells to treated cells. Untreated control cell numbers increased approximately 2.5 times between the 48 and 72 hour time points, whereas the TGF-β1 treated cells increased by 2 times. In this experiment using HEC-1B cells, TGF-β1 had the overall effect of increasing cell volume and decreasing proliferation. This effect of TGF- β1 on HEC-1B morphology and growth has previously been reported by Boyd & Kaufman, 1990.

Ishikawa morphological changes

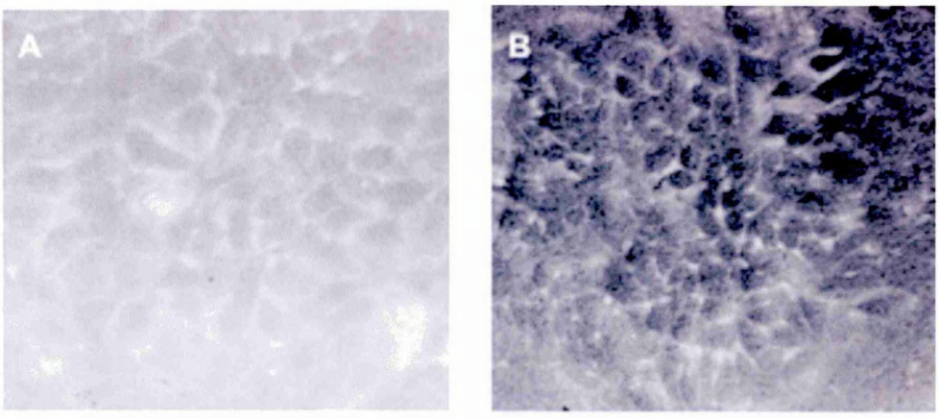

Fig 24 Morphological changes in Ishikawa under reduced-serum conditions with no TGF-β1 at A: 48 hours and B: 72 hours Live cells visualised after 48 & 72 hours using phase contrast microscopy. Magnification x200

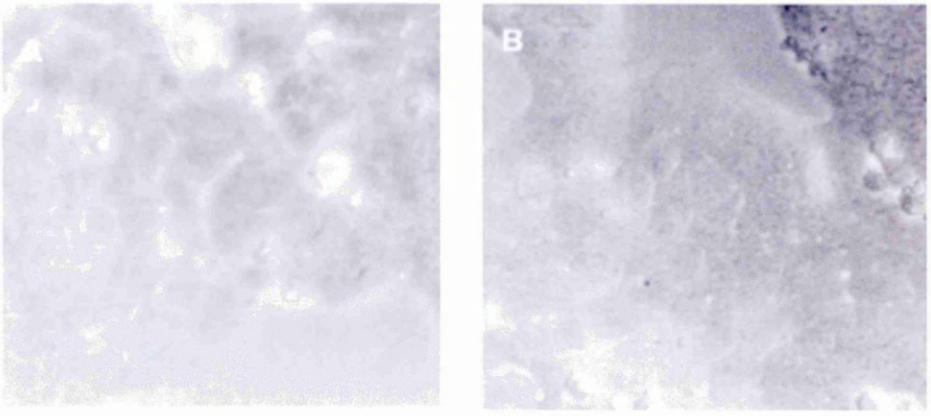

Fig 25 Morphological changes in Ishikawa with 10ng/ml TGF-β1 at A: 48 hours and B: 72 hours Live cells visualised after 48 & 72 hours using phase contrast microscopy. Magnification x200

Table 15 Ishikawa cell count x 10^4		
	48 hours	72 hours
No TGF-β1	14	16.5
	12	18
	13.5	19.5
Average	**13.2**	**18**
10ng/ml TGF-β1	12	17.5
	10.5	18
	10.5	13.5
Average	**11**	**16.3**

By comparing Figure 24 and 25, it can be seen that treatment with TGF-β1 had little effect on Ishikawa cell volume, but after 48 hours of stimulation small patches of cells appeared to have detached from the flask, leaving areas free of cell growth.

After performing cell counts of the stimulated and unstimulated Ishikawa cells (Table 15), the results were expressed in Graph 6. After both 48 and 72 hours there was only a very slight increase in the number of untreated cells to treated cells. Additionally, little change was observed between the 48 and 72 hour time points for both treated and untreated cells. This suggests that TGF-β1 has significantly less effect on the morphology and proliferation of Ishikawa cells compared to HEC-1B cells under the conditions used. ISK cells have previously been reported to show inhibition of proliferation in response to TGF-β1 (Anzai, et al 1992).

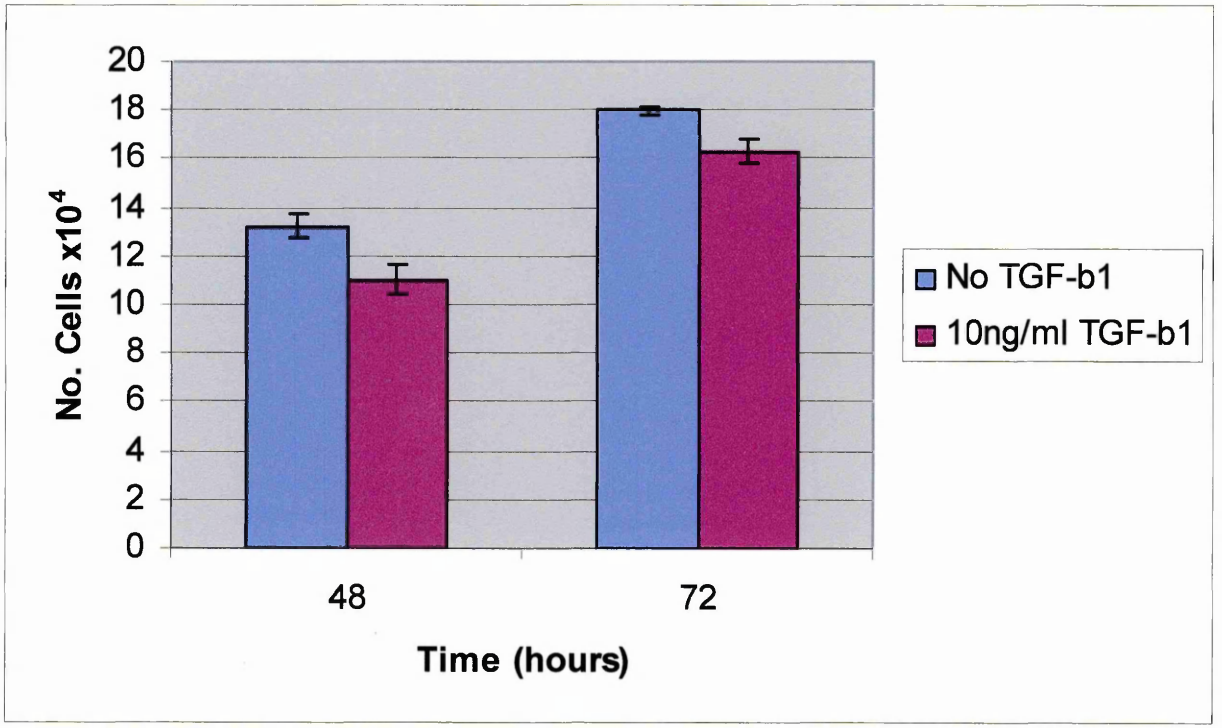

Graph 6 Ishikawa cell counts from morphology study following treatment with 10ng/ml TGF-β1. Cells were cultured in reduced-serum (1%) medium and were either untreated (blue) or treated with 10ng/ml TGF-β1(purple) for 48 and 72 hours prior to counting trypsinised cells using a haemocytometer. Data indicates a very modest reduction in cell numbers with TGF-β1 treatment compared to unstimulated controls. The stimulation experiment was performed once, in triplicate (overall n=3). Data is presented as mean ± SEM.

3.2 CLONING OF FULL LENGTH HUMAN PTEN INTO CMV-pEGFP-N1 AND SUBCELLULAR LOCALISATION OF PTEN PROTEIN

The localisation of PTEN has been described as mainly cytoplasmic but has also been reported as nuclear in some cells, and its localisation has not previously been described in HEC-1B or Ishikawa endometrial cell lines. Changes in the localisation of PTEN in the cell are a possible mechanism of regulating its function.

To enable the rapid study of PTEN localisation in various cell lines, full length human PTEN was cloned into a GFP plasmid vector to create a C-terminal fusion protein which can be detected by fluorescent microscopy using a standard FITC filter. The production of GFP-PTEN permitted the transfection of cultured cells, regardless of the state of endogenous PTEN, and the subsequent ability to add stimulating compounds to these transiently transfected cells. The fusion protein could be rapidly visualised without the need for detection using antibodies, which may be difficult to detect if cellular levels of PTEN are very low.

The overall cloning strategy is outlined in Chapter 2, Section 2.3.1. Briefly, full-length PTEN amplified by PCR and the CMV-PEGFP-N1 vector were subjected to double-digestion with two restriction enzymes, *Eco*RI and *Sal*I, to create a single cohesive end from each enzyme on both DNA sources. Subsequent ligation of the cut fragments to form a EGFP-PTEN chimera can only occur in one direction, thus ensuring that the PTEN fragment is inserted into the vector and later transcribed and translated in the correct orientation (5'→3').

The detection of other cellular compartments, proteins or organelles could also be accomplished in transfected cells using a primary antibody bound by a secondary antibody linked to a fluorescent moiety that is not green, eg red, cyan or magenta. This would enable the study of the localisation of GFP-PTEN to such cellular compartments by overlapping the two differently coloured images and noting areas of co-localisation, indicated by a colour change (eg an overlap of green and red is seen as yellow).

3.2.1 Extraction of RNA from whole human blood

Total RNA was extracted from the whole blood of four members of staff using TRI Reagent. The yield and purity of each sample was assessed by reading the absorbance at 260 and 280nm and the results shown in Table 16. Peripheral blood was chosen because PTEN mutations in lymphocytes are very rare even in haematological malignancies, therefore cells from healthy individuals was most likely to be wild-type for PTEN.

Table 16 Staff total RNA yield and purity

Staff Number	A260nm	A280nm	ratio	µg/µl
1	0.065	0.033	1.74	0.52
2	0.101	0.059	1.84	0.81
3	0.085	0.046	1.816	0.68
4	0.082	0.044	1.832	0.66

3.2.2 RT-PCR of full-length human PTEN for cloning

3.2.2.1 Analytical scale preparation of cDNA and digestion with restriction endonucleases *Mse* I and *Hha* I

cDNA was synthesised as described in Chapter 2, Section 2.3.3 from each of the four staff members and amplified using PTEN primers 1 and 4 to yield a

450bp fragment, shown in Figure 26. This fragment can be used in an analytical digest with *Mse* I and *Hha* I to distinguish between PTEN derived from pure RNA, (contains an *Mse* I site only), or from genomic contamination, (contains a *Hha* I site only). The PCR products were therefore digested with *Mse* I and *Hha* I (Figure 27). From this gel it can be clearly observed that all four PCR products were only digested with *Mse* I, and were therefore derived from PTEN cDNA and not genomic ΨPTEN. Staff cDNA number 4 was selected for cloning as it gave a good yield of PCR product and the RNA from which it was derived had a high purity ratio (260/280nm).

3.2.2.2 PCR amplification of PTEN with high fidelity *Pfx* polymerase

cDNA was used in the amplification of full-length PTEN as described in Section 2.3.4 using the Pfx3lx PCR programme (Appendix V), and the reactions analysed by agarose gel electrophoresis (see Figure 28). To improve the yield of PCR product, which was poor, a modified version of the programme (Pfx3lx2) was then used which included a 20 minute final extension (Appendix V). The products were again analysed on an agarose gel as shown in Figure 29, and a significant improvement in yield was observed. Several PCR reactions were performed, pooled, and separated on an agarose gel to provide adequate DNA for cloning. The 1.2Kb band was carefully excised from the gel and purified as described in Chapter 2, Section 2.3.5.

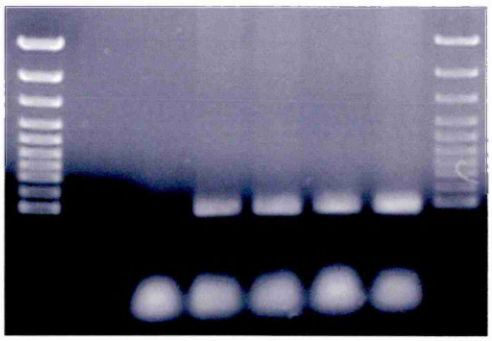

Figure 26
PCR of staff cDNAs (**1 - 4**) with PTEN primers 1&4 to amplify a 450bp fragment. RT-PCR controls (-RT & -RNA), are shown with the four staff samples. **M**= 100bp ladder.

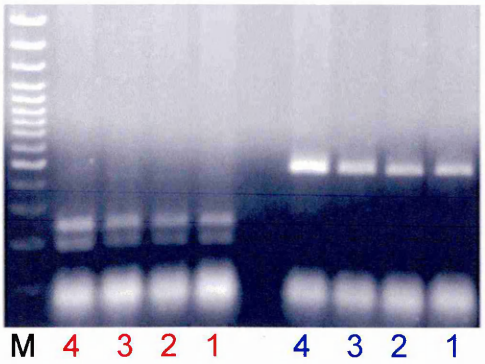

Figure 27
Aliquots of staff PCR samples 1-4 digested with *Mse* I (red) and *Hha* I (blue). **M**= 100bp ladder. The products were cleaved by *Mse*I to yield two distinct bands.

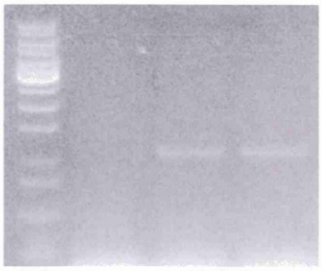

M – Pfx3lx

Figure 28

Electrophoresis of Staff number 4 full-length PTEN PCR product (1.2Kb), using Pfx3lx PCR cycle. PCR Control shown as a dash, **M**= 1Kb ladder.

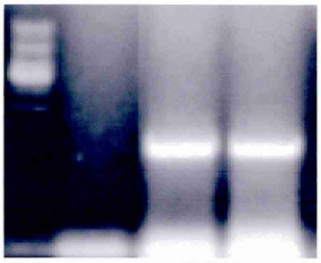

M – Pfx3lx2

Figure 29

Electrophoresis of Staff number 4 full-length PTEN PCR product (1.2Kb), using Pfx3lx2 cycle. PCR Control shown as a dash, **M**= 1Kb ladder.

3.2.3 Digestion and purification of the PTEN fragment for ligation

To create the restriction fragment sites for ligation into the vector, the purified PTEN fragment was digested with *Eco*RI and *Sal* I as described in Chapter 2, Section 2.3.5 and cleaned up as described in the same section. To assess yield a 5µl aliquot was separated on an agarose gel alongside 5µl of double digested and purified pEGFP as shown in Figure 31. From this gel a good yield of both plasmid and insert was observed, with no extraneous bands in either sample (shown in Section 3.2.5).

3.2.5 Preparation of CMV-pEGFP-N1 plasmid for cloning

The CMV-pEFP family of plasmids are widely used for the fluorescent tagging of proteins to be expressed in mammalian cells, and are available for either N or C-terminal fusions. They also include a range of colours, such as ECFP (cyan) and EYFP (yellow) which are point mutants of the standard EGFP (green) fluorescent protein. The vectors are suitable for mammalian expression due to the presence of the strong cytomegalovirus (CMV) promoter. The EGFP-N1 version of the plasmid was chosen for cloning as this was readily available and would attach the GFP moiety to the C-terminus of the mature PTEN protein. As it has been postulated that degradation of PTEN is controlled via the C-terminus, the generation of this clone may yield some insight into the cellular effects of interfering with this process.

3.2.5.1 Transformation of *E.*coli with CMV-pEGFP-N1 and plasmid DNA isolation by Alkaline Lysis

Chemically competent JA221 cells were prepared and transformed with CMV-pEGFP-N1, as described in Chapter 2, Section 2.3.6. Numerous colonies were observed on the selective plate. Plasmid DNA extracted from a single colony by the method described in Chapter 2, Section 2.3.7 was analysed on a 1% agarose gel. 1µl of plasmid was run with a 1Kb marker as illustrated in Figure 30. The preparation was seen to consist of two bands; the upper of these being the open circular form of the plasmid and the lower being the supercoiled form. 5µl of plasmid (~10µg) was used in double restriction digest and purification as described in Chapter 2, Section 2.3.7.

3.2.5.2 Comparison of yield of PTEN and linearised pEGFP after digestion.

To give an estimation of yield of the double digested PTEN and pEGFP after purification, 5µl of each sample was separated on an agarose gel, as shown in Figure 31. The concentration of the PTEN fragment was estimated to be approximately 2.5 times that of the pEGFP fragment. The relative amount of DNA in each sample was used to determine the amount required to perform three ligations with different ratios of vector to insert DNA.

3.2.6 Ligation

Ligations were performed at 1:1, 1:3, and 1:5 ratios of vector : insert (Table 17) based on the PTEN fragment having 2.5 times the concentration of DNA as the vector, and 10µl analysed on an agarose gel (Figure 32). A control ligation was performed using a 100bp marker (Chapter 2, Section 2.3.8), and is shown as an inverted image in Figure 33.

Table 17 Ligation Reactions for pEGFP & PTEN		
Ligation Number	Ratio V:I	V:I (µl)
1	1:1	6.5:2.5
2	1:3	6.5:7.5
3	1:5	6.5:12.5

Table 17 Ligation ratios and volumes of vector (v) and insert (I).

Preparation of pEGFP & Comparison of yield of Digested PTEN & pEGFP

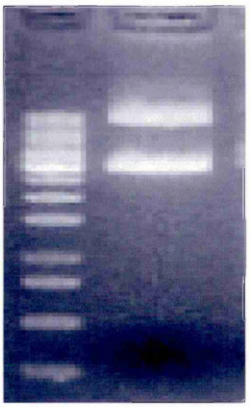

Fig 30

Agarose gel electrophoresis of 1µl pEGFP. **M**= 1Kb marker.

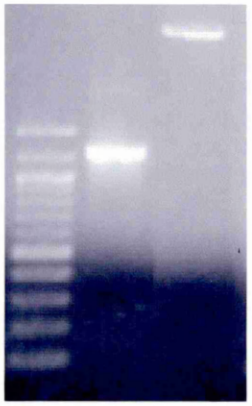

Fig 31

Comparison of yield of double digested products 5µl each of **1:** PTEN, and **2:** pEGFP. **M**= 100bp marker.

Ligation & Ligation Control

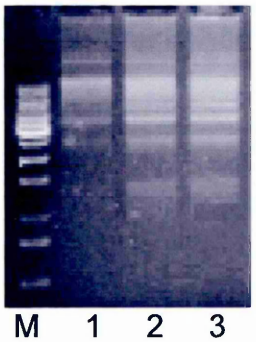

Fig 32

Agarose gel electrophoresis of ligations **1**, **2** & **3** **M**= 1Kb ladder.

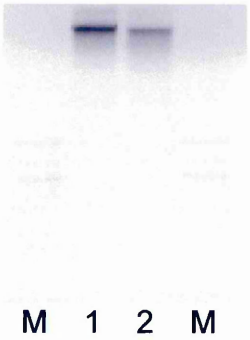

Fig 33

Control ligations of 100bp ladder at **1:** 4°C and **2:** 24°C shown as an inverted image. **M**= 100bp ladder

From Figure 33 it was observed that the ligation of the 100bp ladder was most successful at 4°C, as this gave the highest yield of ligated product. The lower temperature was therefore used in ligations involving PTEN and pEGFP. Figure 32 shows the three ligation reactions and as expected all contain multiple bands, indicating that the ligation was successful insofar that the DNA fragments had been randomly joined.

3.2.7 Introduction of Recombinant Plasmid DNA into *E.*coli cells

3.2.7.1 Plating out and analysis of the transformants

The three ligation reactions were used to transform chemically competent DH5α cells which were plated onto selective L-agar as described in Chapter 2, Section 2.3.9. Chemically competent cells are available commercially and avoid the need for preparing competent cell stocks. Following overnight incubation the number of colonies on each control or ligation plate was noted and shown in Table 18. From the results tabulated it was observed that plates 1 and 5 gave the highest colony numbers. These plates correspond to the ligation ratio of 1:1.

3.2.7.2 Confirmation of the presence of full length PTEN in the recombinant (pRC-2) plasmids

To confirm that the cloning had been successful, two colonies were picked from each ligation plate (with the exception of plate 5 which contained too many colonies) into selective LB for overnight growth. Plasmids were labelled A and B for each plate. The following day plasmids were extracted as previously described in Chapter 2, Section 2.3.7. Each plasmid was digested and aliquots of cut and uncut plasmid analysed on a 1% agarose gel. Gels

with uncut plasmid (Figure 34), and double digested plasmid (Figure 35) are shown overleaf.

Table 18 Results of Transformation			
Plate number	Ligation	µl cells spread	Colonies Formed
1	1	20	71
2	2	20	49
3	3	20	43
4	control	20	130
5	1	50	370
6	2	50	170
7	3	50	108
8	control	20	122

Confirmation of the presence of Recombinant Plasmids Containing Full-Length PTEN

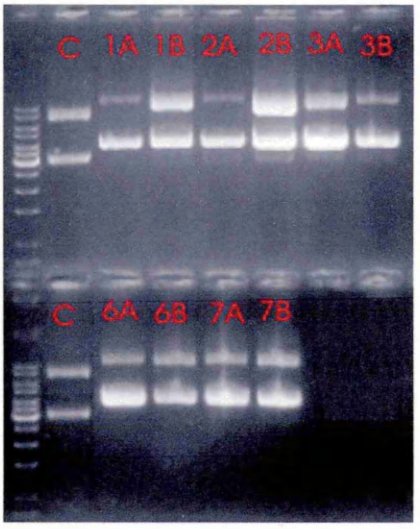

Fig 34

Electrophoresis of uncut plasmids derived from clones 1A to 7B. **C**= uncut pEGFP, **M**= 1Kb marker.

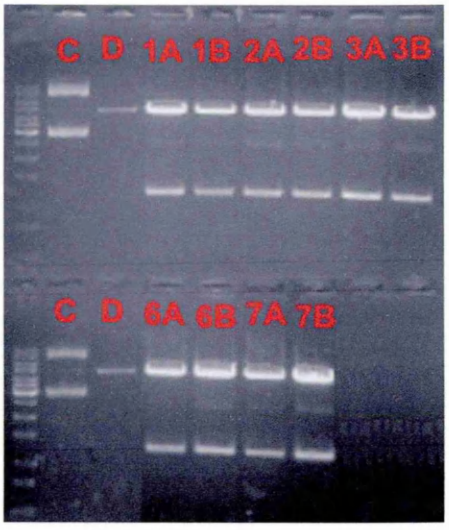

Fig 35

Electrophoresis of *Eco*RI / *Sal* I double digested plasmids derived from clones 1A to 7B. **C**= uncut pEGFP, **D**= linear pEGFP, **M**= 1Kb marker.

All the cultures gave a high yield of plasmid DNA of approximately 1-1.5Kb higher in size when compared to the pEGFP control and 1Kb marker. Upon digestion, all plasmids yielded two bands of approximately 4.7Kb and 1.2Kb. These bands corresponded to linear pEGFP and PTEN, respectively.

3.2.7.3 Preparation of pRC-2 (Clone 6A) plasmid DNA for Sequencing

From Figure 35 it was observed that clone number 6A had the cleanest digest, as the presence of an extra band at approximately 2.5Kb was not detected. In addition, Figure 34 shows that this clone had a high proportion of supercoiled DNA (lower band) to the open circular form upper band), indicating that little damage to the plasmid DNA had occurred during preparation. To confirm the PTEN insert sequence, and to verify that the clone was in-frame with respect to the EGFP tag, the plasmid was propagated and sent for automated sequencing (Chapter 2, Section 2.3.10). The sequencing data is shown in Figure 36 and includes a single strand read with standard EGFP and CMV primers. The read confirmed that pRC-2 contained wild-type PTEN.

Date sent: Fri, 28 Jun 2002 11:47:32 +0100
Subject: LARK TECHNOLOGIES
From: Stephen Foster <stephen@larkuk.co.uk>
To: Eric Blair <g.e.blair@leeds.ac.uk>

EGFP primer

GNGGGCACCCCCCGGTGAACAGCTCCTCGCCCTTGCTCACCATGGTGGCGACCGGTGGATCCCGGGCCCG
CGGTACCGTC
GACTGGACTTTTGTAATTTGTGTATGCTGATCTTCATCAAAAGGTTCATTCTCTGGATCAGAGTCAGTGG
TGTCAGAATA
TCTATAATGATCAGGTTCATTGTCACTAACATCTGGTGTTACAGAAGTTGAACTGCTAGCCTCTGGATTT
GACGGCTCCT
CTACTGTTTTTGTGAAGTACAGCTTCACCTTAAAATTTGGAGAAAAGTATCGGTTGGCTTTGTCTTTATT
TGCTTTGTCA
AGATCATTTTTTGTTAAAGTAAGTACTAGATATTCCTTGTCATTATCTGCACGCTCTATACTGCAAATGC
TATCGATTTC
TTGATCACATAGACTTCCATTTTCTACTTTTTCTGAGGTTTCCTCTGGTCCTGGTATGAAGAATGTATTT
ACCCAAAAGT
GAAACATTTTGTCCTTTTTTAGCATCTTGTTCTGTTTGTGGAAGAACTCTACTTTGATATCACCACACAC
AGGTAACGGC
TGAGGGAACTCAAAGTACATGAACTTGTCTTCCCGTCGTGTGGGTCCTGAATTGGAGGAATATATCTTCA
CCTTTAGCTG
GCAGACCACAAACTGAGGATTGCAAGTTCCGCCACTGAACATTGGAATAGTTTCAAACATCATCTTGTGA
AACANCAGTG
CCCACTGGTCTATAATCCAGATGATTCTTTAACAGGTAGCCTATAATAATACACATAGCCGCCTCTGACT
GGGAATAGTT
ACTCCCTTTTTGGNCTCTGGCCCTTACTTCCCCATANAAATCTANGGCCCTNTTGGCCCTTTAAAANTTN
NCCCCGANGT
AATAATTTGCCCATTTCNTTNNCCCAGTTNGTCCCTTTCCAGTTTTCNNGGNAATGGCNGCACATGATNG
GCCTCNNCCT
NTACCCNNGGGCAAAANCTNCCAAANGGGTTGGAAAANNNCNACCGGGGGGGGNNANGNCCCCAAAGNAT
TT

Date sent: Fri, 28 Jun 2002 11:47:32 +0100
Subject: LARK TECHNOLOGIES
From: Stephen Foster <stephen@larkuk.co.uk>
To: Eric Blair <g.e.blair@leeds.ac.uk>

CMV primer

GNNGGGCCGCNCTATATAAGCAGNAGCTCTCTGGCTAACTAGAGAACCCACTGCTTACTGGCTTATCGAA
ATTAATACGA
CTCACTATAGGGAGACCCAAGCTTCGAATTCAGCATGACAGCCATCATCAAAGAGATCGTTAGCAGAAAC
AAAAGGAGAT
ATCAAGAGGATGGATTCGACTTAGACTTGACCTATATTTATCCAAACATTATTGCTATGGGATTTCCTGC
AGAAAGACTT
GAAGGCGTATACAGGAACAATATTGATGATGTAGTAAGGTTTTTGGATTCAAAGCATAAAAACCATTACA
AGATATACAA
TCTTTGTGCTGAAAGACATTATGACACCGCCAAATTTAATTGCAGAGTTGCACAATATCCTTTTGAAGAC
CATAACCCAC
CACAGCTAGAACTTATCAAACCCTTTTGTGAAGATCTTGACCAATGGCTAAGTGAAGATGACAATCATGT
TGCAGCAATT
CACTGTAAAGCTGGAAAGGGACGAACTGGTGTAATGATATGTGCATATTTATTACATCGGGGCAAATTTT
TAAAGGCACA
AGAGGCCCTAGATTTCTATGGGGAAGTAAGGACCAGAGACAAAAAGGGAGTAACTATTCCCAGTCAGAGG
CGCTATGTGT
ATTATTATAGCTACCTGTTAAAGAATCATCTGGATTATAGACCAGTGGCACTGTTGTTTCACAAGATGAT
GTTTGAAACT
ATTCCAATGTTCAGTGGGCGGAACTTGCAATCCTNAGTTTGTGGTCTGCCANCTAAAGGTGAANATTTAT
TCCTCCANTT
CAGGACCCACACGACGGGNAGACAAGTTCATGTNCTTTGANTTCCCTCAACCGTTACCTGGGTGTGGGGA
ATTNAAAANA
AANTTNTTCCNCAACAAAANAGAGCTAAAAAGGNCAAATGTTCNCTTTNGGGNAANAATTCTTNNNCCNG
ACCGGGGAAC
CTNAAAAANTNAAANGGGGTTTTGGGNCCAAAANCCTAGCCTTGGCNATNAANCGNCNAAANANNAGNAA
TTT

Figure 36

pRC-2 Clone 6A Sequence data acquired using CMV & EGFP primers.

3.2.8 Sub-cellular distribution and localisation of pRC-2

Although it has been widely reported that PTEN is mainly a cytoplasmic protein, evidence exists that it can localise to the plasma membrane and the nucleus in a manner which may be cell-line specific (Ginn-Pease & Eng, 2003). The observation of PTEN in the nucleus suggests that it may interact with an as yet unidentified protein to modulate transcription, but as yet there is no direct evidence to support this. In this section, the localisation and distribution of PTEN was studied in endometrial cell lines by transfection with pRC-2. The monkey cell line COS-7 was also used in initial transfections as this cell line has a very flat morphology which is easy to visualise using fluorescent microscopy. A commercial lipid-based transfection reagent was chosen to deliver pRC-2 into COS-7, HEC-1B and Ishikawa cell lines. These cationic lipid reagents bind to DNA and permit transfer across the cell membrane, and are a less time-consuming alternative methods, such as calcium phosphate.

3.2.8.1 Preparation of Ultrapure Supercoiled Plasmid DNA

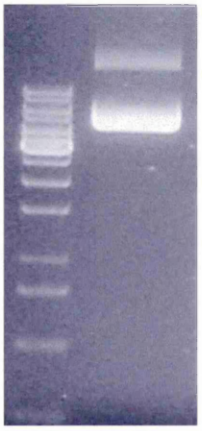

Figure 37

Electrophoresis of **1:** pRC-2, 1µl. **M** = 1Kb ladder

Preparation of high quality, supercoiled pRC-2 plasmid DNA was performed using a Sigma miniprep kit according to the manufacturer's guidelines (Chapter 2, section 2.3.11). To assess the quality of the plasmid, a 1µl aliquot was analysed by agarose gel electrophoresis, as shown in Figure 37. Samples of plasmid (5µl) were diluted 1:200 in sterile water to measure absorbance at 260nm. A stock solution of 1µg/µl was prepared and small aliquots frozen.

Initial transfections were performed with 0.6-1.0μg of pRC-2 or pEGFP and 2μl of Lipofectamine (LF) or Lipofectamine 2000 (LF2K), as described in Chapter 2 Section 2.3.11. Transfection into both the COS-7 and HEC-1B cell lines was highly inefficient in all conditions, with less than 10% transfectants visible on each coverslip. Many of the cells were observed to have detached from the coverslips during the fixing process of submerging in cold methanol, indicating poor adherence to the glass surface. Additionally, the presence of the fusion protein did not appear to be toxic as the nuclei of transfected cells were visibly normal and several could be seen in a state of mitosis. This experiment was performed several times in triplicate and on several separate occasions. Images were captured from wells transfected with 0.8μg of plasmid, (see Figures 38 and 39), and are representative of the distribution observed in all transfection conditions in each individual experiment.

Transfection of COS-7 Cell Line with pRC-2

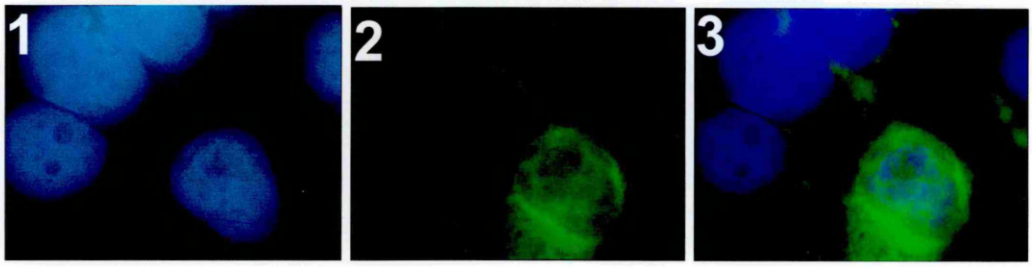

a 0.8µg pRC-2 and 2µl LF

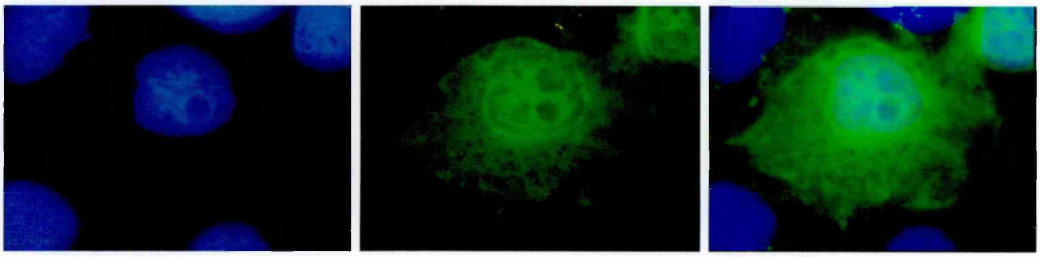

b 0.8µg pRC-2 and 2µl LF2K

Figure 38

Transfection of COS-7 cell line with **a** 0.8µg pRC-2, and 2µl LF and **b** 0.8µg pRC-2 and 2µl LF2K. Filters used were **1** DAPI for the nucleus and **2** FITC for EGFP. Composite images are shown in **3**. Magnification x400.

Transfection of HEC-1B with pRC-2

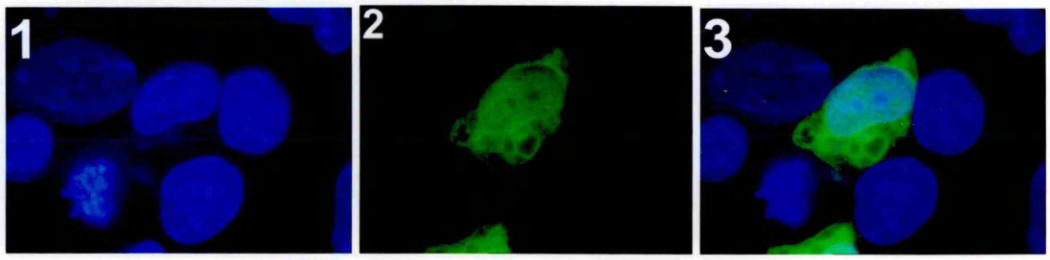

a 0.8µg pRC-2 and 2µl LF

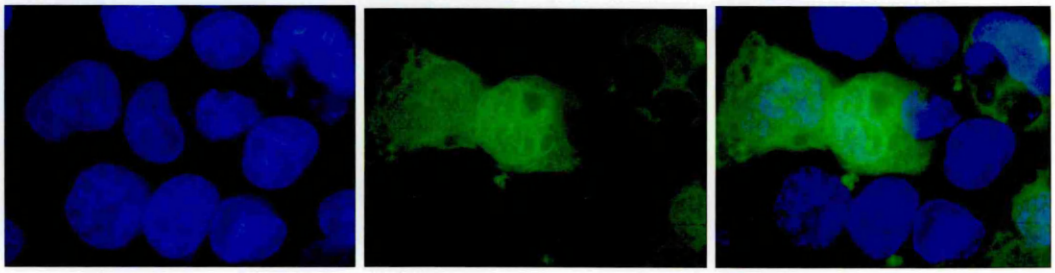

b 0.8µg pRC-2 and 2µl LF2K

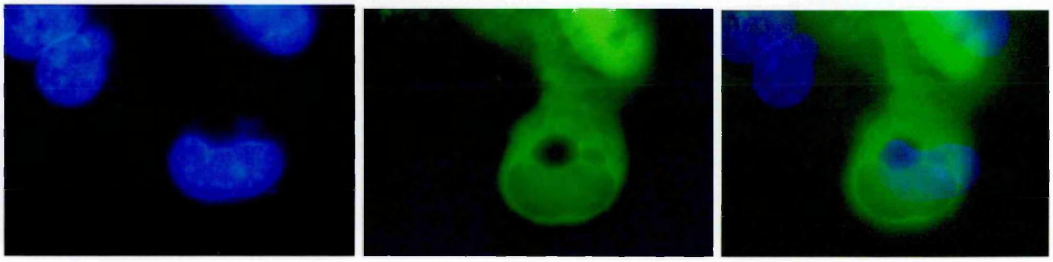

c 0.8µg pEGFP and 2µl LF2K

Figure 39

Transfection of HEC-1B cell line with **a** 0.8µg pRC-2 and 2µl LF and **b** 0.8µg pRC-2 and 2µl LF2K. Filters used were **1** DAPI for the nucleus and **2** FITC for EGFP. Composite images are shown in **3**. Magnification x400.

From the previous images it was noted that the green pRC-2 signals showed a distinctly cytoplasmic distribution in both cell lines, with prominant delineation around the nuclear membrane or perinuclear region. Cytoplasmic localisation of PTEN has been reported in endometrial stromal cells, whilst P-PTEN was observed in the nucleus (Guzeloglu-Kayisli, et al 2003). Varying amounts of protein and 'speckles' appeared in the approximate location as the nucleus, as described in neuronal cells by Lachyankar, et al (2000). Overall expression levels varied widely within the visible cells. The patterns of distribution and expression levels were comparable between pRC-2 and pEGFP. Of the two transfection reagents used, Lipofectamine 2000 (LF2K) gave a higher yield of transfected cells (Figure 38b & 39b) and was therefore selected to perform further investigation.

3.2.9.3 Optimisation of Transfection

HEC-1B and Ishikawa cells were seeded onto coverslips coated in polylysine, (Chapter 2, Section 2.3.12), and were observed to exhibit greater adherence as fewer cells became detached during the fixing process. Transfection rates were scored visually from several experiments performed independently with duplicate samples. Figures 40 to 43 show transfection levels using 2µl LF2K, and 0.6-1.0µg of pRC-2 for these cell lines at 200- and 400-times magnification.

Optimisation of HEC-1B Cell Line Transfection

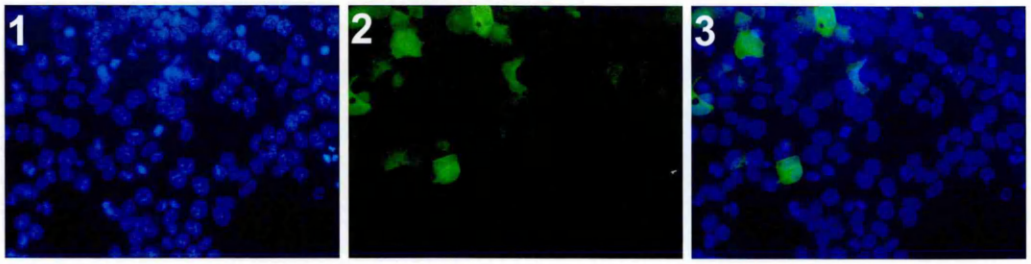

a 0.6µg pRC-2 and 2µl LF2k x200

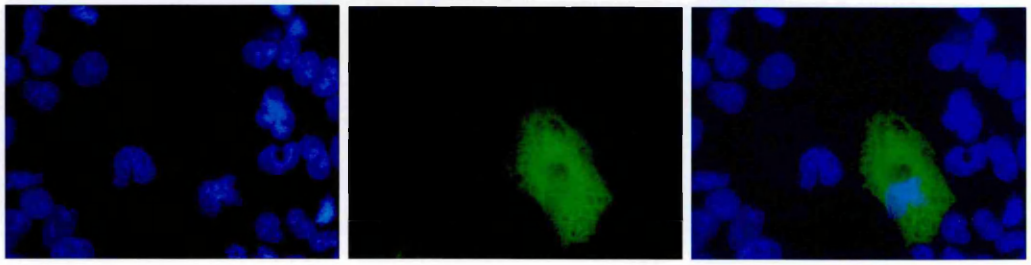

ai 0.6µg pRC-2 and 2µl LF2k x400

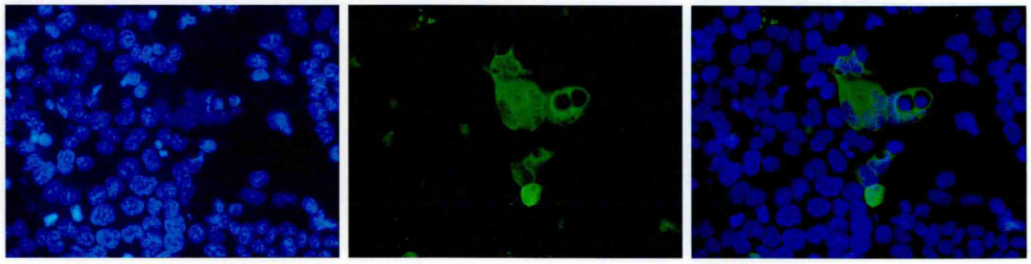

b 0.7µg pRC-2 and 2µl LF2k x200

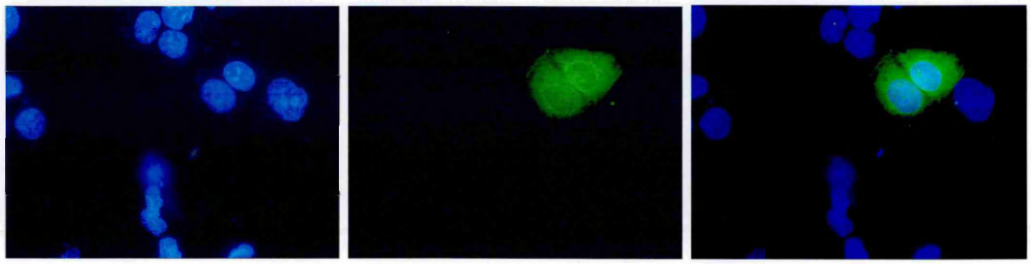

bi 0.7µg pRC-2 and 2µl LF2k x400

Figure 40

Transfection of HEC-1B cell line grown on polylysine with 0.6 to 1.0µg pRC-2 and 2µl LF2K, **a-d**. Filters used were **1** DAPI for the nucleus and **2** FITC for EGFP. Composite images are shown in **3**. Magnification x200 & x400.

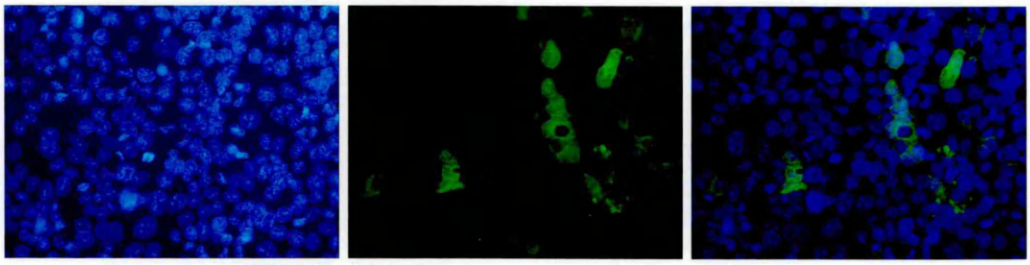

c 0.8µg pRC-2 and 2µl LF2k x200

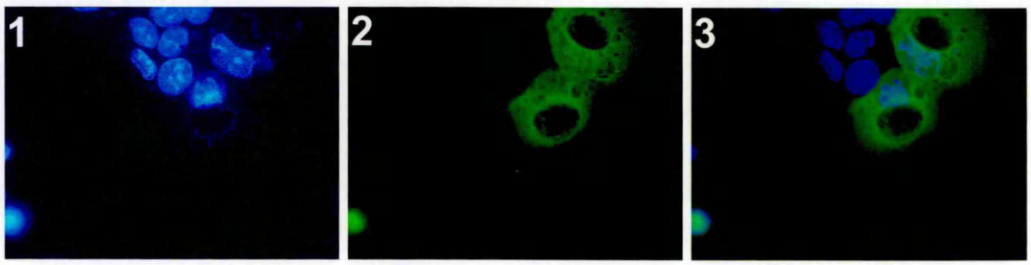

ci 0.8µg pRC-2 and 2µl LF2k x400

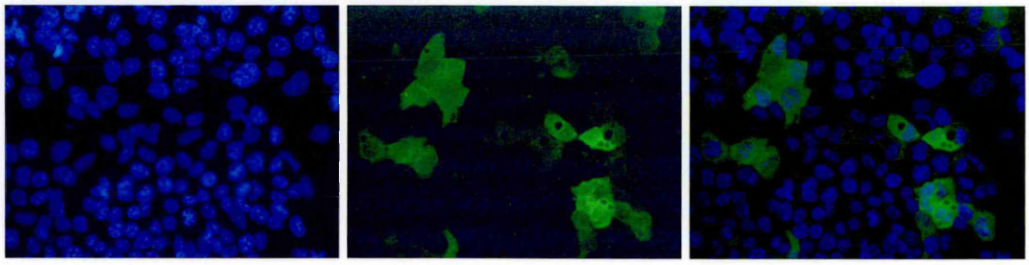

d 1.0µg pRC-2 and 2µl LF2k x200

Figure 40 (Continued)

Transfection of HEC-1B cell line grown on polylysine with 0.6 to 1.0µg pRC-2 and 2µl LF2K, **a-d**. Filters used were **1** DAPI for the nucleus and **2** FITC for EGFP. Composite images are shown in **3**. Magnification x200 & x400.

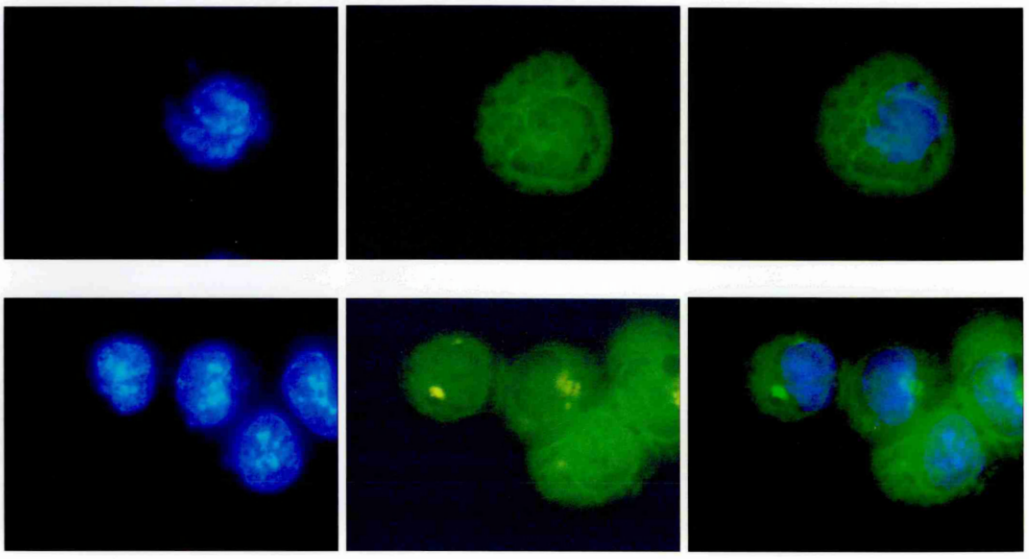

Figure 41

High power images of HEC-1B cell line grown on polylysine with 0.8 µg pRC-2 and 2µl LF2K. Magnification x1000.

Optimisation of Ishikawa Cell Line Transfection

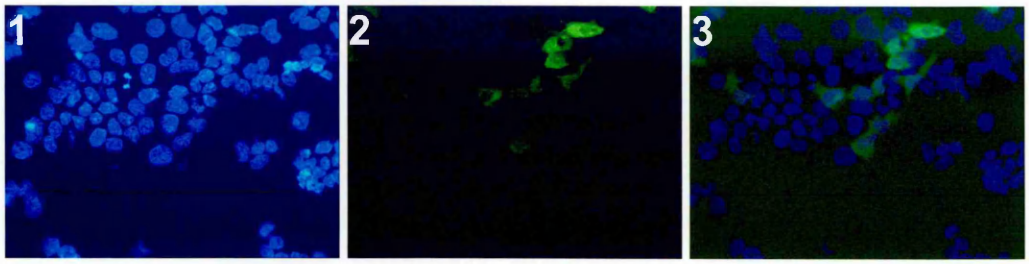

a 0.6µg pRC-2 and 2µl LF2k x200

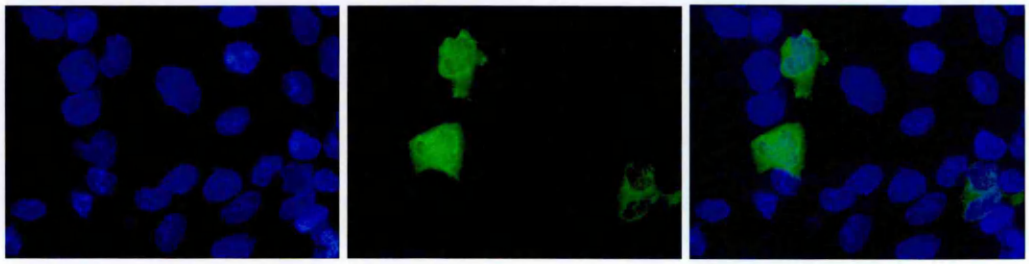

ai 0.6µg pRC-2 and 2µl LF2k x400

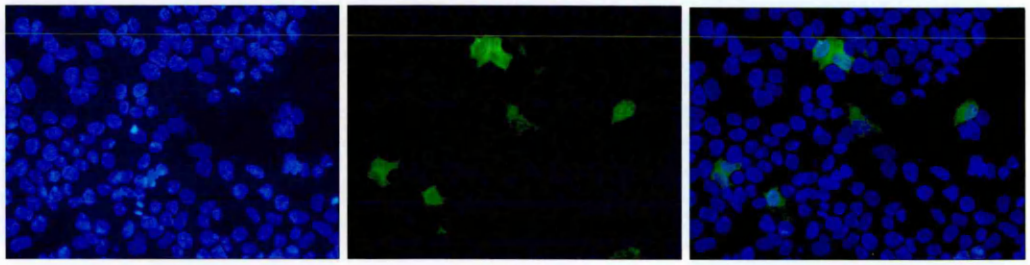

b 0.7µg pRC-2 and 2µl LF2k x200

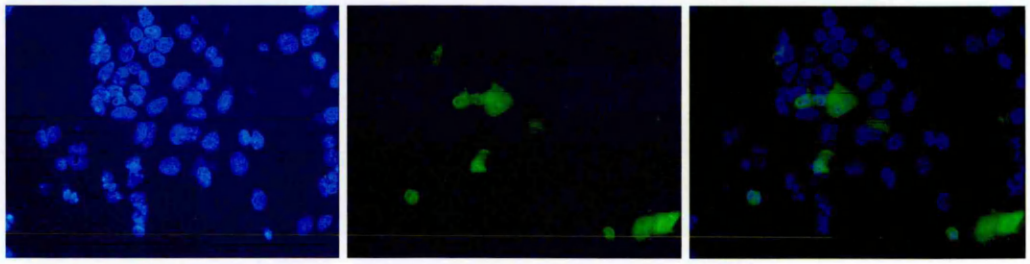

c 0.8µg pRC-2 and 2µl LF2k x200

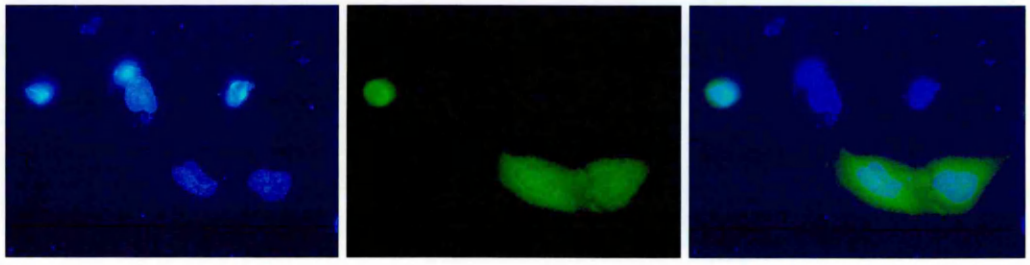

ci 0.8µg pRC-2 and 2µl LF2k x400

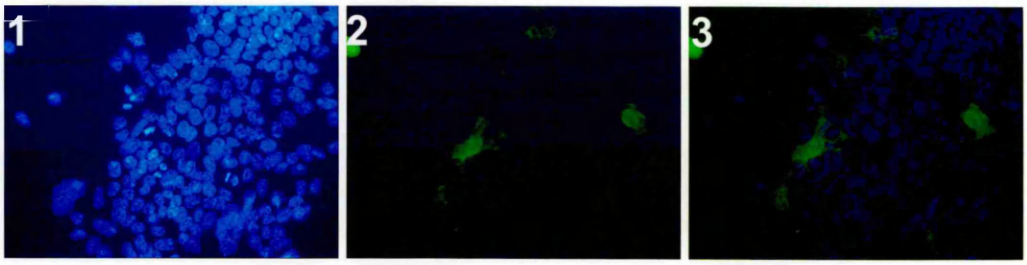

d 0.9µg pRC-2 and 2µl LF2k x200

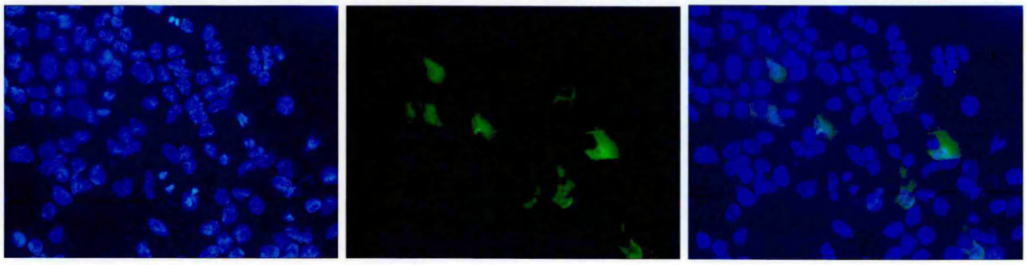

e 1.0µg pRC-2 and 2µl LF2k x200

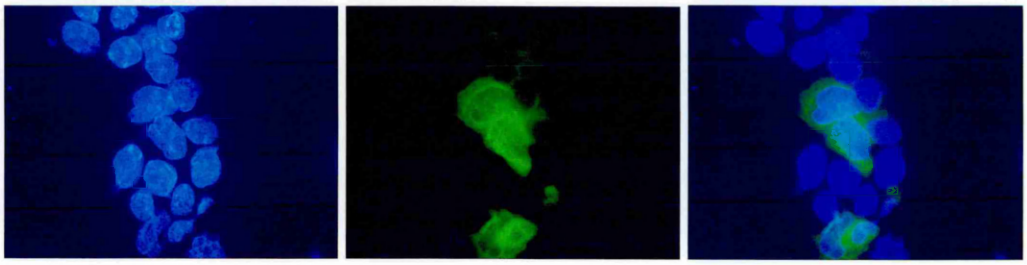

ei 1.0µg pRC-2 and 2µl LF2k x400

Figure 42

Transfection of Ishikawa cell line grown on polylysine with 0.6 to 1.0µg pRC-2 and 2µl LF2K, **a-ei**. Filters used were **1** DAPI for the nucleus and **2** FITC for EGFP. Composite images are shown in **3**. Magnification x200 & x400.

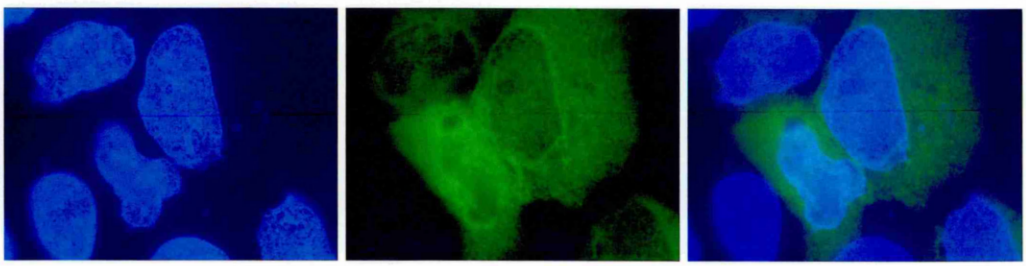

Figure 43

High power image of Ishikawa cell line grown on polylysine with 0.8 µg pRC-2 and 2µl LF2K. Magnification x1000.

The results for HEC-1B indicated that the best transfection rates of 50-70% were obtained using 0.8-1.0μg of pRC-2 (Fig 40 c-d). The majority of the transfected cells were seen to be expressing the PTEN protein at low levels, but a greater number of cells expressed the protein highly in proportion to increasing the amount of pRC-2 used.

The data obtained for Ishikawa cells showed that the best transfection rates of 30-50% were again obtained using 0.8-1.0μg of pRC-2 (Fig 42 c-ei). The majority of the transfected Ishikawa cells were seen to be expressing the GFP protein at low levels, but as observed with HEC-1B a greater number of cells expressed the protein highly in proportion to increasing the amount of pRC-2 used. Although Ishikawa cells do not express PTEN protein, the nuclei of transfected cells were observed undergoing division, and reconstitution of PTEN did not appear to cause apoptosis as nuclear fragmentation was not observed.

3.2.9.4 Stimulation of Transfected Cell Lines

Localisation of PTEN in HEC-1B and Ishikawa cell lines was investigated under stimulation using TGF-β1 or oestrogen, a hormone which influences cellular conditions in the endometrium. Oestrogen plays a major role in regulating the architecture of the endometrium during the menstrual cycle, and may therefore cause morphological changes in endometrial cells which could be linked to a change in PTEN protein localisation. Although TGF-β1 did not appear to modify PTEN protein levels in the experiments previously described here, it is worthwhile investigating whether the cytokine can change the localisation of the protein. Such changes in location within the cell may indicate sequestration to specific compartments which may have an

impact on the cellular function of PTEN in attenuating PI3K, and therefore growth regulation.

Briefly, cells were transfected with 0.8µg pRC-2 in the presence of 2µl LF2K and stimulated with the relevant compound as described in Chapter 2, Section 2.3.13. As cellular response to hormones and cytokines can be rapid, short incubation times of 1-2 hours were used. Longer incubations of up to 24 hours were employed to detect any delayed or long-lasting response.

3.2.9.4.1 Oestrogen stimulation of HEC-1B and Ishikawa cell lines

Concentrations of oestrogen (10 and 100nM) were chosen on the basis of published work (Campbell, et al 2001). Transiently transfected cells were stimulated with hormone and fixed for fluorescent microscopy after 2, 6 or 24 hours. These experiments were performed in triplicate on several separate occasions. Results for oestrogen stimulation of Ishikawa and HEC-1B cells lines are shown in Figures 44 to 47 and are representative of all the experiments.

Oestrogen Stimulation of Transfected Ishikawa Cell Line

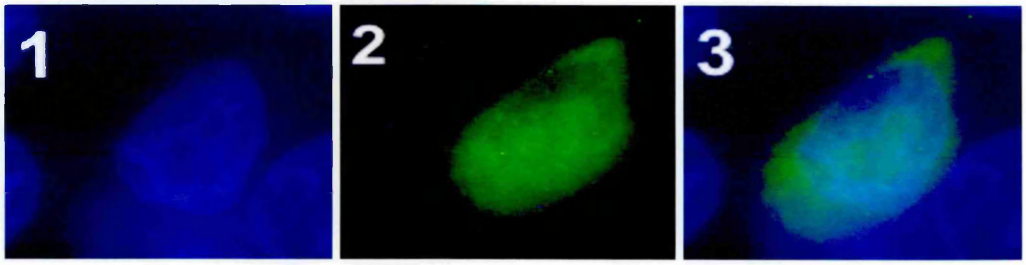

a 10nM oestrogen, 2 hrs x200

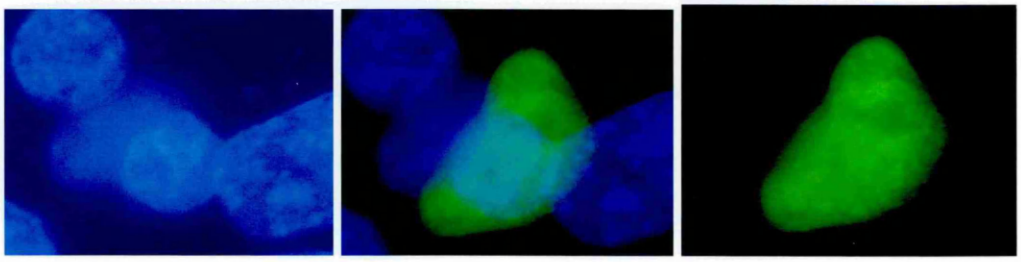

b 10nM oestrogen, 24 hrs x200

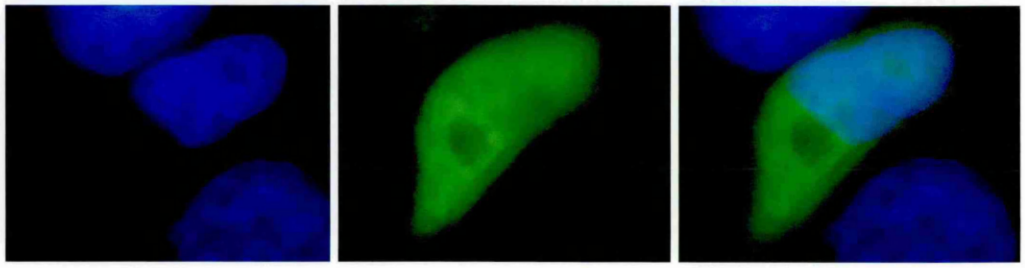

c 100nM oestrogen, 2 hrs x200

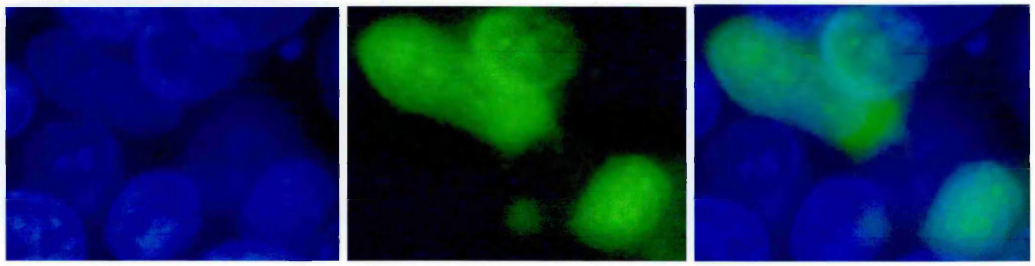

d 100nm oestrogen, 24hrs x200

Figure 44

Stimulation of transfected Ishikawa cell line with 10-100nM oestrogen for 2 and 24 hours **a-d**. Filters used were **1** DAPI for the nucleus and **2** FITC for EGFP. Composite images are shown in **3**. Magnification x200

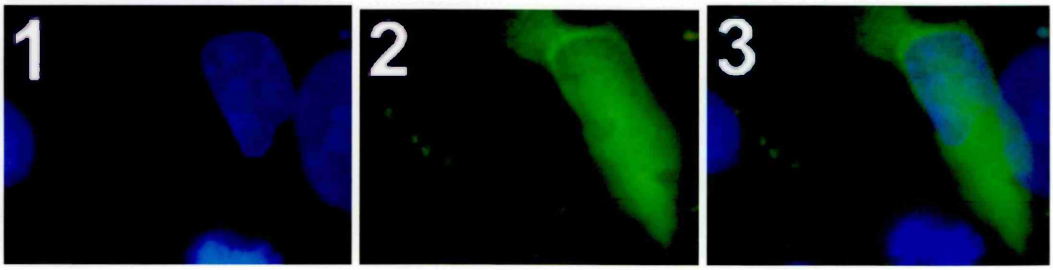

100nm oestrogen, 24hrs

Figure 45

High power image of transfected Ishikawa cell stimulated with 100nM oestrogen for 24 hrs. Filters used were **1** DAPI for the nucleus and **2** FITC for EGFP. Composite images are shown in **3.** Magnification x1000.

Oestrogen Stimulation of Transfected HEC-1B Cell Line

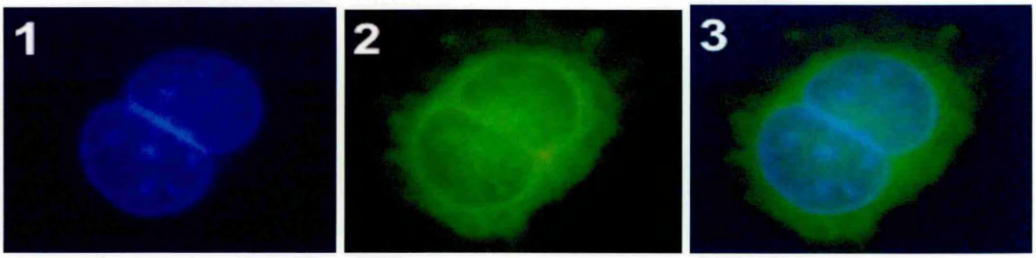

a 10nM oestrogen, 2hrs x200

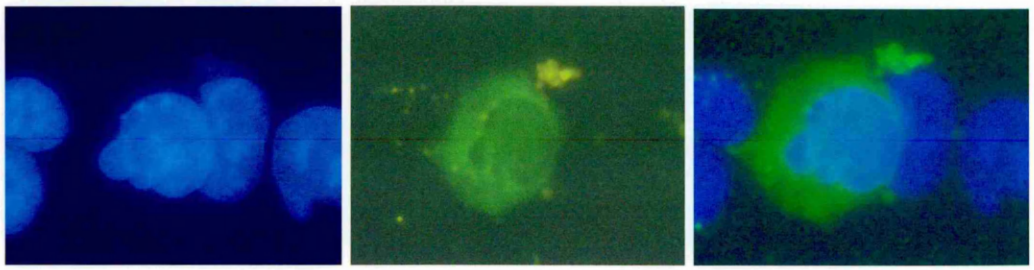

b 10nM oestrogen, 6hrs x200

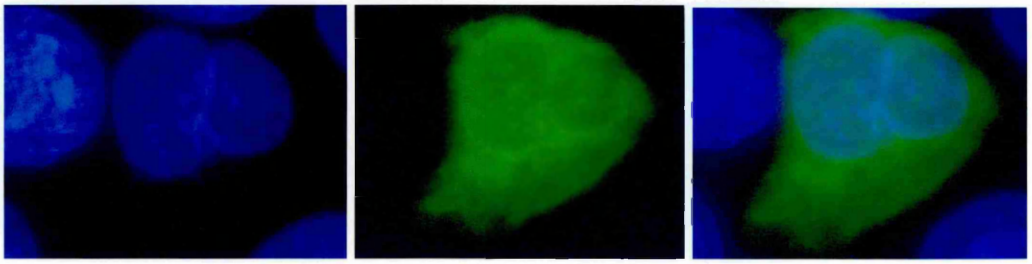

c 10nM oestrogen, 24hrs x200

Figure 46

Stimulation of transfected HEC-1B cell line with 10-100nM oestrogen for 2 and 24 hours **a-c**. Filters used were **1** DAPI for the nucleus and **2** FITC for EGFP. Composite images are shown in **3**. Magnification x200

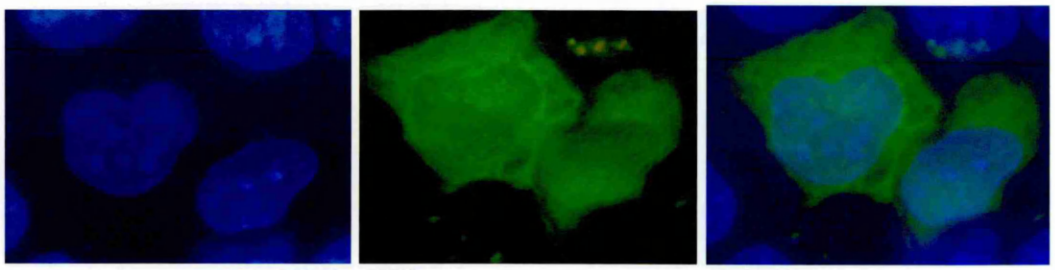

d 100nM oestrogen, 2hrs x200

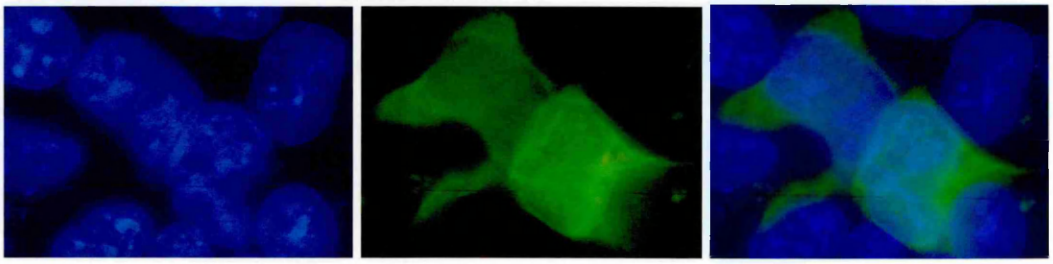

e 100nM oestrogen, 6 hrs x200

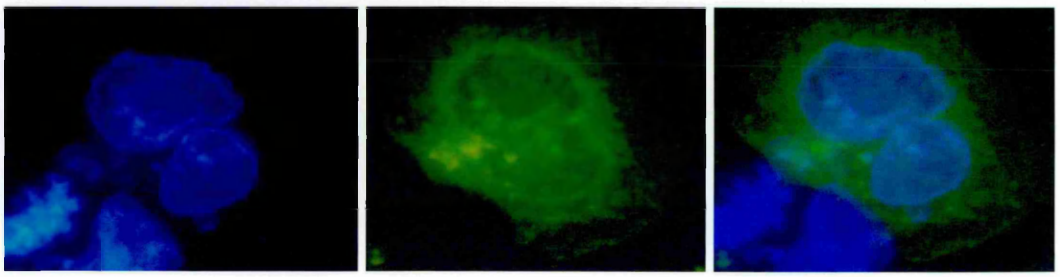

f 100nM oestrogen, 24hrs x200

Figure 46 (Continued)

Stimulation of transfected HEC-1B cell line with 10-100nM oestrogen for 2,6 and 24 hours **d-f**. Filters used were **1** DAPI for the nucleus and **2** FITC for EGFP. Composite images are shown in **3.** Magnification x200.

The results shown in Figure 44 and 45 indicated no discernable change in the distribution of PTEN in Ishikawa cells with the concentrations of hormone and incubation times used. Ishikawa cells are known to express functional oestrogen receptors (Nishida, 2002), but stimulation with this hormone appeared to have little effect on PTEN localisation. Cells from this experiment were very difficult to photograph compared to HEC-1B due to cloudiness on the coverslips which prevented good focussing of the microscope. This may represent morphological changes, eg rounding of the cells, but this experiment would need to be repeated using confocal microscopy to fully assess this observation.

The images presented in Figure 46 indicated no change in the overall distribution of PTEN in HEC-1B with the concentrations of hormone and incubation times used. As with the Ishikawa cell line, stimulation of transiently transfected HEC-1B cells appears to have little or no effect on the localisation of PTEN protein contributed by pRC-2.

3.2.9.4.2 TGF-β1 Stimulation of HEC-1B cell line

Transiently transfected HEC-1B cells were stimulated with either 2ng/ml or 5ng/ml of cytokine, as these concentrations were previously used in the investigation of PTEN mRNA and protein expression. As for oestrogen, short incubation times of 1, 2 and 6 hours were used as cellular responses to cytokines can be rapid. Results for TGF-β1 stimulation of the HEC-1B cells line are shown in Figure 47.

TGF-β1 Stimulation of Transfected HEC-1B Cell Line

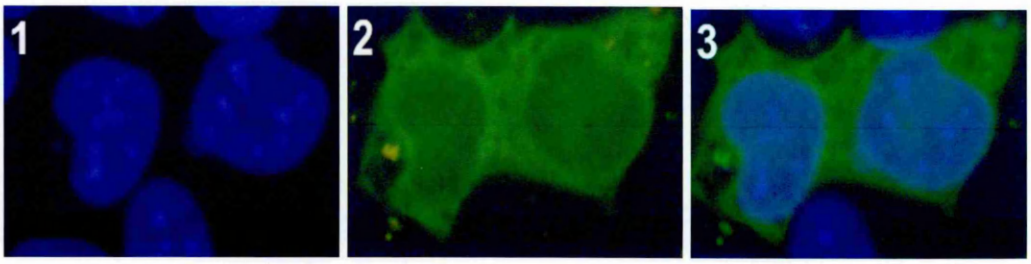

a 2ng TGF-β1, 1hr x200

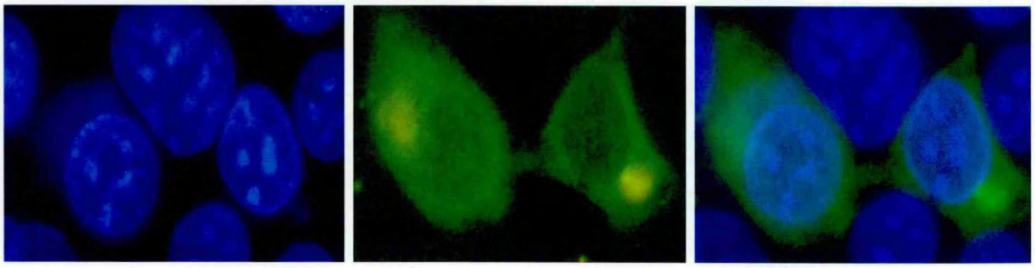

b 2ng TGF-β1, 2hr x200

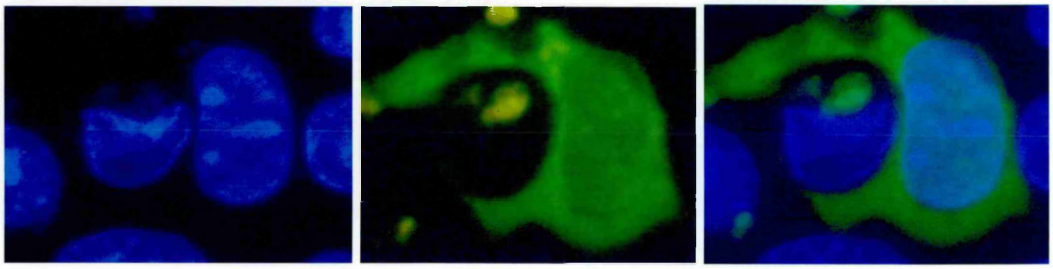

c 2ng TGF-β1,6hrs x200

Figure 47

Stimulation of transfected HEC-1B cell line with 2 and 5ng/ml TGF-β1 for 1,2 and 6 hours **a-c**. Filters used were **1** DAPI for the nucleus and **2** FITC for EGFP. Composite images are shown in **3.** Magnification x200.

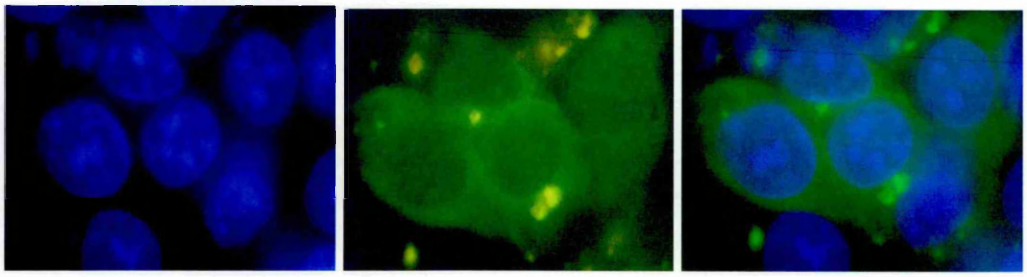

d 5ng TGF-β1, 1hr x200

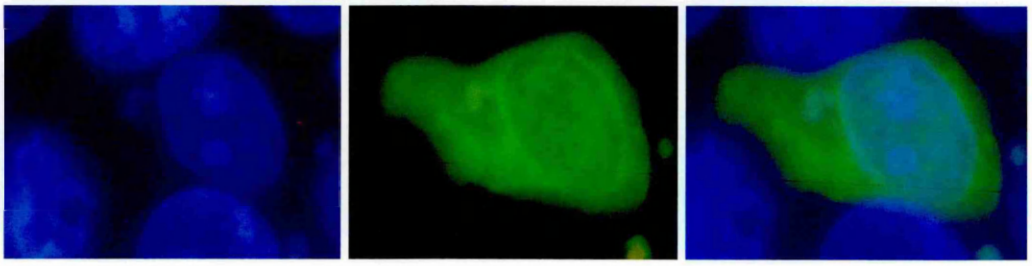

e 5ng TGF-β1, 2hrs x200

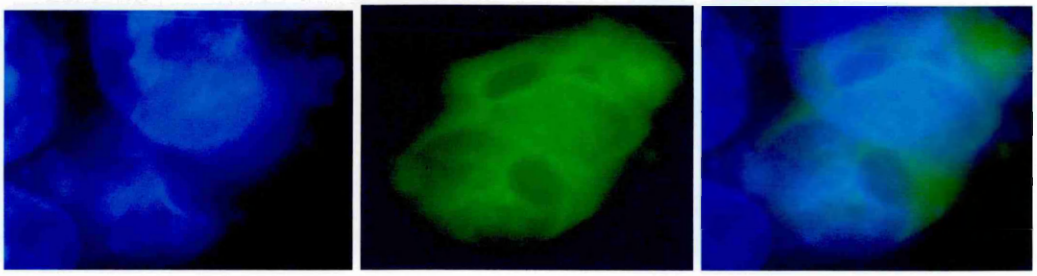

f 5ng TGF-β1, 6hrs x200

Figure 47 (Continued)

Stimulation of transfected HEC-1B cell line with 2 and 5ng/ml TGF-β1 for 1,2 and 6 hours **d-f**. Filters used were **1** DAPI for the nucleus and **2** FITC for EGFP. Composite images are shown in **3.** Magnification x200.

Figure 47 shows the results of stimulating transiently transfected HEC-1B cells with TGF-β1. No discernable change in the localisation of PTEN encoded by pRC-2 was observed with the concentrations of hormone and incubation times used.

Although no changes in the distribution of PTEN were detected in the stimulation experiments performed, it is possible that if any response occurred it was too rapid for observation or so slow that it occurred outside of the 24 hour maximum incubation time used.

3.2.9.5 Localisation of pRC-2 to Subcellular compartments

A comparison of the localisation of PTEN encoded by pRC-2 with colligin (ER marker) and mannosidase II (golgi marker) was performed to determine any co-localisation of PTEN to the ER or golgi. Localisation to specific regions of the cell may indicate partitioning of PTEN and have implications for the phosphatases' ability to gain access to its substrates. Additionally, close association with the ER may be important for the nuclear translocation of PTEN, the mechanism of which has not yet been described.

As described in Chapter 2, Section 2.3.14, transiently transfected HEC-1B and Ishikawa cell lines were probed with antibodies against colligin (Hsp47), an ER-resident protein, or golgi-specific anti-mannosidase II. Any overlap between the green signal from pRC-2 and the red signal from colligin or mannosidase II show as a yellow colour on the merged images.

Results for localisation with colligin are presented in Figures 48a/b and 49a/b for HEC-1B and Ishikawa cell lines respectively. Localisation studies with mannosidase II are shown in Figures 50 a/b and 51a/b for HEC-1B and Ishikawa cell lines respectively, and represent several separate experiments.

Localisation of Colligin & pRC-2 in HEC-1B Cell Line

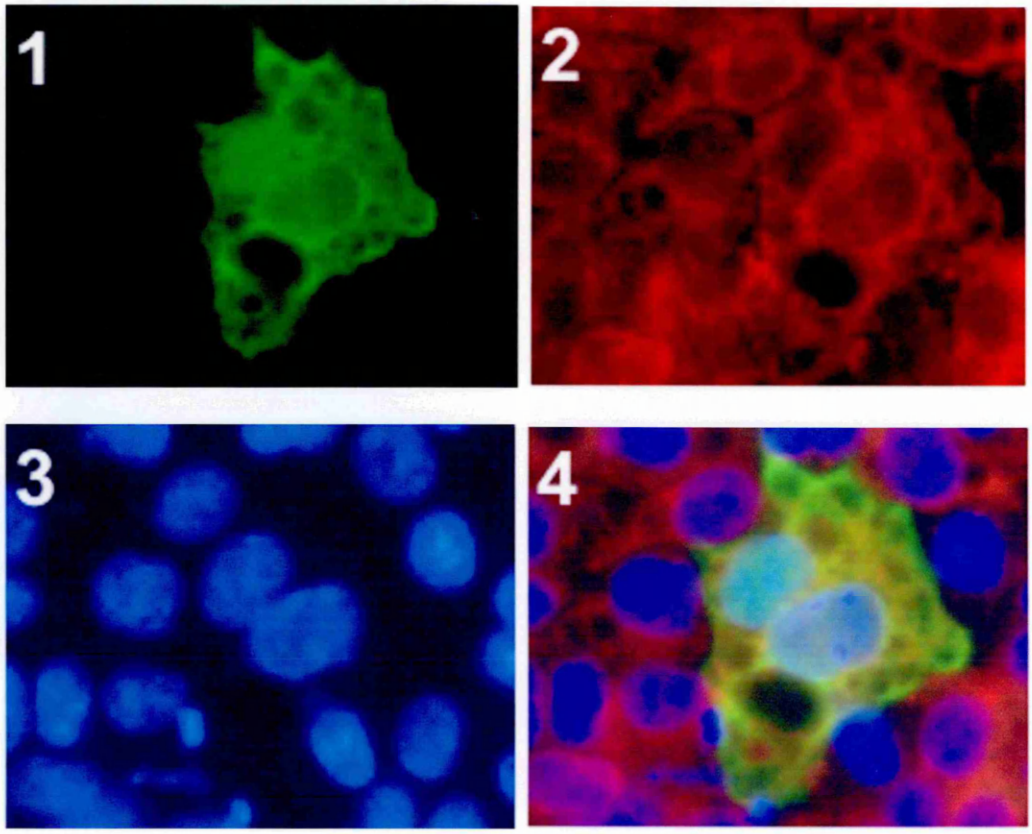

Figure 48a

Anti-colligin staining of HEC-1B transiently transfected with pRC-2. Filters used were **1** FITC for EGFP,**2** Texas red for AlexaFluor 594 (Colligin),**3** DAPI for the nucleus. Composite image shown in **4**.

Magnification x400.

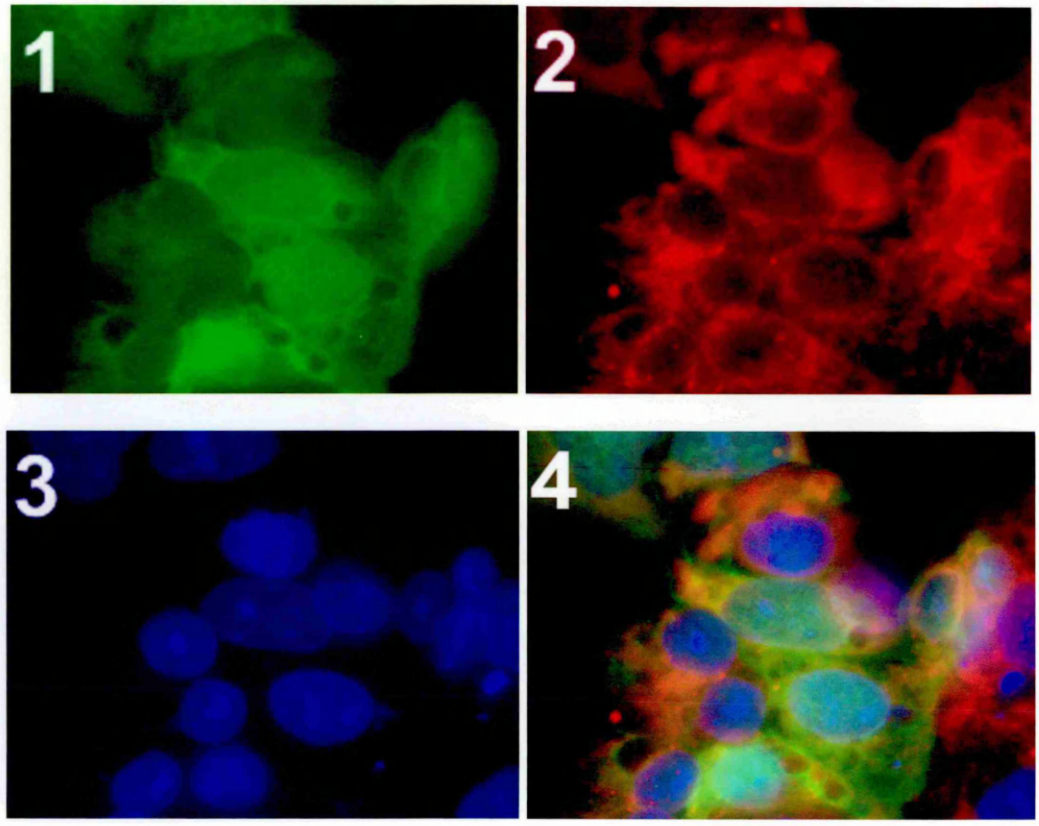

Figure 48b

Anti-colligin staining of HEC-1B transiently transfected with pRC-2. Filters used were **1** FITC for EGFP,**2** Texas red for AlexaFluor 594 (Colligin),**3** DAPI for the nucleus. Composite image shown in **4**.

Magnification x400.

Localisation of Colligin & pRC-2 in Ishikawa Cell Line

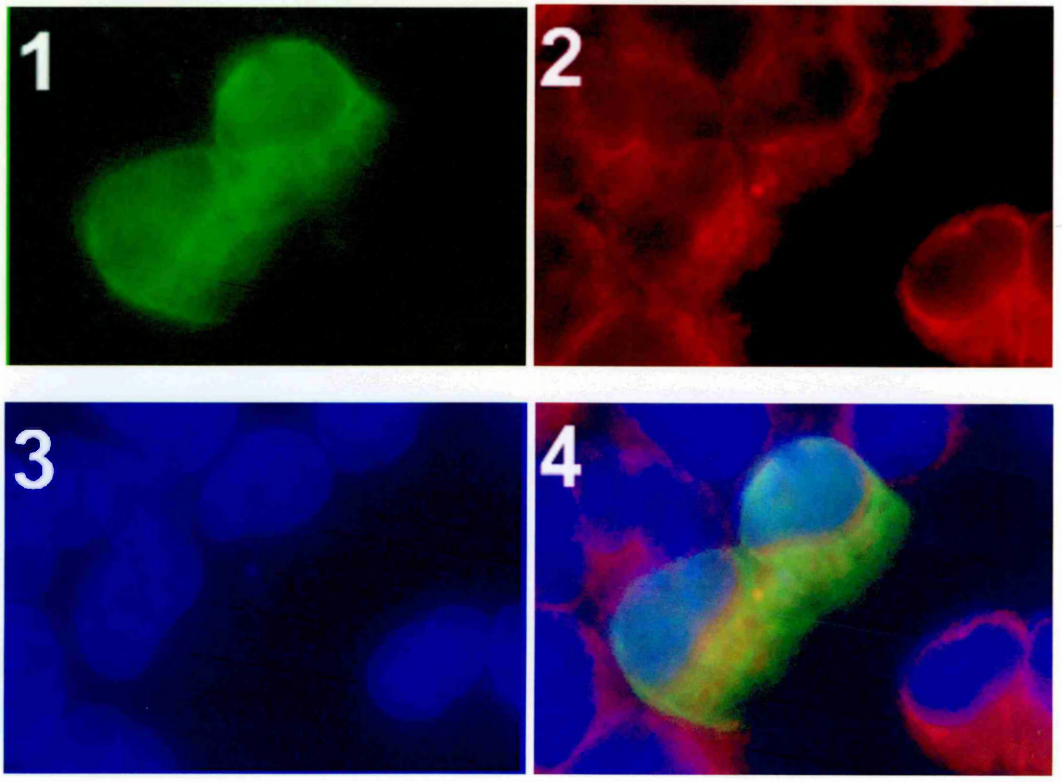

Figure 49a

Anti-colligin staining of Ishikawa transiently transfected with pRC-2. Filters used were **1** FITC for EGFP,**2** Texas red for AlexaFluor 594 (Colligin),**3** DAPI for the nucleus. Composite images are shown in **4**. Magnification x400.

Localisation of Colligin & pRC-2 in Ishikawa Cell Line

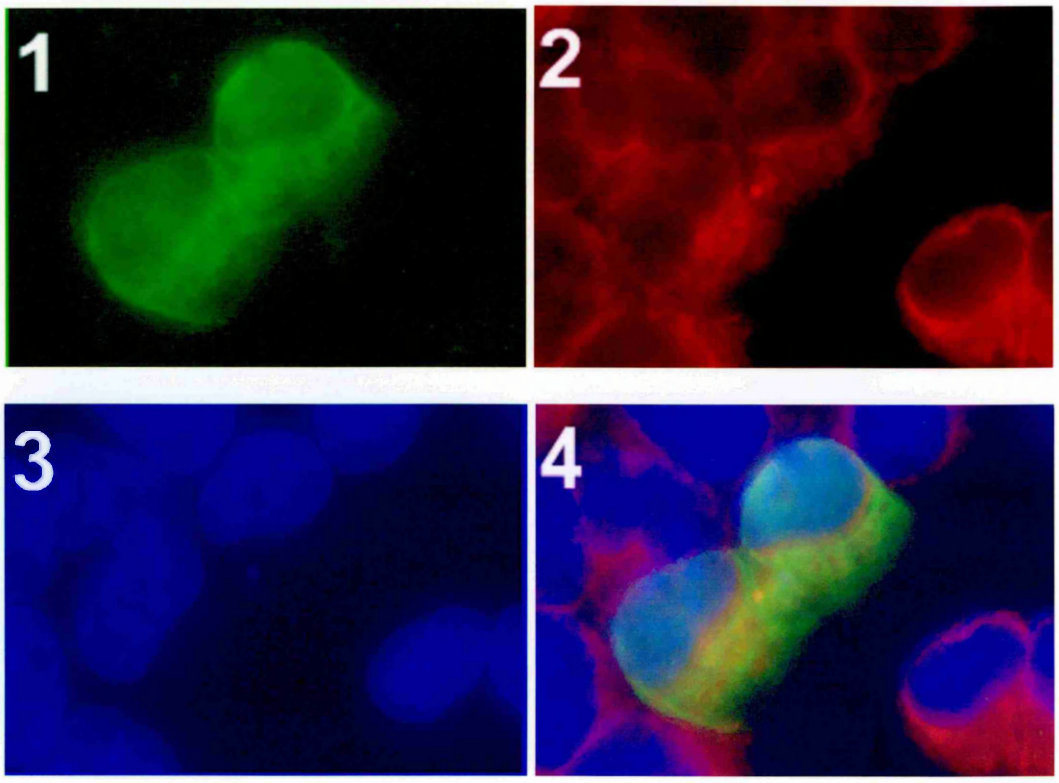

Figure 49a

Anti-colligin staining of Ishikawa transiently transfected with pRC-2. Filters used were **1** FITC for EGFP,**2** Texas red for AlexaFluor 594 (Colligin),**3** DAPI for the nucleus. Composite images are shown in **4**. Magnification x400.

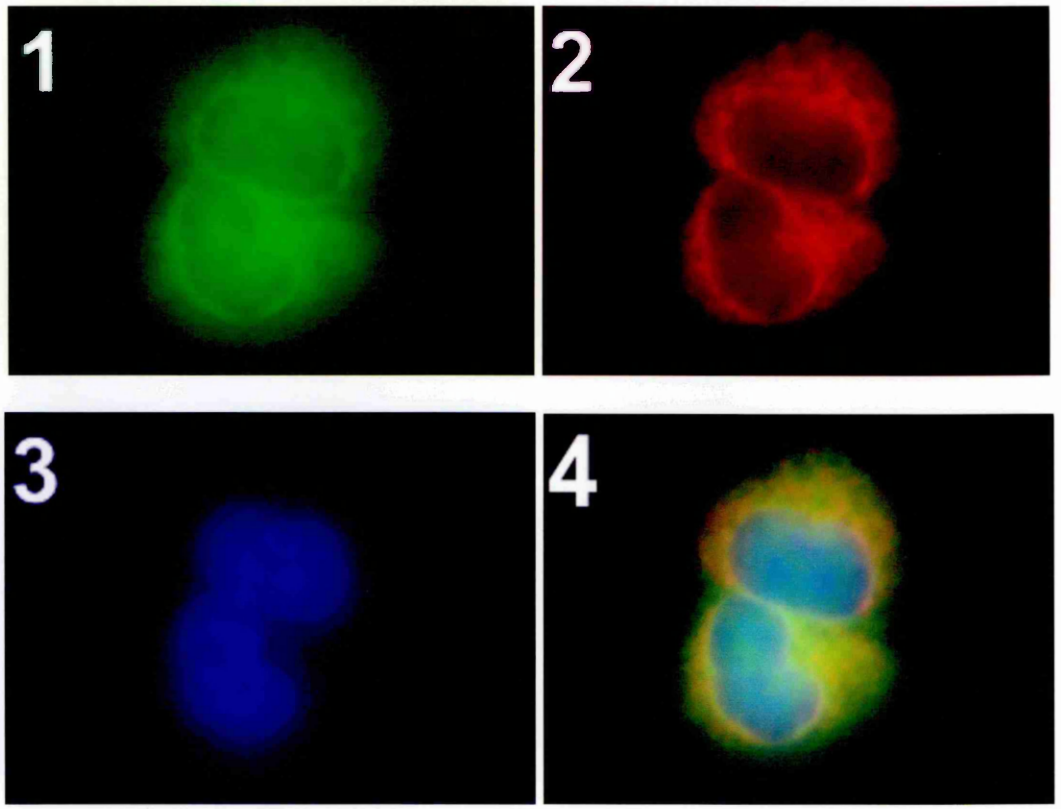

Figure 49b

Anti-colligin staining of Ishikawa transiently transfected with pRC-2. Filters used were **1** FITC for EGFP,**2** Texas red for AlexaFluor 594 (Colligin),**3** DAPI for the nucleus. Composite images are shown in **4**. Magnification x400.

Localisation of Mannosidase II & pRC-2 in HEC-1B Cell Line

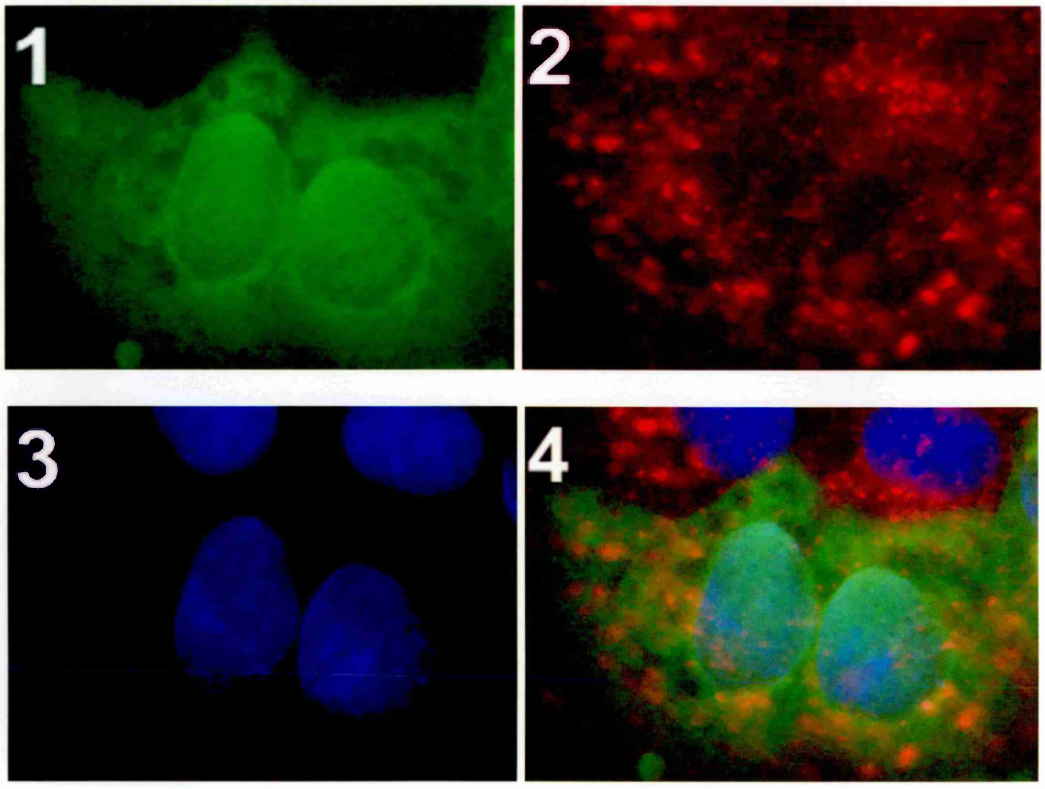

Figure 50a

Anti-Mannosidase II staining of HEC-1B transiently transfected with pRC-2. Filters used were **1** FITC for EGFP,**2** Texas red for AlexaFluor 594 (Mannosidase II),**3** DAPI for the nucleus. Composite images are shown in **4**. Magnification x400.

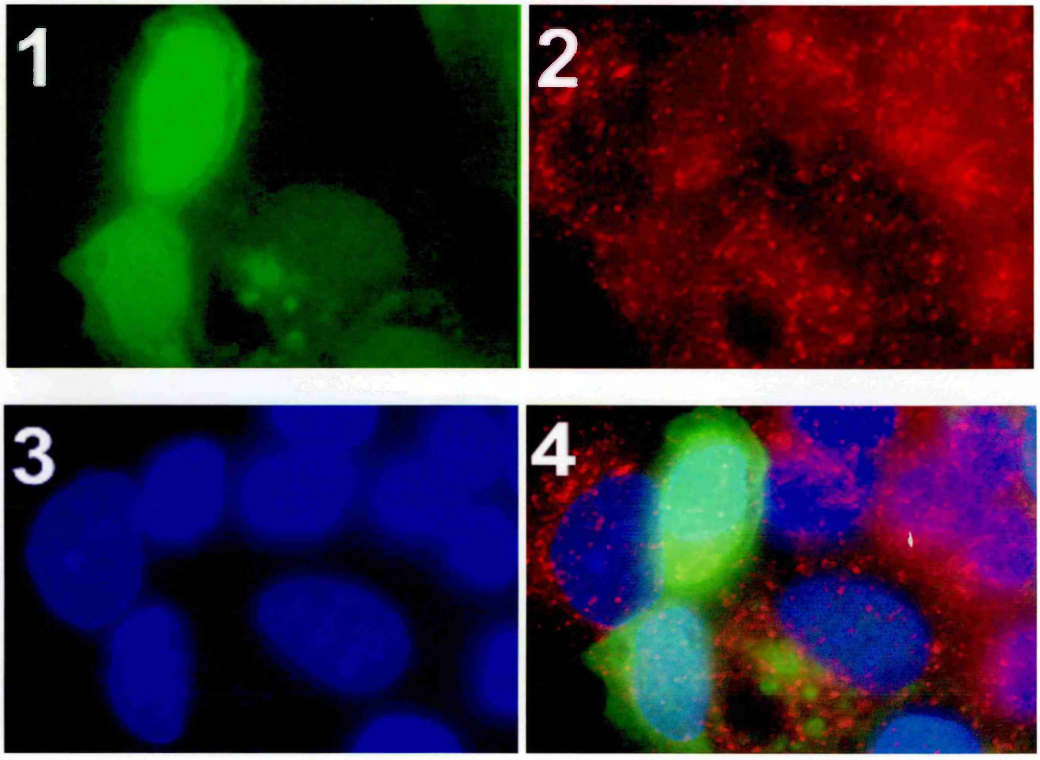

Figure 50b

Anti-Mannosidase II staining of HEC-1B transiently transfected with pRC-2. Filters used were **1** FITC for EGFP,**2** Texas red for AlexaFluor 594 (Mannosidase II),**3** DAPI for the nucleus. Composite images are shown in **4**. Magnification x400.

Localisation of Mannosidase II & pRC-2 in Ishikawa Cell Line

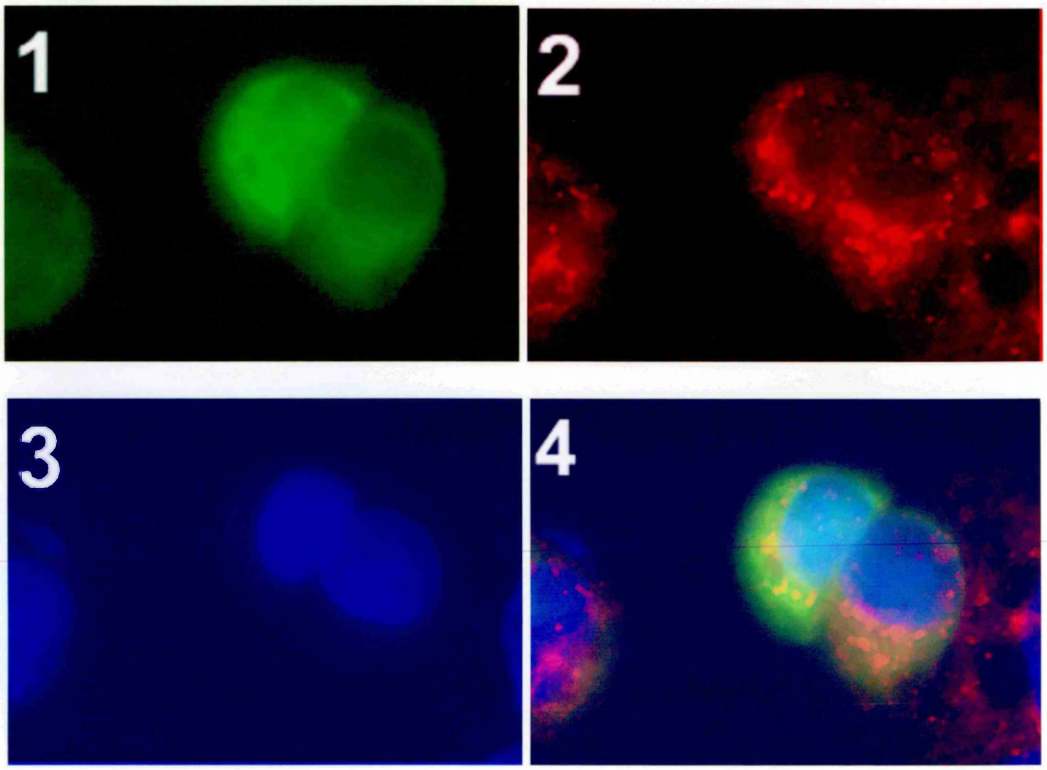

Figure 51a

Anti-Mannosidase II staining of Ishikawa transiently transfected with pRC-2. Filters used were **1** FITC for EGFP,**2** Texas red for AlexaFluor 594 (Mannosidase II),**3** DAPI for the nucleus. Composite images are shown in **4**. Magnification x400.

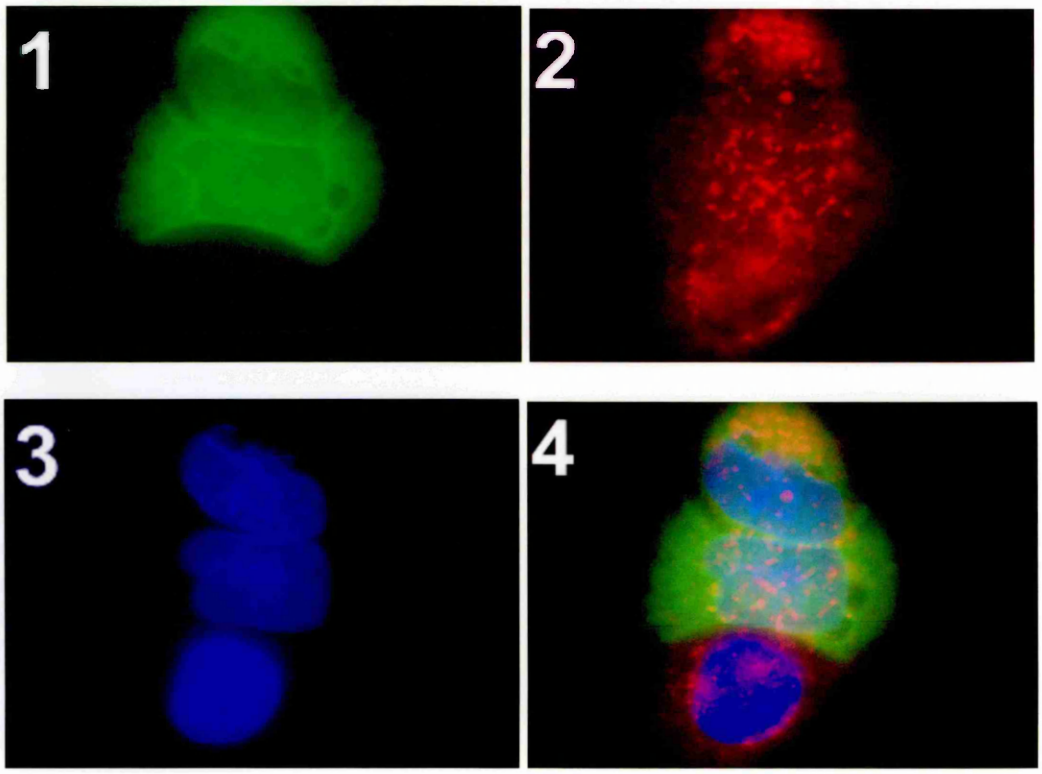

Figure 51b

Anti-Mannosidase II staining of Ishikawa transiently transfected with pRC-2. Filters used were **1** FITC for EGFP,**2** Texas red for AlexaFluor 594 (Mannosidase II),**3** DAPI for the nucleus. Composite images are shown in **4**. Magnification x400.

As the images in Figures 48a and b show, there was some degree of overlap between PTEN and colligin giving a yellow colour on the composite images. This suggests that a proportion of the PTEN fusion protein was present in the ER, and that the presence of the GFP moiety did not prevent entry into this compartment. Additional signals derived from the FITC filter once demonstrate the presence of a small amount of exogenous PTEN in the cytoplasm and nuclear region.

Figures 50a and b show that there was no discernable overlap between pRC-2-derived PTEN and the golgi marker Mannosidase II in HEC-1B cells. The fusion protein was therefore not specifically localised to the golgi. However, the staining of the golgi was indistinct and diffuse particularly in transfected cells. The poor definition was possibly due to the polyclonal nature of the anti-Mannosidase antibody, which could be less specific than a monoclonal.

Figures 49a & b show there was some degree of overlap between pRC-2 and Colligin in Ishikawa cells, giving a yellow colour on the composite images. This suggests that at least some of the PTEN fusion protein was present in the ER, and that as observed in HEC-1B cells the presence of the GFP moiety did not exclude entry into this compartment. Additional signals derived from the FITC filter once again demonstrated the presence of exogenous PTEN in the cytoplasm and nuclear region.

Figures 51a and b show that there was very little overlap between pRC-2-derived PTEN and the golgi marker Mannosidase II in Ishikawa cells. The fusion protein was therefore not specifically localised to the golgi, as there was a partial overlap of colours in only a small proportion of cells. The

staining of the golgi was again indistinct and diffuse particularly in transfected cells, although somewhat clearer definition of the golgi was observed in the Ishikawa cell line.

3.2.9.6 Co-localisation of exogenous PTEN to endogenous PTEN in HEC-1B

To determine whether endogenous PTEN in transfected cells would demonstrate a different staining pattern to exogenous PTEN-EGFP, transfected HEC-1B cells were incubated with anti-PTEN primary (BD Biosciences) and AlexaFluor 594-labelled secondary antibodies (Chapter 2, Section 2.3.14). The images obtained are presented in Figures 52 a and b. In Figure 52 a low expression level of endogenous PTEN can be observed in non-transfected cells which has been detected by the anti-PTEN antibody and visualised under a Texas red filter. In contrast, the level of exogenous PTEN in transfected cells is significantly increased, suggesting that the endogenous cellular level of PTEN protein is fairly low.

From these images, a total overlap between the red and green images was observed, suggesting that both sources of PTEN localise to the same cellular regions. It should be noted, however, that if the anti-PTEN antibody is capable of binding to PTEN-GFP, then this experiment would not discriminated between the endogenous and exogenous forms of PTEN. The antibody's ability to bind to PTEN-GFP could be tested by Western blot against protein lysates from transfected Ishikawa cells which contain no endogenous PTEN protein.

Co-Localisation of PTEN and PTEN-EGFP in HEC-1B Cell Line

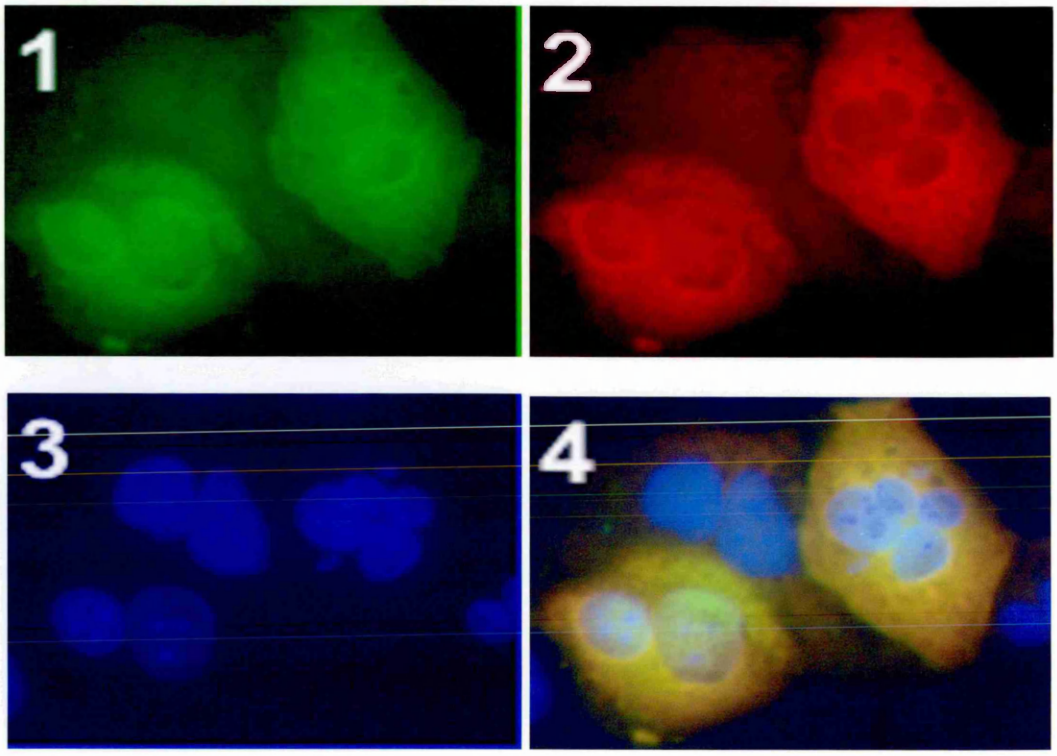

Figure 52a

Anti-PTEN staining of HEC-1B transiently transfected with pRC-2. Filters used were **1** FITC for EGFP,**2** Texas red for AlexaFluor 594 (PTEN),**3** DAPI for the nucleus. Composite images are shown in **4**. Magnification x400.

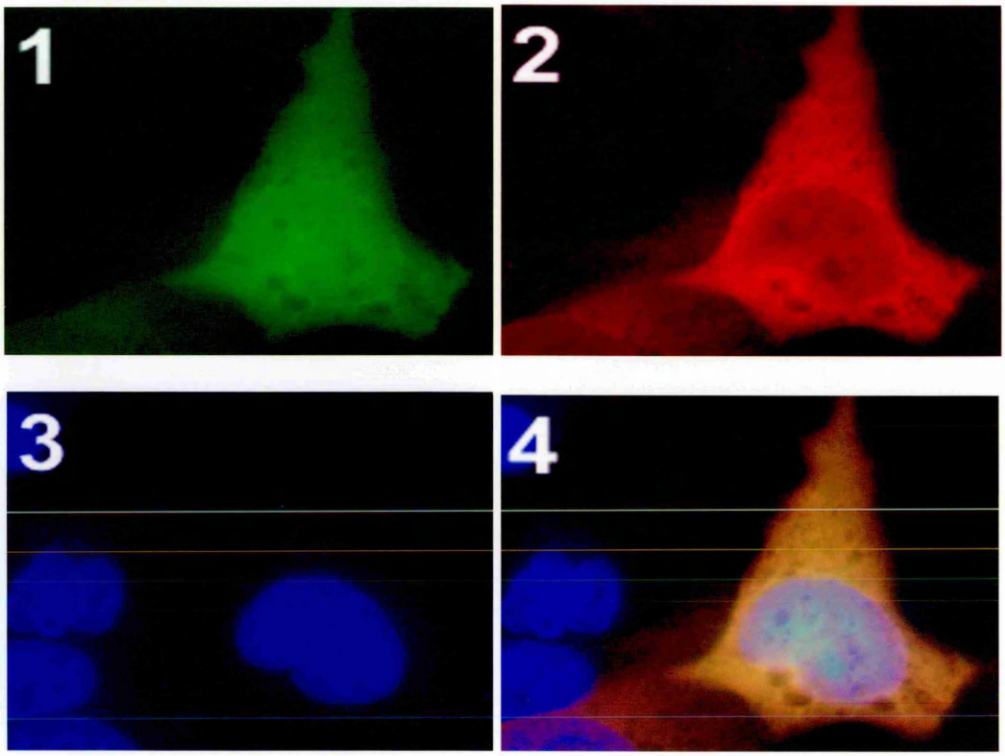

Figure 52b

Anti-PTEN staining of HEC-1B transiently transfected with pRC-2. Filters used were **1** FITC for EGFP,**2** Texas red for AlexaFluor 594 (PTEN),**3** DAPI for the nucleus. Composite images are shown in **4**. Magnification x1000

3.3 MUTATIONAL ANALYSIS OF PTEN EXONS 5 & 8 IN ENDOMETRIAL DNA SAMPLES BY SINGLE STRAND CONFORMATIONAL POLYMORPHISM ANALYSIS (SSCP)

Various studies have been conducted into the mutation status of genomic PTEN in fresh tumour tissue of diverse origin, but little work has been published using archival material (paraffin fixed and frozen samples which may have been stored for several years). This is mainly due to technical difficulties associated with retrieving DNA from paraffin embedded tissue sections. Extracted DNA can be highly fragmented and overall yields low, and the isolation of DNA from only one cell type is difficult if the section contains a mixture of cells.

Due to the availability of a large repository of archival endometrial carcinomas, complete with histologically normal cervical sections, a study of PTEN mutations was performed for the 43 patients available (a total of 127 samples). Because a histologically normal sample was available for each accompanying tumour specimen, any mutations in PTEN could be compared between normal and tumour DNA, thus such changes could be described as early or late events. Published results for fresh tumours described a range of mutations which were mainly clustered in exons 5 and 8 of PTEN, and therefore prompted my focus on these two exons. The electrophoretic technique of SSCP was chosen as a relatively simple and rapid method of analyzing the 127 samples for both exons, a total of 508 PCR samples.

SSCP is an electrophoretic method which is capable of detecting single base changes in a population of small DNA strands which are otherwise identical in sequence to a known sequenced control. Single stranded DNA forms

stable intramolecular secondary structures in solution, therefore differences in base sequence will manifest as differences in single-strand conformations. This technique distinguishes between these conformations by virtue of differences in DNA mobility through the gel. When compared to the control, sequence variations can be observed as 'bandshifts' which display a change in migration pattern. Controls used in SSCP analysis were derived from peripheral blood lymphocytes, in which mutations in PTEN are uncommon (Dahia, et al 1999). These samples were donated by members of staff and denoted as rDNA, gDNA, C1 and SJ1. Sequencing of these controls was peformed to verify a wild-type PTEN sequence.

Small PCR fragments of <250bp in length are required for a good detection rate using this method. For this reason, Exons 5 and 8 were 'split' into two overlapping PCR reactions using primer pairs AB and CD, which contain a small region of overlap to amplify the entirety of each exon in these two reactions.

3.3.1 Preparation of DNA Samples for SSCP Analysis

3.3.1.1 Extraction of human DNA from whole blood and archival material

Extraction of DNA from whole blood and archival material was performed as described in Chapter 2, Section 2.3.2 and stored at -70°C prior to use in PCR reactions.

3.3.1.2 PCR amplification of Patient & Control DNA samples for SSCP Analysis

3.3.1.2.1 PCR amplification of samples for Exon 5

PCR products for Exons 5AB and 5CD were obtained for each patient sample from Dr K Feeley, University of Sheffield UK. PCR was performed using the conditions described in Chapter 2, Section 2.4.2 using the PTEN I programme (Appendix V). The presence of PCR products for 5AB (137bp) and 5CD (186bp) were confirmed by 15% PAGE.

Due to a very low yield of product amplified for 5AB in the PCRs sent to me, aliquots of all remaining patient DNA samples were requested from Dr Feeley. All patient DNA samples available, and controls, were therefore subjected to repeated PCR for 5AB using the RIS2-2 cycle (Appendix III) with the conditions described previously. PCRs were analysed by agarose gel electrophoresis, and the majority of samples exhibited an improved yield of the 5AB fragment when compared to PCR products generated by the PTEN I programme. Examples of these PCRs are illustrated in Figure 53 which shows the typical yield of some of the original samples, and Figure 54 which shows the improved yield using the RIS2-2 PCR cycle.

PCR samples provided for exon 5CD showed good amplification in the majority of patient DNA samples; an example is shown in Figure 55. Control 5CD DNA (RDNA) is shown in Figure 56.

PCR of Patient and Control samples for Exon 5AB

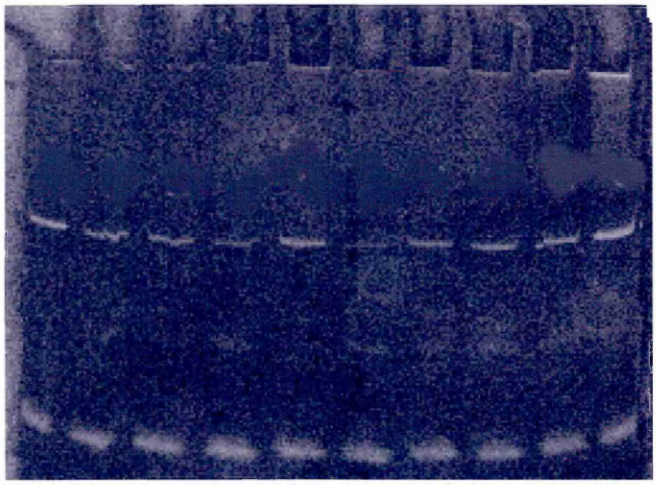

Figure 53 15% PAGE of 5AB patient samples 92-222, 10µl/ lane, PTEN I cycle.

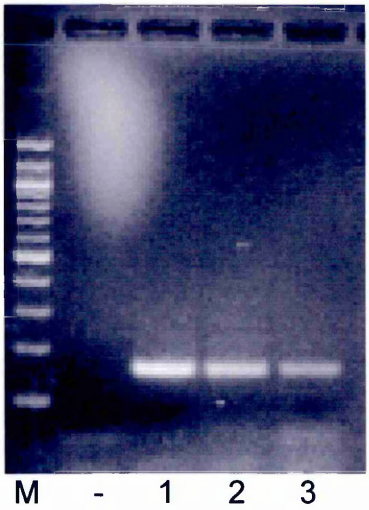

Figure 54 5AB PCR of **1:** control rDNA **2:** patient 49 **3:** patient 52x, 10µl/lane, RIS2.2 cycle. Dash indicates PCR control, **M:** 100bp ladder.

PCR of Patient and Control samples for Exon 5CD

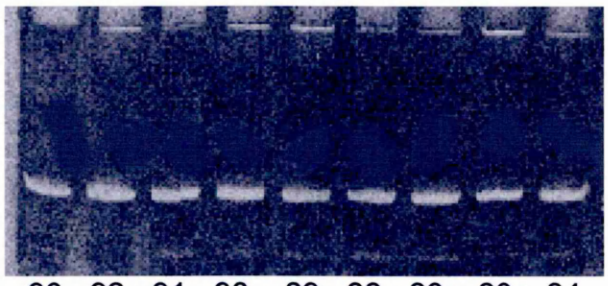

Figure 55 15% PAGE of 5CD PCR for patient samples 84-93, 10µl/ lane, PTEN I cycle.

Figure 56 5CD PCR of **1:** control rDNA, 10µl per lane, PTEN I cycle. Dash indicates PCR control. **M:**100bp ladder.

3.3.1.2.2 PCR amplification of samples for Exon 8

PCR products for Exons 8AB were obtained for each patient sample from Dr K Feeley, as described, and the presence of the 8AB fragment (188bp) confirmed by 15% PAGE. For Exon 8CD, PCR was performed on available patient DNA using the PTEN I cycle (Chapter 2, Section 2.4.2). The presence of the 8CD (245bp) fragment was confirmed by agarose gel electrophoresis. For exon 8AB, all patient DNA samples showed good amplification; an example is shown in Figure 57. Control DNA amplified using PTEN I cycle is shown in Figure 58. PCR of all patient DNA samples available for exon 8CD was performed as previously described. Control DNA is shown in Figure 59.

PCR of Patient and Control samples for Exon 8 AB

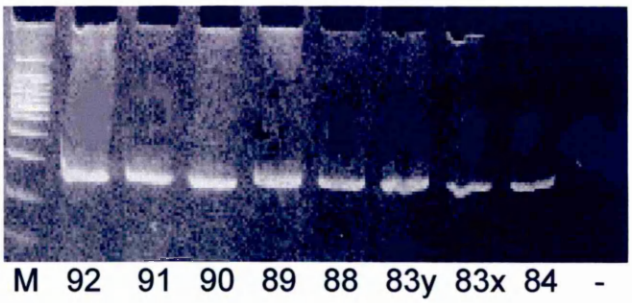

Figure 57 15% PAGE of 8AB PCR for patient samples 84-92, 10µl/ lane, PTEN I cycle. **M**= 100bp ladder.

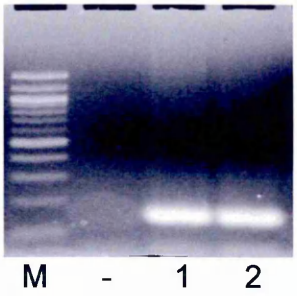

Figure 58 8AB PCR of controls **1:** RDNA, **2:** gDNA, 10µl per lane. Dash indicates PCR control

PCR of Control samples for Exon 8 CD

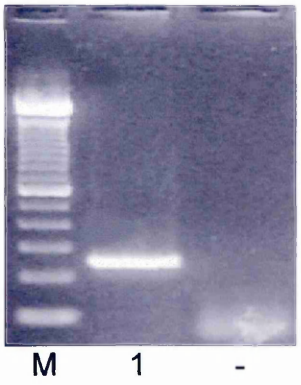

Figure 59 8CD PCR of **1:** Control gDNA, 10µl. Dash indicates PCR control **M**= 100bp

3.3.2 Preparation of Control PCR products for sequencing

To provide normal sequence controls for SSCP, PCR was performed using DNA derived from peripheral blood donated by four staff members. PTEN mutations are very rare in white blood cells, so these samples were likely to have normal sequences from which to compare patient DNA. Staff control DNA (rDNA, gDNA, C1 and SJ1) to be used as controls was purified as described in Chapter 2, Section 2.4.3, following PCR with AB and CD primer pairs for both exons as previously described for patient DNA (Section 2.4.2). Sequence information was obtained from Lark as electropherograms (see Figures 60 to 68). Adequate sequences were obtained for exon 5AB, 5CD and 8AB, for either g- or r-DNA, C1 and SJ1 control samples. The sequences showed a high degree of sequence homology to PTEN cDNA with few ambiguous bases. These samples were regarded as suitable controls for these exon fragments. Sequence data for the 8CD control was not obtained due to poor read quality after several attempts, but was still used on the relevant gels.

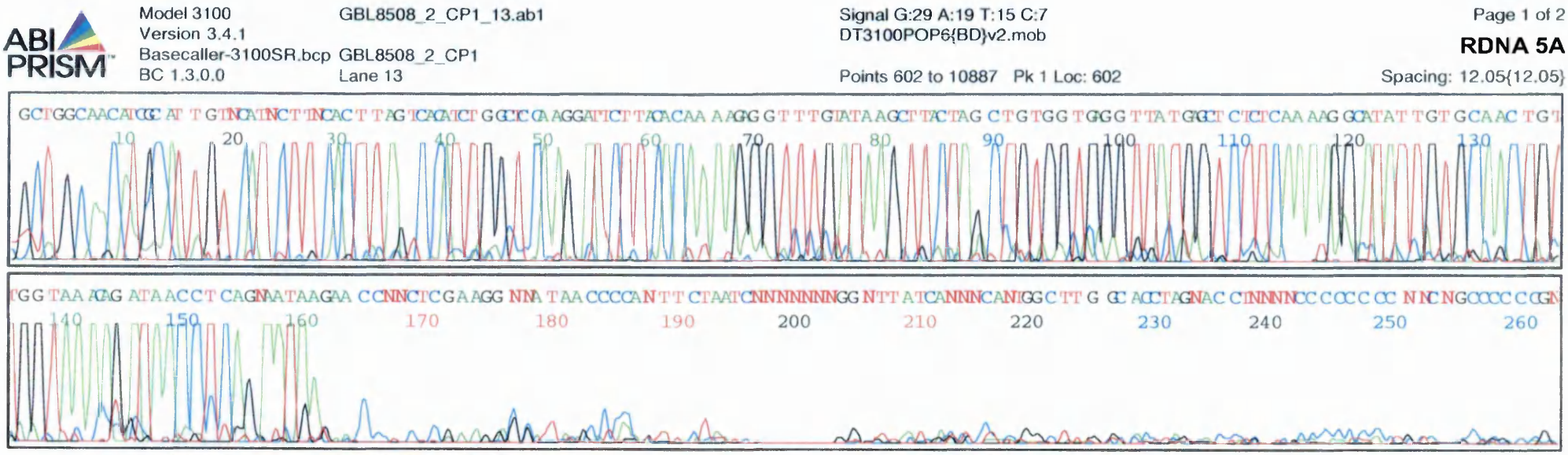

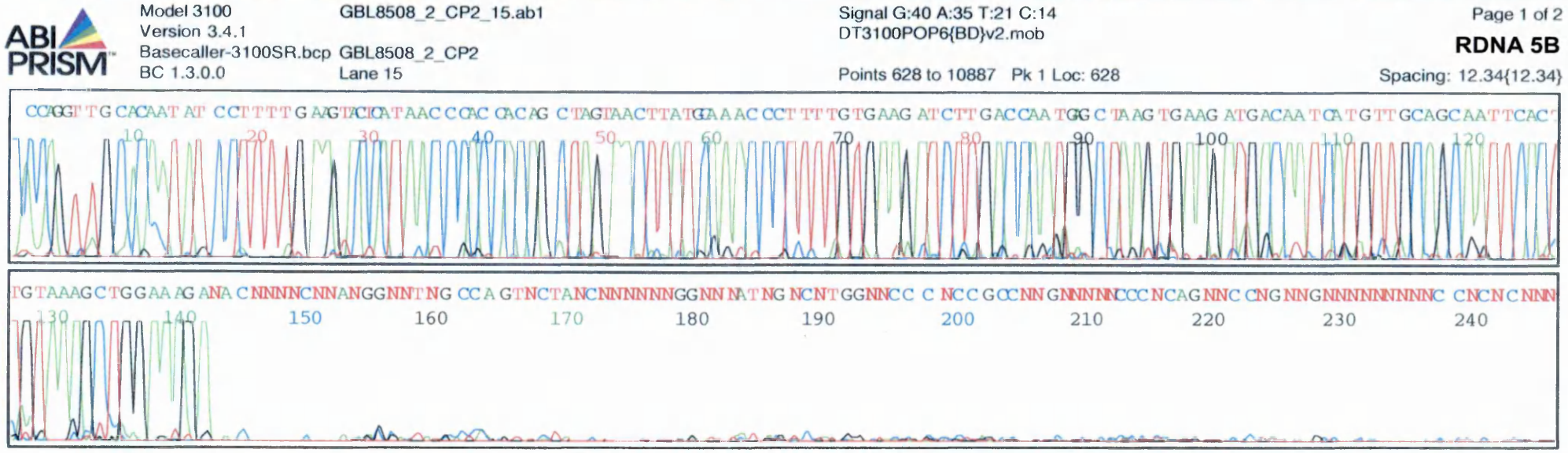

Figure 60 rDNA control 5AB sequence

No electropherogram for gDNA 5A

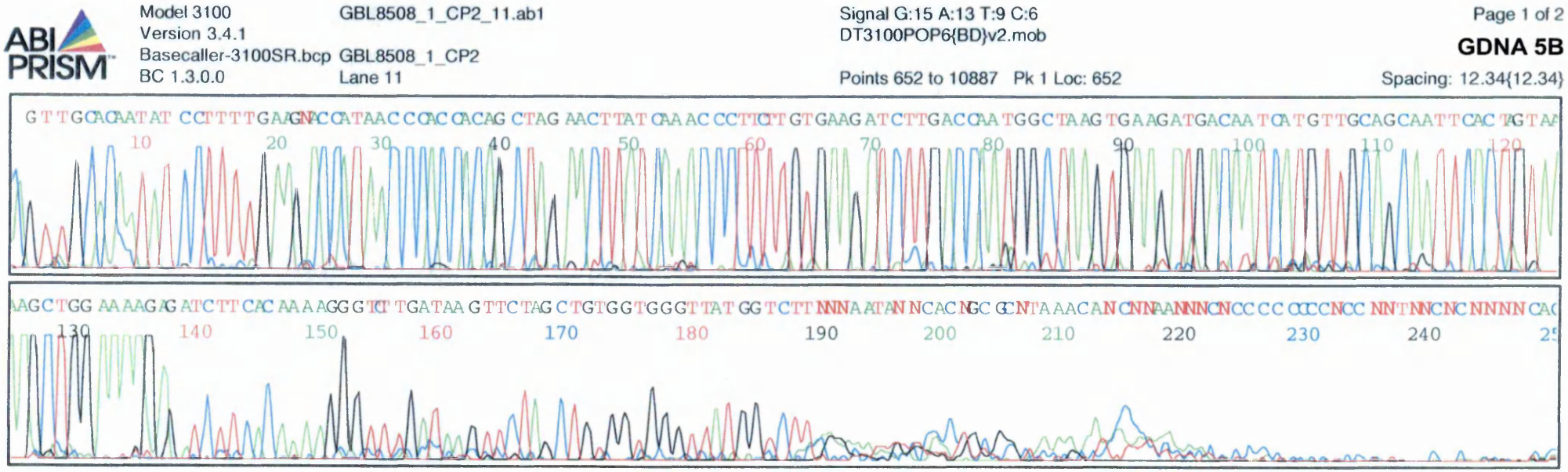

Figure 61 gDNA control 5B sequence

PTEN C AGA GTT GCA CCA TAT CCT TTT GAA GAC CAT AAC CCA CCA CAG CTA GAA CTT ATC AAA CCC TTT TGT

RDNA 5A G TCT CAA CGT GTT ATA GGA AAA CTT CTG GTA TTG GGT GGT GTC GAT CTT GAA TAG TTT GGG AAA ACA

RDNA 5B .....GTT GCA CCA TAT CCT TTT GAA GAC CAT AAC CCA CCA CAG CTA GAA CTT ATC AAA CCC TTT TGT

GDNA 5A .....AAA CGT GTC ATA GNC AAA NTT CTG GTA TTG GGT GGT GTC GAT CTT GAA TAG TTT GGG AAA ACA

GDNA 5B.....GTT GCA CCA TAT CCT TTT GAA GAC CAT AAC CCA CCA CAG CTA GAA CTT ATC AAA CCC TTT TGT

GAA GAT CTT GAC CAA TGG CTA AGT GAA GAT GAC AAT CAT GTT GCA GCA ATT CAC TGT AAA GCT GGA AAG

CTT CTA GAA CTG GTT ACC GCT TCA CTT CTA CTG TTA GTA CA.....

GAA GAT CTT GAC CAA TGG CTA AGT GAA GAT GAC AAT CAT GTT GCA GCA ATT CAC TGT AAA GCT GGA AAG

CTT CTA GAA ATA.....

GAA GAT CTT GAC CAA TGG CTA AGT GAA GAT GAC AAT CAT GTT GCA GCA ATT CAC TGT AAA GCT GGA AAG

Figure 62

5AB Sequence data for rDNA & gDNA controls compared to PTEN cDNA. Grey indicates ambiguous bases or those differing from published sequence. Dotted line indicates the point at which the read degenerated.

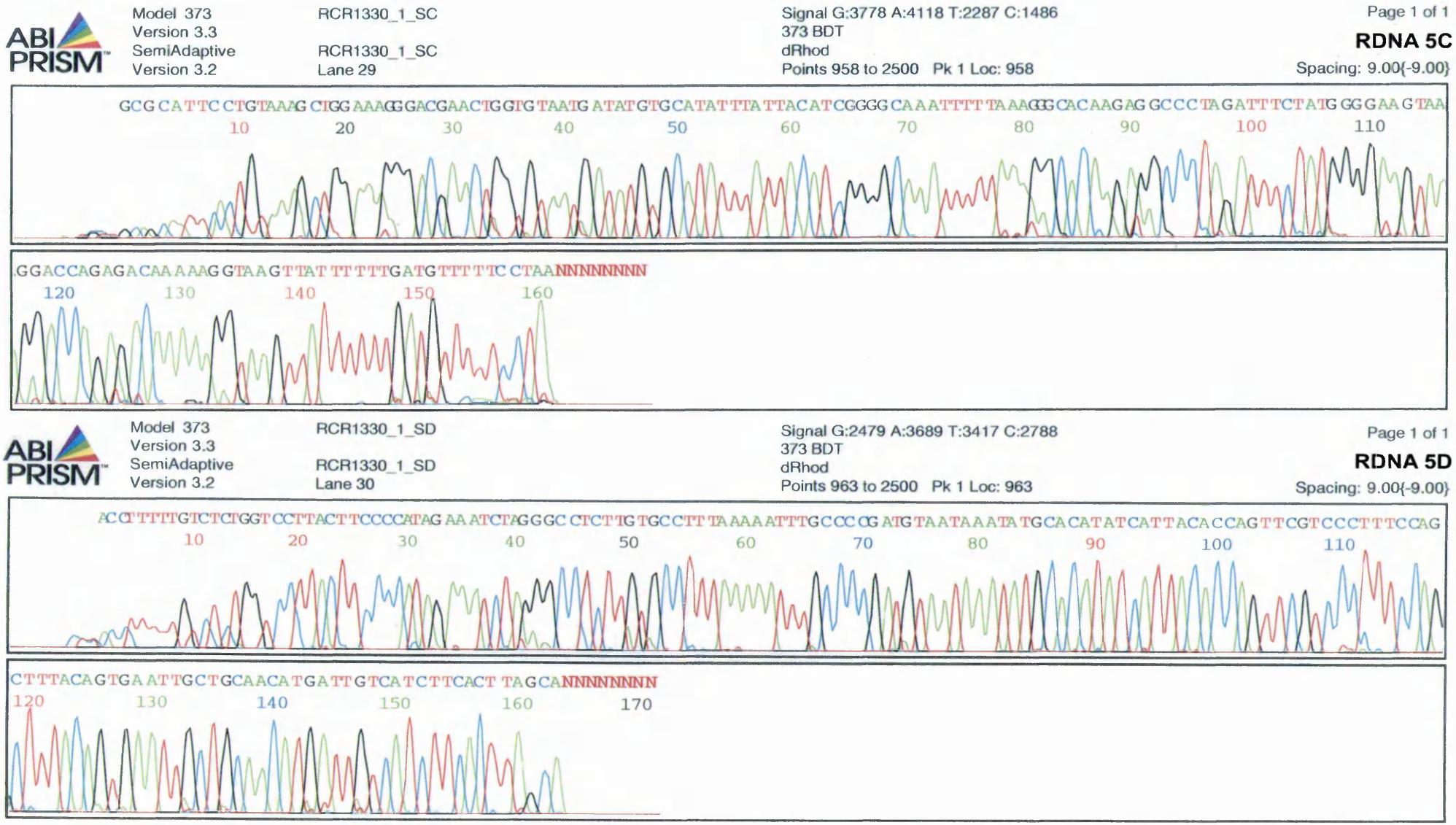

Figure 63 rDNA control 5CD sequences

PTEN GAA GCA ACT GGT GTA ATG ATA TGT GCA TAT TTA TTA CAT CGG GGC AAA TTT TTA AAG GCA CAA GAG

RDNA 5C CTT CGT TGA CCA CAT TAC TAT ACA CGT ATA AAT AAT GTA GCC CCG TTT AAA AAT TTC CGT GTT CTC

RDNA 5D GAAGCA ACT GGT GTA ATG ATA TGT GCA TAT TTA TTA CAT CGG GGC AAA TTT TTA AAG GCA CAA GAG

GCC CTA GAT TTC TAT GGG GAA GTA AGG ACC AGA GAC AAA AAG

CGG GAT GTA AAG ATA CCC CTT CAT TCC TGG TCT CTG TTT TTC

GCC CTA GAT TTC TAT GGG GAA GTA AGG ACC AGA GAC AAA AAG

Figure 64

rDNA control 5CD Sequence data for rDNA & gDNA controls compared to PTEN cDNA

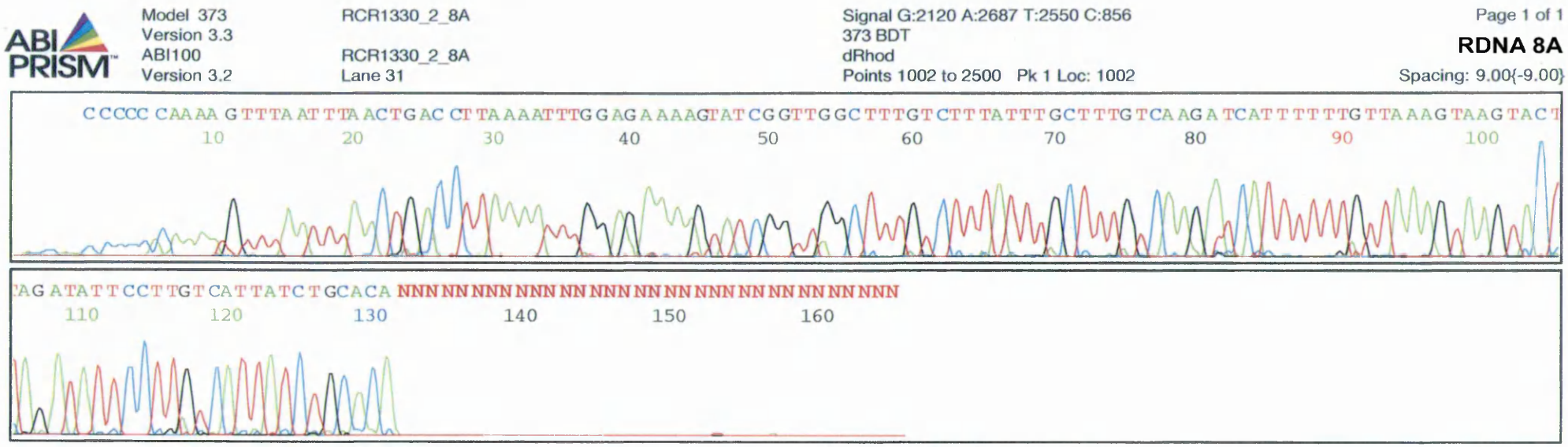

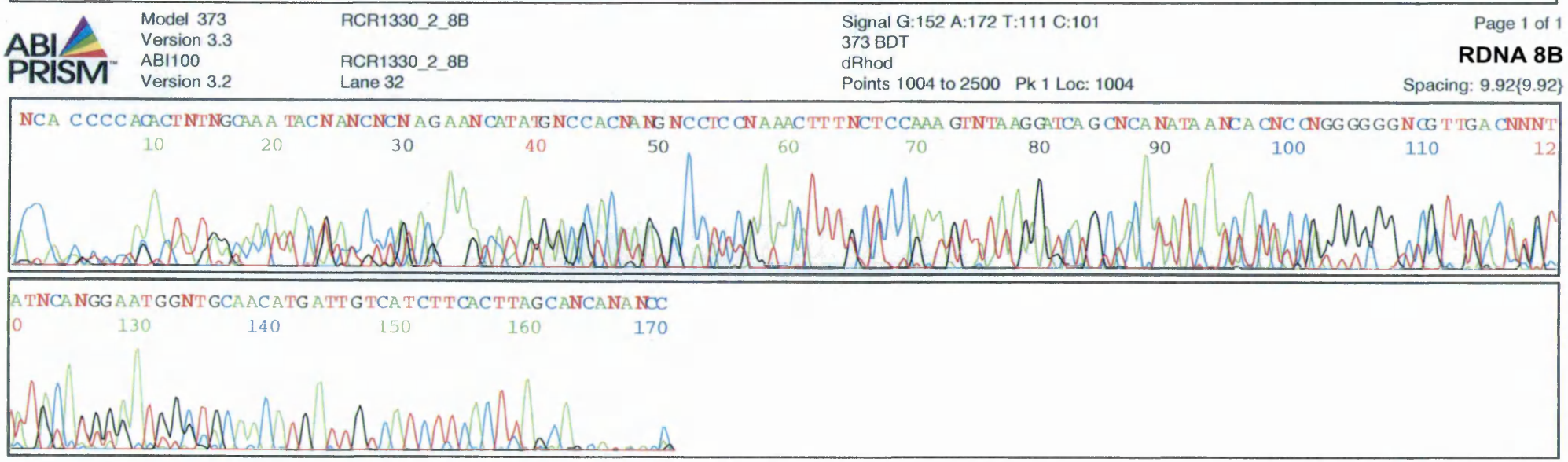

Figure 65 rDNA control 8AB sequences

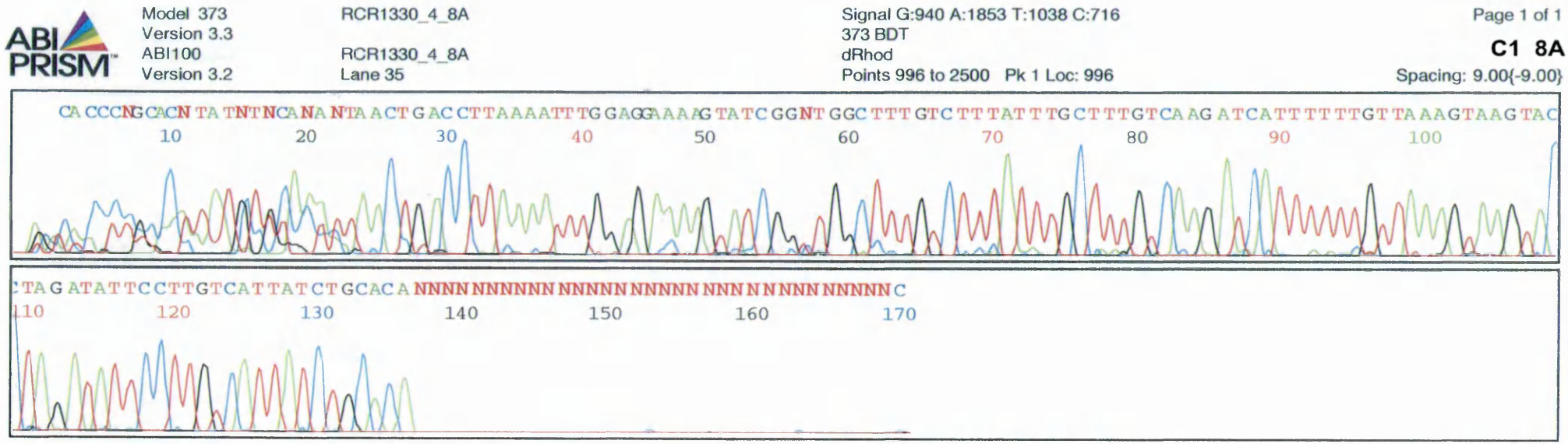

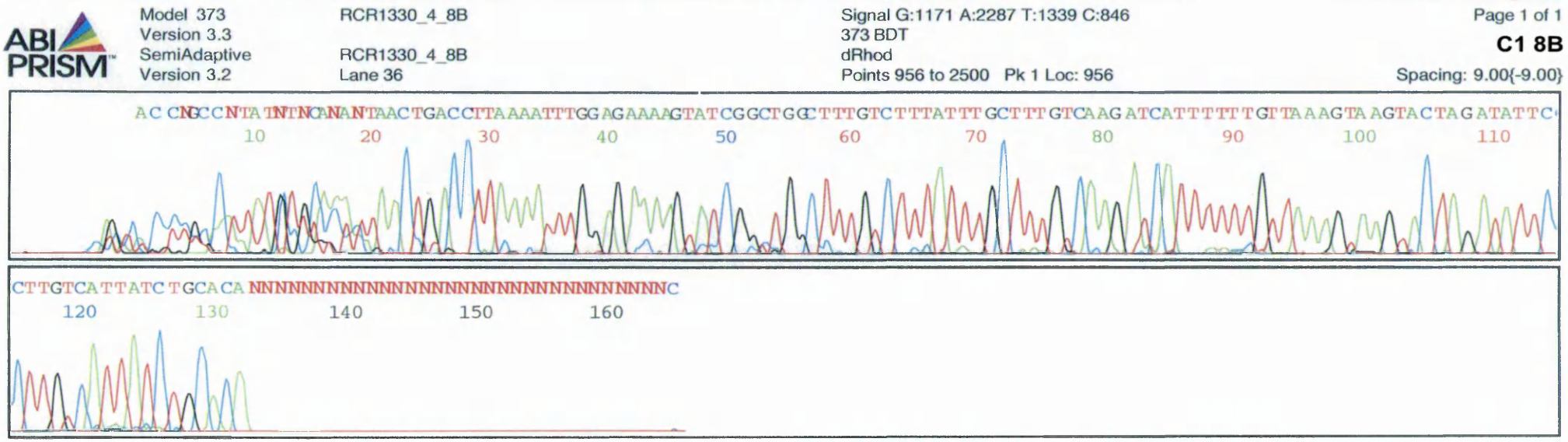

Figure 66 C1 control 8AB sequences

Figure 67 SJ1 control DNA 8AB

PTEN GT GCA GAT AAT GAC AAG GAA TAT CTA GTA CTT ACT TTA ACA AAA AAT GAT CTT GAC AAA GCA AAT

RDNA 8A CA CGT CTA TTA CTG AAC CTT ATA GAT CAT GAA TGA AAT TGT TTT TTA CTA GAA CTG TTT CGT TTA

RDNA 8B NO READ.....

SJ1 8A CA CGT CTA TTA CTG AAC CTT ATA GAT CAT GAA TGA AAT TGT TTT TTA CTA GAA CTG TTT CGT TTA

SJ1 8B GT GCA GAT AAT GAC AAG GAA TAT CTA GTA CTT ACT TTA ACA AAA AAT GAT CTT GAC AAA GCA AAT

C1 8A CA CGT CTA TTA CTG AAC CTT ATA GAT CAT GAA TGA AAT TGT TTT TTA CTA GAA CTG TTT CGT TTA

C1 8B GT GCA GAT AAT GAC AAG GAA TAT CTA GTA CTT ACT TTA ACA AAA AAT GAT CTT GAC AAA GCA AAT

AAA GAC AAA GCC AAC CGA TAC TTT TCT CCA AAT TTT AAG

TTT CTG TTT CGG TTG GCT ATG AAA AGA GGT TTA AAA TTC

.....

TTT CTG TTT CGG TTG GCT ATG AAA AGA GGT TTA AAA TTC

AAA GAC AAA GCC AAC CGA TAC TTT TCT CCA AAT TTT AAG

TTT CTG TTT CGG TNG GCT ATG AAA AGA GGT TTA AAA TTC

AAA GAC AAA GCC AAC CGA TAC TTT TCT CCA AAT TTT AAG

Figure 68

8AB Sequence data for rDNA, SJ1 & C1 controls compared to PTEN cDNA. Grey indicates ambiguous bases or those differing from published sequence. Dotted line indicates the point at which the read degenerated.

3.3.3 SSCP Analysis

PCR products were initially separated using a minigel (8 x 10 cm) system. This method, however, was revised due to poor band migration. Increased band separation and detection sensitivity was observed using an 18x24 cm large gel format, therefore this method was selected to analyse the PCR products for all exon fragments. SSCP was performed as described in Chapter 2, Section 2.4.4 using 0.5 - 0.6% MDE/10% glycerol gels running overnight at 4°C to avoid heat generation. Bands were detected initially by manual silver staining (Section 3.3.3.2), which gave a high background and poor band definition, and later with a silver staining kit as described in Chapter 2, Section 2.4.4.2.

Results of SSCP are shown in Figures 69 and 70, for exon 5 (Section 3.3.3.1-2) and Figures 76 and 77 for exon 8 (Section 3.3.3.3-4). Samples were carefully compared to the band migration pattern of one or more of the controls (rDNA, gDNA, C1 or SJ1). Samples showing band shifts were noted and re-run on separate gels to confirm the presence of the aberrant bands (highlighted in red), where sufficient sample was available. The results for each exon were tabulated to include histological details for each sample, where available (Tables 19 to 22).

3.3.3.1 Exon 5AB SSCP Results

Fig 69a

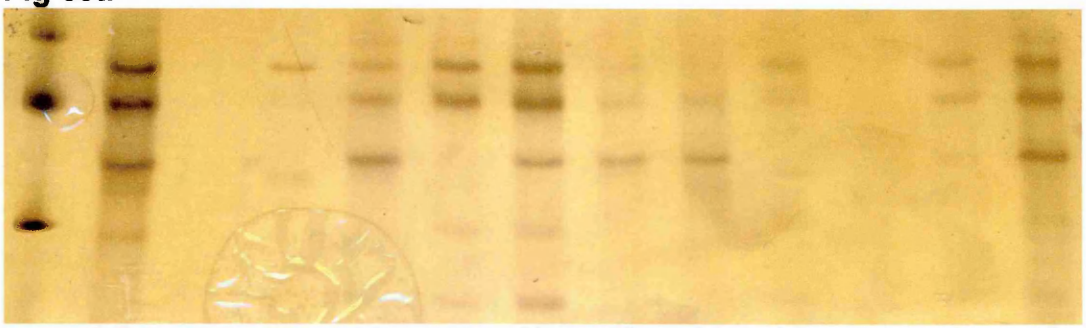

rDNA 24 25 27 28 30x 30y 31 35 36 45 46x

Fig 69b

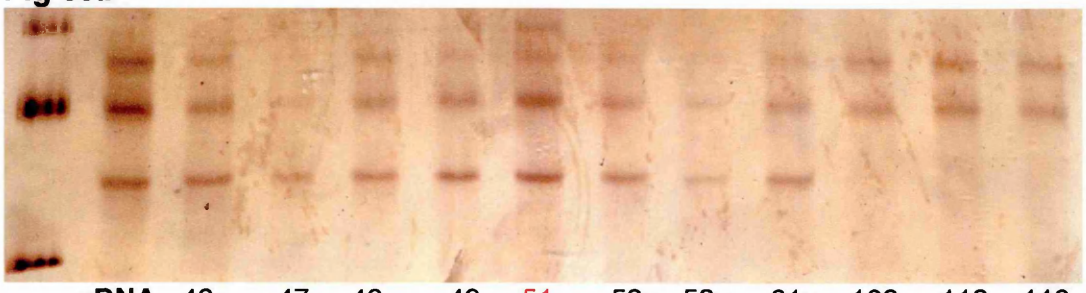

gDNA 46y 47 48 49 51 52x 52y 61x 102 112 113

Fig 69c

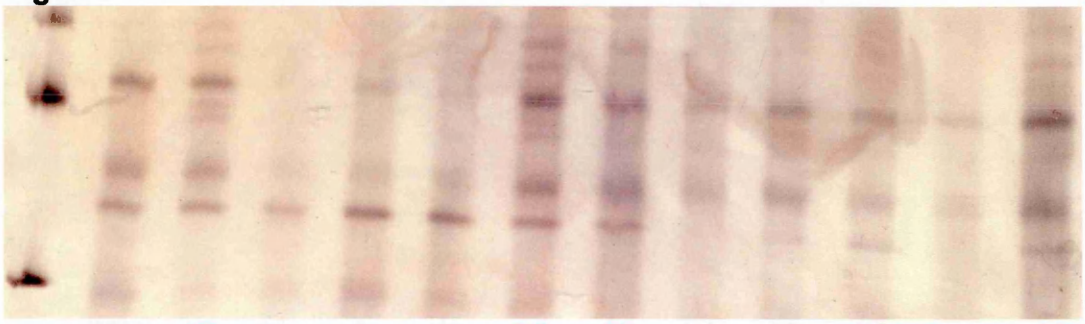

rDNA 18 68x 69 73 74 75 76 77 78 79 80

Fig 69d

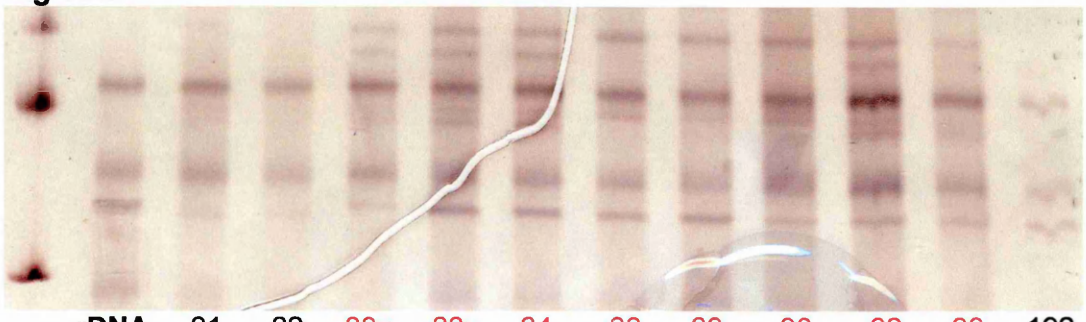

rDNA 81 82 83x 83y 84 88 89 90 92 93 192

Figure 69 a-d SSCP results for exon 5ABSamples with bandshifts are numbered in red. Controls rDNA and/or gDNA are included with 100bp marker on each gel (lane 1).

Fig 69e

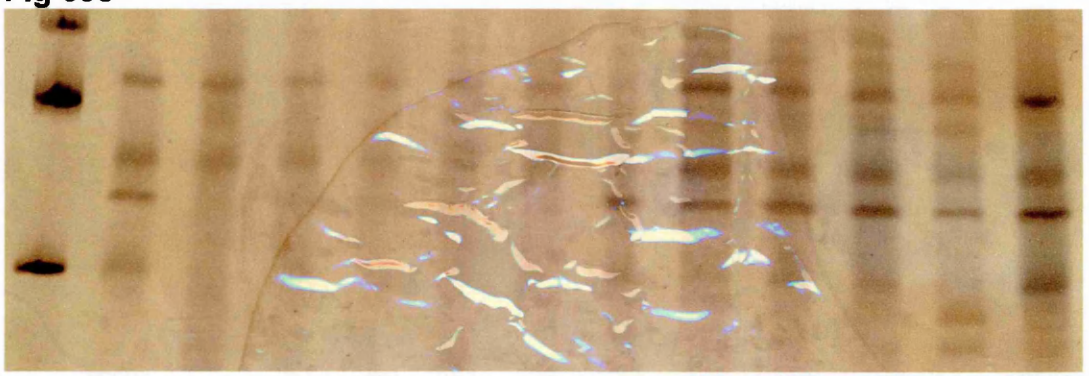

rDNA 114 134 135 137 138 151 152 153 159 160 **gDNA**

Fig 69f

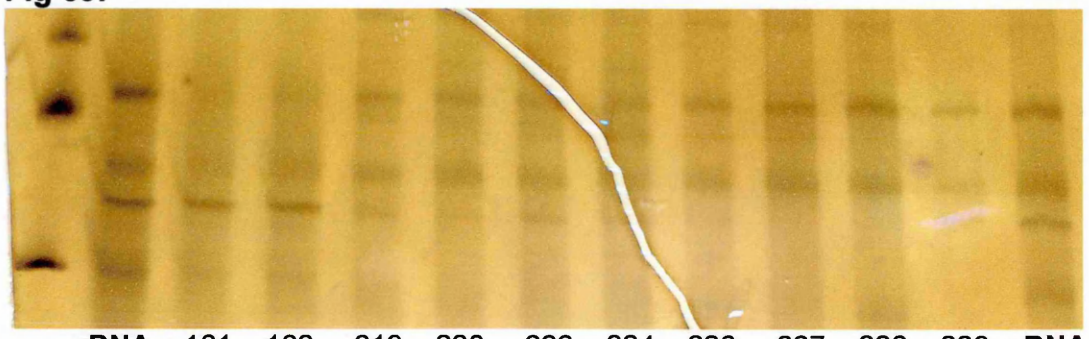

rDNA 161 162 219 220 222 224 226 227 228 229 **gDNA**

Fig 69g

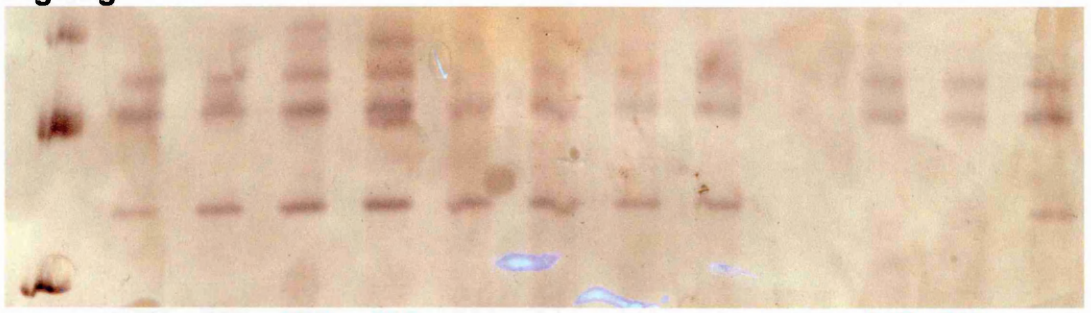

rDNA 207 208 209 210 211 212 214x 216 217 218 **gDNA**

Fig 69 e-g SSCP results for exon 5AB

Samples with bandshifts are numbered in red. Controls rDNA and/or gDNA are included with 100bp marker on each gel (Lane 1).

Table 19 Bandshift Summary Exon 5AB			
Sample	ID	Tissue	Histology
18	95/23231e	Endometrium	AH?
51	94/18507c	Endometrium	AH?
74	97/12804 ln	Endometrium	Com H
83x	97/21010 jx	Endometrium	AdCa 2 & AH
83y	97/21010 jy	Endometrium	AdCa 2 & AH
84	97/21010 a	Cervix	Normal
88	98/4189 2a	Cervix	Normal
89	98/4189 2d	Endometrium	AdCa 2
90	98/4189 2c	Endometrium	AdCa 2 & AH
92	98/11642 h	Endometrium	AdCa 3
93	98/11642 g	Endometrium	AH?
152	94/11672 c	Endometrium	H
153	94/11672 b	Cervix	Normal
159	94/20749 c	Endometrium	H
160	95/6941 c	Endometrium	H
208	97/3404 f	Endometrium	Marginal
209	94/4094 f	Endometrium	-

Table 19 Bandshift Summary for Exon 5AB showing samples in which aberrant bands were detected. Where available, tissue and histological description are included. **H:** hyperplasia, **AH:** atypical hyperplasia, **Com H:** complex hyperplasia, **AdCa (x):** adenocarcinoma (grade), **?:** histological grouping unclear.

3.3.3.2 Exon 5CD SSCP Results

Fig 70a

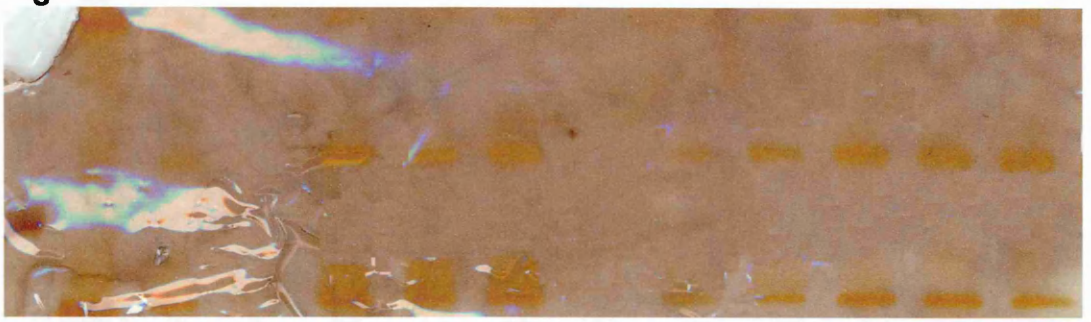

rDNA 18 18a 20 21 22 24 25 27 28 134 135

Fig 70b

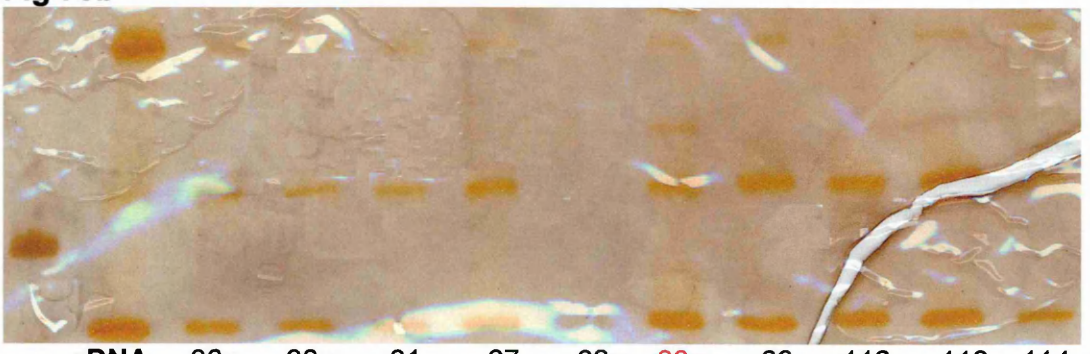

rDNA 30x 30y 31 67 68x 68y 69 112 113 114

Fig 70c

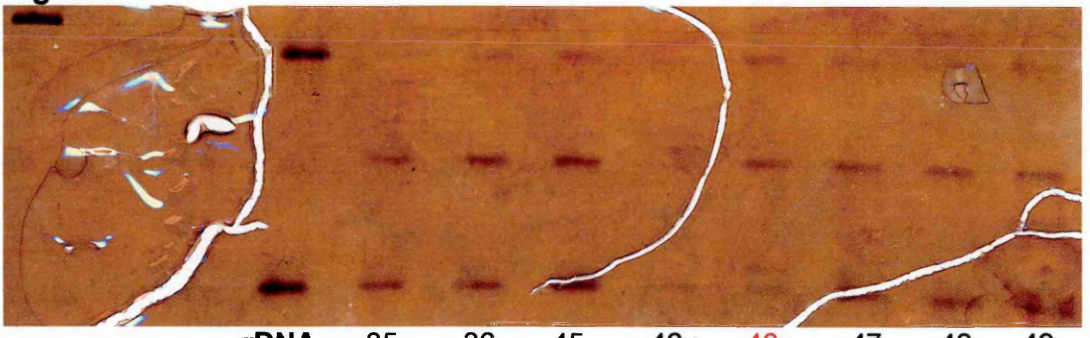

rDNA 35 36 45 46y 46x 47 48 49

Fig 70d

rDNA 35 36 45 - 46x 46y 47 48 49 **C1**

Figure 60 a-d SSCP results for exon 5CD. Samples with bandshifts are numbered in red. Controls rDNA and/or gDNA are included with 100bp marker on each gel.

Fig 70e

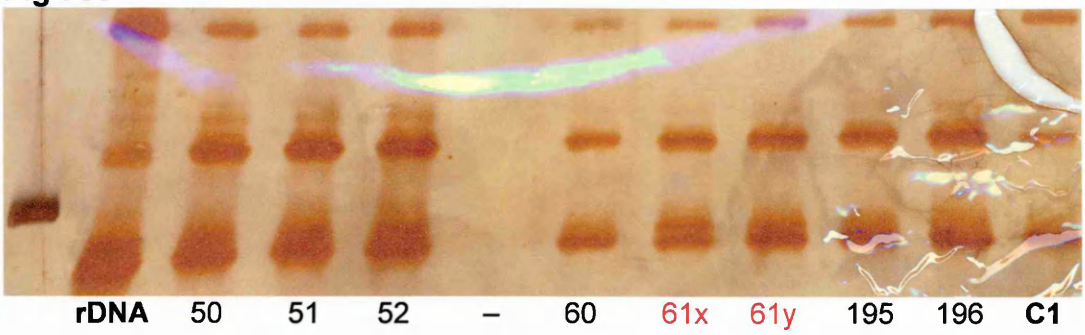

Fig 70f

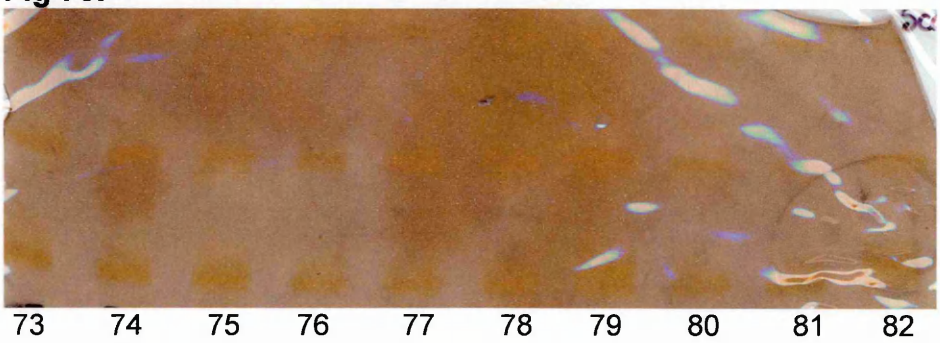

Fig 70g

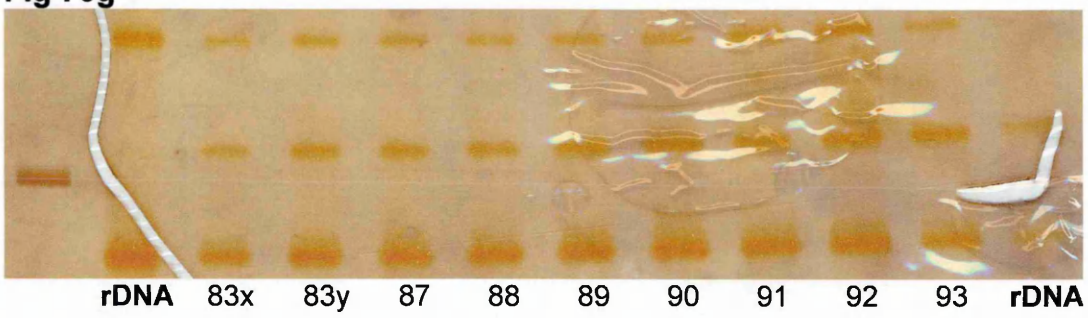

Fig 70h

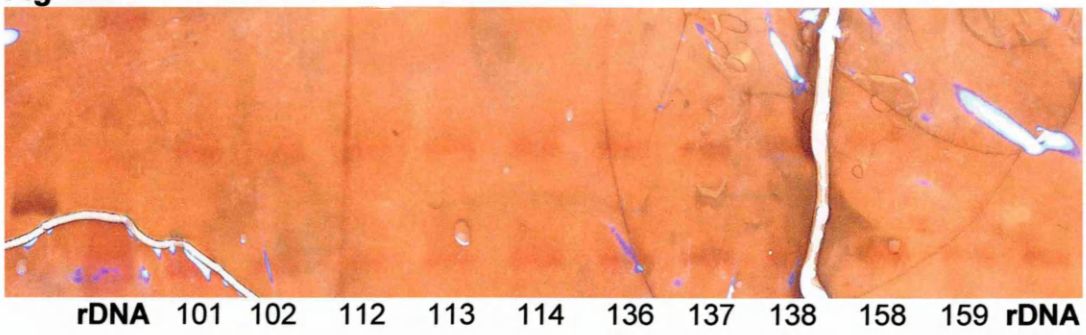

Figure 60 e-h SSCP results for exon 5CD. Samples with bandshifts are numbered in red. Controls rDNA and/or gDNA are included with 100bp marker on each gel (lane 1).

Fig 70i

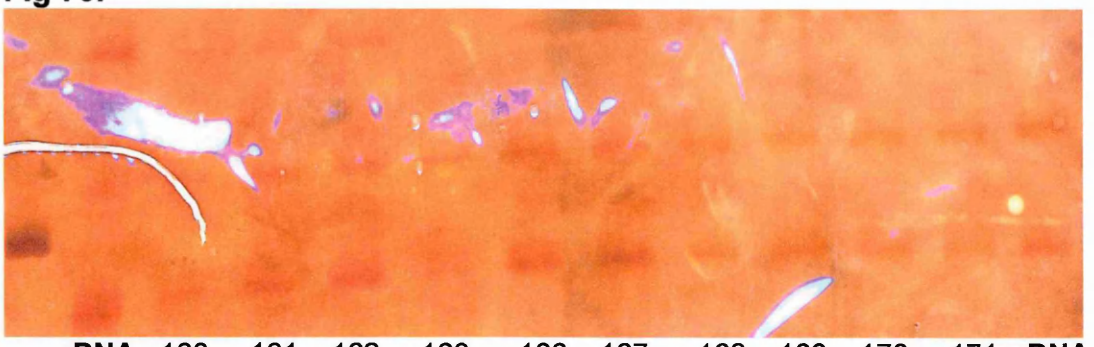

rDNA 160 161 162 163 166 167 168 169 170 171 **rDNA**

Fig 70j

rDNA 205 206 207 208 209 210 211 212 214 215 **rDNA**

Fig 70k

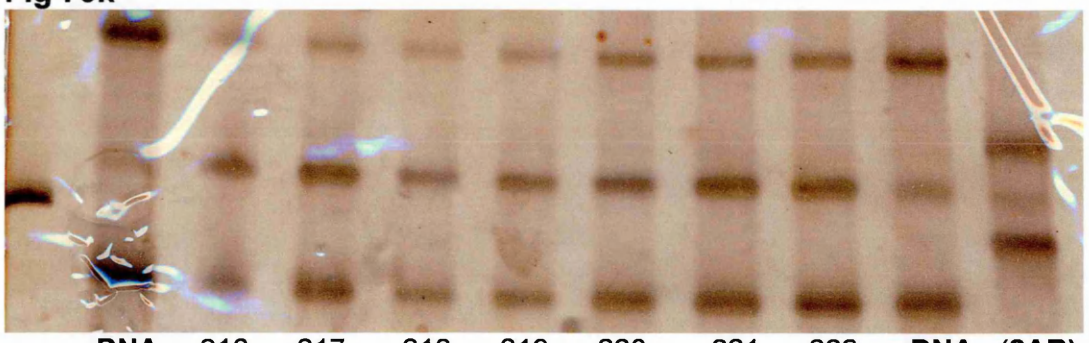

rDNA 216 217 218 219 220 221 222 **rDNA** **(8AB)**

Fig 70l

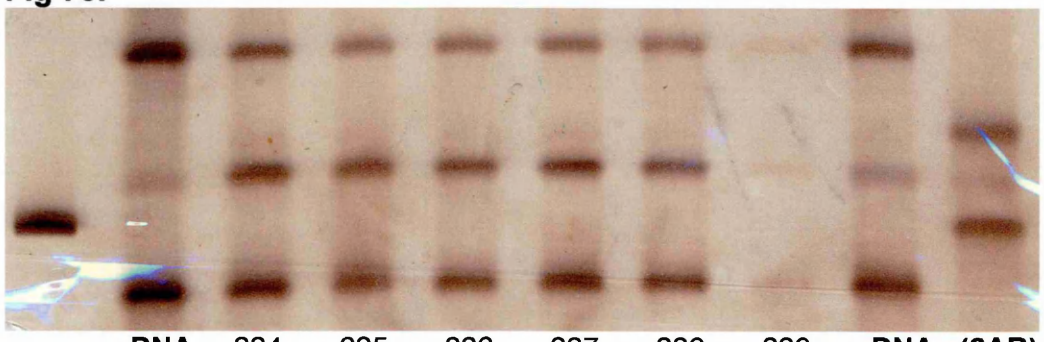

rDNA 224 225 226 227 228 229 **rDNA** **(8AB)**

Figure 60 i-l SSCP results for exon 5CD. Samples with bandshifts are numbered in red. Controls rDNA and/or gDNA are included with 100bp marker on each gel (lane 1).

Fig 70m

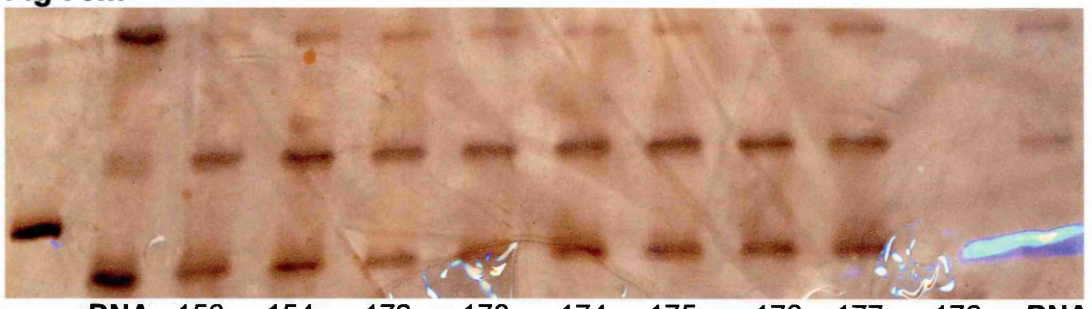

Fig 70n

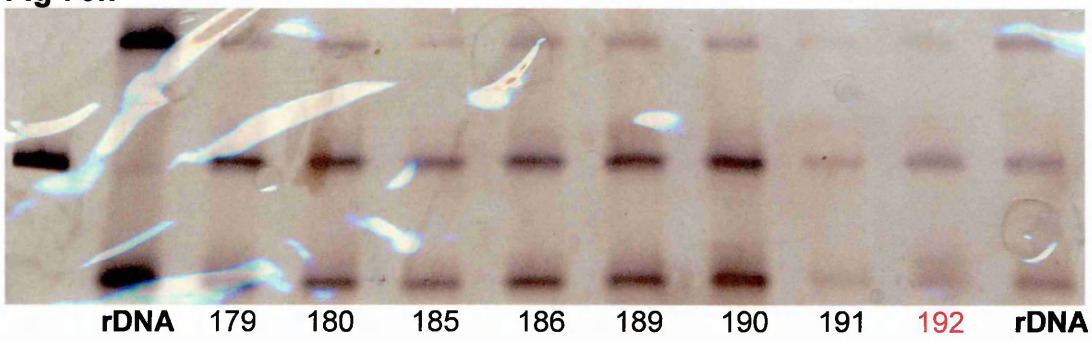

Fig 70o

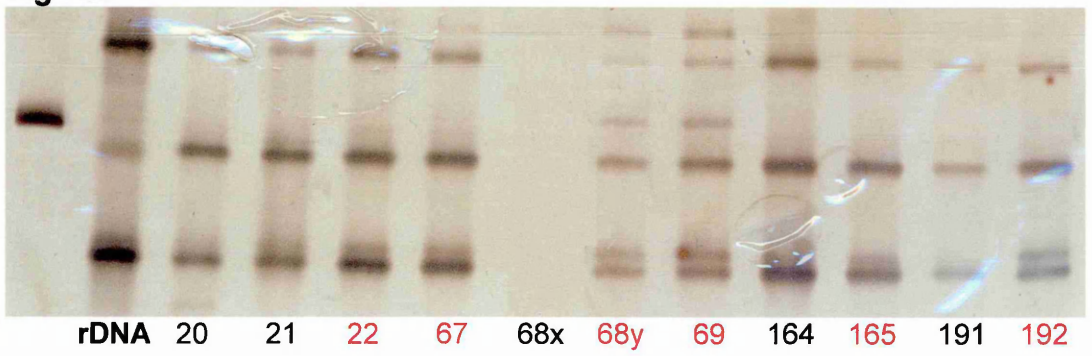

Fig 60 m-o SSCP results for exon 5CD. Samples with bandshifts are numbered in red. Controls rDNA and/or gDNA are included with 100bp marker on each gel (lane 1).

Table 20 Bandshift Summary Exon 5CD			
Sample	ID	Tissue	Histology
22	96/11307 h	Endometrium	-
46x	94/5212 lbx	Endometrium	AdCa 3 + AH?
61x	95/22466 5fx	Endometrium	IECa / Sev AH
61y	95/22466 5fy	Endometrium	IECa / Sev AH
67	97/9145 3b	Cervix	Normal
68y	97/9145 32y	Endometrium	AdCa 2
69	97/9145 lb3	Endometrium	AH / IECa
165	94/21552 3a	Cervix	Normal
192	97/3362 e	Endometrium	-

Table 22 Bandshift Summary for Exon 5CD showing samples in which aberrant bands were detected. Where available, tissue and histological description are included. **AH:** atypical hyperplasia, **Com H:** complex hyperplasia, **Sev AH:** severe atypical hyperplasia, **AdCa (x):** adenocarcinoma (grade), **IECa**: intraepithelial carcinoma, **?:** histological grouping unclear.

Exon 5 Summary

SSCP separation for the 5AB exon fragment was good, however interpretation of the bands was difficult due to multiple additional bands observed in each sample. Patient samples could not be sequenced due to inadequate read quality after several attempts.

Figures 70a-j show gels developed by manual silver staining. Sensitivity was very low and background staining high for the majority of gels. Figures 70k-o demonstrate the improvement of gels stained with the PlusOne silver staining kit (Chapter 2, Section 2.4.4.2).

With regard to exon 5CD, sequencing was performed on sample 46x, which exhibited a bandshift, and also samples 45, 46y and 47 obtained from the same patient. Sequence data was successfully obtained (Figures 71 to 74) but the readings were incomplete, containing ambiguous bases and low signal strength, especially with the 5C primer.

The readable portions of data were aligned with the PTEN cDNA sequence for comparison (Figure 75). No conclusions as to the success of bandshift detection could be made from the sequence data obtained, due to the high number of ambiguous bases or base changes.

Overall figures for the incidence of bandshifts in exon 5 were as follows. For exon 5AB, 26% (11/43) of patients demonstrated bandshifts from a corresponding total of 13% (17/127) of all samples. For exon 5CD, 14% (6/43) of patients demonstrated bandshifts from a corresponding total of 7% (9/127) of all samples. The total bandshift detection rate for exon 5 was 40% (17/43) of patients, from 20% (26/127) of the samples used.

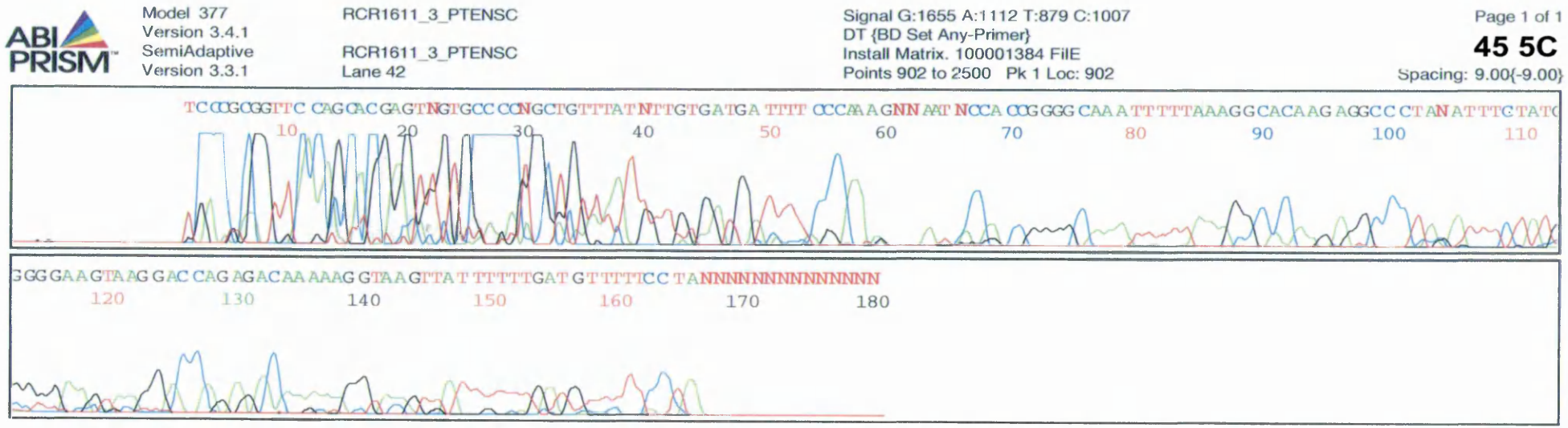

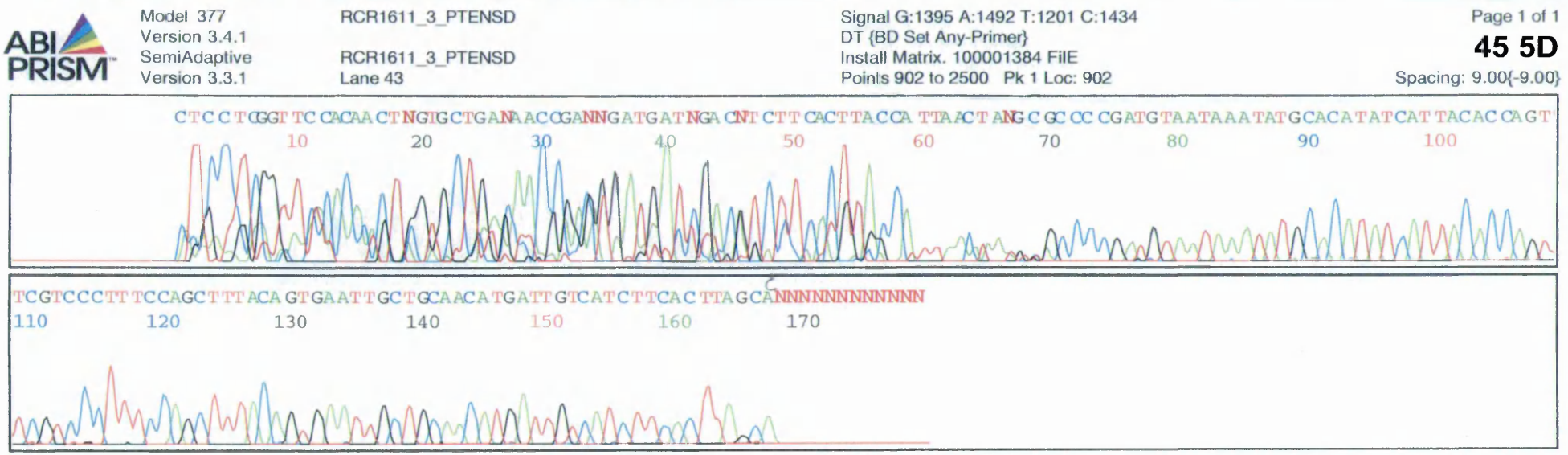

Figure 71 Exon 5CD Sequence data for Patient 45

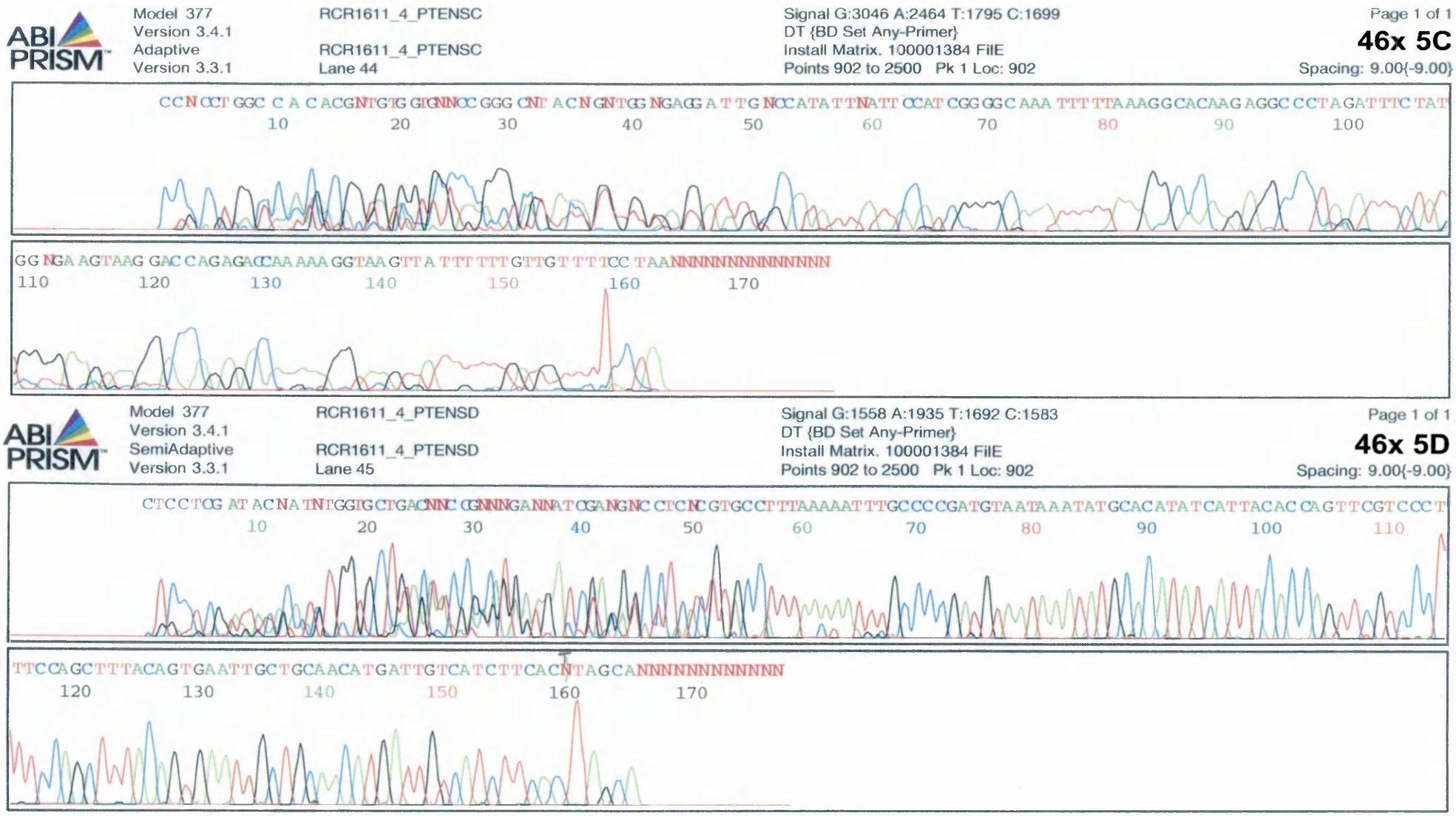

Figure 72 Exon 5CD Sequence data for Patient 46x

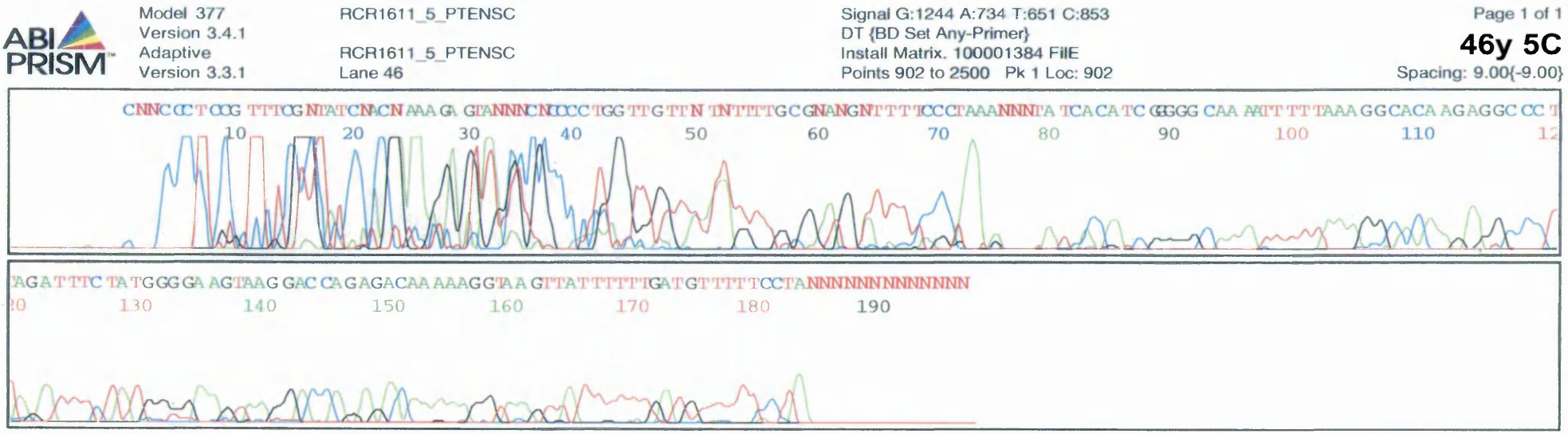

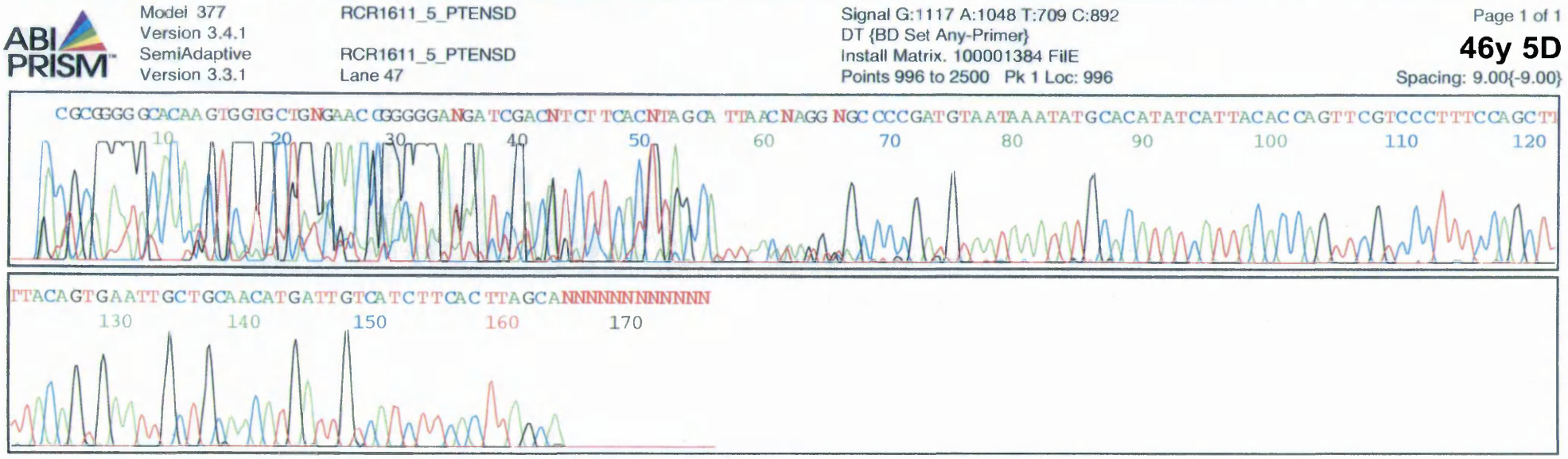

Figure 73 Exon 5CD Sequence data for Patient 46y

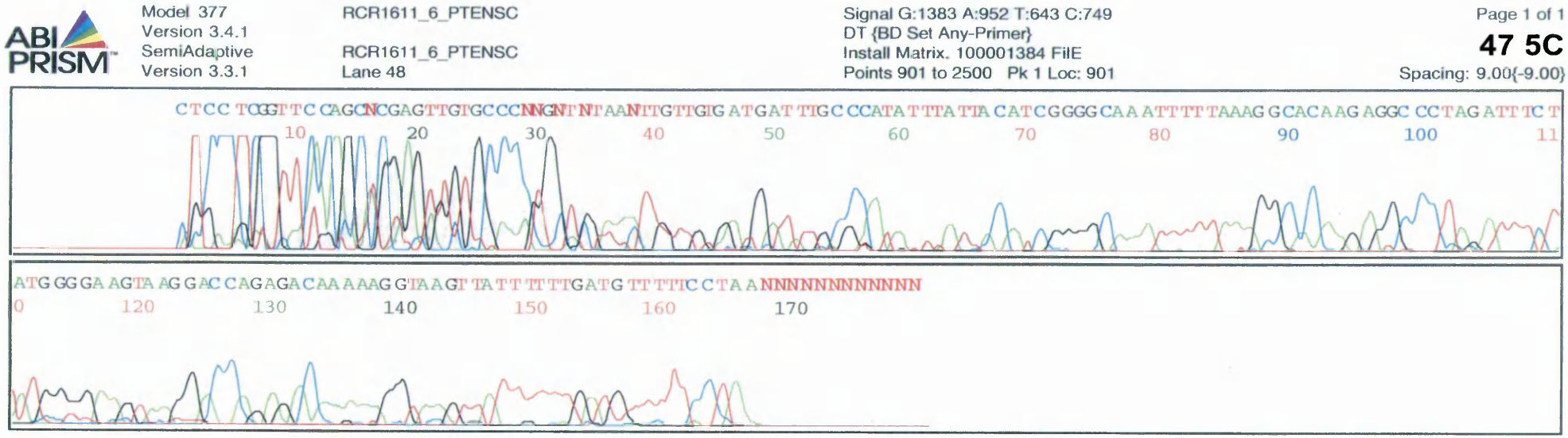

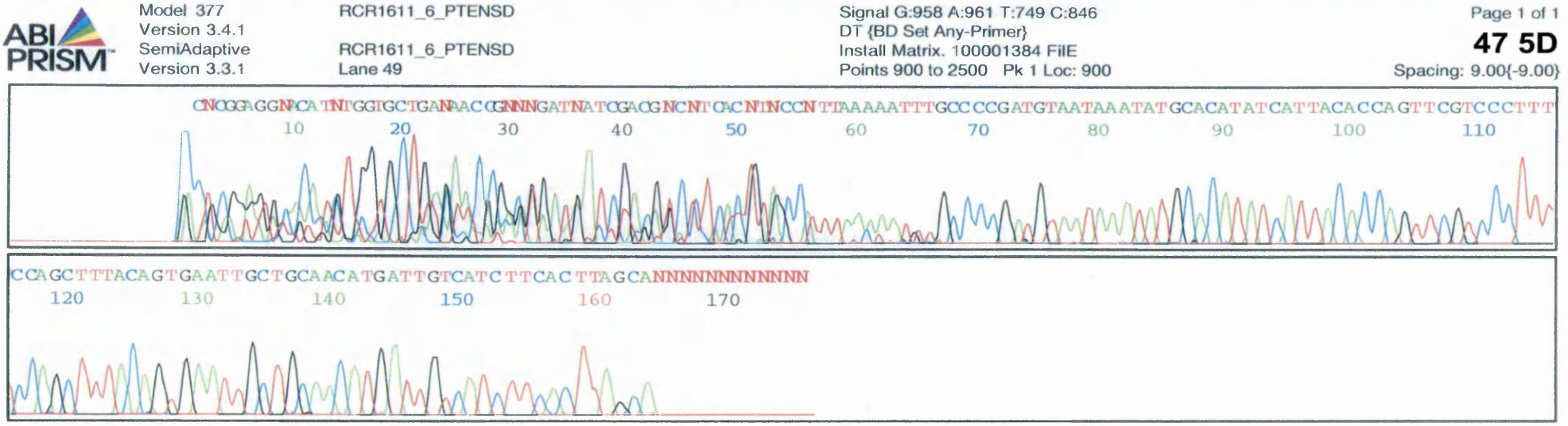

Fig 74 Exon 5CD Sequence data for Patient 47

```
PTEN 5C GAA CGA ACT GGT GTA ATG ATA TGT GCA TAT  TTA TTA CAT CGG GGC AAA TTT TTA AAG GCA CAA GAG
 45 5C  CTG  TTT ATN TTG  TGA TGA TTT  TCC CAA AGN NAA TNC CAC CGG GGC AAA TTT TTA AAG GCA CAA GAG
 45 5D  CTT GCT TGA CCA CAT TAC TAT  ACA CGT ATA AAT AAT GTA GCC CCG CGN ATC AAT TAC  CAT  TCA  CTT
46x 5C  GGG CNT ACN GNT GGN GAG GAT TGN CCA TAT TNA TTC CAT CGG GGC AAA TTT TTA AAG GCA CAA GAG
46x 5D  CCT  GCT TGA CCA CAT TAC TAT  ACA CGT ATA AAT AAT GTA GCC CCG TTT AAA AAT TTC CGT  GCN  CTC
46y 5C  ..................................................... TAA ANN  NTA TCA CAT CGG GGC AAA TTT TTA AAG GCA CAA GAG
46y 5D  CCT GCT TGA CCA CAT TAC TAT  ACA CGT ATA  AAT AAT GTA GCC CCG NGG ANC AAT TAC GAT  NCA CTT
47 5C  NTN TAA  NTT GTT GTG ATG ATT  TGC CCA TAT  TTA  TTA CAT CGG GGC AAA  TTT TTA AAG GCA CAA GAG
47 5D  CCT GCT TGA CCA CAT TAC TAT  ACA CGT ATA AAT  AAT GTA GCC CCG  TTT  AAA AAT TNC CNT  NCA CTN

GCC CTA GAT TTC TAT GGG GAA GTA AGG ACC AGA GAC AAA AAG
GCC CTA NAT TTC TAT GGG GAA GTA AGG ACC AGA GAC AAA AAG
.......................................................................................
GCC CTA GAT TTC TAT GGN GAA GTA AGG ACC AGA GAC AAA AAG
CNG NAG CTA NNA.......................................................................
GCC CTA GAT TTC TAT GGG GAA GTA AGG ACC AGA GAC AAA AAG
CTN CAG CTA GNA.......................................................................
GCC CTA GAT TTC TAT GGG GAA GTA AGG ACC AGA GAC AAA AAG
CNG CAG CTA NTA GNN...................................................................
```

Figure 75 Exon 5CD Sequence data for patient samples 45, 46x / y & 47 aligned with PTEN cDNA. Base changes indicated in non-bold type, non-readable sections shown by dashed line. N indicates ambiguous bases.

3.3.3.3 Exon 8AB SSCP Results

Fig 76a

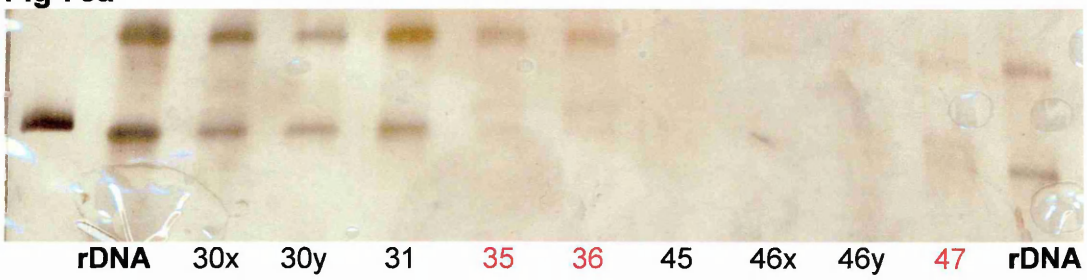

Fig 76b

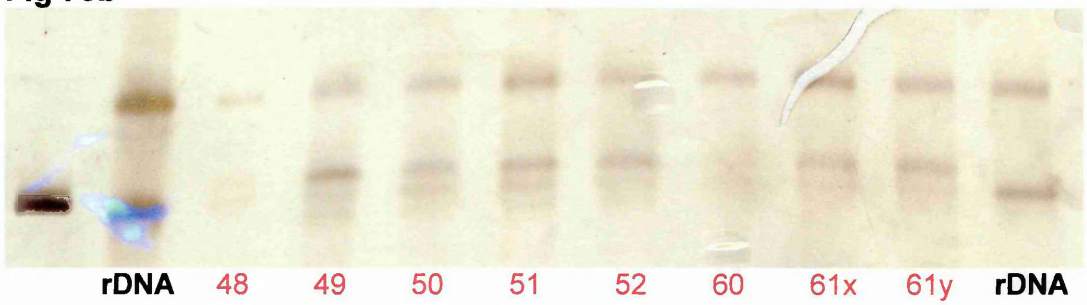

Fig 76c

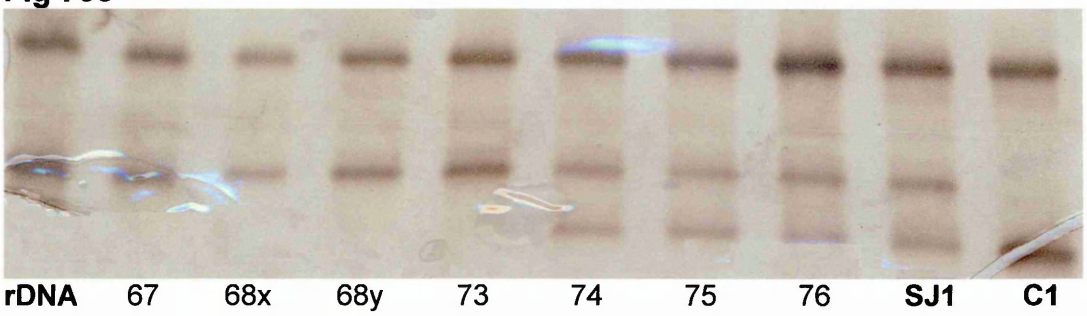

Fig 76d

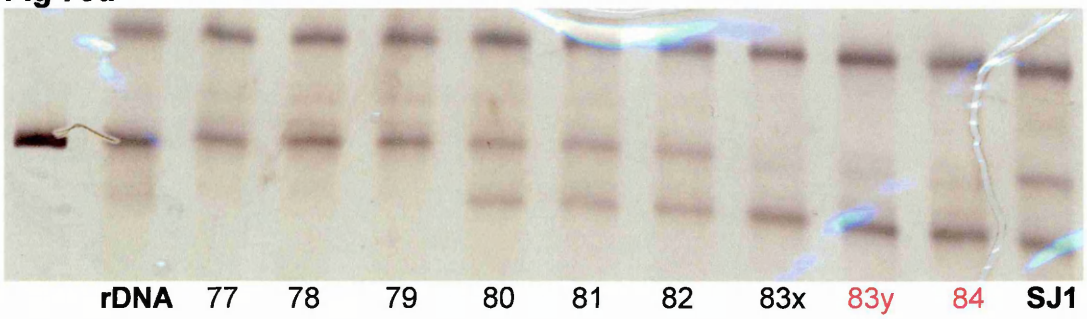

Figure 76 a-d SSCP results for exon 8AB Samples with bandshifts are numbered in red. Controls rDNA and/or C1 and SJ1 are included with 100bp marker on each gel (lane 1).

Fig 76e

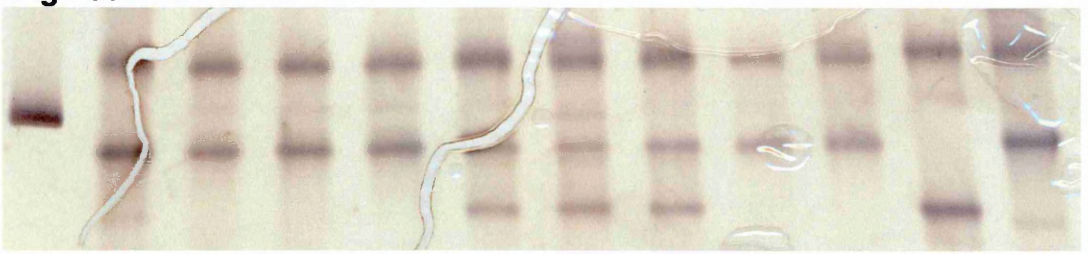

rDNA 88 89 90 91 92 93 101 102 **C1** **rDNA**

Fig 76f

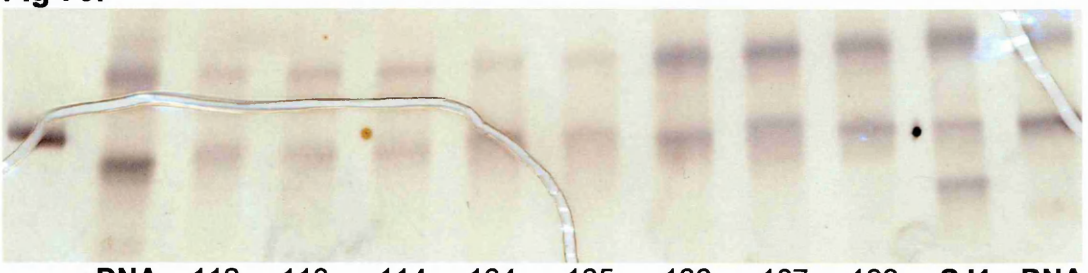

rDNA 112 113 114 134 135 136 137 138 **SJ1** **rDNA**

Fig 76g

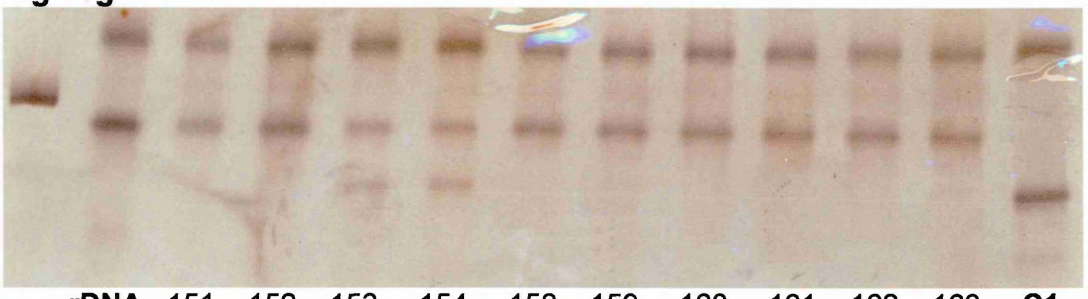

rDNA 151 152 153 154 158 159 160 161 162 163 **C1**

Fig 76h

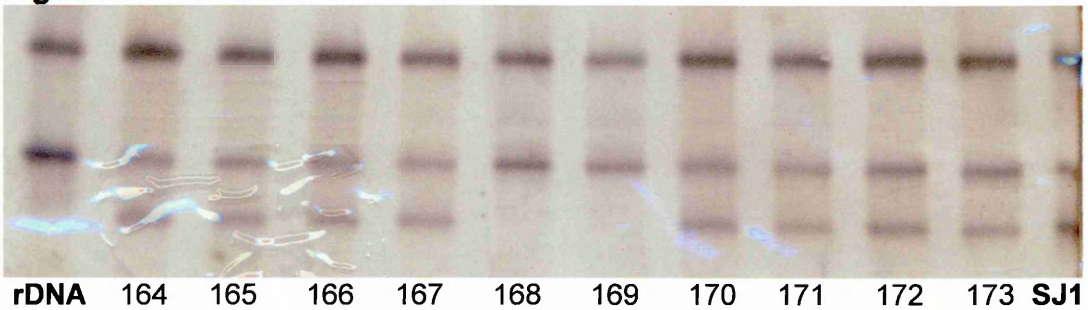

rDNA 164 165 166 167 168 169 170 171 172 173 **SJ1**

Figure 76 e-h SSCP results for exon 8AB Samples with bandshifts are numbered in red. Controls rDNA and/or C1 and SJ1 are included with 100bp marker on each gel (lane 1).

Fig 76i

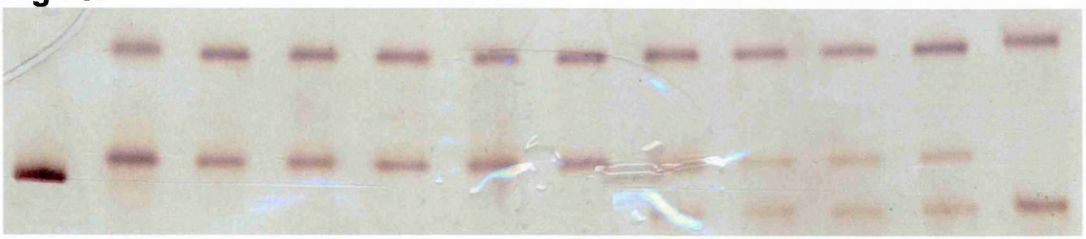

rDNA 174 175 176 177 178 179 180 185 186 **C1**

Fig 76j

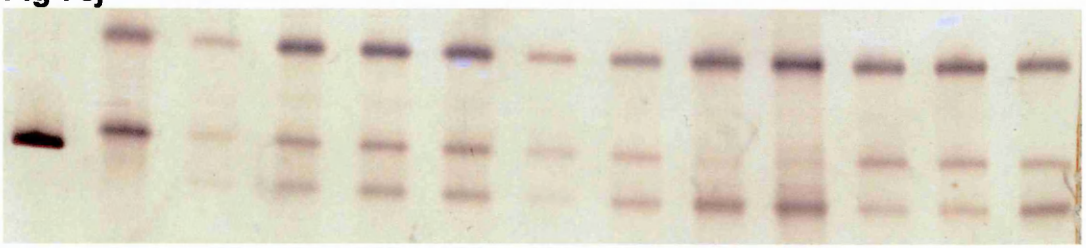

rDNA 187 188 189 190 191 192 193 194 195 196 **SJ1**

Fig 76k

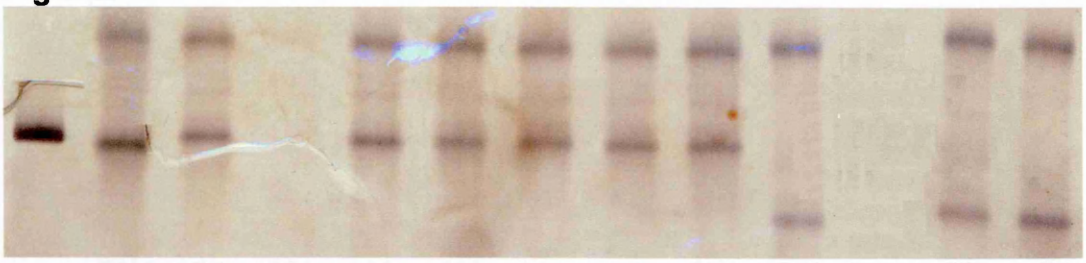

rDNA 200 201 202 203 204 205 206 207 - 208 **C1**

Fig 76l

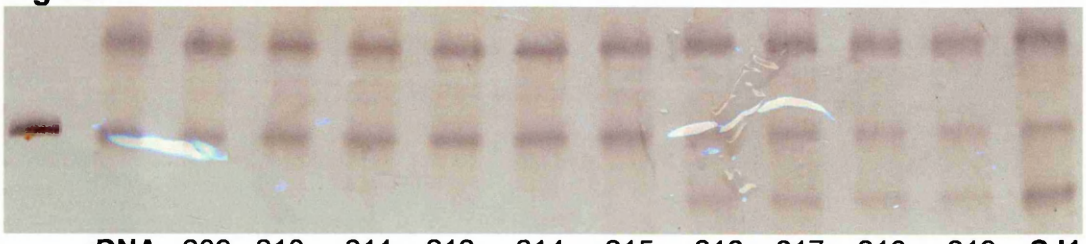

rDNA 209 210 211 212 214 215 216 217 218 219 **SJ1**

Fig 76m

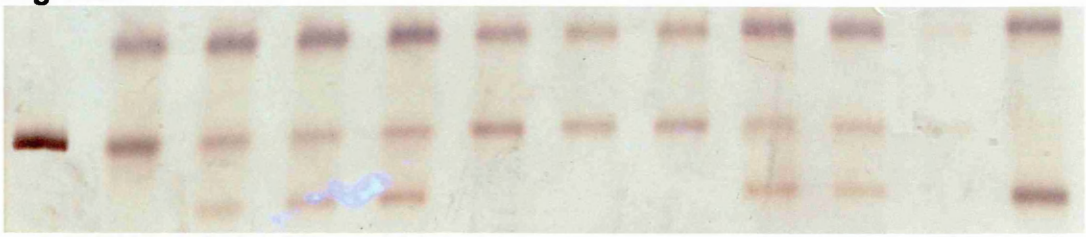

rDNA 220 221 222 224 225 226 227 228 229 **C1**

Figure 76 i-m SSCP results for exon 8AB Samples with bandshifts are numbered in red. Controls rDNA and/or C1 and SJ1 are included with 100bp marker on each gel (lane 1).

Fig 76n

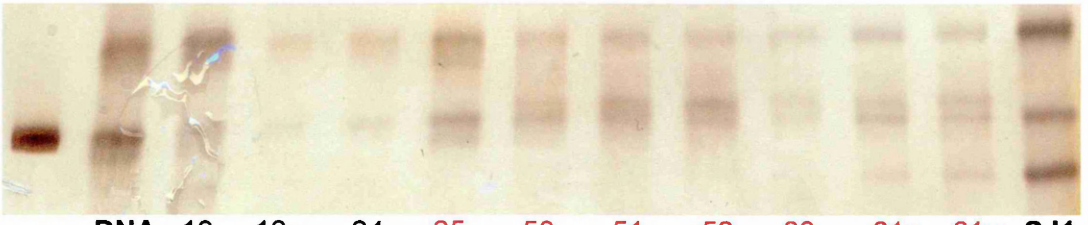

Fig 76o

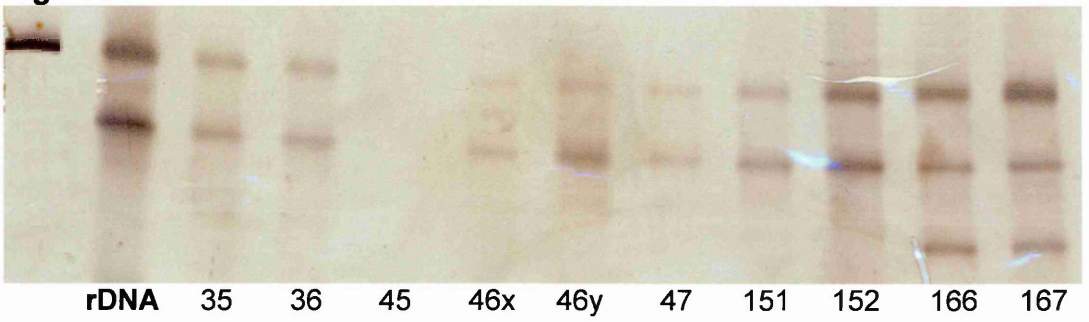

Figure 76 n-o SSCP results for exon 8AB. Samples with bandshifts are numbered in red. Controls rDNA and/or C1 and SJ1 are included with 100bp marker on each gel (lane 1).

Table 21 Bandshift Summary Exon 8AB			
Sample	ID	Tissue	Histology
25	96/17667 c	Endometrium	Com H
35	97/23720 1a	Cervix	Normal
36	97/23720 1p	Endometrium	AH (B'gr)
47	94/5212 1j	Cervix	-
48	98/1372 la	Cervix	Normal
49	98/1372 ld	Endometrium	AH
50	94/18507 a	Cervix	Normal
51	94/18507 c	Endometrium	AH?
52	94/18507 f	Endometrium	Ad Ca 3
60	95/22466 5c	Cervix	Normal
61x	95/22466 5fx	Endometrium	IE Ca / Sev AH
61y	95/22466 5fy	Endometrium	IE Ca / Sev AH
83y	97/21010 j	Endometrium	AdCa2 + Ah
84	97/21010 a	Cervix	Normal
92	98/11642 h	Endometrium	Ad Ca 3
194	98/10452 j	Endometrium	-

Table 21 Bandshift Summary for Exon 8 AB showing samples in which aberrant bands were detected. Where available, tissue and histological description are included. **AH:** atypical hyperplasia, **Com H:** complex hyperplasia, **Sev AH:** severe atypical hyperplasia, **IECa**: intraepithelial carcinoma, **AdCa (x):** adenocarcinoma (grade), **?:** histological grouping unclear.

3.3.3.4 Exon 8CD SSCP Results

Fig 77a

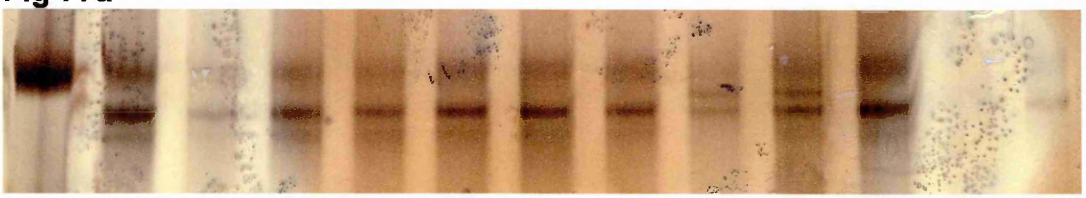

gDNA 80 81 82 83y 84 88 89 90 92 101 102

Fig 77b

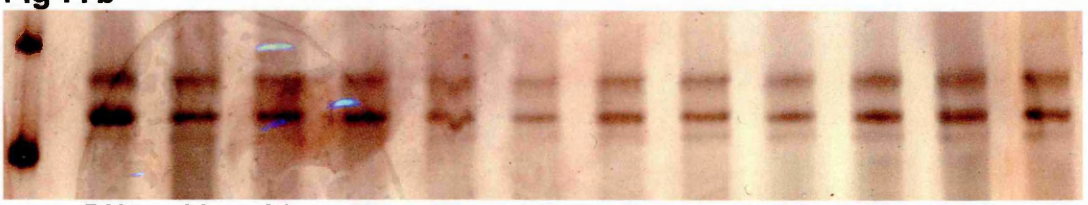

gDNA 20 21 27 28 48 49 81 82 83y 84 88

Fig 77c

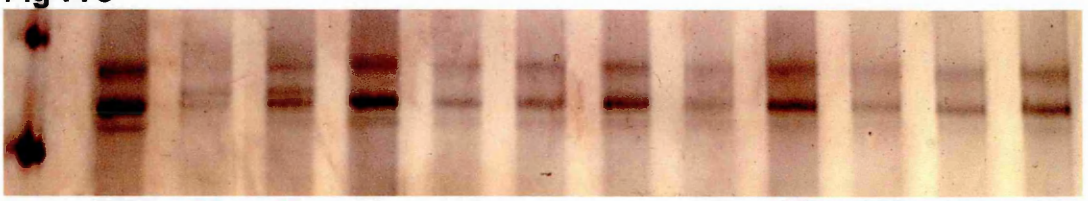

gDNA 89 90 92 112 113 114 135 137 138 151 152

Fig 77d

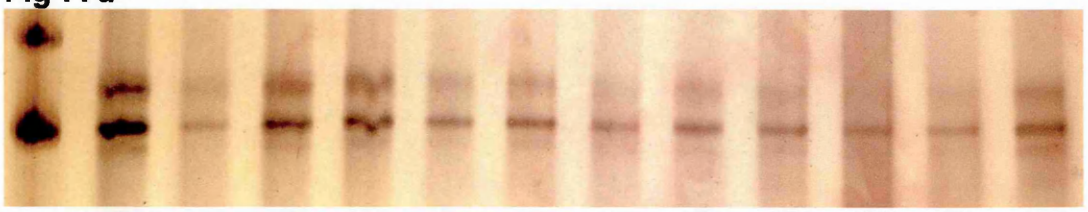

gDNA 153 159 160 161 162 168 169 174 175 176 177

Fig 77e

gDNA 167 171 172 179 180 185 186 188

Figure 77 a-e SSCP results for exon 8CD. Samples with bandshifts are numbered in red. Control gDNA is included with 100bp marker on each gel (lane 1).

Fig 77f

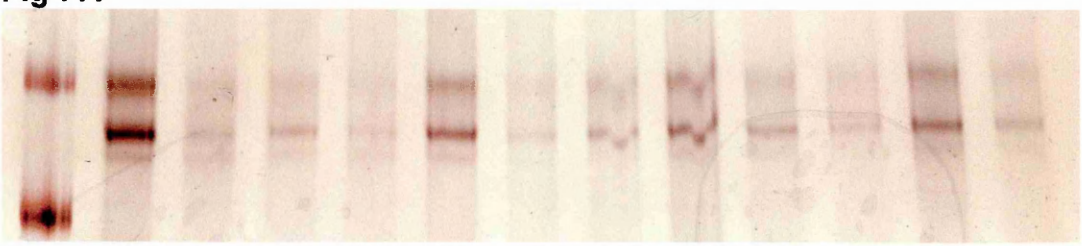

gDNA 189 190 192 193 194 195 196 202 52y 61x 61y

Fig 77g

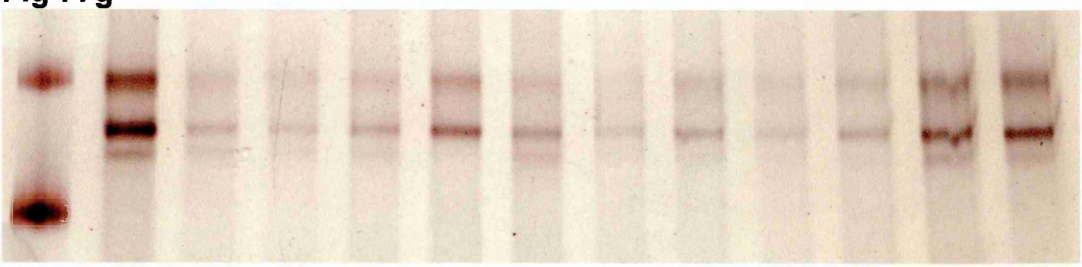

gDNA 67 68x 73 75 79 80 81 102 134 165 166

Figure 77 f-g SSCP results for exon 8CD. Samples with bandshifts are numbered in red. Control gDNA is included with 100bp marker on each gel (lane 1).

Table 22 Bandshift Summary Exon 8CD			
Sample	ID	Tissue	Histology
89	98/4189 2d	Endometrium	AdCa 2
90	98/4189 2c	Endometrium	AdCa 2 & AH

Table 22 Bandshift Summary for Exon 8 CD showing samples in which aberrant bands were detected. Where available, tissue and histological description are included. **AH:** atypical hyperplasia, **AdCa (x):** adenocarcinoma (grade).

Exon 8 Summary

Exon 8AB generated very good SSCP gels with clean, well-separated bands and very little background (Figures 76a-o). Sequences for patient samples sent for contained many ambiguous bases (data not shown) and were difficult to interpret. SSCP for exon 8CD fragments demonstrated much lower separation than for 8AB, and altering the gel composition had little effect in improving this (data not shown). Again, sequencing of patient samples 89 and 90 in which aberrant bands were detected contained many ambiguous bases (data not shown).

Figures for the incidence of bandshifts in exon 8 were as follows. For exon 8AB, 21% (9/43) of patients demonstrated bandshifts from a corresponding total of 12% (16/127) of all samples. For exon 8CD, 2% (1/43) of patients demonstrated bandshifts from a corresponding total of 2% (2/127) of all samples. The total bandshift detection rate for exon 8 was 23% (10/43) of patients, from 14% (18/127) of the samples used.

3.3.3.5 Patients with multiple bandshifts

Eight samples corresponding to five patients displaying bandshifts in more than one exon are shown in Table 23. Six samples carry an exon 5 AB or 8AB bandshift, with 4 samples carrying changes in both of these exon portions. This may reflect the sensitivity of the SSCP technique for the different exon portions. It is interesting to note that 6 out of the 8 samples (75%) displaying aberrations in two exons are histologically advanced lesions (adenocarcinomas). The higher grade of the samples (2 and 3) denotes increasing depth of invasion into the tissue underlying the endometrium.

Table 23 Samples with Bandshifts in Multiple exons		
Sample	Histology	Exons
51	AH?	5AB & 8AB
61x*	IECa / Sev AH	5CD & 8AB
61y*	IECa / Sev AH	5CD & 8AB
83y†	AdCa2 + AH	5AB & 8AB
84†	Normal	5AB & 8AB
89§	AdCa2	5AB & 8CD
90§	AdCa2 + AH	5AB & 8CD
92	AdCa3	5AB + 8AB

Table 23 Samples displaying bandshifts in multiple exons, with histological descriptions. Symbols indicate samples belonging to the same patient. **AH:** atypical hyperplasia, **Sev AH:** severe atypical hyperplasia, **IECa**: intraepithelial carcinoma, **AdCa (x):** adenocarcinoma (grade), **?:** histological grouping unclear.

CHAPTER 4

DISCUSSION

4.1 Discussion of Results

Understanding the molecular mechanisms which underlie the initiation and progression of cancer is central to the development of novel therapeutic strategies. Since its discovery in 1997, the PTEN tumour suppressor has proven to be the first of an emerging species of lipid phosphatase involved in multiple cellular processes, which now includes SHIP and myotubularin phosphatase (Wishart & Dixon, 2002). The existence of PTEN and its several homologues, such as PTEN 2, TPTE and TPIP across the spectrum of eukaryotic organisms highlights the evolutionary importance of this enzyme. The central role of PTEN in the control of multiple signalling pathways, and its interaction with other cell-cycle proteins, have placed it amongst the hierarchy of tumour suppressor genes including pRb and p53. Recently, PTEN has proven to be much more that just a tumour suppressor by exhibiting a fundamental role in the development and organisation of tissues as diverse as neurones and immune cells.

Significantly, the high occurrence of PTEN mutation or loss of expression is a feature of certain cancers, including endometrial and prostate carcinomas, although the reasons for such tissue specificity are not yet fully understood. The exceptionally high incidence of PTEN aberrations in endometrial carcinomas (~80%) has provoked many studies, and unlike other somatic cancers, loss of PTEN is an early event in the development of EC. Clearly, PTEN has a fundamental role in endometrial pathology, and it is hoped that

by dissecting this role advances will eventually be made in the diagnosis and treatment of endometrial carcinoma.

The aims of this thesis were therefore to investigate the role of PTEN in endometrial carcinoma by three distinct approaches. These included analysis of the effect of TGF-β1 on PTEN expression in EC cell lines, cloning of human PTEN cDNA and assessing sub-cellular localisation of the protein under various conditions, and the detection of novel mutations in EC archival DNA.

The effect of TGF-β1 on PTEN expression in EC cell lines

TGF-β1 has previously been shown to both up- and down-regulate PTEN mRNA or protein levels in various cell lines, in a manner which may indicate cell-line specificity, but this has not been previously reported in cells of endometrial origin. Compounds which up-regulate PTEN may represent future anti-cancer therapies, and therefore merit investigation.

For this study, cell lines were chosen which expressed wild-type (HEC-1B) or mutant (Ishikawa) PTEN protein. This permitted the study of the effects of the cytokine on growth and cellular morphology in the presence or absence of endogenous PTEN protein, in addition to modulation of PTEN mRNA and protein levels.

The results presented in Chapter 3, Section 1 indicated a modest up-regulation of PTEN mRNA expression in both HEC-1B and Ishikawa cell lines in response to TGF-β1. Similar results have been reported by Lee, et al (1999) in the human monocytic leukaemia cell line U937, but this group did not describe a possible pathway for the data described. Serum deprivation

also appeared to have a small up-regulatory effect on PTEN mRNA expression. This could be accounted for by the lack of growth factors, which when present in the medium could suppress PTEN protein function, and possibly mRNA expression. Functionality of the TGF-β1 receptor signalling to Smads in HEC-1B and ISK cell lines was confirmed by the time and dose-dependant up-regulation of the classically TGF-β1-responsive gene PAI-1. Additionally, the effects of high cell density on increasing PTEN mRNA expression were ruled out, as plating HEC-1B cells at high density displayed no difference in PTEN expression to cells grown at a lower density (Chapter 3.1.5)

Analysis of PTEN and P-PTEN protein levels indicated very little change from the controls which were not stimulated with cytokine. This suggests that the effects of TGF-β1 occurred mainly at the transcriptional level, or that the protein analysis methods used were not sensitive enough to detect subtle post-translational changes. It remains unclear, however, which of the three putative PTEN phosphorylation sites in the C-terminus (Ser380 and Thr382/383) are phosphorylated under differing cellular conditions. At the time that the work described here was performed, only an anti-P-PTEN (Ser380) antibody was commercially available. The use of a new anti-P-PTEN antibody (CST, UK), which detects phosphorylation of all three C-terminal sites (Ser380 and Thr382/383), may increase the sensitivity of the Western blot for P-PTEN.

Effects of TGF-β1 on endometrial cell morphology agree with published data (Boyd & Kaufman, 1990 & Anzai, et al 1992) in that the cytokine increases cell volume and/or decreases proliferation of the HEC-1B and ISK cell lines.

The mechanisms underlying the regulatory effects of TGF-β1 on PTEN are yet to be described. TGF-β1 may exert growth suppression on these cell lines via several mechanisms described in Chapter 1. These may include cell cycle restriction via the transcription factor Sp1 which increases expression of the cyclin inhibitor $p15^{INK}$, increased FOXO activity, or by inhibition of c-myc. The presence of a Sp1 consensus site in the promoter region of PTEN has been noted by Sheng, et al (2002), and this may represent a pathway of transcriptional modulation by TGF-β1.

Cloning of Human Full-Length PTEN and localisation of Transfected PTEN protein in Endometrial cell lines.

PTEN has been described as a cytoplasmic protein in the majority of cell lines and tissues, which would appear to correlate with a lack of nuclear location signal (NLS). However, nuclear PTEN has been reported in a number of studies and it is likely that other proteins are involved in its transport both to the nucleus and to various cellular compartments.

Other phosphatases have been observed to be shuttled between the nucleus and cytoplasm in synchrony with the cell cycle, including CDC25B (Davezac, et al 2000) and CDC14 (Li, et al 1997b). The discovery of a nuclear $PI3,4,5P_3$ cycle, which is still poorly understood, supports the theory that PTEN may have a role in the nucleus (Lachyankar, et al 2000). The extent to which nuclear PTEN responds to modulation by external stimuli, such as growth factors and hormones, is also not fully understood.

The results of transfection of pRC-2 into HEC-1B and Ishikawa cell lines are partially consistent with a recently published report by Ginn-Pease & Eng

(2003). This group used full-length PTEN cloned into both a vector without a fluorescent tag and also into the pEGFP-C1 vector, to transiently transfect the MCF-7 breast cancer cell line. The paper reported accumulation of transfected PTEN around the nuclear membrane and in the general location of the nucleus, which increased at G_0 -G_1 and decreased during S-phase. Co-localisation of PTEN with the nuclear protein CDK2 during G1 was also observed. Additionally, the presence of PTEN in the nucleus was confirmed by Western blot of nuclear and cytoplasmic extracts prepared from the transfected cells. The presence of the N-terminal EGFP moiety did not reportedly affect PTEN entry into the nucleus or the cell cycle. The results shown in Chapter 3, Section 2 are strikingly similar to those of Ginn-Pease & Eng (2003) in that strong staining in the perinuclear and nuclear regions, but also ubiquitous cytoplasmic localisation, were observed in the endometrial cell lines. Some vault proteins can accumulate at the nuclear membrane adjacent to nuclear pores, and as PTEN can bind the major vault protein via its C2 domain (Yu, et al 2002) this may be a mechanism of transport into the nucleus. Other proteins, such as β-catenin, may bind directly to the nuclear pore to mediate their own transport, but in this case the mechanism is unknown (Suh & Gumbiner, 2003).

A further possibility proposed by Ginn-Pease and Eng is that PTEN may have a more rare form of NLS called a nuclear-cytoplasmic shuttling sequence, or a bipartite NLS. Such bipartite sequences have previously been reported in p53 (Liang & Clarke, 1999), and the CDK inhibitor $p27^{KIP1}$ has been shown to require an interaction with Jab1/CSN5 for CRM1-mediated nuclear export (Tomoda, et al 2002).

A lack of detectable change in subcellular localisation of PTEN encoded by pRC-2 in endometrial cell lines in response to stimulation by oestrogen and TGF-β1 was observed (Chapter 3, Section 2). With respect to oestrogen, Mutter, et al (2000) has described ubiquitous expression of PTEN in both the nucleus and cytoplasm of oestrogen-exposed dividing endometrial glandular and stromal cells. A further study by Guzeloglu-Kayisli, et al (2003) demonstrated a rapid and short-lived increase in total PTEN and nuclear P-PTEN in endometrial cells in response to oestrogen. This increase declined after 15 minutes and was absent in cells treated over longer periods (3 to 24 hours), suggesting that any increase in PTEN is extremely rapid and transitory. As the unstimulated distribution of PTEN-EGFP was observed to be both perinuclear/nuclear and cytoplasmic, oestrogen may not affect localisation of PTEN under the experimental conditions used. Cells stimulated with TGF-β1 also demonstrated no change in exogenous PTEN localisation, suggesting that with consideration to the lack of endogenous PTEN increase shown by Western blot in Chapter 3, the cytokine does not modify levels of the protein.

Co-localisation of PTEN in endometrial cell lines with markers for the ER and Golgi shown in Chapter 3, Section 2 has not previously been described. Localisation of the murine testis-specific homologue of PTEN, called PTEN-2, to the golgi in transfected COS-7 cells has been demonstrated by Wu, et al (2001), who cloned PTEN-2 into pEGFP-N3. This localisation was shown to require the N-terminal domain of PTEN-2 containing four potential transmembrane domains, which may play a role in vesicular trafficking through the golgi network.

In the HEC-1B and ISK cell lines used in this study, very little co-localisation was observed between the golgi protein mannosidase II and PTEN. Although detection of the golgi with the non-commercial polyclonal antibody did not appear to be very specific, it is more likely that PTEN simply does not associate with the golgi in the same manner as testis-specific PTEN-2. Co-localisation of PTEN with the endoplasmic reticulum resident chaperone protein colligin (Hsp47) was detected in both endometrial cell lines as illustrated in Chapter 3, Section 2. As the ER is continuous with the outer nuclear membrane, it is possible that PTEN localises with colligin if it has been localised to the perinuclear region perhaps via one of the theoretical mechanisms previously described.

Recently, PTEN has been detected in lipid rafts within intestinal cells, which may affect PTEN-mediated attenuation of PI3K by specific localisation of the protein (Li, et al 2004). Lipid rafts and their stabilising caveolin proteins, are distinct micromembrane domains which have been implicated in signal transduction and can associate with many transduction elements, including receptor tyrosine kinases, PKC, G-proteins and Ras-MAPK components (Pike, L. J., 2003 & Smart, et al 1999). PTEN and other protein tyrosine phosphatases have previously been shown to form complexes with caveolin-1, which may regulate the function of these proteins (Caselli, et al 2002).

Mutation Analysis of PTEN Exons 5 & 8 in Archival Endometrial DNA by SSCP

A large variety of PTEN mutations have now been described in EC and other cancers. The SSCP technique used in this thesis was based on previous

reports (Rhei, et al 1997, Aveyard, et al 1999 & Cinti, et al 2000) in which a commercial mutation detection gel solution and silver staining kit were used to give superior separation and detection of bands. The results of SSCP analysis shown in Chapter 3, Section 3 indicate that excellent separation and staining was achieved for all samples with the exception of exon 8CD PCR products. From the total of total of 43 patients, 27 (63%) were found to have at least one sample containing a bandshift. This figure is in agreement with the published PTEN mutation rate in EC of 20-85%, which includes the earliest hyperplasias to the highest grade adenocarcinomas.

The SSCP technique, whilst being relatively simple, rapid, and up to 95% effective for some genes, is also extremely sensitive to changes in temperature and primer concentration (Hennessy, Teare & Ko, 1998). The latter of these variables may account in part for the poor separation of 8CD products. As stated in Chapter 3, sequencing data was difficult to obtain for the great majority of samples exhibiting bandshifts. The quality of DNA derived from archival material is notoriously fragile, and can generate not only low yields of PCR product but also reduce the specificity of the reaction and lead to spurious amplification. This is the main reason why archival DNA is not commonly used in such studies, where fresh tissue is preferred.

The PCR products for all samples appeared to consist of a single clean band, but insufficient PCR product was problematic in some samples, particularly in exon 5AB. Although non-specific amplicons were visually undetectable on the agarose gel, the presence of very small amounts of extraneous PCR product could be a cause for interference in sequencing as the technique is very sensitive to contamination.

A further explanation for the sequencing difficulties encountered is that more than one cell type was present in the tissue samples when DNA was extracted. Potentially, strands of DNA with slightly different sequences could therefore have been present in the samples prior to PCR, causing multiple amplicons of the same apparent size to be generated. As the tissue handling and DNA extraction were performed by our collaborators, this element of the study was essentially beyond my control.

Despite the associated technical hurdles, SSCP is still being used to effectively detect PTEN mutations and thereby increase our understanding of this gene in disease. One recent study has discovered three polymorphisms in PTEN from Japanese patients with type-2 diabetes, these being c.-9C→G in the 5' UTR of exon 1, IVS5-11T→G in intron 4 and c.859T→C in exon 8 (Ishihara, et al (2003). The most common polymorphism in the 5' UTR of exon 1 was shown to cause increased PTEN expression when cloned and expressed in two cell lines. Exposure of the transfected cells to insulin showed a significant reduction in P-Akt/PKB compared to a control of wild-type PTEN, and this polymorphism may therefore contribute to insulin resistance in type-2 diabetes in this population.

4.2 Future Work

Although several compounds have been shown to positively affect PTEN mRNA expression including progesterone, TGF-β1, and NGF, or protein levels, (vitamin D3 analogues, BDNF and BMP), few studies have proposed mechanisms which may underlie these observations. Additionally, few groups have analysed both mRNA and protein expression of PTEN in response to stimulation. It is not clear, therefore, how many studies in which increased PTEN mRNA was detected would also demonstrate a change in protein levels. As the regulation of PTEN may involve both transcriptional and post-translational events which may be further complicated by cell-type specificity, it is worthwhile investigating both levels of response for a complete picture. The fundamental question still remains as to how constitutive expression of PTEN is maintained, and how the compounds mentioned above actually affect changes in mRNA expression.

Recently, a study by Han, et al 2003 on mouse PTEN revealed a strong promoter in the 5' UTR at -551 to -220 upstream of the translation start codon. This promoter drives the production of an mRNA transcript with a shorter 5' UTR which was translated at 100-fold higher efficiency that the full-length 5' UTR transcript. The group also demonstrated constitutive activation of the promoter via Sp1. It would be of interest to determine whether this is also the case for the constitutive expression of human PTEN. For this purpose, the entire human 5'UTR upstream of exon 1 would be cloned into a reporter vector containing the luciferase gene, such as pGL-2-Basic (Promega). A range of clones with successively smaller portions of 5'UTR would also be created, and the clones transfected into a suitable mammalian

cell line. Degree of promoter activity would be assessed after 24-48 hours by fluorescence of cell extracts in the luciferase assay, in which luciferin is added to the extracts and light levels determined by scintillation counter. To assess the ability of Sp1 to initiate transcription, the transcription factor would be cloned into a Drosophila expression vector containing a strong promoter, such as pAC5.1 (Invitrogen) which is driven by the actin 5C promoter. Co-transfection of the Sp1 and PTEN 5'UTR clones into Drosophila SL2 cells (which contain no Sp factors) followed by the luciferase assay would be used to determine the degree of promoter activity in each PTEN clone. Clones exhibiting significantly higher levels of promoter activity would then be sequenced to determine whether one or more transcripts are present. As TGF-β1 may affect PTEN transcription via Sp1, it would be interesting to stimulate co-transfected cells with the cytokine to ascertain whether treatment enhances promoter activity.

To further investigate the presence of nuclear PTEN in endometrial cell lines, the following approach could be taken. Firstly, transfected cells would be imaged using a confocal microscope with the ability to scan and create 3-D images to more accurately assess the location of PTEN-EGFP. Secondly, nuclear and cytoplasmic protein extracts would be prepared from transfected cells using a commercially available kit such as NE-PER (Pierce-Endogen). The two fractions would be used in Western blot and probed with an anti-PTEN antibody, with anti-β-actin as a control to demonstrate the purity of the nuclear fraction. As a lack of nuclear PTEN has been associated with some high-grade tumours, a cell line in which nuclear PTEN has been reported, such as MCF-7 breast cancer cells, would be used as a control.

REFERENCES

Abate-Shen, C. et al (2003) Nkx3.1; Pten mutant mice develop invasive prostate adenocarcinoma and lymph node metastases. *Cancer Res.* **63**, 3886-3890.

Abbott, R. T., et al (2003) Analysis of the PI-3-Kinase-PTEN-AKT pathway in human lymphoma and leukemia using a cell line microarray. *Mod Pathol.* **16**, 607-612.

Abe, T., et al (2003) PTEN decreases in vivo vascularisation of experimental gliomas in spite of proangiogenic stimuli. *Cancer Res.* **63**, 2300-2305.

Abraham, R. T., (2002) Identification of TOR Signalling Complexes: More TORC for the Cell Growth Engine. *Cell* **111**, 9-12.

Adey, et al, (2000) Threonine phosphorylation of the MMAC1/PTEN PDZ binding domain both inhibits and stimulates PDZ binding. *Cancer Res.* **60**, 35-37.

Aggerholm, A., et al (2000) Mutational analysis of the tumour suppressor gene MMAC1/PTEN in malignant myeloid disorders. *Eur. J. Haematol.* 65, 109-113.

Ahmed, S. F., et al (1999) Balanced translocation of 10q and13q, including the PTEN gene, in a boy with a human chorionic gonadotropin-secreting tumor and the Bannayan-Riley-Ruvalcaba syndrome. *J. Clin. Endocrinol. Metab.* **84**, 4665-4670.

Ahmad, F., et al (2000) Cyclic nucleotide phosphodiesterase 3B is a downstream target of protein kinase B and may be involved in regulation of effects of protein kinase B on thymidine incorporation in FDCP2 cells. *J. Immunol.* **164**, 4678-4688

Alessi, D. R., et al (1996a) Mechanism of activation of protein kinase B by insulin and IGF-1. *EMBO J.* **15**, 6541-6551.

Alessi, D. R., et al (1996b) Molecular basis for the substrate specificity of protein kinase B: comparison with MAPKAP kinase-1 and p70 S6 kinase. *FEBS Lett.* **399**, 333-338.

Alnemi, E. S. (1999) Hidden powers of the mitochondria. *Nat. Cell Biol.* **E40-E42.**

Altiok, S., et al (1999) Heregulin induces phosphorylation of BRCA1 trough phosphatidylinositol 3-kinase/AKT in breast cancer cells. *J. Biol. Chem.* **274,** 32274-32278.

Anzai, Y., et al (1992) Effects of transforming growth factors and regulation of their mRNA levels in two human endometrial adenocarcinoma cell lines. *J. Steroid. Biochem. Mol Biol.* **42**, 449-455.

Anzelon, A. N., Wu, H. & Rickert, R. C. (2003) Pten inactivation alters peripheral B lymphocyte fate and reconstitutes CD19 function. *Nat. Immunol.* **4**, 287-294.

Arcaro, A., et al (2002) Two distinct phosphoinositide 3-kinases mediate polypeptide growth factor-stimulated PKB activation. *EMBO J.* **21**, 5097-5108).

Attisano, L. & Lee-Hoeflich, S. T. (2001) The Smads. *Genome Biol.* **2**, 3010.1-3010.8.

Attwell, S., et al (2003) Integration of cell attachment, cytoskeletal localization and signalling by integrin-linked kiase (ILK), CH-ILKBP, and the tumor suppressor PTEN. *Mol. Biol. Cell.* **14**, 4813-4825.

Audo, I., et al (2003). Vitamin D analogues increase p53, p21, and apoptosis in a xenograft model of human retinoblastoma. *Invest. Ophthalmol. Vis. Sci.* **44**, 4192-4199.

Aveyard, J. S., et al (1999) Somatic mutation of PTEN in bladder carcinoma. *Br. J. Cancer.* **80**, 904-908.

Baca M. (2003) Analysis of SH2 ligands and identification of sites of interaction. *Methods Mol Biol.* **249**, 111-20.

Backlund, L. M., et al (2003) Short postoperative survival for glioblastoma patients with a dysfunctional Rb1 pathway in combination with no wild-type PTEN. *Clin. Cancer Res.* **9,** 4151-4158.

Bae, S. K., et al (1999) Egr-1 mediates transcriptional activation of IGF-II gene in response to hypoxia. *Cancer Res.* 59, 5989-5994.

Baeza, N., et al (2003) PTEN methylation and expression in glioblastomas. *Acta Neuropathol.* **106**, 479-485.

Bakin, A. V. et al (2000) Phosphatidylinositol 3-kinase function is required for transforming growth factor beta-mediated epithelial to mesenchymal transition and cell migration. *J. Biol. Chem.* **275**, 36803-36810.

Baldwin, R. L., et al (2000) BRCA1 promoter region hypermethylation in ovarian carcinoma: a population-based study. *Cancer Res.* **60**, 5329-33.

Balendran, A., et al (1999a) PDK1 acquires PDK2 activity in the presence of a synthetic peptide derived from the carboxyl terminus of PRK2. *Curr. Biol.* **9**, 393-404.

Balendran, A., et al (1999b) Evidence that PDK-1 mediates the phosphorylation of p70 S6 kinase in vivo at Thr412 as well as Thr252 *J. Biol. Chem.* **274**, 37400-37406.

Banerjee, P. & Chatterjee, M. (2003) Antiproliferative role of vitamin D and its analogs--a brief overview. *Mol. Cell Biochem.* **253**, 247-254.

Barthel, A., et al (1999) Regulation of *GLUT1* gene transcription by the serine/threonine kinase Akt1. J. Biol. Chem. **274** 20281020286.

Beppu, T., et al (1994) Identification of S-phase cells with PC10 antibody to proliferating cell nuclear antigen (PCNA) by flow cytometric analysis. *J. Histochem. Cytochem.* **42**, 1177-1182.

Bhat, N. R., Shen, Q. & Fan. F. (2003) TAK1-mediated induction of nitric oxide synthase gene expression in glial cells. *J. Neurochem.* **87**, 238-247.

Bhowmick, N. A. et al (2003) TGF-{beta}-induced RhoA and p160ROCK activation is involved in the inhibition of Cdc25A with resultant cell-cycle arrest. *PNAS* Dec 1 **[Epub ahead of print]**

Biggs, III, W. H., et al (1999) Protein kinase B/Akt-mediated phosphorylation promotes nuclear exclusion of the winged helix transcription factor FKHR. Proc. Natl. Acad. Sci. **96**, 7421-7426.

Bilkay, U., et al (2003) Proteus syndrome. *Scand. J. Plast. Reconstr. Surg. Hand. Surg.* **37**, 307-310.

Birck, A., et al (2000) Mutation and allelic loss of the PTEN/MMAC1 gene in primary and metastatic melanoma biopsies. *J. Invest. Dermatol.* **114**, 277-280.

Birkenkamp, K. U. & Coffer, P. J., (2003) FOXO transcription factors as regulators of immune homeostasis: molecules to die for? *J. Immunol.* **171**, 1623-1629.

Bonneau, D. & Longy, M. (2000) Mutations of the human PTEN gene. *Hum Mutat.* 16, 109-122.

Bose, S., et al (1998) Allelic loss of chromosome 10q23 is associated with tumor progression in breast carcinomas. *Oncogene*. **17**, 123-127.

Bose, S., et al (2002) Reduced expression of PTEN correlates with breast cancer progression. *Hum. Pathol.* 33, 405-409.

Boyd, J. A. & Kaufman, D. G. (1990) Expression of transforming growth factor beta 1 by human endometrial carcinoma cell lines: inverse correlation with effects on growth rate and morphology. *Cancer Res.* **50**, 3394-3399.

Brennan, P., et al (1999) $p70^{s6k}$ integrates phosphatidylinositol 3-kinase and rapamycin-regulated signals for E2F regulation in T lymphocytes. *Mol. Cell Biol.* **19**, 4729-4738.

Brown, K. S., et al (2004) FcγRIIb-mediated negative regulation of BCR signalling is associated with the recruitment of the MAPkinase-phosphatase, pac-1, and the 3'-inositol phosphatase, PTEN. *Cell. Signal.* **16**, 71-80.

Brunelle, J. K., et al (2003) c-Myc sensitization to oxygen deprivation induced cell death is dependent on Bax/Bak but independent of p53 and HIF-1.*J. Biol. Chem.* Nov 19 **[Epub ahead of print]**

Brunet, A., et al (1999) Akt promotes cell survival by phosphorylating and inhibiting a Forkhead transcription factor. *Cell*, **96**, 857-868.

Buchholz, T. A. & Wazer, D. E. (2002) Molecular biology and genetics of breast cancer development: a clinical perspective. *Semin. Radiat. Oncol.* **12**, 285-295.

Burgering, B. M. & Medema, R. H. (2003) Decisions on life and death: FOXO Forkhead transcription factors are in command when PKB/Akt is off duty. *J. Leukoc. Biol.* **73**, 689-701.

Caffrey, J. J. et al (2001) Expanding coincident signalling by PTEN through its inositol 1,3,4,5,6-pentakisphosphate 3-phosphatase activity. *FEBS Letts.* **499**, 6-10.

Cai, J., et al (2003) Activation of Vascular Endothelial Growth Factor Receptor-1 Sustains Angiogenesis and Bcl-2 Expression Via the Phosphatidylinositol 3-Kinase Pathway in Endothelial Cells. *Diabetes.* **52**, 2959-2968.

Campbell, R. A., et al (2001) Phosphatidylinositol 3-kinase/AKT-mediated activation of estrogen receptor alpha: a new model for anti-estrogen resistance. *J. Biol. Chem.* **276**, 9817-9824.

Campbell, R. B., et al (2003) Allosteric activation of PTEN phosphatase by phosphatidylinositol 4,5-bisphosphate. *J. Biol. Chem.* **278**, 33617-33620.

Cantley, L. C., & Neel, B. G., (1999) New insights into tumor suppression: PTEN suppresses tumor formation by restraining the phosphoinositide 3-kinase / AKT pathway. *PNAS* **96**, 4240-4245.

Cappellini, A., et al (2003) The Phosphoinositide 3-kinase/Akt pathway regulates cell cycle progression of HL60 human leukaemia cells through cytoplasmic relocation of the cyclin-dependant kinase inhibitor p27(Kip1) and control of cyclin D1 expression. *Leukemia*, **11**, 2157-2167.

Cardone, M. H., et al, (1998) Regulation of cell death protease caspase-9 by phosphorylation. *Science* **282**, 1318-1321.

Carpenter, C. L. & Cantley, L. C. (1996) Phosphoinositide kinases. *Curr. Opin. Cell Biol.* **8**, 153-158.

Carroll, B. T., et al (1999) Polymorphisms in PTEN in breast cancer families. *J. Med. Genet.* **36**, 94-96.

Casamassima, A & Rozengurt, E. (1998) Insulin-like growth factor I stimulates tyrosine phosphorylation of p130(Cas), focal adhesion kinase, and paxillin. Role of phosphatidylinositol 3'-kinase and formation of a p130(Cas).Crk complex. *J. Biol. Chem.* **273**, 26149-26156.

Caselli, A., et al (2002) Some protein tyrosine phosphatases target in part to lipid rafts and interact with caveolin-1. *Biochem. Biophys. Res. Commun.* **296**, 692-697.

Chen, C. R. et al (2002) E2F4/5 and p107 as Smad cofactors linking the TGFbeta receptor to c-myc repression. *Cell.* **110**, 19-32.

Chen, H., et al (1999) A testis-specific gene, TPTE, encodes a putative transmembrane tyrosine phosphatase and maps to the pericentromeric region of human chromosomes 21 and 13, and to chromosomes 15, 22, and Y. *Hum. Genet.* **105**, 399-409.

Chen, F. et al (2003a) Phosphorylation of PPARgamma via active ERK1/2 leads to its physical association with p65 and inhibition of NF-kappabeta. *J. Cell Biochem.* **90**, 732-744.

Chen, T. C., et al (2003b) Evaluation of vitamin D analogs as therapeutic agents for prostate cancer. *Recent Results Cancer Res.* **164**, 273-288.

Cheng, J. Q., et al (1992) AKT2, a putative oncogene encoding a member of a subfamily of protein-serine/threonine kinases, is amplified in human ovarian carcinomas. *Proc. Natl. Acad. Sci.* U.S.A. **89**, 9267-9271.

Cheng, J. Q., et al (1996) Amplification of *AKT2* in human pancreatic cells and inhibition of AKT2 expression and tumorigenicity by antisense RNA. *Proc.Natl. Acad. Sci.* U.S.A. **93**, 3636-3641.

Cheney, I. W., et al (1998) Suppression of tumorigenicity of glioblastoma cells by adenovirus-mediated MMAC1/PTEN gene transfer. *Cancer Res.* **58**, 2331-2334.

Cheney, I. W., et al (1999) Adenovirus-mediated gene transfer of MMAC1/PTEN to glioblastoma cells inhibits S phase entry by the recruitment of $p27^{Kip1}$ into cyclin E/CDK2 complexes. *Cancer Res.* **59**, 2318-2323.

Cheong, J-W., et al (2003) Phosphatase and tensin homologue phosphorylation in the C-terminal regulatory domain is frequently observed in acute myeloid leukaemia and associated with poor clinical outcome. *Br. J. Haematol.* **122**, 454-456.

Cheong, J. W., et al (2003a) Phosphatase and tensin homologue phosphorylation in the C-terminal regulatory domain is frequently observed in acute myeloid leukaemia and associated with poor clinical outcome. *Br. J. Haematol.* **122**, 454-456.

Cheong, J. W., et al (2003b) Constitutive phosphorylation of FKHR transcription factor as a prognostic variable in acute myeloid leukemia. *Leuk Res.* **27**, 1159-1162.

Ciechomska, I., et al 2003 Inhibition of Akt kinase signalling and activation of Forkhead are indispensable for upregulation of FasL expression in apoptosis of glioma cells. *Oncogene*, **22 (48)**, 7617-7627.

Cinti, C. et al (2000) Genetic alterations of the retinoblastoma-related gene RB2/p130 identify different pathogenetic mechanisms in and among Burkitt's lymphoma subtypes. *Am. J. Pathol.* **156**, 751-760.

Cohen, G. B., Ren, R., & Baltimore, D. (1995) Modular binding domains in signal transduction proteins. *Cell* **80**, 237-248.

Comer, F. I. & Parent, C. A. (2002) PI 3-kinases and PTEN: how opposites chemoattract. *Cell* **109**, 541-544.

Crescenzi, E., et al (2000) Differential expression of antiapoptotic genes in human endometrial carcinoma: bcl-XL succeeds bcl-2 function in neoplastic cells. *Gynecol. Oncol.* **77**, 419 (doi: 10.1006/gyno.2000.5803).

Crescenzi, E. & Palumbo, G. (2001) Bcl-2 exerts a pRb-mediated cell cycle inhibitory function in HEC-1B endometrial carcinoma cells. *Gynecol. Oncol.* **81**, 184-192.

Cuevas, B., et al (1999) SHP-1 regulates Lck-*induced phosphatidylinositol 3-kinase phosphorylation and activity. J.* Biol. Chem. **274**, 27583-27589.

Dahia, P. L. M. et al (1998) A highly conserved processed PTEN pseudogene is located on chromosome 9p21. *Oncogene*, **16**, 2403-2406.

Dahia, P. L. et al (1999) PTEN is inversely correlated with the cell survival factor Akt/PKB and is inactivated via multiple mechanismsin haematological malignancies. *Hum Mol Genet.* **8**, 185-193.

Dahia, P. L. M. (2000) PTEN, a unique tumor suppressor gene. *Endocr. Relat. Cancer*, **7**, 115-129.

Datta, S. R., et al, (1997) Akt phosphorylation of BAD couples survival signals to the cell-intrinsic death machinery. *Cell* **91**, 231-241.

Davezac, N., et al (2000) Regulation of CDC25B phosphatases subcellular localization. *Oncogene.* **19**, 2179-2185.

Davies, M. A., et al (1998) Adenoviral transgene expression of MMAC/PTEN in human glioma cells inhibits Akt activation and induces anoikis. *Cancer Res.* **58**, 5285-5290.

Davies, M. A., et al (1999) Regulation of Akt/PKB activity, cellular growth, and apoptosis in prostate carcinoma cells by MMAC/PTEN. *Cancer Res.* **59**, 2551-2556.

Davies, M. P. A., et al (1999b) Mutation in the PTEN/MMAC1 gene in archival low grade and high grade gliomas. *Br. J. Cancer.* **79**, 1542-1548.

Deleris, P., et al (2003) SHIP-2 and PTEN are expressed and active in vascular smooth muscle cell nuclei, but only SHIP-2 is associated with nuclear speckles. *J. Biol. Chem.* **278**, 38884-38891.

Dent, P., et al (2003) MAPK pathways in radiation responses. *Oncogene.* **22(37)**, 5885-96.

Denu, J. M. & Dixon, J. E. (1995) A catalytic mechanism for the dual-specificity phosphatase. *PNAS* **92**, 5910-5914.

Deocampo, N. D., et al (2003) The role of PTEN in the progression and survival of prostate cancer. *Minerva Endocrinol.* **28**, 145-153.

Depowski, P. L., et al (2001) Loss of expression of the PTEN gene protein product is associated with poor outcome in breast cancer. *Mod. Pathol.* **14**, 672-676.

Dery, M. C., et al (2003) Regulation of Akt expression and phosphorylation by 17beta-estradiol in the rat uterus during estrous cycle. *Reprod. Biol. Endocrinol.* **1**, 47.

Derynck, R. & Zhang, Y. E. (2003) Smad-dependent and Smad-independent pathways in TGF-β family signalling. *Nature*, **425,** 577-584.

Di Christofano, A., et al (1998) Pten is essential for embryonic development and tumour suppression. *Nat. Genet.* **19**, 348-355.

Di Christofano, A., & Pandolfi, P. P., (2000) The multiple roles of PTEN in tumor suppression. *Cell* **100**, 387-390.

Diehl, J. A., et al (1998) Glycogen synthase kinase-3β regulates cyclin D1 proteolysis and subcellular localization. *Genes Dev.* **12**, 3499-3511.

Di Guglielmo, G. M., et al (2003) Distinct endocytic pathways regulate TGF-beta receptor signalling and turnover. *Nat. Cell Biol.* **5**, 410-421. Erratum in: *Nat. Cell Biol.* **5**, 680.

Dimmeler, S., et al (1999) Activation of nitric oxide synthase in endothelial cells by Akt-dependent phosphorylation. *Nature.* **399**, 601-605.

Dong, C. et al (2000) Microtubule binding to Smads may regulate TGFβ activity. *Mol. Cell* **5**, 27-34.

Dowdy, S. C., Mariana, A. & Janknecht, R. (2003) HER2/Neu- and TAK1-mediated up-regulation of the transforming growth factor beta inhibitor Smad7 via the ETS protein ER81. *J. Biol. Chem.* **278**, 44377-44384.

Downward, J (1998) Mechanisms and consequences of activation of protein kinase B/Akt. *Curr. Opin. Cell* Biol. **10**, 262-267.

Downward, J. (1999) How Bad phosphorylation is good for cell survival. *Nat. Cell Biol.* **E33-E35**.

Ebert, M. P., et al (2002) Reduced PTEN expression in the pancreas overexpressing transforming growth factor-beta 1. *Br. J. Cancer.* 86, 257-262.

Eckmann, L., et al (1997) D-myo-Inositol 1,4,5,6-tetrakisphosphate produced in human intestinal epithelial cells in response to Salmonella invasion inhibits phosphoinositide 3-kinase signaling pathways. *PNAS* **94**, 14456-14460.

Eng, C. (2003) PTEN: one gene, many syndromes. *Hum. Mutat.* **22**, 183-198

Evangelou, A., et al (2000) Down-regulation of transforming growth factor beta receptors by androgen in ovarian cancer cells. *Cancer Res.* **60**, 929-935.

Farrow, B. & Evers, B. M. (2003) Activation of PPARgamma increases PTEN expression in pancreatic cancer cells. *Biochem. Biophys. Res. Commun.* **301**, 50-53.

Feng, X.H, Lin. X, & Derynck. R. (2000) Smad2, Smad3 and Smad4 cooperate with Sp1 to induce p15 (Ink4B) transcription in response to TGF-beta. *EMBO J.* **19**, 5178-93.

Fernandez, M. & Eng, C. (2002) The expanding role of PTEN in neoplasia: A moleculae for all seasons? *Clin. Cancer Res.* **8**, 1695-1698.

Figueroa, C & Vojtek, A. B. (2003) Akt negatively regulates translation of the ternary complex factor Elk-1. *Oncogene*, **22**, 5554-5561.

Fisslthaler, B., et al (2003) Insulin enhances the expression of the endothelial nitric oxide synthase in native endothelial cells: a dual role for Akt and AP-1. *Nitric Oxide*, **8**, 253-261.

Flanagan, L., et al (2003) Efficacy of Vitamin D compounds to modulate estrogen receptor negative breast cancer growth and invasion. *J. Steroid. Biochem. Mol. Biol.* **84**, 181-192.

Flint, A. J., Tiganis, T., Barford, T. & Tonks, N. K. (1997) Development of "substrate-trapping" mutants to identify physiological substrates of protein tyrosine phosphatases. *Natl. Acad. Sci.* **94**, 1680-1685.

Foster, B. A., et al (1999) Pharmacological rescue of mutant p53 conformation and function. *Science* **286**, 2507-2510.

Frasor, J., et al (2003) Profiling of estrogen up- and down-regulated gene expression in human breast cancer cells: insights into gene networks and pathways underlying estrogenic control of proliferation and cell phenotype. *Endocrinology*. **144**, 4562-74.

Freeburn, R. W., et al (2002) Evidence that SHIP-1 contributes to phosphatidylinositol 3,4,5-trisphosphate metabolism in T lymphocytes and can regulate novel phosphoinositide 3-kinase effectors. *J. Immunol.* **169**, 5441-5450.

Freedman, D. A. & Levine, A. J. (1998) Nuclear export is required for degradation of endogenous p53 by MDM2 and human papillomavirus E6. *Mol. Cell. Biol.* **18**, 7288-7293.

Friedenauer, D., & Berlet, H. H., (1989) Sensitivity and variability of the Bradford protein assay in the presence of detergents. *Anal. Biochem.* **178**, 263-268.

Frisk, T., et al (2002) Silencing of the PTEN tumor-suppressor gene in anaplastic thyroid cancer. *Genes Chromosomes Cancer.* **35**, 74-80.

Fruman, D. A., Meyers, R. E. & Cantley, L. C. (1998) Phosphoinositide kinases. *Annu. Rev. Biochem.* **67**, 481-507.

Fujii, G. H. et al (1999) Transcriptional analysis of the PTEN/MMAC1 pseudogene, ψPTEN. *Oncogene* **18**, 1765-1769.

Fujimoto, J., et al (1996) Sex steroids regulate the expression of plasminogen activator inhibitor-1 (PAI-1) and its mRNA in uterine endometrial cancer cell line Ishikawa. *J. Steroid. Biochem.* **59**, 1-8.

Fujita, E. J., et al (1999) Akt phosphorylation site found in human caspase-9 is absent in mouse caspsae-9. *Biochem. Biophys. Res. Commun.* **264**, 550-555.

Fujita, N., Sato, S. & Tsururo, T. (2003) Phosphorylation pf $p27^{Kip1}$ at threonine 198 by p90 ribosomal protein S6 kinases (RSKs) promotes its binding to 14-3-3 and cytoplasmic localisation. *J. Biol. Chem.* **278**, 49254-49260.

Fukuchi, T., et al (1998) β-Catenin mutation in carcinoma of the uterine endometrium. *Cancer Res.* **58**, 3526-3528.

Furnari, F. B., Huang, H.-J. S., & Cavenee, W. K. (1998) The phosphoinositol phosphatase activity of PTEN mediates a serum-sensitive G1 growth arrest in glioma cells. *Cancer Res.* **58**, 5002-5008.

Gagnon, V., et al (2003) Akt activity in endometrial cancer cells: regulation of cell survival through cIAP-1. *Int. J. Oncol.* **23**, 803-810.

Gao, X., Neufeld, T. P., & Pan, D (2000) Drosophila PTEN regulates cell growth and proliferation through PI3K-dependent and -independent pathways. *Dev. Biol.* **221**,404-418.

Gao, N., et al (2003) Role of PI3K/AKT/mTOR signalling in the cell cycle progression of human prostate cancer. *Biochem. Biophys. Res. Comm.* **310**, 1124-1132.

Gao, Q. L., et al (2003b) PTEN coding product: a marker for tumorigenesis and progression of endometrial carcinoma] *Ai. Zheng.* **22**, 640-644.

Georgescu, M. M. et al, (1999) The tumor-suppressor activity of PTEN is regulated by its carboxyl-terminal region. *PNAS* **96**, 10182-7.

Georgescu, M. M,. (2000) Stabilization and productive positioning roles of the C2 domain of PTEN tumor suppressor. *Cancer Res.* **60**, 7033-7038.

Gera, J. F. (2003) AKT activity determines sensitivity to mTOR inhibitors by regulating cyclin D1 and c-myc expression. *J. Biol. Chem.* **[Epub ahead of print]**

Germain, et al (2000) Ubiquitination of free cyclin D1 is independent of phosphorylation on threonine 286. *J. Biol. Chem.* **275**, 12074-12079.

Gesbert, F. et al., (2000) BCR/ABL regulates expression of the cyclin-dependant kinase inhibitor $p27^{Kip1}$ through the phosphatidylinositol 3-kinase/AKT pathway. *J. Biol. Chem.* **50**, 39223-39230.

Gimm, O., et al (2000) Differential nuclear and cytoplasmic expression of PTEN in normal thyroid tissue, and benign and malignant epithelial thyroid tumors. *Am. J. Pathol.* **156**, 1693-1700.

Gimm, O., et al (2000b) Expression of the PTEN tumour suppressor protein during human development. *Hum. Mol. Genet.* **9**, 1633-1639.

Ginn-Pease, M. E. & Eng, C. (2003) Increased nuclear phosphatase and tensin homologue deleted on chromosome 10 is associated with G_0 -G_1 in MCF-7 cells. *Cancer Res.* **63**, 282-286.

Giraud, J., et al (2003) Nutrient-dependent and insulin-stimulated phosphorylation of IRS-1 SER302 correlates with increased insulin signalling. *J. Biol. Chem.* **[Epub ahead of print]**

Goetze, S. et al (2003) Leptin induces endothelial cell migration through Akt, which is inhibited by PPARgamma-ligands. *Hypertension.* **40**, 748-54.

Gold, L. I. (1999) The role for transforming growth factor-β (TGF-β) in human cancer. *Crit. Rev. Oncogen.* **10**, 303-360.

Gomez-Manzano, C. et al (2003) Mechanisms underlying PTEN regulation of vascular endothelial growth factor and angiogenesis. *Ann. Neurol.* **53**, 109-117.

Gottschalk, A. R., et al (2001) $p27^{Kip1}$ is required for PTEN-induced G1 growth arrest. *Cancer Res.* **61**, 2105-2111.

Graff, J. R., et al (2000) Increased AKT activity contributes to prostate cancer progression by dramatically accelerating prostate tumor growth and diminishing $p27^{Kip1}$ expression. *J. Biol. Chem.* **275**, 24500-24505.

Grimes, C. A & Jope, R. S (2001) The multifaceted roles of glycogen synthase kinase 3β in cellular signalling. *Prog. Neuro.* **65**, 391-426.

Gryfe, R., et al (2000) Tumor microsatellite instability and clinical outcome in young patients with colorectal cancer. *N. Engl. J. Med.* **342**, 69-77.

Gu, J., et al (1998) Tumor suppressor PTEN inhibits intergrin- and growth factor- mediated mitogen-activated protein (MAP) kinase signalling pathways. *J. Cell Biol.* **143**, 1375-1383.

Gu, J., et al (1999) Shc and FAK differentially regulate cell motility and directionality modulated by PTEN. *J. Cell Biol.* **146**, 389-403.

Guipponi, M., et al (2000) Genomic structure of a copy of the human TPTE gene which encompasses 87 kb on the short arm of chromosome 21. Hum. Genet. **107**, 127-31.

Guldberg, P., et al (1997) Disruption of the MMAC1/PTEN gene by deletion or mutation is a frequent event in malignant melanoma. *Cancer Res.* **57**, 3660-3603.

Guo, S., et al (1999) Phosphorylation of serine 256 by protein kinase b disrupts transactivation by FKHR and mediates effects of insulin on insulin-like metabolic and longevity signals in *C. elegans. Nature* **401**, 33-34.

Gustin, J. A., et al (2001) The PTEN tumor suppressor protein inhibits tumor necrosis factor-induced nuclear factor kappa B activity. *J. Biol. Chem.* **276**, 27740-27744.

Guzeloglu-Kayisli, O., et al (2003) Regulation of PTEN (phosphatase and tensin homolog deleted on chromosome 10) expression by estradiol and progesterone in human endometrium. *J. Clin. Endocrinol. Metab.* **88**, 5017-5026.

Halvorsen, O. J., Haukaas, S. A. & Akslen, L. A. (2003) Combined loss of PTEN and p27 expression is associated with tumor cell proliferation by Ki-67 and increased risk of recurrent disease in localized prostate cancer. *Clin. Cancer Res.* **9**, 1474-1479.

Healy, E., et al (1998) Prognostic significance of allelic losses in primary melanoma. *Oncogene.* **16**, 2213-2218.

Heldin, N. E., (1999) Lack of responsiveness to TGF-beta1 in a thyroid carcinoma cell line with functional type I and type II TGF-beta receptors and Smad proteins, suggests a novel mechanism for TGF-beta insensitivity in carcinoma cells. *Mol. Cell Endocrinol.* **153**, 79-90.

Hendriks, Y. M. C. et al (2003) Bannayan-Riley-Ruvalcaba syndrome: further delineation of the phenotype and management of PTEN mutation-positive cases. *Fam. Cancer.* **2**, 79-85.

Hennessy, L. K., Teare, J., & Ko, C. (1998) PCR conditions and DNA denaturants affect reproducibility of single-strand conformation polymorphism patterns for BRCA1 mutations. *Clin. Chem.* **44**, 879-882.

Hesselager, G., et al (2003) Complementary effects of platelet-derived growth factor autocrine stimulation and *p53* or *Ink4a-Arf* deletion in a mouse glioma model. *Cancer Res.* **63**, 4305-4309.

Hinton, H. J. & Welham, M. J. (1999) Cytokine induced protein kinase B activation and Bad phosphorylation do not correlate with cell survival of hematopoietic cells. *J. Immunol.* **162**, 7002-7009.

Hirashima, Y., et al (2003) Insulin down-regulates insulin receptor substrate-2 expression through the phosphatidylinositol 3-kinase/Akt pathway. *J. Endocrin.* **179,** 253-266.

Hisatake, J. et al (2001) Novel vitamin D(3) analog, 21-(3-methyl-3-hydroxy-butyl)-19-nor D(3), that modulates cell growth, differentiation, apoptosis, cell cycle, and induction of PTEN in leukemic cells. *Blood.* **97**, 2427-2433.

Hlobilkova, A., et al (2000) Cell cycle arrest by the PTEN tumor suppressor is tager cell specific and may require protein phosphatase activity. *Exp. Cancer Res.* **256**, 571-577.

Hooshmand-Rad, R, et al., (1997) Involvement of phosphatidylinositide 3'-kinase and Rac in platelet-derived growth factor-induced actin reorganisation and chemotaxis. *Exp. Cell. Res.* **234**, 434-441.

Hooshmand-Rad, R, et al., (2000) the PI 3-kinase isoforms p110α and p110β have different roles in PDGF- and insulin-mediated signalling *J. Cell Sci*, **113**, 207-214.

Hu, P., et al (1993) Cloning of a novel, ubiquitously expressed human phosphatidylinositol 3-kinase and identification of its binding site on p85. *Mol. Cell Biol.* **13**, 7677-7688.

Hu, X. et al (2001) Differential effects of transforming growth factor on cell cycle regulation molecules in human myeloid leukaemic cells. *Oncogene* **20**, 6840-6850.

Huang, H., et al (1999) PTEN affects cell size, cell proliferation and apoptosis during Drosophila eye development. *Development* **126**, 5365-5372.

Huang, Y. E., et al (2003) Receptor-mediated regulation of PI3Ks confines PI(3,4,5)P_3 to the leading edge of chemotaxing cells. *Mol. Biol. Cell* **14**, 1913-1922.

Hubbard, S. R., Mohammadi, M., & Schlessinger, J. (1998) Autoregulatory mechanisms in protein-tyrosine kinases. *J. Biol. Chem.* **273**, 11987-11990.

Hurley, J. H., Tsujishita, Y., & Pearson, M. A. (2000) Floundering about at cell membranes: a structural view of phospholipid signalling. *Curr. Opin. Struct. Biol.* **10**, 737-743.

Hurley, J. H, Meyer, T. (2001) Subcellular targeting by membrane lipids. *Curr. Opin. Cell Biol.* **13**, 146-52

Iijima, M. & Devreotes, P (2002) Tumour suppressor PTEN mediates sensing of chemoattractant gradients. *Cell* **109**, 599-610.

Ishihara, H., et al (2003) Association of the polymorphisms in the 5'-untranslated region of PTEN gene with type 2 diabetes in a Japanese population. *FEBS Lett.* **554**, 450-454.

Jiang T & Qiu Y (2003) Interaction between Src and a C-terminal proline-rich motif of Akt is required for Akt activation. *J. Biol. Chem.* **278**, 15789-93.

Jiang, Z., et al (2003) Reactive oxygen species mediate TGF-β1-induced plasminogen activator inhibitor-1 upregulation in mesangial cells. *Biochem. Biophys. Res. Comm.* **309**, 961-966.

Johnston, A. M., Pirola, L., & Van Obberghen, E., (2003) Molecular mechanisms of insulin receptor substrate protein-mediated modulation of insulin signalling. *FEBS Letts.* **546**, 32-36.

Kalesnikoff, J., et al (2003) The role of SHIP in cytokine-induced signalling. *Rev. Physiol. Biochem. Pharmacol.* **149**, 87-103.

Kane, L. P. (1999) Induction of NF-κB by the Akt/PKB kinase. *Curr. Biol.* **9**, 601-604.

Kang, Y-H. et al (2002) Promoter methylation and silencing of PTEN in gastric carcinoma. *Lab. Invest.* **82**, 285-291.

Keeton, M. R., et al (1991) Identification of regulatory sequences in the type I plasminogen activator inhibitor gene responsive to transforming growth factor β. *J. Biol. Chem.* **34**, 23048-23052.

Kennedy, S. G., et al (1999) Akt/protein kinase B inhibits cell death by preventing the release of cytochrome *c* from mitochondria. *Mol. Cell Biol.* **19**, 5800-5810.

Kensler, T. W., et al (2000) Conceptually new deltanoids (vitamin D analogs) inhibit multistage skin tumorigenesis. *Carcinogenesis.* **21**, 1341-1345.

Keski-Oja, J., et al (1998) Regulation of mRNAs for type-1 plasminogen activator inhibitor, fibronectin, and type I procollagen by transforming growth

factor-beta. Divergent responses in lung fibroblasts and carcinoma cells. *J. Biol. Chem.* **263**, 3111-3115.

Kihana. T., et al (1998) Association of replication error positive phenotype with lymphocyte infiltration in endometrial cancers. *Jpn. J. Cancer Res.* **89**, 895-902.

Kim, A. H., et al (2001) Akt phosphorylates and negatively regulates apoptosis signal-regulating kinase 1. *Mol. Cell Biol.* **21**, 893-901.

Kim, A. H., et al (2002) Akt1 regulates a JNK scaffold during excitotoxic apoptosis. *Neuron*, **35**, 697-709.

Kim, B., et al (2003) Cilostazol Enhances CK2 Phosphorylation and Suppresses Tumor Necrosis Factor-{alpha}-induced Increased Phosphatase and Tensin Homolog Deleted from Chromosome 10 Phosphorylation and Apoptotic Cell Death in SK-N-SH Cells. J. Pharmacol. Exp. Ther. **308**, 97-104.

Kim, S. et al (2003) Down-regulation of the tumor suppressor PTEN by the TNFα/NIK/NF-κB pathway is linked to a default IκB-alpha autoregulatory loop. *J. Biol. Chem.* Nov 17 Epub

Kirit, M. A., et al (2000a) The PI3 kinase, p38 SAP kinase, and NF-κB signal transduction pathways are involved in the survival and maturation of lipopolysaccharide-stimulated human monocyte-derived dendritic cells. *Blood*, **96**, 1039-1046.

Kitamura, T., et al (1999) Insulin-induced phosphorylation and activation of cyclic nucleotide phosphodiesterase 3B by the serine-theonine kinase Akt. *Mol. Cell. Biol.*, **19**, 6286-6296.

Klippel, A., et al (1994). The interaction of small domains between the subunits of phosphatidylinositol 3-kinase determines enzyme activity. *Mol. Cell Biol.* **14**, 2675-2685.

Koch, A., et al (1999) Childhood hepatoblastomas frequently carry a mutated degradation targeting box of the β-Catenin gene. *Cancer Res.* **59**, 269-273.

Kocher, O., et al (2003). Targeted disruption of the PDZK1 gene in mice causes tissue-specific depletion of the HDL Receptor SR-BI and altered lipoprotein metabolism. *J. Biol Chem.* **278**, 52820-52825.

Konopka, B., et al (2003) The coexistence of ERBB2, INT2, and CMYC oncogene amplifications and PTEN gene mutations in endometrial carcinoma. *J. Cancer Res. Clin. Oncol.* **[Epub ahead of print]**

Kops, G. J., et al (1999) Direct control of the Forkhead transcription factor AFX by protein kinase B. *Nature* **398**, 630-634.

Kornmann, M.,Tangvoranuntakul, P. & Korc, M. (1999) TGF-beta-1 up-regulates cyclin D1 expression in COLO-357 cells, whereas suppression of cyclin D1 levels is associated with down-regulation of the type I TGF-beta receptor. *Int. J. Cancer.* **83**, 247-254.

Koruso, H., et al (1997) Heterodimeric phosphoinsitide 3-kinase consisting of p85 and p110β is synergistically activated by the βγ subunits of G proteins and phosphotyrosyl peptide. *J. Biol. Chem.* **272**, 24252-24256.

Koul, D., et al (2001) Tumor suppressor MMAC/PTEN inhibits cytokine-induced NFκB activation without interfering with the IκB degradation pathway. *J. Biol. Chem.* 276, 11402-11408.

Kretzschmar, M. et al (1999) A mechanism of repression of TGFbeta/ Smad signaling by oncogenic Ras. *Genes Dev.* **13**, 804-816.

Krex, D, et al (2003) Genetic analysis of a multifocal glioblastoma multiforme: a suitable tool to gain new aspects in glioma development. *Neurosurgery.* **53**, 1377-1384.

Kurose, K., et al (2002) Frequent somatic mutations in PTEN and TP53 are mutually exclusive in the stroma of breast carcinomas. *Nat Genet.* **32**, 355-357. Erratum in: *Nat Genet* **32**, 681.

Kutz, S. M. et al (2001) TGF-beta1-induced PAI-1 gene expression requires MEK activity and cell-to-substrate adhesion. *J. Cell Sci.* **114**, 3905-3914.

Kwon, T., et al (2000) Akt protein kinase inhibits Rac1-GTP binding through phosphorylation at serine 71 of Rac1. *J. Biol. Chem.* **275**, 423-428.

Kwon, C. H., et al (2003) mTor is required for hypertrophy of Pten-deficient neuronal soma in vivo. *PNAS* **100**, 12923-12928.

Kyriakis,J. M., 1999 Activation of the AP-1 transcription factor by inflammatory cytokines of the TNF family. Gene Expr. **7**, 217-231.

Lachyankar, M. B., et al (2000) A role for nuclear PTEN in neuronal differentiation. *J. Neurosci.* **20**, 1404-413.

Laemmli, U. K. (1970) Cleavage of structural proteins during the assembly of the head of bacteriophage T4. *Nature.* **227**, 680-685.

Lee, J. O. et al, (1999) Crystal structure of the PTEN tumor suppressor: Implications for its phosphoinositide phosphatase activity and membrane association. *Cell* **99**, 323-334.

Lee, J., et al (1999b) TGF-beta1 inhibition of apoptosis through the transcriptional up-regulation of Bcl-X(L) in human monocytic leukemia U937 cells. *Exp. Mol. Med.* **31**, 126-133.

Lee, J., et al (2000) hCds1-mediated phosphorylation of BRCA1 regulates the DNA damage response. *Nature* **404**, 201-204.

Lee, J. H., et al (2003) Cilostazol Prevents Focal Cerebral Ischemic Injury by Enhancing CK2 Phosphorylation and Suppression of PTEN Phosphorylation in Rats. *J. Pharmacol. Exp. Ther.* Nov 21 **[Epub ahead of print]**

Leever, S. J., Vanhaesebroeck, B & Waterfield, M. D (1999) Signalling through phosphoinositide 3-kinases: the lipids take centre stage. *Curr. Opin. Cell Biol.* **11**, 219-225.

Le Good, J. A., et al (1998) Protein kinase C isotypes controlled by phosphoinositide 3-kinase through the protein kinase PDK-1. *Science.* **281**, 2042-2045.

Lei, X. et al (2002) Autocrine TGFβ supports growth and survival of human breast cancer MDA-MB-231 cells. *Oncogene* **21**, 7514-7523.

Leslie, N. R. (2001) Targeting mutants of PTEN reveal distinct subsets of tumour suppressor functions. *Biochem J.* **357**, 427-35.

Leslie, N. R., et al (2003) Redox regulation of PI 3-kinase signalling via inactivation of PTEN. *EMBO J.* **22**, 5501-5510.

Levine, R. L., et al (1998) PTEN mutations and microsatellite instability in complex atypical hyperplasia, a precursor lesion to uterine endometrioid carcinoma. *Cancer Res.* **58**, 3254-3258.

Lhuillier, L. & Dryer, S. E. (2003) Developmental regulation of neuronal K(Ca) channels by TGFbeta1: an essential role for PI3 kinase signaling and membrane insertion. *J. Neurophysiol.* **88**, 954-964.

Li, D. M. & Sun, H. (1997) TEP1, encoded by a candidate tumor suppressor locus, is a novel protein tyrosine phosphatase regulated by transforming growth factor beta. *Cancer Res.* **57**, 2124-2129.

Li, D. M. & Sun, H. (1998) PTEN/MMAC1/PEP1 suppresses the tumorigenicity and induces G1 cell cycle arrest in human glioblastoma cells. *PNAS* **95**, 15406-15411.

Li, J., et al (1997) PTEN, a putative protein tyrosine phosphatase gene mutated in human brain, breast, and prostate cancer. *Science* **275**, 1943-1947. **Li, J-M. et al** (1995) Transforming growth factor beta activates the promoter of cyclin-dependent kinase inhibitor p15INK4B through an Sp1 consensus site. *J. Biol. Chem.* **270**, 26750-26753.

Li, L., et al (1997b) A family of putative tumor suppressors is structurally and functionally conserved in humans and yeast. *J. Biol. Chem.* **272**, 29403-29406.

Li, L., Liu, F. & Ross, A. H. (2003b) PTEN regulation of neural development and CNS stem cells. *J. Cell Biochem.* **88**, 24-8.

Li, P. et al (2001) Antagonism between PTEN/MMAC1/TEP-1 and androgen receptor in growth and apoptosis of prostatic cancer cells. *J. Biol. Chem.* **276**, 20444-20450.

Li, P., et al (2003) AKT-independent protection of prostate cancer cells from apoptosis mediated through complex formation between the androgen receptor and FKHR. *Mol. Cell Biol.* **23**, 104-18.

Li, X., et al (2004) Akt2, phosphatidylinositol 3-kinase, and PTEN are in lipid rafts of intestinal cells: Role in absorption and differentiation. *Gastroenterology.* **126**, 122-135.

Liang, S. H. & Clarke, M. F. (1999) A bipartite nuclear localization signal is required for p53 nuclear import regulated by a carboxyl-terminal domain. *J. Biol. Chem.* **274**, 32699-32703.

Liao. Y. & Hung, M. C (2003) Regulation of the activity of p38-mitogen-activated protein kinase by Akt in cancer and adenoviral protein E1A-mediated sensitization to apoptosis. *Mol. Cell Biol.* **19**, 6836-6848.

Liliental, J. et al, (2000) Genetic deletion of the Pten tumor suppressor gene promotes cell motility by activation of Rac1 and Cdc42 GTPases. *Curr. Biol.* **10**, 401-404.

Lim, M. A., et al (2003) Nuclear ttranslocation of 3'-phosphoinositide-dependant protein kinase 1 (PDK-1): a potential regulatory mechanism for PDK-1 function. *PNAS*, **100**, 14006-14011.

Lin, H. K. et al (2001) Akt suppresses androgen-induced apoptosis by phosphorylating and inhibiting androgen receptor. *PNAS*, **98**, 7200-7205.

Liu, J. & Kagan, J. (1999) Method to distinguish between the MMAC1/PTEN gene and its pseudogene in RT-PCR analysis of point mutations. *Biotechniques.* **26**, 19-22, 24.

Liu, W., Asa, S. L. & Ezzat, S. (2002) Vitamin D and its analog EB1089 induce p27 accumulation and diminish association of p27 with Skp2 independent of PTEN in pituitary corticotroph cells. *Brain. Pathol.* **12**, 412-419.

Lopez-Ilascala, M., et al (1997) Linkage of G protein-coupled receptors to the MAPK signaling pathway through PI 3-kinase gamma. *Science*. **275**, 394-397.

Lu, Y., et al (1999) The PTEN/MMAC1/TEP tumor suppressor gene decreases cell growth and induces apoptosis and anoikis in breast cancer cells. *Oncogene.***18**, 7034-7045.

Lutz, M. & Knaus, P. (2002) Integration of the TGF-β pathway into the cellular signalling network. *Cell. Signal.* **14**, 977-988.

Lynch, et al (1999) Integrin-linked kinase regulates phosphorylation of serine 473 of protein kinase B by an indirect mechanism. *Oncogene.* **18**, 8024-8032.

Maehama, T., & Dixon, J. E., (1998) The tumor suppressor, PTEN/MMAC1, dephosphorylates the lipid second messenger, phosphatidylinositol 3,4,5-trisphosphate. *J. Biol. Chem.* **273**, 13375-13378.

Maehama, T., & Dixon, J. E., (1999) PTEN: a tumour suppressor that functions as a phospholipids phosphatase. *Trends Cell Biol.* **9**, 125-128.

SCF^{SKP2}. *Curr. Biol.* **11**, 263-267.

Mahimainathan, L. & Ghosh, C. G. (2004) Inactivation of platelet-derived growth factor receptor by the tumor suppressor PTEN provides a novel mechanism of action of the phosphatase. J. Biol. Chem. 2004 Jan 12 **[Epub ahead of print]**

Maier, D., et al (1999) The PTEN lipid phosphatase domain is not required to inhibit invasion of glioma cells. *Cancer Res.* **59**, 5479-5482

Mao, J. H., et al (2003) Genetic analysis of a multifocal glioblastoma multiforme: a suitable tool to gain new aspects in glioma development. *Neurosurgery*. **53**, 1377-1384.

Mamillapalli, R, et al (20001) PTEN regulates the ubiquitin-dependant degradation of the CDK inhibitor p27KIP1 though the ubiquitin E3 ligase.

Maniatis, T., Sambrook, J. & Fritsch, E. F. (1989) Molecular Cloning: A Laboratory Manual. Second Edition, Cold Spring Harbour Laboratory Press, ISBN 0879693096.

Marsh, D. J., et al (1998) Mutation spectrum and genotype-phenotype analyses in Cowden disease and Bannayan-Zonana syndrome, two hamartoma syndromes with germline PTEN mutation. *Hum. Mol. Genet.* **7**, 507-515.

Marsh, D. J. et al (1999) PTEN mutation spectrum and genotype-phenotype correlations in Bannayan-Riley-Ruvalcaba syndrome suggest a single entity with Cowden syndrome. *Hum. Mol. Genet.* **8**, 1461-1472.

Martini, M., et al (2002) Possible involvement of hMLH1, p16(INK4a) and PTEN in the malignant transformation of endometriosis. *Int. J. Cancer.* **102**, 398-406.

Massague, J. (2000) How cells read TGF-β signals. *Nat. Rev. Mol. Cell. Biol.* **1**, 169-178.

Matsushima-Nishiu, M., et al (2001) Growth and gene expression profile analysis of endometrial cancer cells expressing exogenous PTEN. *Cancer Res.* **61**, 3741-3749.

Maxwell, G. L. et al (2000) Racial disparity in the frequency of PTEN mutations, but not microsatellite instability, in advanced endometrial cancers. *Clin. Cancer Res.* **6**, 2999-3005.

Maxwell, G. L. et al (2001) Favorable survival associated with microsatellite instability in endometrioid endometrial cancers. *Obstet. Gynecol.* **97**, 417-422.

Mayo, L. D. & Donner, D. B. (2002) The PTEN, Mdm2, p53 tumor suppressor-oncoprotein network. *Trends Biochem. Sci.* **27**, 462-467.

Mayo, M. W., et al (2002) PTEN blocks tumor necrosis factor-induced NF-kappa B-dependent transcription by inhibiting the transactivation potential of the p65 subunit. *J. Biol. Chem.* **277**, 11116-11125.

Medema, R. H., et al (2000) AFX-like Forkhead transcription factors mediate cell-cycle regulation by Ras and PKB through p27kip1. *Nature* **404**, 782-787.

Melendez, B., et al (2003) Coincidental LOH regions in mouse and humans: evidence for novel tumor suppressor loci at 9q22-q34 in non-Hodgkin's lymphomas. *Leuk. Res.* **27**, 627-633.

Meng, T. C., et al (2003) Reversible oxidation and inactivation of protein tyrosine phosphatases in vivo. *Mol. Cell.* **9**, 387-399.

Mercie, P. (1998) Nuclear transcription factor kappa B (NF-kappa B). *Rev. Med. Interne.* **12**, 945-7.

Merril, C. R. (1990) Silver staining of proteins and DNA. *Nature.* **343**, 779-780.

Merks, J. H. M., et al (2003) PTEN harmatoma tumour syndrome: variability of an entity. *J. Med. Genet.* **40**, E111.

Mhashilkar, A. M., et al (2003) MDA-7 negatively regulates the β-Catenin and PI3K signalling pathways in breast and lung tumor cells. *Mol. Therapy* **8**, 207-219.

Mighell, A. J., et al (2000) Vertebrate pseudogenes. *FEBS Letts.* **468**, 109-114.

Minaguchi, T. et al (2001) PTEN mutation located only outside exons 5, 6, and 7 is an independent predictor of favorable survival in endometrial carcinomas. *Clin. Cancer Res.* **7**, 2636-2642.

Mincey, B. A. (2003) Genetics and the management of women at high risk for breast cancer. *The Oncologist* **8**, 466-473.

Miralem, T & Avraham, H. K. (2003) Extracellular matrix enhances heregulin-dependant BRCA1 phosphorylation and suppresses BRCA1 expression through its C terminus. *Mol. Cell Biol.* **23**, 579-593.

Molinari, A. M. et al (2000) Estradiol induces functional inactivation of p53 by cellular redistribution. *Cancer Res.* **60**, 2594-2597.

Moorehead, R. A., et al (2001) Inhibition of mammary epithelial apoptosis and sustained phosphorylation of Akt/PKB in MMTV-IGF-II transgenic mice. *Cell Death Differ.* **8**, 16-29.

Moorehead, R. A., et al (2003) IGF-II regulates PTEN expression in the mammary gland. *J. Biol. Chem.* **278**, 50422-50427.

Mosmann, T. (1983) Rapid colorimetric assay for cellular growth and survival: application to proliferation and cytotoxicity assays. *J. Immunol. Meth.* **65**, 55.

Mutter, G. L. et al (2000) Changes in endometrial PTEN expression throughout the human menstrual cycle. *J. Clin. Endocrinol. Metab.* **85**, 2334-2338.

Mutter, G. L, et al (2000b) Altered PTEN expression as a diagnostic marker for the earliest endometrial precancers. *J. Natl. Cancer. Inst.* **92**, 924-930.

Myers, M. P., et al (1997) P-TEN, the tumor suppressor from human chromosome 10q23, is a dual-specificity phosphatase. *PNAS* **94**, 9052-9057.

Myers, M. P., et al (1998) The lipid phosphatase activity of PTEN is critical for its tumor supressor function. *PNAS* **95**, 13513-8.

Nakamura, N., et al (2000) Forkhead transcription factors are critical effectors of cdell death and cell cycle arrest downstream of PTEN. *Mol. Cell. Biol.* **20**, 8969-8982.

Nakatani, K., et al (1999) Up-regulation of Akt3 in estrogen receptor-deficient breast cancers and androgen-independent prostate cancer lines. *J. Biol. Chem.* **274**, 21528-21532.

Nakayama, K-I., Hatakeyama, S & Nakayama, K., (2001) Regulation of the cell cycle at the G_1-S transition by proteolysis of cyclin E and $p27^{KIP1}$. *Biochem. Biophys. Res. Comm.* **282**, 853-860.

Nan, B., et al (2003) The PTEN tumor suppressor is a negative modulator of androgen receptor transcriptional activity. *J. Mol. Endocrin.* **31**, 169-183.

Nicholson, K. M., Streuli, C. H. & Anderson, G. E. (2003) Autocrine signalling through erbB receptors promotes constitutive activation of protein kinase B/Akt in breast cancer cell lines. *Breast Cancer Res. Treat.* **81**, 117-128.

Nishida, M. (2002) The Ishikawa cells from birth to the present. *Hum. Cell.* **15**, 104-117.

Nystrom, E. N. & Quon, M. Y. (1999) Insulin signalling: metabolic pathways and mechanisms for specificity. *Cell Signal.* **11**, 563-574.

Odom, A. R. et al, (2000) A role for nuclear inositol 1,4,5-trisphosphate kinase in transcriptional control. *Science*. **287**, 2026-2029.

Oft, M., Heider, K-H. & Beug, H. (1998) TGFβ signalling is necessary for carcimona invasiveness and metastasis. *Curr. Biol.* **8**, 1243-1252.

Okkenhaug, K., & Vanhaesebroeck, B (2001) http://www.stke.org/cgi/content/full/OC_sigtrans:2001/65/pel

Okkenhaug, K., & Vanhaesebroeck, B (2003) PI3K-signalling in B- and T-cells: insights from gene-targeted mice. *Biochem Soc Trans.* **31**, 270-4.

Ong, S. H., et al (2001) Stimulation of phosphatidylinositol 3-kinase by fibroblast growth factor receptors is mediated by coordinated recruitment of multiple docking proteins. *PNAS* **22**, 6047-6079.

Orbo, A., et al (2003) Loss of expression of MLH1, MSH2, MSH6, and PTEN related to endometrial cancer in 68 patients with endometrial hyperplasia. *Int. J. Gynecol. Pathol.* **22**, 141-148.

Ozes, O. N., et al (1999) NF-kappaB activation by tumour necrosis factor requires the Akt serine-threonine kinase. *Nature* **401**, 82-85.

Palacios, J. & Gamallo, C. (1998) Mutations in the β-Catenin gene (*CTNNB1*) in endometrioid ovarian carcinomas. *Cancer Res.* **58**, 1344-1347.

Paramio, J. M., et al (1999) PTEN tumour suppressor is linked to the cell cycle control through the retinoblastoma protein. *Oncogene* **18**, 7462-7468.

Patel, L. et al (2001) Tumor suppressor and anti-inflammatory actions of PPARgamma agonists are mediated via upregulation of PTEN. *Curr. Biol.* **11**, 764-768.

Payrastre, B., et al (2001) Phosphoinositides. Key players in cell signalling, in time and space. *Cell. Signal.* **13**, 377-387.

Paz K., et al (1999) Phosphorylation of insulin receptor substrate-1 (IRS-1) by protein kinase B positively regulates IRS-1 function. *J. Biol. Chem.* **274**, 28816-22.

Perren, A., et al (1999) Immunohistochemical evidence of loss of PTEN expression in primary ductal adenocarcinomas of the breast. *Am. J. Pathol.* **155**, 1253-1260.

Perren, A., et al (2000) Mutation and expression analyses reveal differential subcellular compartmentalization of PTEN in endocrine pancreatic tumors compared to normal islet cells. *Am. J. Pathol.* **157**, 1097-1103

Persad, S., et al (2001) Tumor suppressor PTEN inhibits nuclear accumulation of β-Catenin and T cell/lymphoid enhancer factor 1-mediated transcriptional activation. *J. Cell Biol.* **153**, 1161-1173.

Pervin, S., Singh, R & Chaudhuri, G (2003) Nitric-oxide-induced Bax integration into the mitochondrial membrane commits MDA-MB-468 cells to apoptosis: essential role of Akt. *Cancer Res.* **63**, 5470-5479.

Petiot, A., Faure, J., Stenmark, H., & Gruenberg, J. (2003) PI3P signalling regulates receptor sorting but not transport in the endosomal pathway. *J. Biol. Chem.* **162**, 971-979.

Pieper, G. M., (1998) Review of alterations in endothelial nitric oxide production in diabetics. *Hypertension*, **31**, 1047-1060.

Piero, G., et al (2002) Microsatellite instability, loss of heterozygosity, and loss of hMLH1 and hMSH2 protein expression in endometrial carcinoma. *Hum. Pathol.* **33**, 347-354.

Pike, L. J. (2003) Lipid rafts: Heterogeneity on the high seas. *Biochem. J.* Dec 8 **[Epub ahead of print]**

Poetsch, M., Dittberner, T. & Woenckhaus, C. (2001) PTEN/MMAC1 in malignant melanoma and its importance for tumor progression. *Cancer Genet. Cytogenet.* **125**, 21-26.

Polakis, P. (1998) The many partners of β-Catenin. *Transduction Labs Insights* **4**, 1-4.

Poulsen, M. K., et al (2003) The Combined Effect of Triple Therapy With Rosiglitazone, Metformin, and Insulin Aspart in Type 2 Diabetic Patients. *Diabetes Care.* **26**, 3273-3279.

Plyte, S., et al (2000) Constitutive activation of the Ras/MAP kinase pathway and enhanced TCR signaling by targeting the Shc adaptor to membrane rafts. *Oncogene* **19,** 1529-1537.

Pullen, N., et al (1998) Phosphorylation and activation of p70s6k by PDK1. *Science.* **279**, 707-710.

Radu, et al (2003) PTEN induces cell cycle arrest by decreasing the level and nuclear localisation of cyclin D1. Mol. Cell Biol. 23, 6139-6149.

Ramaswamy, S., et al (1999) Regulation of G1 progression by the PTEN tumor suppressor protein is linked to inhibition of the phosphatidylinositol 3-kinase/Akt pathway. *PNAS* **96**, 2110-2115.

Reiss, M. (1999) TGF-β and cancer. *Microbes Infect.* **1**, 1327-1347.

Reis, R. M., et al (2000) Genetic profile of gliosarcomas. *Am. J. Pathol.* **156**, 425-432.

Ren, Y., & Wu, J. (2003) Simultaneous suppression of Erk and Akt/PKB activation by Gab1 pleckstrin homology (PH) domain decoy. *Anticancer Res.* **23**, 3231-3236.

Rena, G., et al (1999) Phosphorylation of the transcription factor forkhead family member FKHR by protein kinase. *B. J. Biol. Chem.* **274**, 17179-17183.

Rennie, P. S. & nelson, C. C. (1999) Epigenetic mechanisms for progression of prostate cancer. *Cancer Metastasis Rev.* **17**, 401-409.

Rhei, E., et al (1997) Mutation analysis of the putative tumor suppressor gene PTEN/MMAC1 in primary breast carcinomas. *Cancer Res.* **57**, 3657-3659.

Ricci, R. et al (2003) PTEN as a molecular marker to distinguish metastatic from primary synchronous endometrioid carcinomas of the ovary and uterus. *Diagn. Mol. Pathol.* **12**, 71-8.

Risinger. J. L., et al (1997) PTEN/MMAC1 mutations in endometrial cancers. *Cancer Res.* 57, 4736-4738.

Risinger, J. I., et al (1998) PTEN mutation in endometrial cancers is associated with favorable clinical and pathologic characteristics. *Clin. Cancer Res.* **4**, 3005-3010.

Risinger, J. I., et al (2003) Promoter hypermethylation as an epigenetic component in Type I and Type II endometrial cancers. *Ann. N. Y. Acad. Sci.* **983**, 208-212.

Rizo, J. & Sudhof, T. C. (1998) C2 domains, structure and function of a universal $C2^{+}$-binding domain. *J. Biol. Chem.* **273**, 15879-15882.

Robertson, G. P., et al (1998) In vitro loss of heterozygosity targets the PTEN/MMAC1 gene in melanoma. *PNAS* **95**, 9418-9423.

Robinson, S & Cohen, A. R. (2000) Cowden disease and Lhermitte-Duclos disease: characterization of a new phakomatosis. *Neurosurgery*. **46**, 371-383.

Rodriguez-Borlando, L., et al (2003) Phosphatidylinositol 3-kinase regulates the CD4/CD8 T cell differentiation ratio. *J. Immunol.* **170,** 4475-4482.

Rogers, S., Wells, R., & Rechsteiner M (1986) Amino acid sequences common to rapidly degraded proteins: the PEST hypothesis. *Science* **234,** 364-368

Romieu-Mourez, R. (2002) Protein kinase CK2 promotes aberrant activation of nuclear factor-kappaB, transformed phenotype, and survival of breast cancer cells. *Cancer Res.* **62**, 6770-6778.

Salvesen, H. B. et al (2001) PTEN methylation is associated with advanced stage and microsatellite instability in endometrial carcinoma. *Int. J. Cancer.* **91**, 22-26.

Sanson, M., et al (1999) Germline mutations of p53 but not p16/CDKN2 or PTEN/MMAC1 tumor suppressor genes predispose to gliomas. *.Ann Neurol.* **46**, 913-916.

Seminario, M. C., et al (2003) PTEN expression in PTEN-null leukaemic T cell lines leads to reduce proliferation via slowed cell cycle progression. *Oncogene* **22**, 8195-8204.

Schlessinger, J. (2003) Autoinhibition control. *Science*, **300**, 750-752.

Sharma, M., Chuang, W. W. & Sun, Z. (2002) Phosphatidylinositol 3-kinase/Akt stimulates androgen pathway through GSK3β inhibition and nuclear β-catenin accumulation. *J. Biol. Chem.* **277**, 30935-30941.

Shepherd, P. R., Withers, D. J. & Siddle, K. (1998) Phosphoinositide 3-kinase: the key switch mechanism in insulin signalling. *Biochem. J.* **333**, 471-490.

Shi, Y. et al (2003) Mechanisms of TGF-β signalling from cell membrane to the nucleus. *Cell* **113**, 685-700.

Shin, I., et al (2002) PKB/Akt mediates cell-cycle progression by phosphorylation of p27(Kip1) at threonine 157 and modulation of its cellular localization. *Nat. Med.* **8**, 1145-1152.

Simpson, D. J., et al (2000) Loss of pRb expression in pituitary adenomas is associated with methylation of the RB1 CpG island. *Cancer Res.* **60**, 1211-1216.

Simpson, L., et al (2001) PTEN expression causes feedback upregulation of insulin receptor substrate 2. *Mol. Cell Biol.* **21**, 3947-3958.

Smart, E. J., et al (1999) Caveolins, liquid-ordered domains, and signal transduction. *Mol. Cell Biol.* **19**, 7289-7304.

Snabboon, N. B., et al (2003) The PTEN tumor suppressor is a negative modulator of androgen receptor transcriptional activity. *J. Mol. Endocrinol.* **31**, 169-183.

Somani, et al (1997) Src kinase activity is regulated by the SHP-1 protein-tyrosine phosphatase. *J. Bio. Chem.* **272**, 21113-21119.

Soria, J-C. et al (2002) Lack of PTEN expression in non-small cell lung cancer could be related to promoter methylation. *Clin. Cancer Res.* **8**, 1178-1184.

Stambolic, V., et al (1998) Negative regulation of PKB/Akt-dependent cell survival by the tumor suppressor PTEN. *Cell* **95**, 29-39.

Stambolic, V. et al (2001) Regulation of PTEN transcription by p53. *Mol. Cell* **8**, 317-325.

Stambolic, V. (2002) PTEN: a new twist on β-Catenin? *Trends Pharm. Sci.* **23**,104-106.

Steck, P., et al (1997) Identification of a candidate tumor suppressor gene, MMAC1, at chromosome 10q23.3, that is mutated in multiple advanced cancers. *Nat. Genet.* **15**, 356-362.

Stephens, L. R., Jackson, T. R., & Hawkins, P. T (1993) Agonist-stimulated synthesis of phosphatidylinositol(3,4,5)-trisphosphate: a new intracellular signalling system? *Biochim. Biophys. Acta.* **1179**, 27-75.

Stoyanov, B., et al (1995). Cloning and characterization of a G protein-activated human phosphoinositide-3 kinase. *Science* **269**, 690-693.

Strauss, G., et al (2003) Constitutive caspase activation and impaired death-inducing signalling complex formation in CD95-resistant, long-term activated antigen-specific T cells. *J. Immunol.* **171**, 1172-1182.

Su, J. D., et al (2003) PTEN and phosphatidylinositol 3'-kinase inhibitors up-regulate p53 and block tumor-induced angiogenesis: evidence for an effect on the tumor and endothelial compartment. *Cancer Res.* **63**, 3585-3592.

Suh, E. K. & Gumbiner, B. M. (2003) Translocation of beta-catenin into the nucleus independent of interactions with FG-rich nucleoporins. *Exp. Cell Res.* **290**, 447-456.

Sun, H., et al (2001) Mutational Analysis of the PTEN gene in endometrial carcinoma and hyperplasia. *Am.* J. Clin. Pathol. **115**, 32-38.

Sutphen, R., et al (1999) Severe Lhermitte-Duclos disease with unique germline mutation of PTEN. *Am. J. Med. Genet.* **82**, 290-293.

Suzuki, A., et al (2003) Critical roles of Pten in B cell homeostasis and immunoglobulin class switch recombination. *J. Exp Med.* **197**, 657-667.

Tachibana, M., et al (2002) Expression and prognostic significance of PTEN product protein in patients with esophageal squamous cell carcinoma. *Cancer.* **94**, 1955-1960.

Takeuchi, K. & Ito, F. (2003) Suppression of adriamycin-induced apoptosis by sustained activation of the phosphoinositol-3'-OH kinase-Akt pathway. *Epub ahead of print.*

Takuwa, N., Fukui, Y. & Takuwa, Y. Cyclin D1 expression mediated by phosphatidylinositol 3-Kinase through mTOR-p70^{S6K}-independent signalling in growth factor-stimulated NIH 3T3 fibroblasts. *Mol. Cell Biol.* **19**, 1346-1358.

Tamura, M., et al (1998) Inhibition of cell migration, spreading, and focal adhesions by tumor suppressor PTEN. *Science* **280**, 1614-1617.

Tamura, M., et al (1999) PTEN interactions with focal adhesion kinase and suppression of the extracellular matrix-dependent phosphatidylinositol 3-kinase/Akt cell survival pathway. *J. Biol. Chem.* **274**, 20693-20703.

Tanaka, M., et al., (2000) MMAC1/PTEN inhibits cell growth and induces chemosensitivity to doxorubicin in human bladder cancer cell lines. *Oncogene* **19**, 5406-5412.

Tashiro, H., et al (1997) Mutations in PTEN are frequent in endometrial carcinoma but rare in other common gynecological malignancies. *Cancer Res.* **57**, 3935-3940.

Terakawa, N., Kanamori, Y.,& Yoshida, S. (2003) Loss of PTEN expression followed by Akt phosphorylation is a poor prognostic factor for patients with endometrial cancer. *Endocr. Relat. Cancer.* **10**, 203-208.

Tian, X-X., et al (1999) Restoration of wild-type PTEN expression leads to apoptosis, induces differentiation, and reduces telomerase activity in human glioma cells. *J. Neuropath. Exp. Neurol.* **58**, 472-479.

Tibbles, L. A. & Woodgett, J. R. (1999) The stress-activated protein kinase pathways. Cell Mol. Life Sci. **55**, 1230-1254.

Tibilietti, M. G., et al (1999) Microsatelitte instability in endometrial cancer: Relation to histological subtypes. *Gynecol. Oncol.* **73**, 247-252.

Toda, T. et al (2001) Analysis of microsatellite instability and loss of heterozygosity in uterine endometrial adenocarcinoma. *Cancer Genet. Cytogenet.* **126**, 120-7.

Tolkacheva, T. & Chan, A. M. (2000) Inhibition of H-Ras transformation by the PTEN/MMAC1/TEP1 tumor suppressor gene. *Oncogene.* **19**, 680-9.

Tomoda, K., et al (2002) The cytoplasmic shuttling and subsequent degradation of p27Kip1 mediated by Jab1/CSN5 and the COP9 signalosome complex. *J. Biol. Chem.* **277**, 2302-2310.

Tonks, N. K. & Neel, B. G. (1996) From form to function: signalling by protein tyrosine kinases. *Cell* **87**, 365-368.

Tonks, N. K. & Neel, B. G. (2001) Combinatorial control of the specificity of protein tyrosine phosphatases. *Curr. Opin. Cell Biol.* **13**, 182-95.

Torres, J. & Pulido, R. (2001) The tumour suppressor PTEN is phosphorylated by the protein kinase CK2 at its c terminus. Implications for PTEN stability to proteosome-mediated degradation. *J. Biol. Chem.* **276**, 993-998.

Truica, Cli, Byers, S. & Gelmann, E. P. (2000) Beta-catenin affects androgen receptor transcriptional activity and ligand specificity. *Cancer Res.* **60**, 4709-4713.

Tsuda, H. et al (2002) Different pattern of loss of heterozygosity among endocervical-type adenocarcinoma, endometrioid-type adenocarcinoma and adenoma malignum of the uterine cervix. *Int. J Cancer.* **98**, 713-717.

Tsuruzoe, K., et al (2001) Insulin receptor substrate 3 (IRS-3) and IRS-4 impair IRS-1- and IRS-2-mediated signaling. *Mol. Cell. Biol.* **21**, 26-38.

Ueda, K. et al (1998) Infrequent mutations in the PTEN/MMAC1 gene among primary breast cancers. *Jpn. J. Cancer Res.* **89**, 17-21.

Ueda, T., et al (2002) Activation of the androgen receptor N-terminal domain by interleukin-6 via MAPK and STAT3 signal transduction pathways. *J. Biol. Chem.* **277**, 7076-7085.

Vanhaesebroeck, B et al (1997) Phosphoinositide 3-kinases: a conserved family of signal transducers. *TIBS* **22**, 267-272.

Vanhaesebroeck, B. & Waterfield, M. D. (1999a) Signalling by distinct classes of phosphoinositide 3-kinases. *Exp. Cell Res.* **253**, 239-254.

Vanhaesebroeck, B et al (1999b) Autophosphorylation of p110δ phosphoinositide 3-kinase: a new paradigm for the regulation of lipid kinases in vitroand in vivo. *EMBO J*, **18** (5), 1292-1302.

Vanhaesebroeck, B et al., (1999c) Distinct PI(3)Ks mediate mitogenic signalling and cell migration in macrophages *Nat. Cell Biol*, **1**,

Vanhaesebroeck, B & Alessi, D. R. (2000) The PI3K-PDK-1 connection: more than just a road to PKB. *Biochem. J.* **346**, 561-576.

Vanhaesebroeck, B et al (2001) Synthesis and function of 3-phosphorylated inositol lipids. *Annu. Rev. Biochem.* **70**, 535-602.

Vantomme, N., et al (2001) Lhermitte-Duclos disease is a clinical manifestation of Cowden's syndrome. *Surg Neurol.* **56**, 201-204.

Vazquez, F & Sellers, W. R. (2000) The PTEN tumour suppressor protein: an antagonist of phosphatidylinositol 3-kinase signalling. *Biochim. Biophys. Acta.* **1470** ,M21-M35.

Vazquez, F., et al (2000) Phospholylation of the PTEN tail regulates protein stability and function. *Mol. Cell Biol.* **20**, 5010-5018.

Vazquez, F., et al (2001) Phosphorylation of the PTEN tail acts as an inhibitory switch by preventing its recruitment into a protein complex. *J. Biol. Chem.* **276**, 48627-48630.

Vazquez-Prado, J., Casas-Gonzalez, P. & Garcia-Sainz, J. A., (2003) G protein-coupled receptor cross-talk: pivotal roles of protein phosphorylation and protein-protein interactions. *Cell. Signal.* **15**, 549-557.

Vasudevan, K. M., Gurumurthy, S. & Rangnekar, V. M, (2004) Suppression of PTEN Expression by NF-kappaB Prevents Apoptosis. *Mol. Cell. Biol.* **24**, 1007-1021.

Vinals, F. & Pouyssegur, J. (2001) Transforming growth factor beta1 (TGF-beta1) promotes endothelial cell survival during in vitro angiogenesis via an autocrine mechanism implicating TGF-alpha signalling. *Mol. Cell. Biol.* **21**, 7218-7230.

Virolle, T., et al (2001) The Egr-1 transcription factor directly activates PTEN during irradiation-induced signalling. *Nat. Cell Biol.* **3**, 1124-1128.

Vitari, A. C., et al (2003) WNK1, the kinase mutated in an inherited high blood pressure syndrome, is a novel PKB/Akt substrate. *Biochem. J.* Nov 11**[Epub ahead of print].**

Vlahos, C. J., et al (1994). A specific inhibitor of phosphatidylinositol 3-kinase, 2-(4-morpholinyl)-8-phenyl-4H-1-benzopyran-4-one (LY294002) *J. Biol. Chem.* **269**, 5241-5248.

Waite, K. A. & Eng, C. (2003) From developmental disorder to heritable cancer: it's all in the BMP/TGF-beta family. *Nat. Rev. Genet.* **4**, 763-773.

Waite, K. A. & Eng, C. (2003b) BMP2 exposure results in decreased PTEN protein degradation and increased PTEN levels. *Hum. Mol. Genet.* **12**, 679-684.

Walker, S. M., Downes, C. P., & Leslie, N. R. (2001) TPIP: a novel phosphoinositide 3-phosphatase. *Biochem. J.* **360**, 277-283.

Walker, S. M., et al (2004) The tumour suppressor function of PTEN requires an N-terminal lipid binding motif. *Biochem. J.* Jan 7 **[Epub ahead of print]**

Wan, X., & Helman, L. J. (2003) Levels of PTEN protein modulate Akt phosphaorylation on serine 473 not on threonine 308, in IGF-II-overexpressing rhabdomyosarcomas. *Oncogene*, **22**, 8205-8211.

Wang, C. Y., et al (1998) NF-κB induces expression of the Bcl-2 homologue A1/Bfl-1 to preferentially suppress chemotherapy-induced apoptosis. *Mol. Cell Biol.* **19**, 5923-5929.

Wang, Q., Wang, X. & Evers, B. M. (2003) Induction of cIAP-2 in human colon cancer cells through PKC delta/NF-kappa B. *J. Biol. Chem.* **278**, 51091-51099.

Warnecke, P. M. & Bestor, T. H., (2000) Cytosine methylation and human cancer. *Curr. Opin. Oncol.* **12**, 68-73.

Welch, H. C., et al (2002) P-Rex1, a PtdIns(3,4,5)P3- and Gbetagamma-regulated guanine-nucleotide exchange factor for Rac. *Cell.* **108**, 809-821.

Weng, L. P., et al (1999) PTEN suppresses breast cancer cell growth by phosphatase activity-dependent G1 arrest followed by cell death. *Cancer Res.***59**, 5808-5814.

Weng, L. P., et al (2001a) Transient ectopic expression of PTEN in thyroid cancer cell lines induces cell cycle arrest and cell type-dependent cell death. *Hum. Mol. Genet.***10**, 251-258.

Weng, L. P., et al (2001b) PTEN coordinates G1 arrest by down regulating cyclin D1 via its protein phosphatase activity and up regulating p27 via its lipd phosphatase activity in a breast cancer model. *Hum. Mol. Genet.* **10**, 599-604.

Weng, L. P., et al (2001c) PTEN inhibits insulin-stimulated MEK/MAPK activation and cell growth by blocking IRS-1 phosphorylation and IRS-1/Grb-2/Sos complex formation in a breast cancer model. *Hum. Mol. Genet.* **10**, 605-616.

Weng, L. P., et al (2002) PTEN blocks insulin-mediated ETS-2 phosphorylation through MAP kinase, independently of the phosphoinositide 3-kinase pathway. *Hum. Mol. Genet.* **11**, 1687-1696.

Whang, Y. E., et al (1998) Inactivation of the tumor suppressor PTEN/MMAC1 in advanced human prostate cancer through loss of expression. *PNAS* **95**, 5246-5250.

Whiteman, D. C. et al, (2002) Nuclear PTEN expression and clinicopathologic features in a population-based series of primary cutaneous melanoma. *Int. J. Cancer.* **99**, 63-67.

Wick, W., et al (1999) PTEN gene transfer in human malignant glioma: sensitization to irradiation and CD95L-induced apoptosis. *Oncogene* **18**, 3936-3943.

Wishart, M. J. & Dixon, J. E. (2002) PTEN and myotubularin phosphatases: from 3-phosphoinositide dephosphorylation to disease. *Trends Cell Biol.* **12**, 579-585.

Wolf, B. B. & Green, D. R. (1999) Suicidal tendencies: apoptotic cell death by caspase family proteinases. *J. Biol. Chem.* **274**, 20049-20052.

Wolfrum, C., et al (2003) Insulin regulates the activity of forkhead transcription factor Hnf-3beta/Foxa-2 by Akt-mediated phosphorylation and nuclear/cytosolic localisation. *Proc. Natl. Acad. Sci.* **100**, 11624-11629.

Wong, Y. F., et al (1999) Clinical and pathamolgical significance of microsatellite instability in endometrial cancer. *Int. J. Gynecol Cancer* **9**, 406-410.

Woods, I K. M. (3003) The Role of Phosphatidylinositol 3'-Kinase and Its Downstream Signals in erbB-2-Mediated Transformation. *Mol. Cancer Res.* **1**, 551-560.

Wu, R. C & Li, S. A. H., (2000) Transcriptional activation of $p21^{WAF1}$ by PTEN/MMAC1 tumor suppressor. *Mol. Cell Biochem.* **203**, 59-71.

Wu, X. et al (2000) Evidence for regulation of PTEN tumor suppressor by a membrane-localized multi-PDZ domain containing scaffold protein MAGI-2. *PNAS* **97**, 4233-4238.

Wu, Y. et al (2000a) Interaction of the tumor suppressor PTEN/MMAC with a PDZ domain of MAGI3, a novel membrane-associated guanylate kinase. J. Biol. Chem. **275**, 21477-21485.

Wu. Y. et al (2000b) PTEN 2, a golgi-associated testis-specific homologue of the PTEN tumor suppressor lipid phosphatase. *J. Biol. Chem.* **276**, 21745-21753

Wu, R-C., et al (2002) Loss of cellular adhesion to matrix induces p53-independent expression of PTEN tumor suppressor. *BMC Mol. Biol.* **3**, 11.

Wymann, M. P., et al (1996) Wortmannin inactivates phosphoinositide 3-kinase by covalent modification of Lys-802, a residue involved in the phosphate transfer reaction. *Mol. Cell Biol.* **16**, 1722-1733.

Wymann, M. P. & Pirola, L. (1998) Structure and function of phosphoinositide 3-kinases. *Biochim. Biophys. Acta.* **1436(1-2)**, 127-50.

Wymann, M. P., et al (2003) Phosphoinositide 3-kinase signalling-which way to target? Trends Pharm. Sci. **24**, 366-376.

Yaginuma, Y., et al (2000) Abnormal structure and expression of PTEN/MMAC1 gene in human uterine cancers. *Mol. Carcinogen.* **27**, 110-116.

Yang, E. S. & Burnstein, K. L. (2003) Vitamin D inhibits G1 to S progression in LNCaP prostate cancer cells through p27Kip1 stabilization and Cdk2 mislocalization to the cytoplasm. *J. Biol. Chem.* **278**, 46862-46868.

Yang, H-Y, et al (2000) Oncogenic signals of HER-2/*neu* in regulating the stability of the cyclin-dependant kinase inhibitor p27. *J. Biol. Chem.* **32**, 24734-24739.

Yeon, J. E., et al (2003) Potential role of PTEN phosphatase in ethanol-impaired survival signaling in the liver. *Hepatology.* **38**, 703-714.

Yokoyama, Y, et al (2000) Expression of PTEN and PTEN pseudogene in endometrial carcinoma. *Int. J. Mol. Med.* **6**, 47-50.

Yu, G., et al (2002) Methylation profiling of twenty promoter-CpG islands of genes which may contribute to hepatocellular carcinogenesis. BMC Cancer. **2**, 29.

Yu, Z., et al (2002) PTEN associates with the vault particles in HeLa cells. *J. Biol. Chem.* **277**, 40247-40252.

Yu, Y., et al (2003) Src family protein-tyrosine kinases alter the function of PTEN to regulate phosphatidylinositol 3-kinase/AKT cascades. *J. Biol. Chem.* **278**, 40057-40066.

Yue, J. & Mulder, K. M. (2001) Transforming growth factor-beta signal transduction in epithelial cells. *Pharmacol. Ther.* **91**, 1-34.

Zhang, J., Vanhaesebroeck, B., & Rittenhouse, S. E., (2002) Human platelets contain p110δ phosphoinositide 3-kinase. *Biochem, Biophys. Res, Comm.* **296**, 178-181.

Zhang, Y., et al (2003) Role of phosphatase PTEN in the activation of extracellular signal-regulated kinase by estradiol in endometrial carcinoma cells. *Chin. Med. J.* **116**,383-387.

Zheng, H-C. et al (2003) Role of PTEN and MMP-7 expression in growth, invasion, metastasis and angiogenesis of gastric carcinoma. *Path. Int.* **53**, 659-666.

Zheng, H-C. et al (2003b) Growth, invasion, metastasis, differentiation, angiogenesis and apoptosis of gastric cancer regulated by expression of PTEN encoding products. *World J. Gastroenterol.* **9**, 1662-1666.

Zhong, H., et al (2000) Modulation of hypoxia-inducible factor 1α expression by the epidermal growth factor/phosphatidylinositol 3-kinase/PTEN/AKT/FRAP pathway in human prostate cancer cells: implications for tumor angiogenesis and therapeutics. *Cancer Res.* **60**, 1541-1545.

Zhong, L., et al (2003) Directional sensing requires Gβγ-mediated PAK1 and PIXα-dependant activation of Cdc42. *Cell* **114**, 215-227.

Zhou, D., et al (2001) A *Salmonella* inositol polyphosphatase acts in conjunction with other bacterial effectors to promote host cell actin cytoskeleton rearrangements and bacterial internalization. *Mol. Microbiol.* **39**, 248-260.

Zhou, M. et al (2003) PTEN reverses MDM2-mediated chemotherapy resistance by interacting with p53 in acute lymphoblastic leukemia cells. *Cancer Res.* **63**, 6357-6362.

Zhou, X., et al (2001b) Association of germline mutation in the PTEN tumour suppressor gene and Proteus and Proteus-like syndromes. *Lancet.* **358**, 210-211.

Zhou, X. P., et al (1999) Mutational analysis of the PTEN gene in gliomas: molecular and pathological correlations. *Int. J. Cancer.* **84**, 150-154.

Zhou, X. P., et al (2000) Epigenetic PTEN silencing in malignant melanomas without PTEN mutation. *Am. J. Pathol.* **157**, 1123-1128.

Zhou, X. P., et al (2000b) Germline and germline mosaic PTEN mutations associated with a Proteus-like syndrome of hemihypertrophy, lower limb asymmetry, arteriovenous malformations and lipomatosis. *Hum. Mol. Genet.* **9**, 765-768.

Zhou, X. P., et al (2002) PTEN mutational spectra, expression levels, and subcellular localization in microsatellite stable and unstable colorectal cancers. *Am. J. Pathol.* **161**, 439-447.

Zhou, X. P., et al (2003b) Germline PTEN promoter mutations and deletions in Cowden/Bannayan-Riley-Ruvalcaba syndrome result in aberrant PTEN protein and dysregulation of the phosphoinositol-3-kinase/Akt pathway. *Am. J. Hum. Genet.* **73**, 404-411.

Zhou, X. P., et al (2003c) Germline Inactivation of PTEN and Dysregulation of the Phosphoinositol-3-Kinase/Akt Pathway Cause Human Lhermitte-Duclos Disease in Adults. *Am. J. Hum. Genet.* **73**, 1191-1198.

Zhu, X., et al (2001) PTEN induces G1 cell cycle arrest and decreases cyclin D3 levels in endometrial carcinoma cells. *Cancer Res.* **61**, 4569-4575.

Zhu, X-F., et al (2003) Ceramide induces cell cycle arrest and upregulates p27Kip in nasopharangeal carcinoma cells. *Cancer Letts.* **193**, 149-154.

Zimmerman, S. & Moelling, K., (1999) Phosphorylation and regulation of raf by akt (protein kinase B). *Science* **286**, 1741-1744.

Zysman, M. A., Chapman W. B & Bapat B. (2002) Considerations when analyzing the methylation status of PTEN tumor suppressor gene. *Am. J. Pathol.* **160**, 795-800. Erratum in: *Am. J. Pathol* **160**, 2311.

Zundel, W., et al (2000) Loss of PTEN facilitates HIF-1-mediated gene expression. *Genes Dev.* **14**, 391-396.

APPENDIX I

MEDIA AND BUFFER COMPOSITION

1. Cell Culture Media Composition

HEC-1B Cell Line

McCoy's 5A Modified Medium

For Complete Medium (CM) add the following to 500ml of McCoy's:

1% L-Glutamine

1% Penicillin-Streptomycin

10% Foetal Calf Serum

For Reduced-Serum Medium (RSM) add the following to 500ml McCoy's:

1% L-Glutamine

1% Penicillin-Streptomycin

1% Foetal Calf Serum

Ishikawa Cell Line

Minimal Essential Medium Eagle

For Complete medium (CM) add the following to 500ml of MEME:

1% L-Glutamine

1% Penicillin-Streptomycin

1% non-essential amino acids

5% Foetal Calf Serum

COS-7 Cell Line

Dulbecco's Modified Eagles Medium (DMEM) with Glutamax

For complete medium (CM) add the following to 500ml of DMEM :

1% Penicillin-Streptomycin

10% Foetal Calf Serum

2. Agarose Gel Electrophoresis

10x TAE Buffer:

Tris	32.3 g
EDTA	2.48 g
Glacial Acetic Acid	11.7 ml

Make up to 1 L with distilled water.

Loading Buffer

Sucrose	25%
Xylene Cyanol FF	0.02%
Bromophenol Blue	0.05%

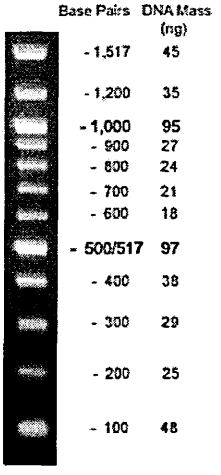

100 bp Ladder

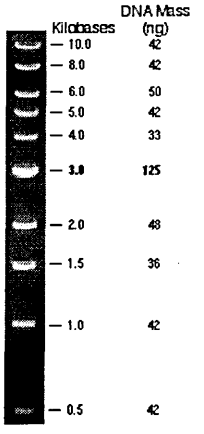

1Kb Ladder

3. Protein Extraction

Activation of Sodium orthovanadate

Prepare a 200 mM solution of sodium orthovanadate. Adjust the pH to 10.0 to give a yellow solution. Boil the solution until it turns colorless and cool to room temperature. Readjust the pH to 10.0 and repeat the boiling and pH adjustment until the solution remains colorless and the pH stabilises at 10.0. Aliquot and store at –20°C.

Protein Lysis Buffer

Glycerol	5ml
SDS	0.5g
DTT	0.5g
1M Sodium fluoride	5ml
2M $Na_4P_2O_7$	0.5ml
1M Na_3VO_4 (activated)	0.05ml
0.1M PMSF	0.5ml
Protease inhibitor Cocktail	300µl
1M Tris pH 6.8	3.125ml

Add distilled water to 50ml, aliquot and store at -20°C.

4. SDS-PAGE & Western Blotting

Resolving Buffer

1.5M Tris/HCl pH 8.8

Stacking Buffer

0.5M Tris/HCl pH 6.8

10x Running Buffer

0.25M Tris/HCl

2M glycine

1% SDS (w/v)

Adjust to pH 8.3

Resolving Gel, 8% (2x minigels of 0.75mm thickness)

Resolving Buffer	3.0ml
Acrylamide	1.6ml
dH2O	3.2ml
10% SDS	80μl

Mix by inverting three times and add:

10% APS	100μl
TEMED	40μl

Stacking gel, 4% (2x minigels of 0.75mm thickness)

Stacking Buffer	1.25ml
Acrylamide	0.5ml
dH_2O	3.1ml
10% SDS	20μl

Mix by inverting three times and add:

10% APS	100μl
TEMED	40μl

Towbin Buffer

Tris	4.84 g
Glycine	21.62 g
Methanol	150 ml

Dissolve in 1L of distilled water.

Chill for 2 hours at –20°C

10x TBS/T

20mM Tris

0.9% Sodium Chloride

Adjust the pH to 7.5 and make up to 1L with distilled water

Add 0.1% TWEEN-20

10x PBS/T

Sodium Chloride	80 g
Potassium Chloride	2 g
Disodium hydrogen orthophosphate	26.8 g
Potassium dihydrogen orthophosphate	2.4 g

Adjust the pH to 7.4 and make up to 1L with distilled water

Add 0.1% TWEEN-20

Coomassie Stain

Dissolve Coomassie R250 in destain to 0.25%

Store at 4°C.

Destain

Methanol	45ml
Acetic acid	5ml

Make up to 100ml with distilled water.

Protein Markers

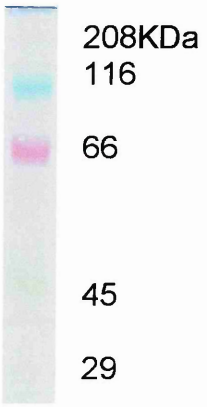

High Range Colour Marker

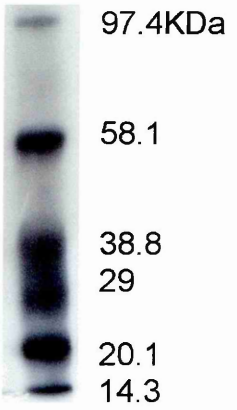

Biotinylated Marker

5. Bacterial Culture

L-Broth

Tryptone	10g
Yeast Extract	5g
Sodium Chloride	5g

Add 900 ml of ultrapure water, adjust pH to 7.5, make up to a final volume of 1L.

Autoclave to sterilise.

L-Agar Selective Plates & Stabs

Add kanamycin to cooled molten L-Agar to final concentration of 50µg/ml. Pour 30ml per Petri dish and allow to set. For stabs pour 15ml into a sterile 50ml Falcon and allow to set at a 45° angle. Store at 4°C for up to 2 weeks.

RNase A Stock Solution

Dissolve 10 mg of RNase A in 1 ml of sterile water. Filter sterilise and store at –20°C.

6. Plasmid Isolation

Alkaline lysis solutions

Solution I

Glucose	50 mM
EDTA	10 mM
Tris-HCl (pH 8.0)	25 mM

Add ultrapure water to a final volume of 100 ml.

Autoclave to sterilise and store at 4°C.

Solution II (Prepared fresh just prior to use):

2M Sodium Hydroxide	100 µl
10% SDS	100 µl
Water	800 µl

Solution III

5M Potassium Acetate	14.7 g

Acetic Acid	5.75 ml

Add distilled water to 50 ml and store at 4°C.

7. Stimulation Stock Compounds

β-17-Estradiol (20μg/ml)

Dissolve the contents of the bottle in 1 ml of ethanol and add 49ml of McCoy's 5A medium. Store at 4°C.

TGFß-1 (2μg/ml)

Dissolve the contents of the vial (2 μg) in 1 ml of sterile 4mM HCl containing 1% BSA. Store aliquots at –70°C.

Normal goat serum

Dilute in PBS to final concentration of 10% with 0.05% Sodium azide.

Aliquot and store at -20°C.

---

8. Extraction of Human DNA from Whole Blood

BufferA

Tris	1.2g
Sucrose	108.5g
Magnesium chloride	1g

Make up to 990ml with distilled water and adjust pH to 8.0.

Autoclave to sterilize. Add 10ml of TritonX-100 and store at 4°C.

Buffer B

Tris	48.44g
EDTA	22.33g
Sodium chloride	8.766g

Make up to 900ml with distilled water and adjust pH to 8.0.

Autoclave to sterilize. Add 100ml of a 10% SDS solution and store at 4^0C.

9. SSCP

Formamide Buffer

Formamide	9.5 ml
10mM EDTA in 10mM NaOH	0.5 ml
Blue / orange dye (Promega)	200 μl

10x TBE Buffer

Tris	112g
Boric Acid	55g
1M EDTA	20ml

Make up to 1 L with distilled water.

SSCP Gel Mix, 80ml

0.5x MDE with 5% glycerol		**0.6x MDE with 10% glycerol**	
2x MDE	20ml	2x MDE	25ml
10x TBE	4.8ml	10x TBE	4.8ml
50% glycerol	8ml	50% glycerol	16ml
Water	47.2ml	Water	34.2ml

Mix by inverting three times.

Add 800μl of freshly prepared 25% Ammonium Persulphate and 80μl of TEMED.

Invert three times, pour between the glass plates and insert the teflon combs.

Manual Silver staining

Gel Fix

Ethanol	100ml
Glacial acetic acid	5ml

Add distilled water to 1L.

Silver stain

0.001% Silver nitrate in distilled water. Store in the dark.

Developer

5M Sodium hydroxide 30ml

Formaldehyde 1.5ml

Make up to 500ml with distilled water. Store in the dark.

Final fix

Sodium carbonate 3.75g

Make up to 500ml with distilled water.

APPENDIX II

PTEN Sequence Data

1. PTEN cDNA Sequence

```
  1 ATG ACA GCC ATC ATC AAA GAG ATC GTT AGC AGA AAC AAA AGG AGA  15
 16 TAT CAA GAG GAT GGA TTC GAC TTA GAC TTG ACC TAT ATT TAT CCA  30
 31 AAC ATT ATT GCT ATG GGA TTT CCT GCA GAA AGA CTT GAA GGC GTA  45
 46 TAC AGG AAC AAT ATT GAT GAT GTA GTA AGG TTT TTG GAT TCA AAG  60
 61 CAT AAA AAC CAT TAC AAG ATA TAC AAT CTT TGT GCT GAA AGA CAT  75
 76 TAT GAC ACC GCC AAA TTT AAT TGC AGA GTT GCA CAA TAT CCT TTT  90
 91 GAA GAC CAT AAC CCA CCA CAG CTA GAA CTT ATC AAA CCC TTT TGT 105
106 GAA GAT CTT GAC CAA TGG CTA AGT GAA GAT GAC AAT CAT GTT GCA 120
121 GCA ATT CAC TGT AAA GCT GGA AAG GGA CGA ACT GGT GTA ATG ATA 135
136 TGT GCA TAT TTA TTA CAT CGG GGC AAA TTT TTA AAG GCA CAA GAG 150
151 GCC CTA GAT TTC TAT GGG GAA GTA AGG ACC AGA GAC AAA AAG GGA 165
166 GTA ACT ATT CCC AGT CAG AGG CGC TAT GTG TAT TAT TAT AGC TAC 180
181 CTG TTA AAG AAT CAT CTG GAT TAT AGA CCA GTG GCA CTG TTG TTT 195
196 CAC AAG ATG ATG TTT GAA ACT ATT CCA ATG TTC AGT GGC GGA ACT 210
211 TGC AAT CCT CAG TTT GTG GTC TGC CAG CTA AAG GTG AAG ATA TAT 225
226 TCC TCC AAT TCA GGA CCC ACA CGA CGG GAA GAC AAG TTC ATG TAC 240
241 TTT GAG TTC CCT CAG CCG TTA CCT GTG TGT GGT GAT ATC AAA GTA 255
256 GAG TTC TTC CAC AAA CAG AAC AAG ATG CTA AAA AAG GAC AAA ATG 270
271 TTT CAC TTT TGG GTA AAT ACA TTC TTC ATA CCA GGA CCA GAG GAA 285
286 ACC TCA GAA AAA GTA GAA AAT GGA AGT CTA TGT GAT CAA GAA ATC 300
301 GAT AGC ATT TGC AGT ATA GAG CGT GCA GAT AAT GAC AAG GAA TAT 315
316 CTA GTA CTT ACT TTA ACA AAA AAT GAT CTT GAC AAA GCA AAT AAA 330
331 GAC AAA GCC AAC CGA TAC TTT TCT CCA AAT TTT AAG GTG AAG CTG 345
346 TAC TTC ACA AAA ACA GTA GAG GAG CCG TCA AAT CCA GAG GCT AGC 360
361 AGT TCA ACT TCT GTA ACA CCA GAT GTT AGT GAC AAT GAA CCT GAT 375
376 CAT TAT AGA TAT TCT GAC ACC ACT GAC TCT GAT CCA GAG AAT GAA 390
391 CCT TTT GAT GAA GAT CAG CAT ACA CAA ATT ACA AAA GTC TGA
```

The putative phosphatase catalytic domain in Exon 5 (boxed) includes the catalytic motif (red) at residues 122-133. N-terminal homology to tensin/auxilin is highlighted in grey. GenBank accession AF067844.

2. PTEN Genomic Sequences

Exons are highlighted in red and include a small portion of the adjacent intron, shown in black. Primer binding regions are shown highlighted in the text.

Exon 1 23338-23417bp

```
ccaccagcag  cttctgccat  ctctctcctc  ctttttcttc  agccacaggc
tcccagacat  gacagccatc  atcaaagaga  tcgttagcag  aaacaaaagg
agatatcaag  aggatggatt  cgacttagac  ttgacctgta  tccatttctg
cggctgctcc  tctttacctt  tctgtcactc
```

Primer PTEN 1

Exon 2 51995-52079 bp

```
ttcagatatt  tctttcctta  actaaagtac  tcagatattt  atccaaacat
tattgctatg  ggatttcctg  cagaaagact  tgaaggcgta  tacaggaaca
atattgatga  tgtagtaagg  taagaatgct  ttgattttct  atttcaaata
ttgatgttta  tattcatgtt  gtgttttcat
```

Exon 3 83481-83526 bp

```
ttcttgatag  tattaatgta  atttcaaatg  ttagctcatt  tttgttaatg
gtggcttttt  gtttgtttgt  tttgttttaa  ggtttttgga  ttcaaagcat
aaaaaccatt  acaagatata  caatctgtaa  gtatgttttc  ttatttgtat
gcttgcaaat  atcttctaaa  acaactatta
```

Exon 4 89015-89058 bp

```
ataactttat  atcactttta  aacttttctt  ttagttgtgc  tgaaagacat
tatgacaccg  ccaaatttaa  ttgcagaggt  aggtatgaat  gtactgtact
atgttgtata  acttaaaccc
```

Exon 5 90987-91225 bp

```
tatgcaacat  ttctaaagtt  acctacttgt  taattaaaaa  ttcaagagtt
tttttttctt  attctgaggt  tatcttttta  ccacagttgc  acaatatcct
tttgaagacc  ataacccacc  acagctagaa  cttatcaaac  ccttttgtga
agatcttgac  caatggctaa  gtgaagatga  caatcatgtt  gcagcaattc
actgtaaagc  tggaaaggga  cgaactggtg  taatgatatg  tgcatattta
ttacatcggg  gcaaattttt  aaaggcacaa  gaggccctag  atttctatgg
ggaagtaagg  accagagaca  aaaaggtaag  ttattttttg  atgtttttcc
tttcctcttc
```

Primers PTEN 4 PTEN 5A & 5B PTEN 5C & 5D

Exon 6 110086-110227 bp

aacattttt ttcaatttgg cttctctttt ttttctgtcc accaggagt
aactattccc agtcagaggc gctatgtgta ttattatagc tacctgttaa
agaatcatct ggattataga ccagtggcac tgttgtttca caagatgatg
tttgaaacta ttccaatgtt cagtggcgga acttgcagta agtgcttgaa
attctcatcc ttccatgtat tggaacagtt ttcttaacca

Exon 7 115821-115987 bp

atcattaaaa tcgtttttga cagtttgaca gttaaaggca tttcctgtga
aataatactg gtatgtattt aaccatgcag atcctcagtt tgtggtctgc
cagctaaagg tgaagatata ttcctccaat tcaggaccca cacgacggga
agacaagttc atgtactttg agttccctca gccgttacct gtgtgtggtg
atatcaaagt agagttcttc cacaaacaga acaagatgct aaaaaaggtt
tgtactttac tttcattggg agaaatatcc aaaataagga cagattaaaa

Exon 8 118862-119086

aaacatcatt aattaaatat gtcatttcat ttctttttct tttctttttt
tttttttta ggacaaaatg tttcactttt gggtaaatac attcttcata
ccaggaccag aggaaacctc agaaaaagta gaaaatggaa gtctatgtga
tcaagaaatc gatagcattt gcagtataga gcgtgcagat aatgacaagg
aatatctagt acttacttta acaaaaaatg atcttgaaaa agcaaataaa
gacaaagcca accgatactt ttctccaaat tttaaggtca gttaaattaa
acattttgtg ggggttggtg acttgtatgt atgtgatgtg tgtttaattc

Primers PTEN 8A & 8B PTEN 8C & 8D

Exon 9 123258-123443 bp

tgttaaaaat atatttcact aaatagttta agatgagtca tatttgtggg
ttttcatttt aaattttctt tctctaggtg aagctgtact tcacaaaaac
agtagaggag ccgtcaaatc cagaggctag cagttcaact tctgtaacac
cagatgttag tgacaatgaa cctgatcatt atagatattc tgacaccact
gactctgatc cagagaatga acctttttgat gaagatcagc atacacaaat
tacaaaagtc tgaatttttt tttatcaaga gggataaaac accatgaaaa

Primer PTEN 2a

APPENDIX III

ψPTEN/PTH2 cDNA Sequence

```
  1 AGG ACA GCC ATC ATC AAA GAG ATC GTT AGC AGA AAC AAA AGG AGA  15
 16 TAT CAA GAG GAT GGA TTC GAC TTA GAC TTG ACC TAT ATT TAT CTA  30
 31 AAC ATT ATT GCT ATG GGA TTT CCT GCA GAA AGA CTT GAA GGC GTA  45
 46 TAC AGG AAC AAT ATT GAT GAT GTA GTA AGG TTT TTG GAT TCA AAG  60
 61 CAT AAA AAC CAT TAC AAG ATA CAC AAT CTT TGT GCT GAA AGA CAT  75
 76 TAT GAC ACC GCC AAA TCT AAT TAC AGA GTT GCG CAA TAT CCT TTT  90
 91 GAA GAC CAT AAC CCA CCA CAG CTA GAA CTT ATC AAA CCC TTT TGT 105
106 GAA GAT CTT GAC CAA TGG CTA AGT GAA GAT GAC AAT CAT GTT GCA 120
121 GCA ATT CAC TGT AAA GCT GGA AAG GGA CGA ACT GGT ATA ATG ATT 135
136 TGT GCA TAT TTA TTA CAT CGG GGC AAA TTT TTA AAG GCA CAA GAG 150
151 GCC CTA GAT TTC TAT GGG GAA GTA AGR ACC AGA GAC AAA AAG GGA 165
166 GTA ACT ATT CCC AGT CAG AGG CGC TAT GTG TAT TAC TAT AGC TAC 180
181 CTG GTA AAG AAT CAT CTG GAT TAT AGA CCA GTG GCA CTG TTG TTT 195
196 CAC AAG ATG ATG TTT GAA ACT ATT CCA ATG TTC AGT GGC GGA ACT 210
211 TGC AAT CCT CAG TTT GTG GTC TGC CAG CTA AAG GTG AAG ATC TAT 225
226 TCC TCC AAT TCA GGA CCC ACA CGA TGG GAG GAC AAG TTC ATG TAT 240
241 TTT GAG TTC CCT CAG CCG TTA CCT GTG TGT GGT GAT ATC AAA GTA 255
256 GAG TTC TTC CAC AAA CAG AAC AAG ATG CTA AAA AAG GAC AAA ATG 270
271 TTT CAC TTT TGG GTA AAT ACA TTC TTC ATA CCA GGA CCA GAG GAA 285
286 ACC TCA GAA AAA GTA GAA AAT GGA AGT CTA TGT GAT CAA GAA ATT 300
301 GAT AGC ATT TGC AGT ATA GAG CGT GCA GAT AAT GAC AAG GAG TAT 315
316 CTA GTA CTT ACT TTA ACA AAA AAT GAT CTT GAC AAA GCA AAT AAA 330
331 GAC AAA GCC AAC CGA TAC TTT TCT CCA AAT GTT AAG GTG AAG CTG 345
346 TAC TTC ACA AAA ACA GTA GAG GAG CCG TCA AAT CCA GAG GCT AGC 360
361 AGT TCA ACT TCT GTA ACA CCA GAT GTT AGT GAC AAT GAA CCT GAT 375
376 CAT TAT AGA TAT TCT GAC ACC ACT GAC TCT GAT CCA GAG AAT GAA 390
391 CCT TTT GAT GAA GAT CAG CAT ACA CAA ATT ACA AAA GTC TGA
```

The nucleotide sequence of ψPTEN/PTH2 cDNA,. Putative phosphatase catalytic domain in Exon 5 (boxed), catalytic motif (red), N-terminal homology to tensin/auxilin (grey), and Putative Tyrosine Phosphorylation site (yellow). *Mse* I sites indicated by blue arrows, *Hha* I sites indicated by green arrows. Bases that differ from PTEN are indicated in bold and underlined. Taken from Dahia, *et al* 1998.

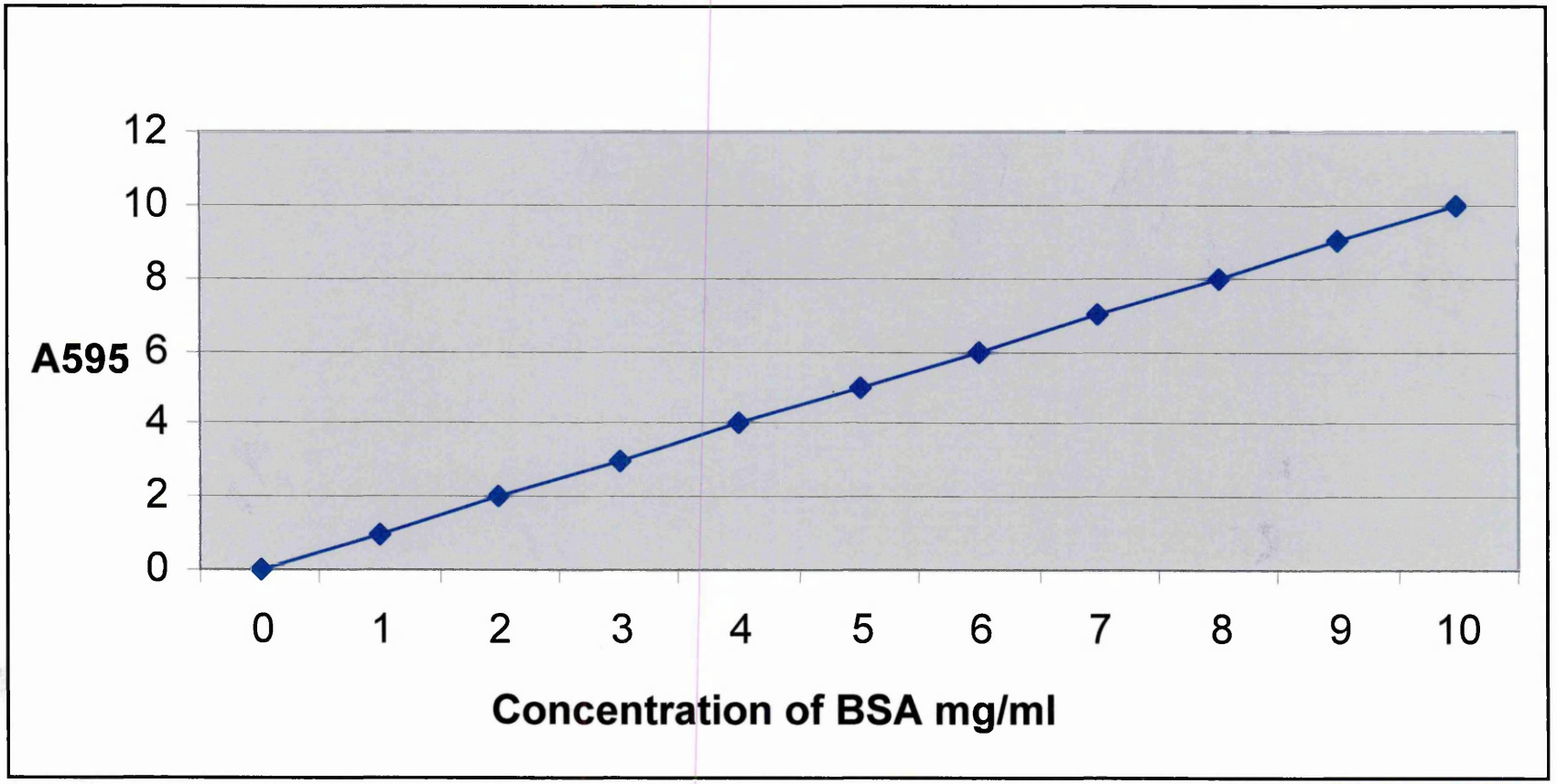

Appendix IV BSA Standard Curve. Graph shows absorbance of BSA standard solutions ranging from 0-10mg/ml at an absorbance of 595nm. Solutions were prepared in duplicate and the mean averages of each reading plotted.

APPENDIX V

PCR PROGRAMMES

PTEN I Cycle

LID ON 110°C

95oC	5 minutes	
95°C	1 minute	x 30
55°C	1 minute	
72°C	1 minute	
72°C	10 minutes	
LID OFF		
4°C	∞	

RIS 2.2 Cycle

LID ON 110°C

95°C	5 minutes	
95°C	2 seconds	x 37
50°C	20 seconds	
72°C	20 seconds	
72°C	10 minutes	
LID OFF		
4°C	∞	

GAPDH Cycle

LID ON 110°C

95°C	5 minutes	
95°C	1 minute	x 30
58°C	1 minute	
72°C	1 minute	
72°C	10 minutes	
LID OFF		
4°C	∞	

PAI-1 Cycle

LID ON 110°C

95°C	5 minutes	
95°C	30 seconds	x30
60°C	30 seconds	
72°C	30 seconds	
72°C	10 minutes	
HEATED LID OFF		
4°C	∞	

Bcl-2 PCR Cycle

HEATED LID ON 110°C

95°C	5 minutes	
95°C	30 seconds	x 35
61°C	30 seconds	
72°C	1 minute 30"	
72°C	10 minutes	

HEATED LID OFF

4°C	∞

Pfx3LX2 PCR Cycle

HEATED LID ON 110°C

95°C	2 minutes	
95°C	1 minute	x 35
55°C	1 minute	
68°C	1 minute	
68°C	20 minutes	

HEATED LID OFF

4°C	∞

APPENDIX VI

Equipment Suppliers

Mini-Gel Submarine Electrophoresis Units

Biometra Ltd, P.O. Box 42, Sale, Manchester.

Protean III Vertical Mini-Gel Electrophoresis Unit & Mini-Gel Electrophoresis Power Pack 300.

BioRad Laboratories Ltd, Marylands Ave., Hemel Hempsted, Herts.

SSCP Gel Vertical Gel Apparatus Hoefer SE660 & 3000v Power Supply

Amersham Biosciences UK Ltd, Pollards Wood, Chalfont St. Giles, Bucks.

PCR Primus Thermocyclers

MWG Biotech (UK) Ltd, Mill Court, Milton Keynes.

APPENDIX VII

1. Purity of RNA from Serum non-Starved HEC-1B Stimulated with TGF-β1

Concentration TGF-ß1 / Time (Hours)	Flask	Conc µg/µl	Ratio 260/280
0ng/4hrs	A	2.15	1.9
	B	1.64	1.7
0ng/8hrs	A	1.79	1.8
	B	2.21	1.86
0ng/24hrs	A	2.87	2.1
	B	2.99	1.78
2ng/4hrs	A	1.3	1.9
	B	1.23	1.81
2ng/8hrs	A	1.38	1.97
	B	1.35	2.01
2ng/24hrs	A	1.44	1.89
	B	1.45	2.08
5ng/4hrs	A	2.13	1.93
	B	1.67	1.86
5ng/8hrs	A	1.4	1.9
	B	1.37	1.84
5ng/24hrs	A	1.82	1.9
	B	2.05	1.92

2. Purity of RNA from Serum-Starved HEC-1B Stimulated with TGF-B1 Experiment 1			
Concentration TGF-ß1 / Time (Hours)	Flask	Conc µg/µl	Ratio 260/280
10% Control	A	1.64	1.65
	B	2.96	1.67
0ng/4hrs	A	3.65	1.76
	B	5.68	1.9
0ng/8hrs	A	3.26	1.9
	B	4.96	1.86
0ng/24hrs	A	1.53	1.88
	B	2.1	1.98
2ng/4hrs	A	5.42	1.8
	B	4.91	1.81
2ng/8hrs	A	1.29	1.86
	B	5.45	1.79
2ng/24hrs	A	6.82	1.84
	B	6.43	1.99
5ng/4hrs	A	4.15	1.83
	B	5.26	1.84
5ng/8hrs	A	1.72	1.75
	B	1.82	1.75
5ng/24hrs	A	7.67	1.89
	B	6.76	1.92

3. Purity of RNA from Serum-Starved HEC-1B Stimulated with TGF-b1 Experiment 2			
Concentration TGF-ß1 /Time (Hours)	Flask	Conc ug/ul	Ratio 260/280
10% Control	A	1.168	1.79
	B	3.37	1.71
0ng/4hrs	A	4.92	1.7
	B	3.24	1.56
0ng/8hrs	A	4.49	1.7
	B	4.09	1.75
0ng/24hrs	A	4.62	1.45
	B	6.1	1.73
2ng/4hrs	A	3.56	1.5
	B	3.97	1.46
2ng/8hrs	A	6.1	1.75
	B	7.83	1.78
2ng/24hrs	A	7.68	1.74
	B	8.1	1.75
5ng/4hrs	A	2.59	1.76
	B	6.94	1.68
5ng/8hrs	A	2.98	1.6
	B	5.99	1.68
5ng/24hrs	A	2.21	1.45
	B	6.11	1.65

4. Purity of RNA from Ishikawa cells Stimulated with TGF-β1			
Concentration TGF-ß1 / Time (Hours)	Flask	Conc µg/µl	Ratio 260/280
0ng/4hrs	A	2.8	1.66
	B	3.3	1.68
0ng/8hrs	A	3.31	1.68
	B	2.96	1.69
0ng/24hrs	A	4.13	1.66
	B	4.11	1.68
2ng/4hrs	A	6.5	1.71
	B	3.6	1.73
2ng/8hrs	A	3.2	1.72
	B	3.15	1.7
2ng/24hrs	A	3.83	1.7
	B	3.04	1.68
5ng/4hrs	A	4.3	1.69
	B	4.5	1.72
5ng/8hrs	A	3.26	1.71
	B	3.2	1.66
5ng/24hrs	A	3.52	1.69
	B	3.82	1.67

APPENDIX VIII

Purity of RNA from HEC-1B Cell Density Experiment			
Days in culture	Flask	Initial Density	
		4x106	9x106
Day 1	A	1.85	1.88
	B	1.83	1.9
	C	1.88	1.89
Day 2	A	1.77	1.8
	B	1.84	1.88
	C	1.8	1.81
Day 3	A	1.8	1.82
	B	1.91	1.9
	C	1.8	1.8
Day 4	A	1.85	1.88
	B	1.86	1.87
	C	1.85	1.89
Day 4 MC	A	1.87	1.89
	B	1.89	1.88
	C	1.79	1.84